Vol. 297, No. 3, November 10, 1994
Completing Volume 297

ISSN 0003-2670

ANALYTICA CHIMICA ACTA

An international journal devoted to all branches of analytical chemistry

ELSEVIER

ANALYTICA CHIMICA ACTA

Scope. *Analytica Chimica Acta* publishes original papers, rapid publication letters and reviews dealing with every aspect of modern analytical chemistry. Reviews are normally written by invitation of the editors, who welcome suggestions for subjects. Letters can be published within **four months** of submission. For information on the Letters section, see inside back cover.

Submission of Papers

Americas

Prof. Harry L. Pardue
Department of Chemistry
1393 BRWN Bldg, Purdue University
West Lafayette, IN 47907–1393
USA

Tel:(+1-317) 494 5320
Fax:(+1-317) 496 1200

Computer Techniques

Prof. J.T. Clerc
Universität Bern
Pharmazeutisches Institut
Baltzerstrasse 5, CH-3012 Bern
Switzerland

Tel:(+41-31) 6314191
Fax:(+41-31) 6314198

Prof. Sarah C. Rutan
Department of Chemistry
Virginia Commonwealth University
P.O. Box 2006
Richmond, VA 23284-2006
USA
Tel:(+1-804) 367 7517
Fax:(+1-804) 367 8599

Other Papers

Prof. Alan Townshend
Department of Chemistry
The University
Hull HU6 7RX
Great Britain

Tel:(+44-482) 465027
Fax:(+44-482) 466410

Prof. Willem E. van der Linden
Laboratory for Chemical Analysis
Department of Chemical Technology
Twente University of Technology
P.O. Box 217, 7500 AE Enschede
The Netherlands
Tel:(+31-53) 892629
Fax:(+31-53) 356024

Prof. Paul Worsfold
Dept. of Environmental Sciences
University of Plymouth
Plymouth PL4 8AA
Great Britain

Tel:(+44-752) 233006
Fax:(+44-752) 233009

Submission of an article is understood to imply that the article is original and unpublished and is not being considered for publication elsewhere. *Anal. Chim. Acta* accepts papers in English only. There are no page charges. Manuscripts should conform in layout and style to the papers published in this issue. See inside back cover for "Information for Authors".

Publication. *Analytica Chimica Acta* appears in 18 volumes in 1995 (Vols. 297–314). *Vibrational Spectroscopy* appears in 2 volumes in 1995 (Vols. 8 and 9). Subscriptions are accepted on a prepaid basis only, unless different terms have been previously agreed upon. It is possible to order a combined subscription (*Anal. Chim. Acta* **and** *Vib. Spectrosc.*).
Our p.p.h. (postage, packing and handling) charge includes surface delivery of all issues, except to subscribers in the U.S.A., Canada, Australia, New Zealand, China, India, Israel, South Africa, Malaysia, Thailand, Singapore, South Korea, Taiwan, Pakistan, Hong Kong, Brazil, Argentina and Mexico, who receive all issues by air delivery (S.A.L.–Surface Air Lifted) at no extra cost. For Japan, air delivery requires 25% additional charge of the normal postage and handling charge; for all other countries airmail and S.A.L. charges are available upon request.

Subscription orders. Subscription prices are available upon request from the publisher. Subscription orders can be entered only by calendar year and should be sent to: Elsevier Science B.V., Journals Department, P.O. Box 211, 1000 AE Amsterdam, The Netherlands. Tel: (+31-20) 5803 642, Telex: 18582, Telefax: (+31-20) 5803 598, to which requests for sample copies can also be sent. Claims for issues not received should be made within six months of publication of the issues. If not they cannot be honoured free of charge. Readers in the U.S.A. and Canada can contact the following address: Elsevier Science Inc., Journal Information Center, 655 Avenue of the Americas, New York, NY 10010, U.S.A. Tel: (+1-212) 633 3750, Telefax: (+1-212) 633 3990, for further information, or a free sample copy of this or any other Elsevier Science journal.
Advertisements. Advertisement rates are available from the publisher on request.

US mailing notice – Analytica Chimica Acta (ISSN 0003-2670) is published 3 times a month (total 54 issues) by Elsevier Science B.V. (Molenwerf 1, Postbus 211, 1000 AE Amsterdam). Annual subscription price in the USA US$ 3677.75 (valid in North, Central and South America), including air speed delivery. Second class postage paid at Jamaica, NY 11431. *USA Postmasters*: Send address changes to Anal. Chim. Acta, Publications Expediting, Inc., 200 Meacham Av., Elmont, NY 11003. Airfreight and mailing in the USA by Publication Expediting.

ANALYTICA CHIMICA ACTA

An international journal devoted to all branches of analytical chemistry

(Full texts are incorporated in CJELSEVIER, a file in the Chemical Journals Online database available on STN International; Abstracted, indexed in: Aluminum Abstracts; Anal. Abstr.; Biol. Abstr.; BIOSIS; Chem. Abstr.; Curr. Contents Phys. Chem. Earth Sci.; Engineered Materials Abstracts; Excerpta Medica; Index Med.; Life Sci.; Mass Spectrom. Bull.; Material Business Alerts; Metals Abstracts; Sci. Citation Index)

VOL. 297 NO. 3 CONTENTS NOVEMBER 10, 1994

(Continued overleaf)

Contents (continued)

ELSEVIER

Analytica Chimica Acta 297 (1994) 313–316

ANALYTICA CHIMICA ACTA

Letter

Fibre optic-based detection of the entire sample plug as a straightforward approach to kinetic measurements in flow-injection systems

J.A. García-Mesa, M.D. Luque de Castro *, M. Valcárcel

Department of Analytical Chemistry, Faculty of Sciences, University of Córdoba, E-14004 Córdoba, Spain

Received 11 July 1994; revised manuscript received 24 August 1994

Abstract

An unsegmented continuous-flow approach based on the use of long tubular flow cells with an axial optical pathlength is reported. The device enables the monitoring of the entire sample plug and uses a spectrophotometric detector furnished with optical fibres. This allows the simple adaptation of the length of the glass tube that functions as the flow cell to the chemical system to be monitored. Recordings resembling those provided by the stopped-flow technique can be obtained without halting the flow, thus facilitating the implementation of reaction rate methods.

Keywords: Flow systems; Fibre optic; Reaction-rate measurements

1. Introduction

UV–visible detectors are the most frequently used in flow-injection (FI) systems. [1,2] Monitoring in hydrodynamic systems normally entails using U-shaped flow-through cells of 10 mm pathlength. The small volume of these cells allows sequential monitoring of the sample plug from head to tail, and thus provides typical transient FI recordings (FI peaks).

A new configuration based on the use of a fibre-optic spectrophotometer is proposed for the monitoring of the entire sample plug. This is accomplished with the aid of a glass tube of variable length and 2-mm i.d. used as the flow cell. In this arrangement dispersion does not lead to loss of sensitivity because at a certain stage the whole sample plug fills the optical path.

1.1. Foundation of the proposed approach

During the passage of an injected sample plug through a flow-injection manifold the volume of solution in which the sample is contained continuously increases due to dispersion. For this reason, the entire injected plug can almost never be monitored; instead, portions sequentially passing the detection point are

* Corresponding author.

SSDI 0003-2670(94)00417-X

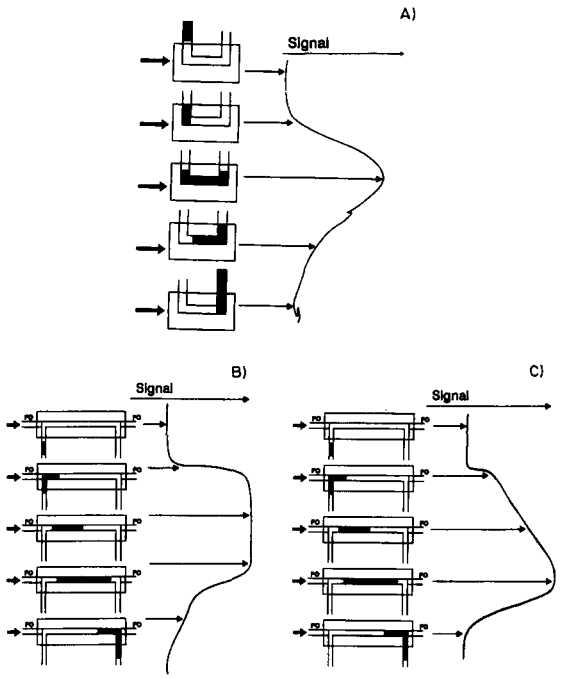

Fig. 1. Recordings obtained on passage of the sample plug through different flow cells: (A) conventional flow cell of 10 mm pathlength. Glass tubing flow cell of long pathlength (B) without chemical reaction; (C) with chemical reaction.

measured resulting in a recording such as that shown in Fig. 1A. However, when the connection between the injection unit and detection point is short and the flow cell is large enough to accommodate the entire injected plug, it almost only disperses in the cell, where it stays over an interval long enough to allow changes during the evolution of the derivatizing reaction to be monitored (Fig. 1C). Hence, the proposed approach can be used to make reaction rate measurements. When no reaction is involved (e.g., injection of a dye) a plateau is obtained (see Fig. 1B).

2. Experimental

2.1. Reagents

Creatinine and picric acid (Sigma); NaOH and K_2MnO_4 (Merck) and bidistilled water obtained from a Millipore Milli-Q system were used. All chemicals were analytical or reagent grade.

2.2. Apparatus

A Gilson Minipuls-3 peristaltic pump; a Rheodyne 5041 injection valve; a Guided Wave spectrophotometer fitted with optical fibres of different diameters (Iberlaser) and connected to a PC equipped with a simple BASIC programme; poly(tetrafluoroethylene) (PTFE) tubing of 0.8 mm i.d. and flow cells made of glass tubing of 2 mm i.d. and different lengths (40–150 cm) were used to build the manifold shown in Fig. 2. The connection between the glass tubing flow cell and the optical fibres is depicted in the detailed view.

3. Results and discussion

Two chemical systems, one without a chemical reaction and one involving a derivatizing reaction, were used in order to test the proposed configuration.

3.1. System without chemical reaction

Potassium permanganate was used as a coloured system to test the manifold; the influence of both types of

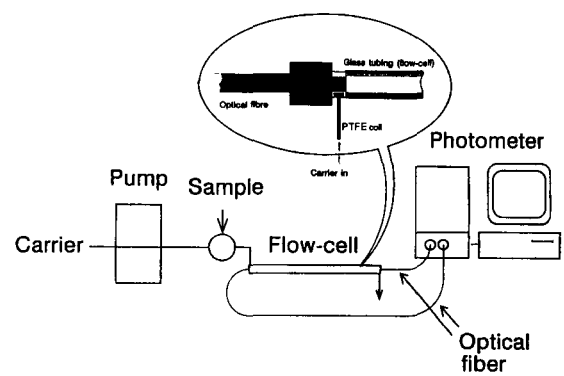

Fig. 2. Flow-injection manifold and detailed view of the long path-beam flow cell and its connection to the fibre optics (for details, see text).

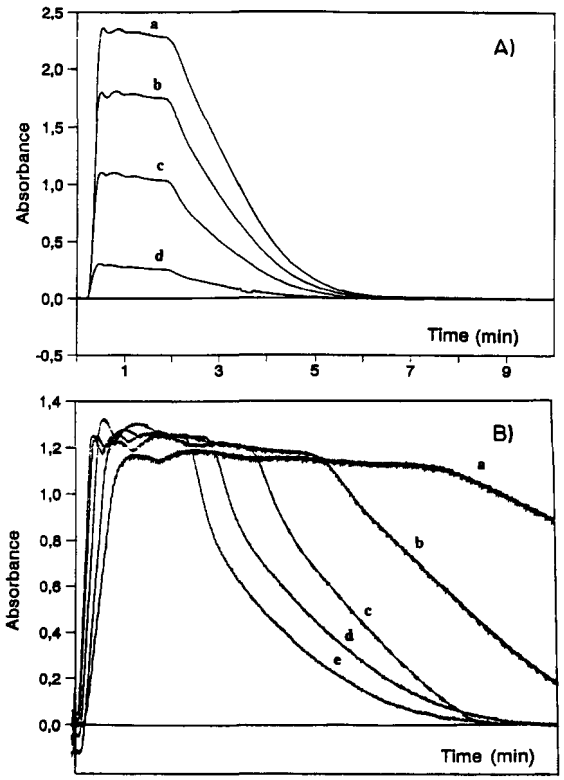

Fig. 3. Study of variables affecting the recordings obtained by using the proposed approach and a system without chemical reaction (I). (A) Influence of the injected volume of dye injected (a = 322, b = 236, c = 136, d = 36 μl). (B) Influence of the flow-rate (a = 1.0, b = 1.5, c = 2.0, d = 2.5, e = 3.0 ml min^{-1}).

variables, viz. flow-injection and chemical ones, was studied.

As can be seen in Fig. 3A, the plateau height and length increased with increasing the injected volume of 90 μM $KMnO_4$ as a result of the increased amount of $KMnO_4$ and length of the injected plug, respectively. Fig. 3B shows the recordings obtained at variable flow-rates and an injected volume of 130 μl of 90 μM $KMnO_4$. The lower the flow-rate was, the longer was the residence time of the plug in the flow cell and hence the wider was the plateau. Increasing flow cell lengths had a similar effect as they also did increase the residence time (Fig. 4A). The slightly lower absorbance obtained with long flow cell lengths could be due to the small cell zones of the pathlength being occupied by the dye as dispersion increased. Fig. 4B shows typical recordings obtained in running the calibration curve.

3.2. System with chemical reaction

The kinetic determination of creatinine based on its reaction with picric acid in alkaline medium [3] was used to check the usefulness of the approach for the development of methods based on reaction rate measurements. The working conditions were optimized by the univariate method, except for the flow cell length and injected volume, which were kept at 40 cm and 36 μl, respectively, in order to maximize the sampling frequency. Creatinine samples were diluted in 0.4 M NaOH and injected into a 5×10^{-3} M picric acid + 0.4 M NaOH carrier in order to minimize recording oscillations ($\lambda_{monitoring} = 525$ nm) due to changes in the refractive index. Table 1 lists the ranges over which the variables were studied and their optimum values.

Fig. 5 shows the recordings obtained in running the calibration curve, whose figures of merit are given in

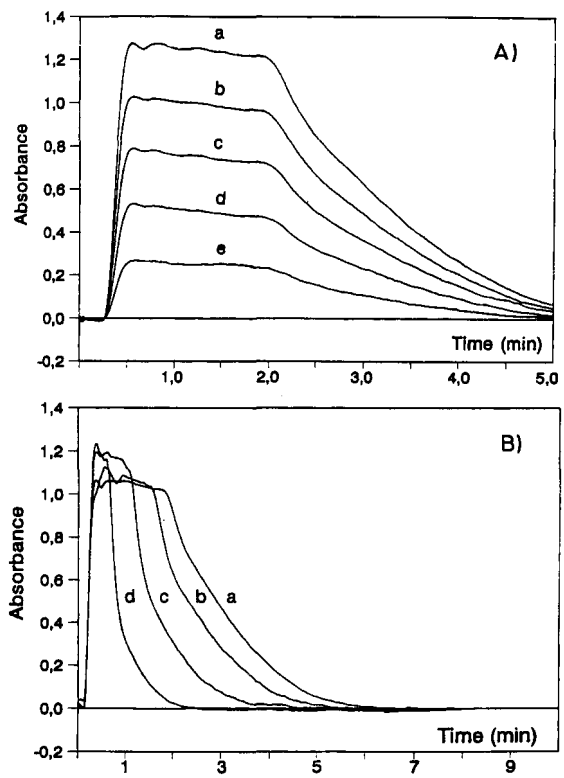

Fig. 4. Study of variables affecting the recordings obtained by using the proposed approach a system without chemical reaction (II). (A) Influence of the flow cell length (a = 150, b = 120, c = 80, d = 40 cm). (B) Influence of the injected dye concentration (a = 90, b = 72, c = 54, d = 36, e = 18 μM K_2MnO_4).

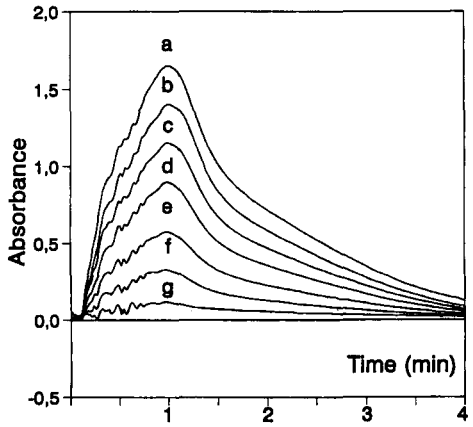

Fig. 5. Calibration recordings used with the reaction rate method for the determination of creatinine (a = 180, b = 150, c = 120, d = 90, e = 60, f = 30, g = 10 μg ml^{-1}).

Table 1. The table also shows the precision of the method, expressed as relative standard deviation obtained in a repeatability study.

Creatinine in synthetic samples was determined in order to estimate the recoveries provided by the method proposed. The results, listed in Table 2, testify to the usefulness of the proposed approach.

4. Conclusion

The use of flow cells with a long pathlength opens new prospects for flow-injection systems. One immediate application of this approach, viz. the obtainment of signal–time measurements similar to those provided by stopped-flow modes, clearly simplifies the experimental set-up required for such methods.

Acknowledgements

The Spanish Comisión Interministerial de Ciencia y Tecnología, CICyT, is thanked for financial support (Project No. PB93-0827).

Table 1
Optimization of the system variables and features of the reaction rate method for determination of creatinine

Optimization

Variables	Range studied	Optimum value
[NaOH], M	0.1–0.5	0.4
[Picric acid], M	1×10^{-3}–1.5×10^{-3}	0.5×10^{-2}
Flow-rate, ml min^{-1}	0.5–2.0	1.0

Features

Equation [a]	Linear range (μg ml^{-1})	r	R.S.D., % [b]	Sampling frequency, h^{-1}
$y = 0.016 + 0.007x$	1–180	0.999	1.9	12

[a] y in milli-absorbance units and x [creatinine] in μg ml^{-1}.
[b] [Creatinine] = 10 μg ml^{-1}.

Table 2
Application of the method to synthetic samples

[Creatinine], μg ml^{-1}	
Added	Found
180	178
150	150
120	122
90	98
60	61
30	34
10	8

References

[1] M. Valcárcel and M.D. Luque de Castro, Flow Injection Analysis: Principles and Applications, Ellis Horwood, Chichester, 1987.
[2] J. Ruzicka and E.H. Hansen, Flow Injection Analysis, Wiley, New York, 1988.
[3] M.C. Gutiérrez, A. Gómez-Hens and D. Pérez-Bendito, Fresenius' J. Anal. Chem., 335 (1989) 576.

ELSEVIER

Analytica Chimica Acta 297 (1994) 317–347

ANALYTICA CHIMICA ACTA

A review of expert systems for chromatography

C.H. Bryant [a,*], A. Adam [a], D.R. Taylor [a], R.C. Rowe [b]

[a] *University of Manchester Institute of Science and Technology, PO Box 88, Manchester M60 1QD, UK*
[b] *Zeneca Pharmaceuticals, Alderley Park, Macclesfield, Cheshire SK10 2NA, UK*

Received 8 February 1994; revised manuscript received 29 April 1994

Abstract

Expert systems for chromatography are reviewed. A taxonomy is proposed that allows present (and future) expert systems in this area to be classified and facilitates an understanding of their inter-relationship. All the systems are described focusing on the reasons for their development, what their purpose was and how they were to be used. The engineering methods, knowledge representations, tools and architectures used for the systems are compared and contrasted in a discussion covering all the stages of the development life cycle of expert systems. The review reveals that too often developers of expert systems for chromatography do not justify their decisions on engineering matters and that the literature suggests that many ideas advocated by knowledge engineers are not being used.

Keywords: Chromatography; Review; Expert systems

1. Introduction

Section 2 compares this work with previous reviews; section 3 introduces some of the concepts and terminology of chromatography and describes how a chromatographic method is developed; section 4 gives a definition of 'expert system' and specifies the scope of this review; section 5 explains why expert systems for chromatography are needed; and section 6 proposes a taxonomy for these systems, describes its purpose and how it was developed.

Sections 7, 8 and 9 are arranged in a taxonomic fashion corresponding to the taxonomy and explain why each system was developed, what its purpose was and how it was to be used.

Sections 11, 12, 13 and 14 discuss the engineering methods, knowledge representations, tools and architectures used in the development of expert systems for chromatography.

2. Previous reviews

Many papers have been published that review artificial intelligence for chemistry but their scope is so wide as to prohibit the inclusion of a review of expert systems for chromatography as detailed as that given here. For an example see [1]. In addition to artificial intelligence for chemistry, the more specific topic of expert systems for

* Corresponding author.

SSDI 0003-2670(94)00209-5

analytical chemistry has been reviewed in a number of papers. Ref. [2] provides an introduction to knowledge representation and explanation facilities for expert systems for analytical chemistry but only gives four references for expert systems for chromatography. Ref. [3] also discusses topics such as knowledge representation but it does not mention any expert systems for chromatography. Ref. [4] compares the use of artificial intelligence languages and expert system shells for building expert systems for limited domains but only reviews one expert system for chromatography.

Three papers [5–7] have been published that specifically review expert systems *for chromatography*. Ref. [5] reviews expert systems for liquid chromatography very briefly. It lacks the authoritative tone that usually accompanies an academic paper: the style of writing is imprecise, some of the analogies used are weak and only two references are given. Ref. [6] does not give any references and only reviews four systems of which only one is an expert system, the other three being simulation programs. Ref. [7] mentions more than sixty [1] computer systems but only about a quarter of these are expert systems for chromatography. This paper reviews all the expert systems for chromatography that [7] reviews and a further eleven expert systems for chromatography that [7] does not mention. Ref. [7] does not make the relationship between different expert systems for chromatography clear; this paper proposes a taxonomy which facilitates an understanding of their inter-relationship. Ref. [7] has a useful explanation of how expert systems in general are structured and introduces some aspects of knowledge engineering. However its analysis of how expert systems *for chromatography* have been engineered is superficial and, in contrast to this paper, no conclusions are drawn on this engineering. This paper reviews expert systems for chromatography comprehensively, covering more than twenty-five systems and gives over eighty references.

[1] This number does not include subsystems of expert systems for chromatography.

3. A brief introduction to chromatography

The aim of this section is to explain *briefly* some concepts and terminology of chromatography and to describe how a chromatographic method is developed, a knowledge of which is assumed later in this paper. Complete definitions, including any relevant mathematical equations, can be found in the references given.

Chromatography is a separation process in which the sample mixture is distributed between two phases in the chromatographic bed (column or plane). One phase is stationary whilst the other passes through the chromatographic bed [8]. Thus the former is referred to as the stationary phase and the latter as the mobile phase (or eluent). Substances to be separated by a chromatographic system must have different relative affinities for these two phases. Thus, a substance with a relatively higher affinity for the stationary phase moves with a lower velocity through the chromatographic system than does a substance with lower affinity. This difference in migration velocity ultimately leads to physical separation of the components in a sample [9].

A component of the sample mixture that leaves the stationary phase is said to be eluted in a process known as elution. The eluting power is the power of the eluent, that is the mobile phase, to elute the components remaining on the stationary phase.

If the substances to be separated do not have widely differing affinities for the stationary phase then the column can be eluted with the same solvent (mobile phase) all the time. However if the affinities vary widely then the composition of the eluting solvent can be gradually changed. This technique is known as gradient elution [10].

Stationary phases are either a solid, porous, surface-active material in small-particle form or a solid support covered with a thin film of liquid [8]. The particle size is related to the efficiency. Column efficiency is inversely related to the rate at which solute molecules spread out as they travel through the stationary phase [10]. The potential of a chromatographic system to separate two compounds is referred to as its selectivity. Most expert systems for chromatography concern

chromatographic systems in which the eluted compounds are transported to a detector and recorded as Gaussian (bell-shaped) curves. The signals are known as peaks and are shown on the chromatogram [8]. The chromatogram is a record of the concentration or mass profile of the sample components as a function of the movement of the mobile phase [11]. The degree of separation of successive solute bands or peaks is referred to as the resolution [10]. The peaks give qualitative and quantitative information on the mixture in question [8]:-

Qualitative. A peak can be identified by injecting the relevant substance and then comparing retention times. The retention time is equal to the period between sample introduction and the detector sensing the maximum of the retained peak. The retention time of a component is always constant under identical chromatographic conditions. The column dimensions, type of stationary phase, mobile phase composition and flow velocity, sample size and temperature provide the chromatographic conditions. Since these conditions vary the capacity factor is better for characterising a compound, although its measurement does require that an unretained component is timed through the column. The capacity factor is the ratio of the time spent by the solute in the stationary phase to the time spent in the mobile phase (or eluent).

Quantitative. The area of a peak is proportional to the amount of a compound injected. Calibration graphs can be drawn to determine unknown concentrations of identified samples.

3.1. Chromatographic modes

Gas chromatography is the branch of chromatography in which the mobile phase is a gas. In HPLC (high performance liquid chromatography) the mobile phase is a liquid.

There are a number of methods, or modes, for liquid chromatography. Adsorption, reversed-phase and ion-pair are three which are relevant to this paper. In adsorption chromatography a relatively polar material is used as the stationary phase and a relatively non-polar solvent as the mobile phase. The different rates at which the various types of molecules in the mixture are adsorbed on the stationary phase provide the separation effect. In reversed-phase chromatography the polarity is reversed: the stationary phase is very non-polar and the mobile phase is relatively polar. Ion-pair chromatography can be used for the separation of ionic compounds. Ionic sample molecules are 'masked' by a suitable counter ion; hence the term pair. [8]

3.2. Method development

Developing a method for chromatography involves five steps:

1. **Method selection**. This step is also known as the first guess. The appropriate chromatographic method, materials and instrumentation are selected.
2. **Optimisation**. The three essential characteristics of any chromatographic separation (retention, selectivity and efficiency) are optimised.
   (a) **Retention optimisation**. A chromatogram is obtained in which the components of interest appear as sharp, symmetrical peaks with a retention time in an optimum range. The retention of components needs to be sufficiently high to achieve separation, but sufficiently low to maintain a reasonable analysis time and good sensitivity.
   (b) **Selectivity optimisation**. The best possible selectivity is sought within the constraints of optimum retention times for each peak.
   (c) **Method (or chromatographic or system or efficiency) optimisation**. After the selectivity has been optimised the efficiency of the chromatographic system is optimised by selecting the most appropriate column, operating conditions and instrumentation.
3. **Method validation**. Finally the method is validated to prove that it meets the analytical requirements.

4. Definition of an expert system

An expert system is a computer program that represents and reasons with knowledge of some specialist subject with a view to solving problems

or giving advice. An expert system should exhibit all of the following features to some degree [12].

- It *simulates human reasoning* about a problem domain, rather than simulating the domain itself.
- It performs reasoning over *representations of human knowledge*, in addition to doing numerical calculations or data retrieval.
- It solves problems by *heuristic or approximate* methods which unlike algorithmic solutions, are not guaranteed to succeed.
- It deals with subject matter of realistic complexity that normally requires a considerable amount of human expertise.
- It must exhibit high performance in terms of speed and reliability in order to be a useful tool.
- It must be capable of explaining and justifying solutions or recommendations to convince the user that its reasoning is in fact correct.

Ref. [12] gives a broad introduction to expert systems. The literature abounds with books on the various aspects of engineering relevant to this paper. Useful texts include [13] for knowledge acquisition, [14] for knowledge representation and [15] for expert system tools and languages.

As stated above an expert system does not simulate the domain itself but human reasoning about the domain. Hence this paper does not review literature that describes work in which the primary aim was to model, quantitatively or qualitatively, aspects of chromatography. Thus [16] is not discussed because it is concerned with *model* based reasoning and Drylab [17] is not included because it *simulates* HPLC development.

5. Why expert systems are needed for chromatography

The introduction of workable expert systems for chromatography would be of great benefit because of the wide range of analytes amenable to chromatography and the complexity of this field with regard to the choice of materials and instruments [18].

An example of the wide range of amenable analytes is seen in the pharmaceutical industry: there is an ever increasing volume of diverse novel compounds which have to be screened in order to develop compounds with diagnostic or therapeutic properties. In principle, each compound needs its own method of analysis; thus the method development process must be repeated in its entirety for each new compound. Most of these new compounds are analysed using some form of chromatography, mainly HPLC. [18]

The choice of materials for HPLC is complex. Many factors affect the choice of mode of separation, packing material, mobile phase, and instrumental operating conditions. The development of an optimum method and the interpretation of the results usually requires a lot of expertise and experience to solve the problems that arise for each particular case.

It is impossible for any individual analyst to become an expert in all the various areas of chromatography. Hence individual analysts working in areas in which they are not experts have to seek assistance from the experts in those areas. Human, as opposed to computer, experts have several drawbacks however. They are often in short supply or unavailable in a particular laboratory. They are usually busy and have little time to spare to help non-experts. Occasionally their expertise is lost because they leave an organisation or die. Sometimes their expertise is temporarily unavailable because they are ill or on leave. When they are available they may not always be in a helpful mood and may not offer consistent advice. Expert systems offer an opportunity to encode chromatographic expertise in computer systems which can be made widely available and which provide advice which is consistent, user-friendly and easily documented.

6. The taxonomy

This section discusses the proposed taxonomy of expert systems for chromatography.

The purpose of the taxonomy is to:

- facilitate the reader's understanding of how the systems are related. The diagrams that show the taxonomy allow it to be quickly assimilated and they can be used for reference.

- allow readers to focus their attention on a class of expert system for chromatography that is of particular interest to them, if they should so wish.
- allow future expert systems for chromatography to be classified and hence illustrate how they are related to previous systems.

The taxonomy was developed as follows. A number of attributes that were candidates for classifying the expert systems were selected. They included the type of expert system, who developed it and where, brief details of how it was implemented and what the domain was. For each system a list of the values of these attributes was compiled. Attempts were made to group the systems into classes where class membership was determined by the values of one of these attributes. It proved impossible to develop a taxonomy that unambiguously classified all the systems if the type of expert system was used to determine class membership: the classes generated were not mutually exclusive for all the systems. Attempts to classify the systems by considering who developed them or where did not give rise to a taxonomy that would, in any way, facilitate the readers understanding of the inter-relationship between the systems. Classifying the systems in terms of how they were implemented was not possible because their implementations could not be accurately compared and contrasted: the range of aspects of the implementations described in the literature varies for different systems. However it was discovered that all the systems could be unambiguously classified if class membership was based on the domain of a system. An analysis of the resulting classes showed that in some cases two or more of these classes were subclasses of a more general class. An examination of these more general classes showed that some of them were subclasses themselves of a yet more general class. Thus a taxonomy was developed, as shown in Fig. 1, Fig. 2 and Fig. 3.

Sections 7, 8 and 9 describe the functionality of the various expert systems for chromatography, presenting them in a taxonomic fashion corresponding to the taxonomy outlined above.

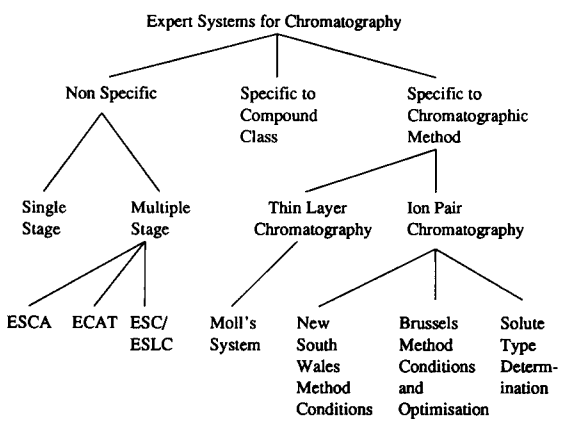

Fig. 1. A taxonomy of expert systems for chromatography.

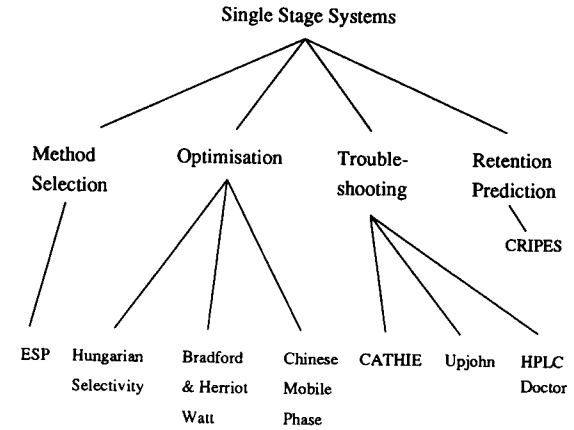

Fig. 2. A taxonomy of single stage expert systems for chromatography.

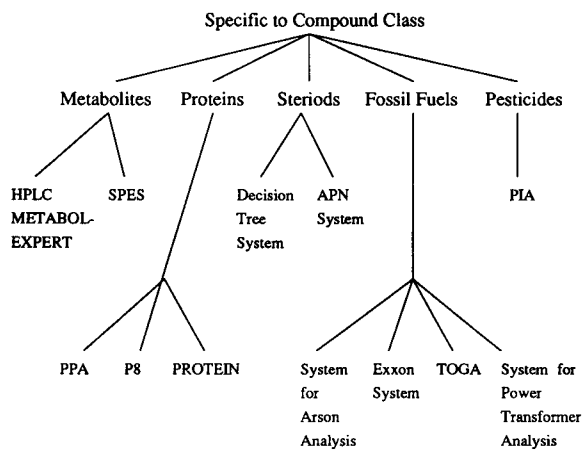

Fig. 3. A taxonomy of expert systems for chromatography that are specific to a class of compounds.

7. Systems not specific to a chromatographic method or class of compounds

This section discusses all the expert systems for chromatography that were not specifically designed for a particular method or a particular class of chemical compounds.

7.1. Systems designed for several stages of the process

This section corresponds to the branch of the taxonomy which is entitled 'Multiple Stage' on Fig. 1 and describes three projects (ESCA, ECAT and ESC/ESLC) which all attempted to implement systems that would give advise to an analyst on several stages of the process of developing a successful HPLC separation.

7.1.1. ESCA

The expert systems in chemical analysis (ESCA) project, Esprit project 1570, started in May 1987, officially finished in May 1990, and involved five partners: Philips Scientific, Cambridge, UK; Catholic University Nijmegen, Netherlands; Organon International B.V., Oss, Netherlands; Philips Research Eindhoven, Netherlands; Philips Research Hamburg, Germany; Brussels Free University, Belgium.

ESCA "was set up to evaluate the merits of expert system technology for use in industrial chemical analysis" [18]. Its aim was to provide expert systems that would illustrate the benefits and shortcomings of expert system technology. ESCA resulted in the publication of around 25 papers. Some of these give general descriptions of the project (see [19–21]).

The knowledge domain chosen for ESCA was HPLC method development in pharmaceutical analysis. "In the pharmaceutical industry an ever increasing volume of diverse novel compounds has to be searched in order to develop compounds with diagnostic or therapeutic properties. In principle, each compound needs its own method of analysis....Most of these... are analysed using some form of chromatography, mainly HPLC" [18]. It was believed that an expert system for HPLC method development "would speed up the process; making it more consistent and better documented" [18] while offering expertise that was not generally available in every laboratory.

Initially the following four domains which covered the entire field of method development in HPLC were selected. Each domain represented a discrete step in the process. Thus the intention was to build four experts systems that could be integrated later.

1. **Selection of initial conditions**
2. **Selection of selectivity optimisation criteria**. It was decided to build an expert system for the *selection of* optimisation criteria because "it is difficult to select the most appropriate criterion in different situations" [18] and the choice greatly affects the outcome of the optimisation. The resulting system helped the user to use a conventional package of computer optimisation programs.
3. **Optimisation of chromatographic parameters**. Chromatographic (or method) optimisation follows selectivity optimisation. The latter results in a method that yields adequate separation in an acceptable amount of time, for the given instrumental conditions. The former optimises these conditions. The aim of the optimisation of the chromatographic parameters is to reduce analysis time and increase the sensitivity of the method. An expert system was developed for this task because the "relations between these parameters are complex. Finding the optimal settings requires the evaluation of a number of equations that are difficult to see through, even after a long period of study." [18]
4. **Validation of the development method**. The expert system developed for this domain was limited to precision testing.

A successful integration of the work of all the participants in the ESCA project required that the project was managed effectively: there was a large number of participants from five organisations that were geographically isolated from one another. Although there were no less than four proposals on how various parts of the work could be integrated, not one of these described how all of the parts could be combined. Furthermore the literature does not provide any evidence that

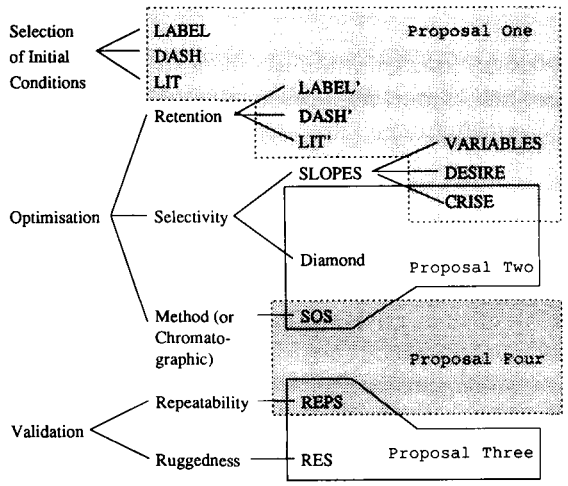

Fig. 4. A mapping between the subdomains of ESCA, the subsystems implemented for each of those subdomains and the proposals for integrating these subsystems. The four polygons correspond to the four proposed integrations and each polygon surrounds those systems that were to be integrated by that proposal.

workers on the ESCA project understood that the success of the integration of a project as large as ESCA could not be left to chance and that consequently there was a need for a plan that described how all the parts would be integrated. This may be because the actual goal of the ESCA project was the development of stand-alone systems [21].

The four parts of the domain covered by the four proposals on how the various parts of the work could be integrated are outlined below.

1. The selection of initial conditions, retention optimisation and selectivity optimisation.
2. Selectivity and chromatographic (or method) optimisation.
3. Method validation.
4. Repeatability testing and troubleshooting.

Fig. 4 shows the ESCA subsystems implemented for each of the ESCA subdomains and shows the four proposals for integrating the subsystems.

Proposal one for integration of ESCA work; selection of initial conditions, retention optimisation and selectivity optimisation. Some of the workers on the ESCA project performed a feasibility study [22,23] for the construction of an integrated system for the selection of initial conditions, retention optimisation, and selectivity optimisation. They proposed to construct the system from the stand-alone expert systems (described in the remaining part of this section) and some additional knowledge which was needed to direct the user through the integrated system.

In the proposed integrated system first-guess conditions were to be selected by one of the expert systems LABEL, DASH or LIT, the choice depending on the application field. After carrying out the first experiment, the retention time range of the solutes was to be evaluated. If there were solutes with capacity factors outside the desired range, then one of the corresponding retention optimisation expert systems LABEL′, DASH′ or LIT′ was to be consulted. The result would be a chromatogram in which all the solutes would have eluted within a reasonable time but two or more peaks may still have overlapped. The selectivity optimisation expert system SLOPES would then have been consulted.

DASH (Drug Analysis System in HPLC) [79] [24] was originally developed for chromatographic method selection and retention optimisation for the purity control of basic compounds, namely CNS (central nervous system)-active and cardiovascular drugs. The system determined the initial conditions to obtain a capacity factor between 3 and 10. "In more than 75% of all cases, correct predictions were obtained for the original family of substances" [22].

DASH′ [24], an extension of DASH, was specifically designed for retention optimisation. DASH′ was a good-second-guess system whereas DASH was a first-guess system. DASH had proved satisfactory when limited to basic drugs. However the integrated ESCA system had to allow for a wider range of compounds. DASH′ was proposed because DASH alone would not have performed satisfactorily for this wider range.

LABEL [25–27] was an expert system for selecting the initial chromatographic conditions for the label claim analysis of pharmaceutical formulations on a cyanopropyl column used in different chromatographic modes. LABEL was developed by one of the partners involved with the project

before ESCA started. "It was included in the project because it covers the situation that one sample must be analysed for different compounds. This is in contrast to DASH" [21].

LABEL contained knowledge for the selection of a suitable detection mode. It only considered UV or electrochemical detection, the latter in the oxidation mode [25,27,28].

LABEL assumed the use of a single stationary phase type, namely a nitrile or cyanopropyl column, which could be used in both normal-phase and reversed-phase chromatography. LABEL selected the mobile phase system, either normal-phase, reversed-phase with water or reversed-phase with buffer, using rules. It then decided if the addition of ion-suppressing agents to the eluting agent was necessary and finally gave the starting composition of the mobile phase. [26]

In 36 of 44 tests performed on LABEL "...success was achieved in a manner that probably could not have been done better by a human chromatography expert" [26].

LABEL/, like DASH/, was specifically designed for retention optimisation: the main task of the expert system was to situate the capacity factor in a suitable range. The optimisation was performed by increasing or decreasing the percentage of organic modifier in the mobile phase, starting from the first-guess composition. [22]

LIT was a small expert system that helped to select all the important parameters of a literature method and checked whether the method could be treated by SLOPES. [21]

SLOPES, the SeLectivity OPtimisation Expert System, was to comprise three different modules: VARIABLES, DESIRE and CRISE. VARIABLES selected the relevant optimisation parameters (the *variables* that need to be considered) and their boundaries (minimum and maximum limits). DESIRE determined the type of the experimental design (the pattern according to which the necessary experiments will be performed such as Simplex or Doehlert) and the number and location of the experiments. Finally, the most suitable optimisation criterion to describe the quality of separation in a chromatogram was selected by CRISE.

CRISE (CRIteria SElection) [29] was an expert system for the selection of objective criteria for systematic optimisation of selectivity. Such criteria must characterise the quality of separation in a chromatogram.

The system was developed for several reasons, but principally because numerous criteria have been suggested, each of which yield different results and the choice depends on a large number of factors. "It is genuinely difficult to select the most suitable criterion in a particular situation" [29].

CRISE consisted of four modules. In the first the most suitable elemental criterion was selected to quantify the extent of separation between two adjacent peaks in the chromatogram. Resolution (R_s), separation factors (S), separation factors corrected for plate counts (S_N) but also expressions such as peak-valley ratios could be used. As R_s, S_N and S do not take into account a possible loss in resolution due to non-ideal situations module 2 investigated whether any corrections were required. Module 3 assisted the user in the selection of weighting-factors to make a difference between peaks according to their relevance or relative importance. In the last module, the elemental criteria were incorporated in the global optimisation criterion that was best suited to quantify the separation quality of the entire chromatogram taking into account the purpose of the chromatogram [30].

The main conclusions of the validation of CRISE were that "(i) the expert system provided clear and unambiguous answers for each consultation and (ii) the expert system and the human expert provided the same answers for all ten cases (19 consultations) considered during the validation" [31].

A hypermedia version of CRISE, **CRISEBOOK** [30], is discussed in the Section 13.2.

Proposal two for integration of ESCA work; selectivity and chromatographic (or method) optimisation. Some of the workers on the ESCA project proposed an integrated system for just two of the domains: selectivity optimisation and chromatographic (or method) optimisation. They proposed to construct the system from three programs: CRISE (see above), Diamond and SOS [31].

Diamond was a package of conventional computer programs which required some expertise to use it. The most difficult decision that a Diamond user needed to make was the selection of the most appropriate optimisation criterion. In the integrated system this decision was to be made with the help of the expert system CRISE. Another expert system, SOS, was to be used to transform the chromatogram with optimum selectivity produced as a result of Diamond into the optimum overall method by establishing the best column conditions, instrumentation, injected amount, etc.

SOS (System Optimisation System) optimised separations in terms of (i) sufficient separation, (ii) sufficient sensitivity and (iii) shortest possible time [32].

To run the system, an initial chromatogram was needed, together with the relevant information of how it was recorded. The system used two databases, one describing the available columns, and the other the available detectors. (These were created once for a given laboratory, but could be modified at any time.) The system used this information to:-

- recommend the optimum column, detector cell, time constant, flow-rate and sample size.
- predict the required analysis time, the 'critical resolution' (that is the lowest value observed for the resolution between a relevant pair of peaks) and the pressure drop over the column.
- provide an explanation of its reasoning in the form of a bar chart and some additional advice to the user.

The optimum result was defined as:

1. The resolution for all relevant pairs of peaks had to exceed a minimum value specified by the user.
2. The signal-to-noise ratio for the smallest relevant peak had to exceed a minimum value specified by the user.
3. The required analysis time had to be as short as possible.

A prototype was implemented in Knowledge Craft [2] but the final system was implemented in Pascal. The developers described the conventional explain facilities provided by expert-system development tools such as Knowledge Craft as "generally not very helpful" [32]. Thus when SOS was reimplemented in Pascal [33] a new set of help and explain facilities was implemented. As a result bar charts could be used to establish which factors were limiting the speed of analysis, which factors caused a particular combination to be invalid and whether or not a major reduction in the analysis time was still feasible.

Proposal three for integration of ESCA work; method validation. The ESCA expert systems discussed so far have not dealt with method validation. A prototype for an integrated expert system for intralaboratory precision testing was implemented [34,35]. It integrated two expert systems described below, one for repeatability testing and the other for ruggedness testing. The architecture of the integrated system is described in Section 13.4.

The purpose of a precision test is to establish the random deviation from the mean in a certain analysis. Precision testing normally consists of repeatability and (interlaboratory) reproducibility tests. In the former, the same sample is analysed under the same conditions by the same analyst a number of times. In the latter, the same sample is tested in different laboratories to examine the precision of the method under slightly changing conditions. Since reproducibility tests involve more than one laboratory they are relatively costly; to reduce these costs a ruggedness test can be performed after the repeatability test but before the reproducibility test. Like a repeatability test, a ruggedness test can be performed in just one laboratory but the effects of using different laboratories are simulated; this detects some of the problems that would usually be discovered during the relatively costly reproducibility test.

The system was developed because method validation was becoming increasingly important as stricter rules were applied by regulatory authorities. Precision testing was a vital step in this validation. The system concentrated on precision tests that could be done in the laboratory where an LC method was developed. For most analysts

[2] Knowledge Craft is described in Section 13

in a routine laboratory, the performance of a precision test was not straightforward. The system was intended to given the analyst validating the method as much certainty as possible that the method would not fail in a collaborative interlaboratory test.

The expert system for repeatability testing was called REPS (REPeatability testing System) [36,37]. The expert system was used to select suitable test procedures for particular applications and to interpret their results. All the algorithms for the calculation of variance were set up in spreadsheets which could interact with the expert system. This is described in Section 13.3.

The system was reimplemented in Pascal in multiple windows environment [84]. This version worked as follows. It started by consulting a system optimisation module to provide the fastest analysis time within the required resolution. The method features to be tested were then defined as the sample preparation and the injection procedure. The user had to input a description of the HPLC method together with information on its expected usage. The system recommended an experimental design based on this input. The user then carried out the experiments and collected data which was input to the system. The system then diagnosed problems with the repeatability of the HPLC method. Each problem diagnosed had a list of actions that could be taken to try to solve the problem. The order in which the actions were presented to the user was such that those which were most likely to solve the problem appeared first.

The expert system for ruggedness testing was called RES (Ruggedness Expert System) [38–40]. RES comprised six modules that represented the major steps in the set-up and interpretation of the ruggedness test. The modules were controlled by a supervisor.

The Factor Choice Module. This selected the factors to be included in the ruggedness test and the factor levels. "Normally, some 50 factors may influence method performance in liquid chromatography. For every method, however, only a small group of factors is expected to be critical in that small changes can cause large effects." [41]. The relevant factors will be different for every chromatographic method. All the relevant factors must be tested but the number of experiments required increases dramatically with the number of factors. Thus the number of factors chosen by the system had to be minimal but sufficient.

The module was based on a rule based system [41]. The expert system approach yielded acceptable results to the problem: it had proved satisfactory for ten of the eleven cases of pharmaceutical formulations tested. This was in contrast to an algorithmic approach; "...the problem of factor choice is difficult to handle in normal programming languages because no algorithms are available, and they are difficult to design because of the many parameters involved and their complex interactions" [41]. The expert system could cope with the problem because the relations between the parameters were organised in frames, rules, handlers and demons [41].

The Design Selection Module. The module selected the experimental design from a set stored in the module. However the user could overrule the decision of the module and even add new designs to the system together with the rules for their selection.

After the user had consulted the factor and design selection modules the experimental design could be stored in a file for reference. The user then performed the experimental work and measured the necessary parameters.

The Statistical Results Module. This performed statistical calculations using algorithms.

The Chemical Results Module. This contained heuristic knowledge. The output from this module consisted of a set of warnings that had to be included in the final method description. The module decided whether one of the two repair modules (described below) should be activated.

The Reselect Factor Levels Module. This was a rule based module which modified the factor levels to a narrower range. The module produced a list of factors and levels that could serve as a *new* input to the design selection module to repeat the ruggedness testing procedure.

The Method Improvement Module. This was derived from SOS, which was described above.

During the validation of RES the factors chosen by an unbiased expert were compared with

those suggested by RES for 11 test cases. In all but one, RES performed satisfactorily.

Proposal four for integration of ESCA work: repeatability testing and troubleshooting. The fourth proposed integration combined REPS, SOS and three other modules which were built to add flexibility to the integrated system [21]. This allowed the user to consult the system in three different situations. It could be used to access the repeatability of a new method, to check the repeatability of a previously validated method and as a trouble-shooting tool. The latter "turned out to be a valuable feature" [21].

Conclusions arising from the ESCA project. Despite the publication of around 25 papers on the ESCA project, the implementation of over a dozen ESCA subsystems and no less than four proposals on how various parts of the ESCA work could be integrated there is no evidence in the literature to suggest that a single integrated system was implemented. Future projects to develop expert systems for chromatography which tackle domains as large as that covered by the ESCA project must be managed more effectively.

7.1.2. ECAT

Workers at Varian Associates in the USA developed ECAT (Expert Chromatographic Assistance Team) [42–44] ECAT was a collection of expert system programs intended to assist the inexperienced chromatographer in HPLC method development. The recommendations of the system were intended to lead the user logically through the entire method development process towards a workable HPLC separation.

ECAT comprised the following four modules connected to an inference engine:

Column and Mobile Phase. This received inputs about the analyte characteristics and made recommendations for the column packing, column geometry, mobile phase liquids and mobile phase modifiers. The module used heuristics which were represented by a set of rules. The module forward chained from the initial factual input about the analyte class(es), querying the user where necessary, in order to develop a more general identity for the class(es), or to conclude the existence of properties associated with the class(es). When the chain of inferencing was exhausted the module searched for key facts to determine which of its recommendations it was to output. The module then gave the user the option of changing some of the decisions that the module made when the rules were initially fired. If the user decided to change any decisions then the module redesigned the separation based on the alternative choice.

Sample Preparation. This helped the user to determine whether or not the sample required pre-treatment in order to enhance some quality of the separation. The module's knowledge base contained sets of rules and facts for determining whether a guard column was needed, and whether the analysis could be aided by solid-phase extraction techniques. A list of recommendations was delivered at the end of the session.

Method Optimisation. This led the user through a series of experiments in which the separation was optimised in both total time and acceptable resolution. This module was limited to a small set of rules which led the user to use a limited range algorithmic optimisation strategies.

Database of Chemical Properties. This contained factual information about specific chemicals and classes of chemicals.

7.1.3. ESC / ESLC

A chromatography expert system was developed by researchers at the Dalian Institute of Chemical Physics in China [45–48]. This system was named ESC (Expert System for Chromatography) in [45] but was referred to as ESLC (Expert System for Liquid Chromatography) in [47].

The strategy for the development of the system was to develop a knowledge and chromatogram base, an inference engine and a user interface. The chromatogram base could be searched by compound, analyte class or author. (The base included literature references for the chromatograms.) Thus the user could either enter the structure of the sample or the sample name or the name of the class to which the analyte belonged [45]. The chromatogram played an important role in that it not only provided a reliable

knowledge base for the system but it was also used to verify the results recommended by the system [47].

The system had five modules:

Separation Mode, Mobile Phase and Stationary Phase Selection.

Selection of the Sample Pretreatment and Detection Method.

Optimisation of the Operating Conditions.

Peak Identification. Four approaches for identifying peaks were considered, one was on-line and the other three were off- line.

Diagnosis of the Hardware System. This was developed because "almost all chromatographs do not possess self-diagnosis at the heart of the system, the column" [45]. It proposed a general strategy for hardware diagnosis involving comparison of the hardware to be used with standards. Any differences found resulted in rules being fired and a diagnosis being proposed.

7.2. Systems designed for one stage of the process only

This section describes those systems shown on Fig. 2 and is organised in a taxonomic fashion corresponding to Fig. 2. All the systems were designed for one stage of the chromatographic process only.

7.2.1. Method selection systems

Researchers at Virginia Tech in the USA developed ESP (Expert Separation Program) [49]. This was an expert system designed to aid the inexperienced analytical chemist in choosing a HPLC method. It did *not* suggest what conditions were required.

ESP began by conducting an interview to gather information on the separation problem. The program then attempted to reduce the number of possible candidate solutions by decomposing the separation problem into independent sub-problems. ESP was menu driven and incorporated how and why explanation facilities. The system's architecture is described in Section 13.4.

The validation of ESP showed that in nine out of 12 test cases ESP suggested a reasonable method [49].

7.2.2. Retention prediction systems

An expert system called CRIPES (Chromatographic Retention Index Prediction Expert System) was developed by researchers at Loughborough University [50,51].

The system used the molecular structure of an analyte to calculate retention indices from empirically derived quadratic expressions for the structural units. The program could also calculate the resolution of pairs of analytes.

During the validation stage the retention of a number of test compounds not previously examined were measured and compared with those calculated by CRIPES. "In many instances there was close agreement between the values, suggesting that generally the prediction method was satisfactory... The database does not yet include sufficient values for interaction between a wide range of substituents to permit a consistently high accuracy in the calculation of retention indices, although in most instances the predictions are within experimental error" [50].

7.2.3. Optimisation systems

Researchers from Bradford and Heriot-Watt Universities developed a system for eluent optimisation in reversed-phase HPLC [52–55]. The input to the system was spectral information from a multichannel diode array detector which provided retention information. This type of detector "provides an extra dimension of information from a single chromatogram... a three-dimensional spectrochromatogram is produced... in which the axes are time, *wavelength* and absorbance" [52].

The approach taken by the system was to perform a gradient elution experiment to determine the appropriate initial solvent strength, followed by response-surface modelling on the resulting spectral information using an iterative regression method to determine the mobile phase composition for optimum resolution.

The iterative regression approach relied upon the correct and unambiguous identification of each solute in each of the chromatograms. If this was not possible, perhaps due to co- elution of two or more peaks, the system then employed a modified Simplex procedure which makes no assumptions based on spectral data.

Peak homogeneity (the extent to which each peak corresponds to just one component of the sample) was assessed by a number of independent modules, the output from which was interpreted by the expert system and used to validate the response surface model constructed by the optimisation procedure.

The system required the column to be preselected, and an operator to prepare the mobile phase, operate the pumps and perform the injections; the developers stated their intention to automate these tasks in the future [52].

Researchers at Zhejiang University in China developed a system for optimisation of the mobile phase composition in reversed-phase HPLC [56].

Workers in Hungary produced an expert system for the prediction of initial HPLC conditions for selectivity optimisation in pharmaceutical analysis [57].

The input data corresponded to the structural formulas of the compounds of interest. Using this data and a database, the system calculated partition coefficients which were correlated with HPLC retention.

7.2.4. Troubleshooting systems

Three troubleshooting systems, HPLC-Doctor [5], CATHIE and PECOD, diagnosed problems with instrumentation whereas another, Upjohn's system, diagnosed problems with methods.

Workers at the Upjohn company in the USA produced a knowledge-based expert system for troubleshooting 21 of the HPLC assay methods frequently used in their laboratories [58]. The aim of the project was to construct an expert system that would advise an entry-level laboratory technician to diagnose problems in a HPLC system.

The problem solving approach of the system was as follows:

1. It gathered the symptoms and other relevant information from the user.
2. It derived the selectivity, capacity factor and resolution from the data.
3. It analysed the assay problem, obtaining more data if necessary.
4. It diagnosed the most probable causes and then ranked them. The results were shown to the user and justifications given.
5. In depth troubleshooting followed for the highly ranked causes in order to identify the cause of the problem.

Milne, from Intelligent Applications Limited in Livingston, produced an expert system called CATHIE [59] for the automatic interpretation of gas chromatographic data and for the provision of an expert analysis of the state of the instrument in order to detect possible failures or deteriorations.

Workers at Tsingham University in China developed a prototype diagnostic expert system called PECOD. "The domain-specific knowledge on the performance, design and operation of packed extraction columns was reviewed, structured and encoded" [60]. The knowledge was represented by combining a production system with conventional programs.

8. Systems specific to a particular class of compounds

This section describes those systems that are shown on Fig. 3 and is organised in a taxonomic fashion corresponding to it.

8.1. Metabolites

Two expert systems for metabolites were developed: SPES and HPLC-METABOLEXPERT. SPES [61] was an expert system for capillary gas chromatography analysis of human ester metabolites.

HPLC-METABOLEXPERT [62] was developed by researchers at the Hungarian Academy of Sciences and the CompuDrug company. The system became commercially available from CompuDrug. The system simultaneously predicted the metabolites of an organic compound and their retention data.

The system was developed because HPLC had acquired a major role in the identification of metabolites in medicinal chemistry which had been growing in importance. The identification procedure was complicated by the problem that compounds with unknown or incompletely known structures and retention times needed to be iden-

tified in a chromatogram that contained mainly the peaks of non-metabolites.

The user had to enter the parent compound via a graphical interface. The system then output a tree-like picture which represented the metabolic transformations. This was produced using a knowledge base of generalised metabolic transformations taken from a standard text.

To obtain the retention predictions the user had to input the chromatographic conditions and retention times of the parent compounds. On requesting the HPLC retention prediction for metabolites, the necessary mobile phase composition and predicted retention times were displayed together with a note about the necessary pH and detection wavelength changes. The prediction was based on the structural differences between the parent compound and the metabolites: the system used a database that contained the retention changes caused by a substituent of the molecule that appeared or disappeared in the physiological metabolic route.

The power of the expert system to predict retention was investigated by measuring synthetic mixtures of parent compounds and metabolites. The differences between the measured and predicted retention times was always less than 8 min and the average difference was 1.8 min.

8.2. Steroids

Two similar expert systems for planning separations of steroids by HPLC were designed by workers in Singapore and Australia [63,64].

The first system that was developed tried to select an appropriate separation system for a given number of compounds. The user had to input a list of compounds which she or he suspected to be present in the sample, and a list of compounds which had to be especially well separated. Candidate separations were created by:

1. establishing the characteristics of the sample, that is the compounds of interest and their polarity.
2. finding a stationary phase of similar polarity.
3. finding an eluent mixture of opposite polarity.
4. finding a compatible detector.

However, this strategy would have produced a large number of candidate solutions so the expert system imposed constraints. These constraints were determined from the list of compounds which had to be especially well separated and other additional queries made to user during the consultation. Candidate solutions that did not meet the constraints were ignored.

The system first searched for a case in the knowledge based in which some or all of the compounds of interest in the sample had been separated. If this failed it searched for a case where similar compounds or class of compounds had been separated. Finally if this failed then the system planned the separation from first principles.

The implementation described was limited to quite simple separations. However this limitation was due to insufficient information in the knowledge base rather than to deficiencies in the system structure or the approach to problem solving [63].

This system is referred to in this paper as the decision tree system for steroids, as explained in Section 12.1.2.

The other system for planning separations of steroids was designed to tackle the problem in the same way but using a different formalism to represent the knowledge. Section 12.1.2. explains why this was attempted and discusses the results. This system is referred to in this paper as the APN (Augmented Planning Network) system for steroids because it used ATNs. ATNs are discussed in Section 12.1.2.

8.3. Biological fluids

Workers at Glaxo have investigated the feasibility of building an expert system for method development in HPLC for bioanalysis, that is the analysis of drugs in biological fluids [66]. They developed a structured approach to method development in this area and they envisaged that the data resulting from it would be used to build the knowledge base for an expert system.

8.4. Proteins

Protein purification involves several stages from the extraction from the source to the final

purification with high-resolution chromatography techniques. Three expert systems for planning the purification of a protein were developed: PROTEIN, PPA and P8.

A prototype expert system called PROTEIN was developed at the University of Reading to assist in the preliminary selection of operations for the recovery and purification steps in the manufacture of proteins. The aim was "...to design large scale protein purification processes with a very high recovery, a virtually pure product and minimum cost Expert knowledge was obtained partially from the literature but mainly from industrial experts..." [67].

"The work showed that expert systems can be a helpful tool to assist in solving the knowledge intensive and heuristic based problem..." [67]. However the system could only amplify the effectiveness of an expert, it could not replace the expert.

Workers in Sweden developed a knowledge-based system called PPA (Protein Purification Advisor) for planning protein purifications [68].

PPA was developed because most researchers had been adopting a trial-and-error approach to protein purification "...without thought for improvement or optimisation of the method, leading to unpredictable and irreproducible results, and rapid exasperation" [68].

PPA was completely user driven in that the users told the system what they knew about the sample, the source material, and the protein they wanted to isolate, and then asked the system for a purification plan. The system then presented a plan. The idea of PPA was not to get a 'perfect' plan but rather to avoid making the most obvious and time consuming errors.

PPA was intended to support users with a varying degree of experience: it was designed to facilitate learning by graduate students and for senior researchers seeking a second opinion. Not only could the user request PPA to formulate a plan but he or she could also describe a complete or partial plan and ask PPA for comments. Further the user could ask for alternative plans and ask why or why not a certain operation had or had not been chosen.

PPA was validated by testing it with 20 different proteins selected by scientists. The resulting plans were discussed with the respective scientists. "In every case the plans were found to be acceptable with some minor variations" [68]. When compared to published procedures for the proteins the plans were found to be very similar.

Three of the people who worked on PPA also worked on P8. P8 was another system for planning protein purifications but P8 used a different planning technique to PPA and was designed for a different type of user.

P8 was a planner "...that planned and provided recommendations for the chromatographic stage of protein purification. The system was developed to meet the requirements for information and decision support among *workers in biochemical research laboratories*" [69]. P8 provided advice on which technique to use, the running conditions for each operation, and measurements to be taken between each purification step. The system was restricted to liquid chromatographic techniques and membrane-bound proteins.

P8 was primarily intended as a research prototype to explore knowledge representation and algorithms for protein purification planning. Thus only "...a limited effort was spent on the user interface" [69].

The techniques for protein purification affect the physical properties of a sample differently but a protein sample requires carefully controlled conditions. Thus a sample has to be adjusted between the steps of a purification but these adjustments need to be kept to a minimum. One of the aims was that P8 would design a plan that involved the minimal number of adjustments.

P8's knowledge base was structured around a set of partial plans. These were represented by a 'technique and decision-point tree', which covered different outcomes of operations in the plan. The knowledge in each decision-point was represented as a rule set. The nodes of the tree corresponded to purification techniques. P8 acted as follows:

1. P8 began by asking questions about the detergent, the amount of sample and protein stability. A rule base then determined what strategy to use. A strategy was essentially an ordering of partial plans.

2. For each partial plan purification techniques were selected, using the corresponding decision tree, until the user acknowledged that the target protein was sufficiently pure. For each purification technique that was selected :-
   (a) A check was made that the sample met the requirements for the technique. Constraint violations were passed on to a module which recommended the adjustments that were necessary before the technique could be employed.
   (b) The running conditions were then selected using a rule base.
   (c) The technique was then performed.
3. Once the target protein was sufficiently pure P8 halted.

Section 13.5 contrasts the two planning techniques of PPA and P8.

8.5. Pesticides

Researchers at the University of Missouri produced an knowledge-based system called PIA (Pesticide Identification Assistant) [70] designed to assist an analytical chemist with the identification of pesticide residues in food products using gas–liquid chromatography. [70]

The intention was that PIA would be able to identify approximately 300 different potential residues found in 234 different food items based on retention data, analysis information and heuristic rules based on food types. The analysis information was used to constrain possible identifications of a chromatographic peak. There was a possibility that a chromatographic response under investigation was due to a residue from outside the set of compounds that the system recognised. Therefore a definite identity could not be established and a variety of heuristic rules allowed the selection of the most probable identity from among the possibilities. Help functions were provided throughout the system. Explanations and suggestions were only available after the probable identification was made. [70]

PIA operated by using Prolog's inference engine directly to perform a number of searches [70]:

1. Prior to attempting residue identification, it performed a search based on the food item in question. This had the effect of gathering heuristics relevant to the sample type into working memory.
2. It tried to identify the residue(s) by:
   (a) searching for a single residue that could account for all the data.
   (b) searching for multiple residues, if no single residue could account for all the data, and finding a possible residue for each peak on the chromatogram.

   Rather than always performing a complete search of possible residues, the system first performed a search among only those residues previously identified in the sample food type, continuing on to a complete search only if the restricted search failed to generate an identification.
3. Finally it searched for information to use in explanations of results, and for suggestions for confirming analyses. However the system was incapable of expanding upon these suggestions or explaining why they were appropriate.

"Currently, eleven of the 234 food items are represented in the system, as well as 18 of the 300 possible compounds. Identification of items drawn from this initial sample is 100%. Obviously, such performance will degrade as the complete database of food items and compounds is incorporated into the system" [70].

8.6. Fossil fuels

Four of the expert systems for chromatography were limited to fossil fuels. Two of these tried to automate the interpretation of data from gas chromatography–mass spectrometry (GC–MS). This is a highly skilled, labour intensive task which is used to identify compounds in fossil fuels.

Researchers at the Georgia Institute of Technology and the University of Alabama, both in the USA, suggested design criteria for a GC–MS based expert system for arson analysis. Since petroleum distillates are "the overwhelming choice of the arsonist" [71] a system specific to this group of compounds was designed. "Ad-

vantage was taken of the high selectivity of mass spectrometry towards aliphatic and aromatic hydrocarbons" [71].

"In the USA about one out of five reported fires is of suspicious origin....The chemical analysis of residual accelerant is an integral part of most investigations into the origin and cause of a fire....The power of GC–MS in accelerant analysis has been demonstrated convincingly on real world samples." [71] The system was developed because of the limitations of human chromatogram interpretation. Data interpretation had almost always been carried out by pattern recognition of chromatograms. This had involved the analyst looking for groups of peaks that were characteristic for fuels commonly encountered. In many cases, chromatograms of suspect samples had been simply arranged side by side to chromatograms of standards. There are many human and technical limitations of chromatogram interpretation. For example it was obvious that factors such as retention time shifts or a mismatch of the chromatographic scale could have caused problems. [71]

Thus a system was designed which tried to automate the process. The system began by acquiring GC–MS data. It tried to categorise chromatographic profiles by establishing the presence of key components. Comparison was made to data from standards stored in the memory of the computer. Retention time information as well as spectral criteria was used. The system then printed a table giving extensive information about the presence or absence of the key compounds and denoting the accelerant standard which was the best match to the unknown sample. The system could then be instructed to print out ion chromatograms for the sample and simultaneously display the best match [71].

The researchers were aware that their system had limitations: "Chemical analysis of fire debris remains a challenging task. There is no substitute for human intuition and a machine will never replace a chemist. The program does fail on occasion for samples that produce overwhelming interferences or have other peculiarities....The program... is of significant help in routine analysis" [71].

Workers in the USA at the University of Houston and at the company Exxon developed an expert system for the interpretation of the GC–MS spectra of fossil fuel distillates.

Interpretation "...of GC–MS spectra is still very labour intensive, in particular for non-routine samples containing hundreds of components, such as fossil fuel distillates....Manual identification... requires a highly skilled professional and is extremely time consuming." [72] Even when a commercially available data system is used, identification "...has to be based on a large number of experienced based, inter-connected decisions, that include a detailed examination of the mass spectra, considering the relative order of elution and a very critical evaluation of the library response" [72].

The Exxon system used the commercially available identification capabilities but it extended them by defining limits of acceptability for the library identification yielded by those systems. These limits were based on *automatic* examination of the spectra, on retention time considerations and on the quality of the matching itself. The system was shown "...to be highly reliable in correctly identifying components in complex hydrocarbon streams, and doing so at a fraction of the time that would be required by a human expert" [72].

Two expert systems for diagnosing the insulation condition of power transformers were developed: TOGA [73] and a system from Xian Jiaotong University in China [74]. The latter worked from the measured chromatograph for the transformer oil. The insulation condition of power transformer was diagnosed as either normal, in need of checking and repair, or the system recommended that the diagnostic period needed shortening.

9. Systems specific to a particular chromatographic method

This section corresponds to the branch of the taxonomy which is entitled 'Specific to Chromatographic Method' on Fig. 1.

9.1. Systems for ion pair chromatography

Three expert systems were developed for ion pair chromatography. One suggested a suitable set of method conditions whereas the other two were mainly concerned with optimisation.

The expert system for suggesting a set of suitable method conditions was developed at the University of New South Wales for ion chromatographic methods using dynamically coated ion-interaction (also known as ion-pair) chromatography [75].

Ion-pair chromatography involves the use of apolar stationary phases with eluents containing a hydrophobic ion of opposite charge sign to that of the analyte ions, that is a counter ion. Two alternative methods exist: 'permanent coating' or 'dynamic coating'. The former requires that the column is first equated with the counter ion, which is then absent from the eluent during the analysis step. The latter uses an eluent containing the counter ion for both the column conditioning and analysis steps. The knowledge acquisition process for the expert system revealed that permanent coating represented less than 20% of ion-pair applications and it was therefore decided to concentrate on the dynamic coating procedure.

The actual rules for defining the method conditions were divided into four stages:

Selection of the method type. This part ascertained the class of ion to be analysed and selected a suitable preliminary method.

Selection of the column. The column was selected by examining the nature of the sample and its matrix.

Selection of the eluent. The eluent was determined chiefly by the class of ions for analysis.

Selection of the detector. The detector was chosen on the basis of the properties of the solute ions and the availability of detector types.

A report was shown to the user which summarised the chosen method conditions. On viewing this it was possible for the user to modify any answers and the system would produce new conclusions. Throughout the consultation help was available for each query that was made of the user.

The system allowed the user to change the conditions for activating some of the rules and the conclusion made by these rules. If any such modifications were made then the rule base was reconfigured to account for these changes. Thus the user could customise the system to include specific preferences.

Researchers in Brussels developed one of the two systems concerned mainly with optimisation [76]. The main purpose of the research was to explore how to introduce optimisation procedures into the expert system rather than to build a system for the domain. Thus only some basic drugs were considered, only one ion-pair reagent was investigated and the detector mode was limited to UV.

The system was based on LABEL. Like LABEL it gave advice on the detection and mobile phase but it also included an experimental design module. The systems comprised four modules:

Introductory Module. This checked whether ion pair chromatography was necessary and possible, and selected the detector settings.

First Guess Module. This advised on the mobile-phase conditions. It began by deciding whether a first guess was indeed possible. If the situation was too complex then it decided that an experimental design should be applied immediately.

Optimisation Module. This used an experimental design when an initial guess approach was likely to give unsatisfactory results, that is when more than one substance was present. A simple design was chosen because the aim of the expert system was not to establish the best optimisation method but to investigate the feasibility of integrating optimisation methods in to an expert system.

The user then tested the method and entered the results in to the system. The system evaluated the results and either advised that the method be used, advised that a good separation could not be obtained using the system selected or adapted the method by calling the fourth module.

Adaptation Module. The input to this module was the chromatographic results of the method proposed by the first guess or optimisation mod-

ules. The module either adapted the method or advised the user that a good separation could not be obtained using the system selected.

The system was validated by following the advice of the system for sixty synthetic mixtures created using a random number generator. "The rate of success was satisfactory" [76].

A rule based system was developed at Texas A&M University in the USA for the determination of solute types in unknown sample mixtures as a first step of selectivity optimisation parameter selection in reversed-phase ion-pair chromatography [77a].

This work illustrated that the nature of the solutes in totally unknown aqueous sample mixtures can be determined by the combination of an experimental procedure and a rule-based retention-shift evaluation strategy that is implemented in a computer program. The approach suggested did not require peak tracking or the use of any other extra-chromatographic information. Other expert systems for selectivity optimisation need extensive a priori chemical information about the sample components in order to make predictions about the expected retention behaviour.

The system comprised three parts:

Data Input. The user entered the retention times of all the peaks observed, together with the respective pH and pairing-ion information. The retention times and chromatograms could be entered in any order.

Type Evaluation. The program tried to label each peak as either SA, SB, WA, WB or N where N = neutral, S = strong, W = Weak, A = acid, and B = base. The retention data of all peaks from all the chromatograms were compared. (At least two chromatograms were required.) Initially all five possible solute types were assigned to all peaks in all chromatograms. Then, recursively using the retention-shift rule set, the program eliminated the impossible solute-type designations for all the peaks.

List Results. The solute-type assignments were then displayed to the user. The user could request the list of rules (and their hierarchical sequence) which were used in the solute- type assignment process, for each individual peak.

When tested with a variety of complex samples, the program correctly identified the type of the first and last eluting peaks and excluded the impossible solute-type designations for the rest of the peaks.

9.2. System for thin-layer chromatography

A system was developed for the identification and separation of samples by thin-layer chromatography (TLC) [77b]. The system was based on an extensive database of pharmaceutical compounds which could be modified by the user. The system was useful for TLC screening and for selecting a TLC separation system for a given sample [7].

10. Synopsis of behaviour and users

Table 1 compares the predominant behaviour of expert systems for chromatography [3] and the types of user for which they were intended. It indicates that only three out of the 18 systems were targeted at users who were novices in the particular domain of each of the systems. Thus most expert systems for chromatography were designed for scientists with some experience of chromatography. The table also shows that the systems exhibit four predominant behaviours: just over a third of them (7 of 18) plan the whole or part of a chromatographic separation, whist the remainder either predict the values of experimental data, diagnose problems or identify sample components.

11. How the knowledge was acquired for the systems

The process of acquiring the knowledge needed for an expert system is called knowledge acquisi-

[3] The systems that were designed for several stages of the chromatographic process (ESCA, ECAT and ESC/ESLC) are not included because they do not have a predominant behaviour: they comprise several subsystems which behave differently.

tion. The knowledge acquisition process is usually divided into three stages: deciding what knowledge is needed, variously referred to as the definition stage or initial analysis; getting knowledge, predominantly from human experts, and interpreting it, usually called elicitation; and 'writing' the knowledge in the internal language of the system, encoding it, usually called representation. Knowledge acquisition is a notoriously slow process and has become known as the 'bottle-neck' in the process of developing expert systems. [78]. It has accounted for a significant proportion of the total work involved in developing expert systems for chromatography. For example the knowledge acquisition phase for the PPA project required approximately six person-months of expert time and in terms of calendar time the project required one year. Future developers of expert systems for chromatography should allow for the knowledge acquisition 'bottle-neck' when planning their projects.

11.1. Sources of expertise and knowledge

Some of the systems relied on the literature as the main source of expertise. This was the case for the expert system for planning separations of steroids that was implemented as a decision tree; the rules were induced from specific examples of validated results of successful separations reported in the literature. Examples of how the expert system should behave were taken and then generalised to a higher-level rule that could guide the inference procedure [63]. ESP used rules drawn from a standard text book [49].

However, the knowledge and expertise for most of the systems was acquired with the help of one or more experts. For example the sources of expertise for the PPA system were specialists on individual separation techniques and researchers on particular classes of proteins [68]. The structure of the knowledge for ECAT was "determined through informal interviewing of experts, and by accumulation of ideas and experience from chromatographers through the literature" [75].

One of the problems of working with experts is that they are usually busy people with little spare time to devote to the development of an expert system. The developers of some of the systems found ways of minimising this problem. For example the researchers, based in New South Wales, that developed the expert system for ion chromatographic methods using dynamically coated

Table 1
Behaviour and users of expert systems for chromatography

Name of expert system	Predominant behaviour				Intended users		
	Plans	Predicts	Diagnoses	Identifies	Experts	Novices	Unspecified
Arson Analysis				Y	Y		
Brussels Method, Conditions and Optimisation	Y						Y
CATHIE			Y				Y
CRIPES		Y					Y
ESP	Y					Y	
Exxon				Y			Y
Hungarian, Selectivity Optimisation		Y			Y		
HPLC METABOL EXPERT		Y					Y
New South Wales, Method Conditions	Y						Y
PECOD			Y				Y
PIA				Y	Y		
PPA	Y				Y	Y	
PROTEIN	Y				Y		
P8	Y				Y		
Power Transformer			Y				Y
Solute Type				Y			Y
Upjohn			Y			Y	
Steroid Systems	Y						Y

ion-pair chromatography [75] developed their system from an extensive database of previously published ion chromatography methods. "The database was searched systematically to find the most commonly used method conditions for different applications. These conditions were then examined by the expert and rules generated for the expert system... This method considerably reduced the amount of time required from the expert but still resulted in the development of a competent expert system." [75]

When help is sought from experts for an expert system project it is important that the most suitable experts are chosen. For a company project this may involve deciding whether to use experts from within the company or from outside. Such a decision was made by the developers of the Upjohn troubleshooting system. The sources of the expertise for the Upjohn troubleshooting system were publications and chromatographic experts in the Pharmaceutical Quality Control Division of the Upjohn company [58]; since the system was to be an 'in-house' system, 'in-house' expertise was adequate.

Using more than one expert in a project can lead to problems. Experts may disagree or use different approaches. For some of the systems the number of experts involved was deliberately limited to one. The developers of CRISE stressed the importance of consistency in the knowledge. They achieved this for CRISE by obtaining almost all the knowledge from a single expert. Knowledge from another source was included in the *periphery* of the system. [29] In the ESCA project four experts separately contributed knowledge for each of the four subdomains. "Although more than one expert could have contributed to a domain, it was decided to avoid any discussion between experts" [18].

Thus previous experience suggests that developers of expert systems for chromatography must carefully consider the number and choice of experts to be consulted, and decide whether 'in-house' or external expertise is to be sought.

11.2. Elicitation techniques employed

For many of the systems the literature does not describe which elicitation techniques were used. However interviewing was used for the majority of those for which the techniques used are described. For a few systems other techniques were employed but they were not described in any detail. For example the knowledge elicitation for the ESCA DASH system was mainly done by interview but other techniques were also used. However they were only described in the vague statement "Sometimes information was exchanged in written form" [79].

The literature on knowledge engineering describes in detail a wide range of techniques for knowledge elicitation that can supplement or replace interviewing [78,80] and gives advice on how and when a given technique should be employed. However the literature on expert systems for chromatography does not mention any of these techniques. Despite the emphasis placed on the techniques by the literature on knowledge elicitation there is no evidence that developers of expert systems for chromatography have used them, considered but rejected using them or were aware of them. Future developers of expert systems for chromatography should consider using the various techniques and describe and justify their choice of technique(s) in any published work.

11.3. Machine induction and neural networks

There is an alternative to the developer of an expert system trying to elicit the expertise from an expert; a computer can be programmed to develop the expertise. This can involve a computer being trained to develop a set of rules or a neural network.

Rule Induction. Rule induction involves a computer system being provided with a number of cases and the system using inductive techniques to create its own rules from the cases.

Neural Networks. A neural network comprises a layer of input elements connected to one or more hidden layers of elements, the last of which is connected to a layer of output elements. Data from the input layer are transmitted through the hidden layer(s) to the output layer in a manner determined by the strengths of the connections between elements. Training modifies the connection strengths, and it is the set of their values in

the trained network which represents the relationship between the input and the output.

There are no reports in the literature to suggest that induction was considered as a method for acquiring the expertise for any of the expert systems for chromatography that have been implemented.

In the conclusion of the paper on the expert system developed in New South Wales for ion chromatographic methods using dynamically coated ion-pair chromatography [75] the authors stated their intention to investigate the potential of neural networks and the Quinlan rule generating system [81] for knowledge acquisition. They proposed to compile rule bases for the ion exclusion and ion exchange methods of chromatography and stated their belief that since these methods are used more frequently the task of manually performing a statistical analysis on a database of literature methods, as was done for the ion pair mechanism, would be extremely difficult due to the large amount of data.

12. The knowledge representations adopted

12.1. Formalisms for knowledge representation

The literature on knowledge representation describes a number of formalisms that can be used such as productions rules, frames, semantic nets and the predicate calculus [14,82]. Ref. [3] includes lucid examples showing how all four formalisms can be used to represent chemical knowledge.

Nearly all the expert systems for chromatography used rules. Despite the emphasis placed on the alternatives to purely rule based systems by the literature on knowledge engineering [12,14] there is no evidence that developers of the rule based systems for chromatography considered using them or were aware of them. Future developers of expert systems for chromatography should consider using the various formalisms and describe and justify their choice of formalism(s) in any published work.

The following sections discuss those few systems which did use other formalisms.

12.1.1. Frames

Frames [83] "...as data structures for storing expectations about typical objects and events have become quite widespread in artificial intelligence applications", p. 169 of [12]. The "...additional structure which can be represented or imposed by frames has considerable value. One demonstration of this is the reconstruction of knowledge bases originally expressed in unstructured production rules into frame systems and the consequent improvement in system understanding and ease of maintenance....The use of frames to represent knowledge about structured domains or structured knowledge continues to increase in popularity...", p. 99 of [14]. Frames "...are mostly used in conjunction with other representations, such as production rules", p. 169 of [12].

It is therefore surprising that the use of the increasingly common combination of production rules and frames was only reported for a few of the expert systems for chromatography. The ESCA system for precision testing was one of these. The usual features of frames such as instantiation, inheritance and demons were used [36,37,41].

12.1.2. Augmented transition networks

The two systems for planning separations of steroids were designed to tackle the same problem in the same way but using different formalisms to represent the knowledge. The first represented a decision tree by a series of rules. The second used an augmented transition network (ATN) [4] and was developed to show that the ATN formalism was "...a more efficient structure for representing the knowledge base of the...system" [64]. However no evidence was presented that proved this. Furthermore the comparison of the ATN and rule formalisms ignored the possibility of using some of the main control strategies for rule based systems, such as allowing rules to be fired more than once, and using meta and context sensitive rules. These omissions render the work as irrelevant to the contemporary

[4] For a description of ATNs see [64].

debate as to which formalism is most efficient for knowledge representation. The work failed to prove that ATNs should be used for future expert systems for chromatography.

12.2. Uncertainty

Uncertainty exists whenever expert systems have to make non- categorical decisions. Uncertainty can be represented using probability theory, certainty factors, fuzzy logic and the Dempster-Shafer theory of evidence [12]. The literature mentions the representation of uncertainty in only a few of the systems. The Upjohn troubleshooting system developed by [58] was implemented in M.1 which is rule-based expert system software which deals with uncertainty by the use of MYCIN style certainty factors. The capability of M.1 in dealing with uncertainty was used to weigh evidence and thereby establish priority for efficient troubleshooting. PROTEIN used certainty factors as well. PIA handled uncertainty "...in an ad-hoc fashion, basically by noting any causes for uncertainty in working memory, assigning a subjective weight, and accumulating the weights associated with each proposed identification" [70]. The Pascal reimplementation of the ESCA REPS also incorporated weighting factors [84].

12.3. Representations not specific to expert systems

Some standard software development representations were used. Data flow diagrams and state transition diagrams were used for the ESCA REPS [36].

Flow charts were used in the development of ESC/ESLC [45,46]. In academic computer science circles flow charts are associated with poor implementation practice [85]. They "...are very limited in their capability for modularisation and structuring..." [86]. It is therefore surprising that flow charts were used in the late 1980s to design a computer program, especially one which was an expert system. Flow charts should not be used to design future expert systems.

13. The software tools and architectures used tools

This section lists the software tools and architectures used to implement expert systems for chromatography.

13.1. Software languages and expert system shells and tools

Table 2 shows which expert systems for chromatography used which languages [5] and the aspects of the each system for which a language was used. The table shows that those systems in which the coding was not in one language alone, the AI languages were mostly used for reasoning, and never for numerical processing, where as conventional languages were mostly used for numerical processing and never for reasoning. This reflects the strengths of the AI languages: they make it possible to represent knowledge quickly and conveniently p. 95 of [87] making it easier to code reasoning. The way in which the conventional languages were used also reflects one of their strengths: they usually provide better facilities than the AI languages for numerical processing.

The aim of Table 3 is to show which expert system shells and tools were used in the development of the systems [6].

13.2. Hypermedia

The developers of CRISEBOOK [30] discussed three problems with 'traditional' expert systems development software:

[5] Prolog and LISP are referred to as artificial intelligence (AI) languages. Third generation languages, such as BASIC, FORTRAN, C and Pascal, will be referred to as conventional languages.

[6] It does not try to review the shells and tools used or to classify them; they are presented in alphabetical order. No description of the shells and tools is given because of the differences between the various versions used for different chromatography systems.

Table 2
Languages used by expert systems for chromatography

Language	Systems that used Language	Used for whole system?	Aspects for which the language was used			
			Reasoning	Numerical processing	Interface	Data capture
Artifical intelligence languages						
Prolog	ESP	N	Y			
MicroProlog	Bradford Herriot Watt System	N	Y			
	Steroid Decision Tree System	Y				
TurboProlog	Exxon System	Y				
	PIA	Y				
	Solute type determination system	Y				
Common	ECAT	Y				
LISP	PPA	N			Y	
SCHEME LISP	ESC/ESLC	N	Y			
Conventional languages						
BASIC and FORTRAN	Brussels ion pair system	N		Y		
	LABEL	N		Y		
C	Chinese mobile phase system	Y				
	ESP	N			Y	
	RES	N		Y		
Lattice C	APN Steroid system	Y				
Pascal	SOS reimplementation	Y				
	REPS reimplementation	Y				
Turbo Pascal	Exxon System	Y				
Unspecified conventional language	Bradford Herriot Watt system	N		Y		Y
	ESC/ESLC	N		Y		

Table 3
Expert system tools and shells used by expert systems for chromatography

Name of tool	Supplier	Systems that used tool	Notes
Epitool	Epitec AB	PPA	Except interface
Expert Systems Environment (ESE)	IBM	PROTEIN	
Goldworks	Gold Hill Computers, Cambridge, MA, USA	REPS	First implementation only
		RES	Factor choice module only
Knowledge Craft	Carnegie Group, Pittsburgh, PA, USA	SOS	Prototype only
Knowledge Engineering System (KES)	Software Architecture and Engineering, Arlington, VA, USA	CRISE DASH LABEL Brussels ion pair system	
M.1	Cimflex-Teknowledge, Palo-Alto CA, USA	Upjohn system	
Nexpert Object	Neuron Data, Palo Alto, CA, USA	SOS	An attempt was made to use it for the reimplementation
Personal Consultant Plus: PC Plus	Texas Instruments	PROTEIN	
Xi-Plus	Expertech, UK	S. Wales method conditions system	
VP-Expert	Paperback Software	CRIPES	

1. Updating and maintaining systems based on this type of software is difficult. "With the conventional present shells it is difficult for the user to make changes owing to the way rules are connected... Adding or changing rules could have repercussions all over the system." [30]
2. To use some of this software requires advanced skills of knowledge engineering.
3. Systems based on this type of software often have a poor user interface.

The developers of CRISEBOOK investigated whether Hypermedia could be used as an alternative to conventional expert systems development software. "Hypermedia is the combination of multimedia and hypertext. In a hypertext document the user does not have to read all information in a sequential way, but is guided by his needs and interests by pieces of information that are linked to each other. Multimedia is a collection of tools producing graphics, sound, and animation, to present data in a more flexible way." [30].

The work on CRISEBOOK did not show whether Hypermedia would make update and maintenance of expert systems easier. The work was inconclusive as to whether advanced skills would be needed to build expert systems with Hypermedia, although the developers of CRISEBOOK reported that the 'scripts' that are developed for Hypermedia are "...entirely readable even for those unfamiliar with programming." [30] CRISEBOOK suggested that Hypermedia would enable better interfaces to be produced because data can be presented in a more flexible manner and because much of the programming associated with interfaces is already present in Hypermedia.

Problems with expert system development software cannot be considered independently. Changing the development software to ease one problem may affect the severity of others or even create new ones. Although CRISEBOOK showed that Hypermedia could help to ease two of the aforementioned problems, it did not prove that Hypermedia would be a better alternative *overall* to 'traditional' expert systems development software.

13.3. Spreadsheets

Two systems were developed by combining expert systems development software and spreadsheets packages.

In REPS spreadsheets were programmed to produce the necessary statistics. The spreadsheet package used was Lotus 1-2-3 (1986) (Lotus Development Co., Cambridge, MA); the expert system tool used, Goldworks, was able to communicate with this. Rules, defined using Goldworks, set up spreadsheets into which the analyst input data, and the rules then interpreted the data processed in the spreadsheet [36].

In CRIPES VP-Exert communicated with spreadsheets written in VP-Planner (Paperback Software) [50].

13.4. Architectures

It was vital for the proposed integration of the ESCA repeatability and ruggedness systems that all the modules of the integrated system used the same concepts as the basis for reasoning so that flexible communication was possible. Simple transfer of files between modules would have been insufficient for two reasons [34]:

1. Most of the facts produced by one module had to be available to all other modules.
2. The modules were not to be consulted in a standard sequence. Trying to implement all possible consultation sequences would have become unrealistically complex.

It was decided to merge all the existing concepts in one common data structure that formed the basis for all the systems. "The blackboard architecture was chosen [7] because it allows integration of modules which use different interfacing or problem solving techniques" [45].

"Blackboards are well known artificial intelligence techniques for the integration of expert systems" [34]. They allow several modules to

[7] The architecture used for the ESCA integrated system varied slightly from a traditional blackboard in that a supervisor module controlled when and which knowledge sources were to be activated.

communicate with each other via a common data structure, the blackboard. In a blackboard architecture "...the knowledge sources trigger themselves when the state of the blackboard is such that they can contribute to the solution of the problem....In an ideal situation several knowledge sources can be activated at the same time. The blackboard architecture offers the possibility for parallel processing." [34].

The ESCA integrated system did not utilise the possibility for parallel processing offered by a blackboard. In fact all but one of the expert systems were designed for serial processing. The exception was ESP [49] which was implemented as two concurrent processes. The interface, implemented in C, was a parent process and the 'intelligence' of the system, the Prolog code, was the child process. Calls to the UNIX operating system kernel allowed concurrent processes to execute, communicating through UNIX pipes.

13.5. Expert planners

Some of the systems can be thought of as planners. For example PPA was a planner that planned a purification process from the original source to the final product. Thus it was a deductive planner as opposed to a reactive planner. Reactive planners, such as P8, immediately respond (without much deduction) to input without forming a complete plan on how the goal should be reached. A deductive planner was developed because reactive planners are "faster but in many senses 'dumber' than deductive planners" [68]. A deductive planner had the advantage that it was possible to plan in advance and, where possible, optimise the plan, and the ability to deal with unanticipated purification tasks by reasoning from general rules. However the designers of the system were aware of the major drawback of deductive planners: they cannot provide dynamic responses to different outcomes of *applied* operations. P8 was designed as a reactive planner because reactive planners do not have this drawback. "Armed with a certain amount of knowledge...one can devise a separation plan in advance. The efficiency of the plan will depend on the actual outcome of the *individual* steps. When the results are known, one is better equipped to plan subsequent steps" [69].

14. Validation and evaluation

"The increasing application of expert systems in routine tasks, and the consequent gradual automation of knowledge intensive work, has led to a need for some kind of assurance of the quality of...", p. 174 of [88] the resulting systems. Hence expert systems need to be validated and evaluated.

14.1. How the systems were validated

Validation involves testing by the developers to estimate the faithfulness with which the expert knowledge has been captured. This involves asking questions such as the following. Does the system offer advice that is appropriate as judged by experts? Is the reasoning correct, consistent and complete? Are the explanations adequate? Do the test problems cover the domain?

Validation is an important stage in the development of an expert system. Unfortunately, due to the nature of expert systems, the standard principles and practices of software engineering for validation are not directly applicable. The workers on the ESCA project stressed this: "Expert systems can only be expected to be useful in practice if they are reliable. Conventional software products can be tested thoroughly through a number of standard procedures. However, for testing expert systems no standard procedures exist" [21].

The validation of only a minority of the expert systems was reported in the literature. For those systems for which a validation was reported one of three approaches was adopted:

(1) Advisory systems for planning were validated by comparing the advice given by the systems with the advice given by experts. For example RES was validated by using 11 test cases, each of which was a liquid chromatography method for the separation of a pharmaceutical sample. For each method an unbiased expert's factor choice was listed before the expert system

was consulted. The factors chosen by the expert and system were then compared.

A slight variation of this approach was used for PPA. Various domain experts were asked to pose problems for the expert system and then decide whether the resulting advice given by the system was acceptable. Twenty different proteins were selected by as many researchers. PPA was then run for each one to produce a plan for its purification. Each of the plans were then discussed with the respective scientist. [68]

(2) Advisory systems for novice users were validated by comparing the performance of the user with and without the help of the system. For example the designers of ESP suggested that "Future [8] validation could take place by asking two similar student groups to solve a set of representative separation problems with and without the aid of ESP" [49].

(3) Predictive expert systems were validated by comparing the results predicted by the systems with corresponding experimental results. To validate CRIPES the retention of a number of test compounds not previously examined were measured and compared with those calculated by CRIPES. The predictive power of HPLC-METABOLEXPERT was investigated for seven parent " molecules and their eight main metabolites by measuring their reversed-phase retention data using various reversed-phase columns and conditions" [62]. The measured and predicted retention data were then compared.

All three approaches involved using some metric of similarity to decide whether two sets of results were similar enough to allow the system to be judged a success. For example for RES the criterion for deciding whether or not a factor choice made by the expert system was acceptable was that the choices of the expert and expert system did not differ by more than two factors. The number of factors selected was allowed to differ only by one: the number of factors was important for the final acceptance of the system because the number had to be small but sufficient.

All the approaches to validation required that a set of tests was selected. The tests were selected in different ways:

Random sets. The tests for the validation of LABEL were randomly chosen. "Initially [9], 50 pharmaceutical formulations were selected at random from the Belgium Drug repertory 1987" [26].

Sets chosen by various experts. The set of tests for the validation of PPA was chosen by a number of domain experts.

Representative sets. The compounds selected from the literature for use in the validation of ESP (see above) were "...*representative* of cases covering the range of possible conclusions that ESP can arrive at" [49].

Sets including specific tests. For example the compounds used in the trials of CRIPES "...included some that were selected to test *specific aspects* of retention prediction" [50].

The 'random sets' and 'sets chosen by various experts' can considered as black box testing and the others can be viewed as clear (or white) box testing.

A notorious problem encountered when developing software is that when it is repaired, following the discovery of an error, the repair itself may introduce new, undetected, errors. This is particularly relevant for expert systems incorporating production rules where adding or changing rules can have repercussions all over the system. The developers of the ESCA expert systems were conscious of this when planning the validation of their systems. To ensure that changes to a knowledge base did not produce unexpected side effects, it was necessary to define a so-called regression test. The expert selected a number of test cases, representing a broad range of possible cases, that were solved by the expert system after each major revision. If the solutions to the test case did not remain the same it was assumed that

[8] The performance of ESP had been measured by a HPLC technician answering ESP's interview questions for a series of compounds from the literature. [49]

[9] Six of these were ignored because they contained compounds that could not be determined by UV or electrochemical detection. [26]

changes had been made that adversely affected previously evaluated knowledge [18]. "The limited nature of the regression test is of course no guarantee that unexpected results will not appear but the choice of a good regression test set will minimise the chance" [18].

14.2. How the systems were evaluated

Evaluation is an investigation of the extent to which the system is useful and acceptable to the users. It involves asking questions such as the following. Is the input and output convenient? Is the nature of the interaction appropriate? Is the system fast enough? Does it fit in with the normal work pattern? Does it threaten the user? Is it being used? Will it be used? Have the goals been achieved? Are there hidden costs?

Given that these questions are so fundamental it seems remarkable that for all but one of the expert systems for chromatography there were no reports in the literature to suggest that any attempt had been made to evaluate the systems. Unless the results of evaluations are published it is impossible for people who were not involved in the development of a system to know how effective a given system was. Future developers of expert systems for chromatography should evaluate their systems and publish the results.

Only the evaluation of the ESCA systems was reported in the literature. It involved testing the expert systems in practical situations in order to evaluate their performance in daily practice. Generally, these tests were performed by external evaluators [21]. An example of such an evaluation, for two of the ESCA subsystems DASH and DASH /, is described in [7]. The literature on the ESCA evaluations included some interesting comments on the process. For example the evaluators of REPS felt the measured performance was "...acceptable for this method, but were pleased to find that the system suggesting actions that could further improve the method. This is a typical advantage of expert systems over conventional software packages....The evaluation of this system proved extremely valuable as it resulted in several additions which enhanced the software considerably" [84].

The ESCA evaluations were carried out by different persons, ranging from experts in method development to students with little or no experience. During the evaluation phase of all the expert systems it became clear that the attitude towards expert systems is strongly dependent on the expertise level of the evaluator. The accessibility of the specialists' expertise was clearly appreciated by inexperienced users. Experienced users could appreciate the quality of advice given by the systems. However when the strategy implemented in a system did not agree with the expertise of experienced users they became dissatisfied with the system because their own experience, probably better adapted to their specific situation, was not considered by the system [21].

15. Conclusions

Expert systems for chromatography have been reviewed. Most are designed for scientists with some experience of chromatography. The predominant behaviour of each is either to plan the whole or part of a chromatographic separation, predict the values of experimental data, diagnose problems or identify sample components.

The domains of the systems vary in their coverage of:

- stages of the chromatographic process.
- compounds to be separated by the chromatograph.
- chromatographic methods.

Thus the systems cover a large number of different subdomains of chromatography. A taxonomy has been proposed that allows expert systems for chromatography to be classified and facilitates an understanding of their inter-relationship.

The literature suggests that the most successful expert systems for chromatography are those which tackle specific aspects of chromatography rather than those which tackle large parts of this domain. Expert system projects which tackle domains as large as that covered by the ESCA project must be managed effectively, particularly if the objective is to produce an integrated system.

Previous expert systems for chromatography show that spreadsheets can be embedded within expert systems for chromatography but fail to prove that Hypermedia is a better alternative *overall* to 'traditional' expert systems development software or that ATNs offer a formalism which is more efficient than rules for knowledge representation.

15.1. Conclusions on the engineering

There are a number of aspects of the software and knowledge engineering that were approached in a similar way for most of the expert systems for chromatography. From this emerges the following stereotypical portrayal of the engineering for a previous expert system for chromatography. The knowledge acquisition accounts for a significant proportion of the total work, and involves interviewing one or more experts. Rules are used to represent the knowledge and they are encoded using an artificial intelligence language or expert system shell or tool. The resulting system is validated but is not evaluated.

Despite the literature on knowledge engineering stressing the importance of evaluating systems and advocating a wide range of techniques for knowledge elicitation and a wide range of formalisms for knowledge representation, developers of expert systems for this 'real world' domain have not responded: nearly all of the developers use interviewing for elicitation and rules for representing knowledge and they do not evaluate their systems. Further research is needed to determine why because developers of expert systems for chromatography often do not justify their decisions on engineering matters in their published work.

15.2. Summary of main conclusions

A taxonomy has been proposed that allows present (and future) expert systems for chromatography to be classified and facilitates an understanding of their inter-relationship.

The literature suggests that many of the ideas advocated by knowledge engineers are not being used by developers of expert systems for chromatography.

Too often developers of expert systems for chromatography do not justify their decisions on engineering matters.

16. Recommendations

Future developers of expert systems for chromatography should:

(i) Either plan their projects so as to allow sufficient time for 'the bottle-neck' in the process of developing expert systems, the knowledge acquisition phase, or consider using other techniques such as neural networks or rule-induction to automatically acquire the expertise.

(ii) Carefully consider the number and choice of experts to be consulted, and decide whether 'in-house' or external expertise is to be sought.

(iii) Consider using the various techniques for knowledge elicitation and formalisms for knowledge representation; and justify their choice in any published work. At the very least they should consider the use of the increasingly common combination of production rules and frames and avoid out-dated formalisms such as flow charts.

(iv) Evaluate their systems, in addition to validating them, and publish the results. Unless the results of evaluations are published it is impossible for people who were not involved in the development of a system to know how effective a given system was.

Acknowledgments

The funding was provided by SERC, under the remit of the Total Technology programme, and by Zeneca Pharmaceuticals.

References

[1] V. Jakus, Collect. Czech. Chem. Commun., 57 (1992) 2413.

[2] T.P. Bridge, M.H. Wiliams and A.F. Fell, Chem. Br., November (1987) 1085.

[3] J. Klaessens and G. Kateman, Fresenius' Z. Anal. Chem., 326 (1987) 203
[4] A.P. Wade, S.R. Crouch and D. Betteridge, Trends Anal. Chem., 7 (1988) 358.
[5] S.A. Borman, Anal. Chem., 58 (1986) 1192.
[6] J.L. Glajch, LC–GC, 6 (1988) 30.
[7] T. Hamoir and D.L. Massart, Adv. Chromatogr., 33 (1993) 97.
[8] V.R. Meyer, Practical High-performance Liquid Chromatography, Wiley, New York, 1988.
[9] J.A. Jonsson, Chromatographic Theory and Basic Techniques, Dekker, New York 1987.
[10] A. Braithwaite and F.J. Smith, Chromatographic Methods, Chapman and Hall, London, 1985.
[11] C.F. Poole and S.A. Schuette, Contemporary Practice of Chromatography, Elsevier, Amsterdam, 1984.
[12] P. Jackson, Introduction to Expert Systems, Addison-Wesley, 2nd edn., 1990.
[13] A. Hart, Knowledge Acquisition for Expert Systems, Kogan Page, London, 1989.
[14] G.A. Ringland and D.A. Duce, Approaches to Knowledge Representation. An Introduction, Research Studies Press Ltd., Taunton, 1988.
[15] P. Harmon, R. Maus and W. Morrissey, Expert Systems. Tools and Applications, Wiley, New York, 1988.
[16] I. Dickinson, Laboratory Robotics and Automation, 4 (1993) 85.
[17] L.R. Snyder, J.W. Dolan and D.C. Lommen, J. Chromatogr., 485 (1989) 65.
[18] J.A. van Leeuwen, L.M.C. Buydens, B.G.M. Vandeginste and G. Kateman, Trends Anal. Chem., 9 (1990) 49.
[19] D. Goulder, T. Blaffert, A. Blokland, L. Buydens, A. Chhabra, A. Cleland, N. Dunand, H. Hindriks and G. Kateman, Chromatographia, 26 (1988) 273.
[20] M. Mulholland, N. Walker, J.A. van Leeuwen, L. Buydens, F. Maris, H. Hindriks and P.J. Schoenmakers, Mikrochim Acta [Wien], II (1991) 493.
[21] L. Buydens, P. Schoenmakers, F. Maris and H. Hindriks, Anal. Chim. Acta, 272 (1993) 41.
[22] T. Hamoir, M. De Smet, H. Pyrins, P. Conti, N.V. Driessche, D.L. Massart, F. Maris, H. Hindriks and P.J. Schoenmakers, J. Chromatogr., 589 (1992) 31.
[23] P. Conti, T. Hamoir, M. De Smet, H. Piryns, N.V. Driessche, F. Maris, H. Hindriks, P.J. Schoenmakers and D.L. Massart, Chemom. Intell. Lab. Syst., 11 (1991) 27.
[24] F. Maris, R. Hindriks, J. Vink, A. Peeters, N.V. Driessche and L. Massart, J. Chromatogr., 506 (1990) 211
[25] G. Musch, M.M. De Smet and D.L. Massart, J. Chromatogr., 348 (1985) 97.
[26] M. De Smet, A. Peeters, L. Buydens and D.L. Massart, J. Chromatogr., 457 (1988) 25.
[27] M. De Smet, G. Musch, A. Peeters, L. Buydens and D.L. Massart, J. Chromatogr., 485 (1989) 237.
[28] G. Musch and D.L. Massart, J. Chromatogr., 370 (1985) 1.
[29] A. Peeters, L. Buydens, D.L. Massart and P.J. Schoenmakers, Chromatographia, 26 (1988) 101.
[30] B. Bourguignon, P. Vankeerberghen and D.L. Massart, J. Chromatogr., 592 (1992) 51.
[31] P.J. Schoenmakers, A. Peeters and R.J. Lynch, J. Chromatogr., 506 (1990) 169.
[32] P.J. Schoenmakers, N. Dunand, A. Cleland, G. Musch and T. Blaffert, Chromatographia, 26 (1988) 37.
[33] P.J. Schoenmakers and N. Dunand, J. Chromatogr., 485 (1989) 219.
[34] J.A. van Leeuwen, L.M.C. Buydens, B.G.M. Vandeginste, G. Kateman and M. Mulholland, Anal. Chim. Acta, 235 (1990) 27.
[35] L.M.C. Buydens, J.A. van Leeuwen, M. Mulholland, B.G.M. Vandeginste and G. Kateman, Trends Anal. Chem., 9 (1990) 58.
[36] M. Mulholland, N. Dunand and A. Cleland, J. Chromatogr., 485 (1989) 283.
[37] M. Mulholland, J.A. van Leeuwen and B. Vandeginste, Anal. Chim. Acta, 223 (1989) 183.
[38] J.A. van Leeuwen, L.M.C. Buydens, B.G.M. Vandeginste, G. Kateman, G.P.J. Schoenmakers and M. Mulholland, Chemom. Intell. Lab. Syst., 10 (1991) 337.
[39] J.A. van Leeuwen, L.M.C. Buydens, B.G.M. Vandeginste, G. Kateman, P.J. Schoenmakers and M. Mulholland, Chemom. Intell. Lab. Syst., 11 (1991) 37.
[40] J.A. van Leeuwen, L.M.C. Buydens, B.G.M. Vandeginste, G. Kateman, P.J. Schoenmakers and M. Mulholland, Chemom. Intell. Lab. Syst., 11 (1991) 161.
[41] J.A. van Leeuwen, B.G.M. Vandeginste and G. Kateman. Anal. Chim. Acta, 228 (1990) 145.
[42] R. Bach, J. Karnicky and S. Abbot, in T.H. Pierce and B.A. Hohne (Eds.), Artificial Intelligence Applications in Chemistry, American Chemical Society, Washington, DC, 1986, p. 278.
[43] S.S. Williams, J.F. Karnicky, J. Excoffier and S.R. Abbot, J. Chromatogr., 485 (1989) 267.
[44] S.S. Williams, Trends Anal. Chem., 9 (1990) 63.
[45] P. Lu and H. Huang, J. Chromatogr., 452 (1988) 175.
[46] Z. Yukui, Z. Hanfa and L. Peichang, J. Chromatogr., 515 (1990) 13.
[47] N. Chen, X. Liang, Y. Zhang and P. Lu, Chinese Science Bulletin, 37 (1992) 1809.
[48] X. Liang, H. Huang, Y. Zhang and P. Lu, Chromatogram, (1990) 215.
[49] M.A. Tischler and E.A. Fox, Comput. Chem., 11 (1987) 235.
[50] R.M. Smith and C.M. Burr, J. Chromatogr., 485 (1989) 325.
[51] C.M. Burr and R.M. Smith, Anal. Proc. (London), 26 (1989) 24.
[52] T.P. Bridge, M.H. Williams and A.F. Fell, J. Liquid Chromatogr., 12 (1989) 23.
[53] T.P. Bridge, M.H. Williams and A.F. Fell, J. Chromatogr., 465 (1989) 59.
[54] T.P. Bridge, M.H. Williams, G.G.R. Seaton and A.F. Fell, Chromatographia, 24 (1987) 691.
[55] T.P. Bridge, M.H. Williams and A.F. Fell, J. Pharmaceut. Biomed. Anal., 6 (1988) 555.

[56] X. Wu, S. Hu, J. Hou and X. Xu, J. Chem. Eng. Chinese Universities, 5 (1991) 136.
[57] G. Szepesi and K. Valko, J. Chromatogr., 550 (1991) 87.
[58] K.M. Kiyoshi Tsuji Jenkins, J. Chromatogr., 485 (1989) 297.
[59] R. Milne, J. Chromatogr., 485 (1989) 341.
[60] X. Wen and W. Fei, Acta Petrolei Sinica (Petroleum Processing Section), 5 (1989) 85.
[61] P.B. Ayscough, S.J. Chinnick, R. Dybowski and P. Edwards, Chem. Ind. (London), 15 (1987) 515.
[62] K. Valko, G. Szabo, J. Rohricht, K. Jemnitz and F. Darvas, J. Chromatogr., 485 (1989) 349.
[63] H. Gunasingham, B. Srinivasan and A.L. Ananda, Anal. Chim. Acta, 182 (1986) 193.
[64] A.L. Ananda, S.M. Foo and H. Gunasingham, J. Chem. Inf. Comput. Sci., 28 (1988) 82.
[65] C.T. Mant, T.W. Lorne Burke, N.E. Zhou, J.M.R. Parker and R.S. Hodges, J. Chromatogr., 485 (1990) 365.
[66] J.C. Pearce, A. Churchill and A.C. Terry, Chemom. Intell. Lab. Syst.: Lab. Inf. Management, 17 (1992) 213.
[67] J.A. Asenjo, B. Byrne and L. Herrera, J. Biotechnol., 11 (1989) 275.
[68] H. Eriksson, K. Sandahl, G. Forslund and B. Osterlund, Chemom. Intel. Lab. Syst., 13 (1991) 173.
[69] H. Eriksson, K. Sandahl, J. Brewer and B. Osterlund, Chemom. Intell. Lab. Syst., 13 (1991) 185.
[70] P. Schneider and S.K. Graham, in H. Berghel, J. Talburt and D. Roach (Eds.), Proceedings of the 1990 Symposium on Applied Computing, p. 101.
[71] G. Holzer, W. Bertsch and Q.W. Zhang, Anal. Chim. Acta, 259 (1992) 225.
[72] T. Aczel, S.G. Colgrove and L. Le, ASTM Spec. Tech Publ., 1019 (Novel Tech. Fossil Fuel Mass Spectrometry), (1989) 159.
[73] C.E. Riese and J.D. Stuart, in T.H. Pierce and B.A. Hohne (Eds.), Artificial Intelligence Applications in Chemistry, American Chemical Society, Washington, DC, 1986, p. 18.
[74] Z. Yan, Y.Z. Wu and Y. Zhou, in Proceedings of the 3rd International Conference on Properties and Applications of Dielectric Materials, 1 (1991) 63.
[75] M. Mulholland, R. Haddad and D.B. Hibbert, J. Chromatogr., 602 (1992) 9.
[76] H. Yuzhu, G. Peeters, G. Musch and D.L. Massart, Anal. Chim. Acta, 223 (1989) 1.
[77] (a) A. Bartha and G. Vigh, J. Chromatogr., 485 (1989) 383; (b) H. Moll, Ph.D. thesis, University of Bern, 1991.
[78] D. Diaper, Knowledge Elicitation. Principles, Techniques and Applications, Ellis Horwood, Chichester, 1989.
[79] R. Hindriks, F. Maris, J. Vink, A. Peeters, M. De Smet, D.L. Massart and L. Buydens, J. Chromatogr., 485 (1989) 255.
[80] M. Meyer and J. Booker, Eliciting and Analysing Expert Judgement: A Practical Guide, Academic Press, London, 1991.
[81] J.R. Quinlan, in D. Michie (Ed.), Expert Systems in the Micro Electronic Age, Edinburgh University Press, Edinburgh, 1979.
[82] B. McGee, in [87], p. 69.
[83] M. Minsky, in P.H. Winston (Ed.), The Psychology of Computer Vision, McGraw-Hill, New York, 1975.
[84] M. Mulholland, N. Walker, F. Maris, H. Hindriks, L. Buydens, I. Blaffert and P.J. Schoenmakers, J. Chromatogr., 550 (1991) 257.
[85] A. Macro, Software Engineering. Concepts and Management, Prentice Hall, 1990.
[86] A. van Mayrhauser, Software Engineering. Methods and Management, Academic Press, London, 1990.
[87] M.F. McTear and T.J. Anderson (Eds.), Understanding Knowledge Engineering, Ellis Horwood, Chichester, 1990.
[88] E. Hollnagel, The Reliability of Expert Systems, Ellis Horwood, Chichester, 1987.

ELSEVIER

Analytica Chimica Acta 297 (1994) 349–368

ANALYTICA CHIMICA ACTA

Dioxetane chemiluminescence detection in liquid chromatography based on photosensitized on-line generation of singlet molecular oxygen; a thorough examination of experimental parameters and application to polychlorinated biphenyls

H.A.G. Niederländer, M.J. Nuijens, E.M. Dozy, C. Gooijer *, N.H. Velthorst

Department of General and Analytical Chemistry, Free University, De Boelelaan 1083, 1081 HV Amsterdam, Netherlands

Received 5 January 1994; revised manuscript received 6 May 1994

Abstract

Experimental parameters influencing sensitivity and selectivity in chemiluminescence detection based on photoinduced production of singlet molecular oxygen in liquid chromatography, an approach introduced in earlier papers, are extensively studied. Normal-phase liquid chromatography is applied in addition to reversed-phase chromatography, using polychlorinated biphenyls (PCBs) as analytes. The photochemical reactor parameters play the most important role. The chemiluminescence detector parameters are generally restrained by the required photochemical reactor conditions. An alternative, commercially available, reagent for addition of singlet molecular oxygen (i.e., ethyl vinyl ether) and a new photochemical reactor construction are introduced and compared to the former ones. The experiments show that the optimum conditions are strongly determined by the individual PCB concerned. Planar PCBs known for their high toxicity, such as the PCBs 77, 126 and 169 can be detected far more sensitively than the non-planar ones. The inherent selectivity of the method is shown for a herring oil sample, spiked with the above PCBs, utilizing normal-phase liquid chromatography with a pyrenyl column.

Keywords: Chemiluminescence; Liquid chromatography; Dioxetanes; On-line photochemical reaction; Photooxygenation; Polychlorinated biphenyls (PCBs); Singlet molecular oxygen

1. Introduction

Previously we have shown that dioxetane chemiluminescence (CL) detection based on photochemical on-line generation of singlet oxygen can be applied as a valuable method in column liquid chromatographic (CLC) systems [1,2], in line with the discussion presented by Shellum and Birks [3]. In our previous investigations the attention was primarily focused on model analytes in reversed-phase eluents. In the present paper a detailed investigation of the influence of various

* Corresponding author.

SSDI 0003-2670(94)00229-F

experimental parameters is presented, considering not only reversed-phase, but also normal-phase CLC conditions. Furthermore, the applicability of the technique to the analysis of polychlorinated biphenyls (PCBs) in a biological matrix will be discussed.

Photochemical on-line generation of singlet oxygen has been involved for CLC detection purposes before [4]; singlet oxygen was reacted with a substituted furan and the resulting change in UV absorption or fluorescence was monitored. Instead, in the present paper emphasis is on dioxetane CL detection.

Dioxetane CL detection based on photochemical generation of singlet oxygen is a detection method that comprises two consecutive chemical processes. Detection is realised by thermally induced decomposition of a substituted dioxetane giving electronically excited compounds, finally leading to chemiluminescence through energy transfer to and subsequent light emission of an added fluorophore (Scheme 1). The substituted dioxetane is produced in an earlier process, by addition of singlet oxygen, generated through photoinduced energy transfer to ground state molecular oxygen, to an addition reagent (Scheme 2). Obviously, the two processes are connected by the dioxetane. Only under the prerequisite that this dioxetane is thermally and chemically sufficiently stable (at room temperature in the solvents used), the two processes can be spatially separated in a CLC system and thus optimized separately. This condition holds for the dioxetane DEDO (3,4-diethoxy-1,2-dioxetane), that is produced from the singlet oxygen reagent chosen previously (1,2-diethoxyethene (DEE)) [1,2].

Below we will describe both processes in more detail. First the dioxetane CL will be discussed, a process that has been extensively studied before [1,2,5] and needs little extra optimization. Secondly, the role of the various experimental variables in the photochemical process will be examined. In our previous papers hardly any attention was paid to these parameters.

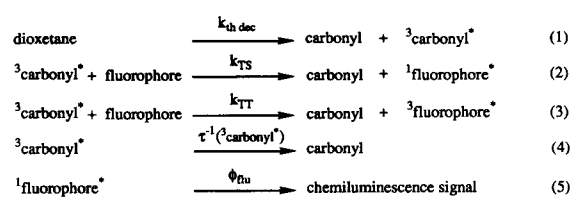

Scheme 1.

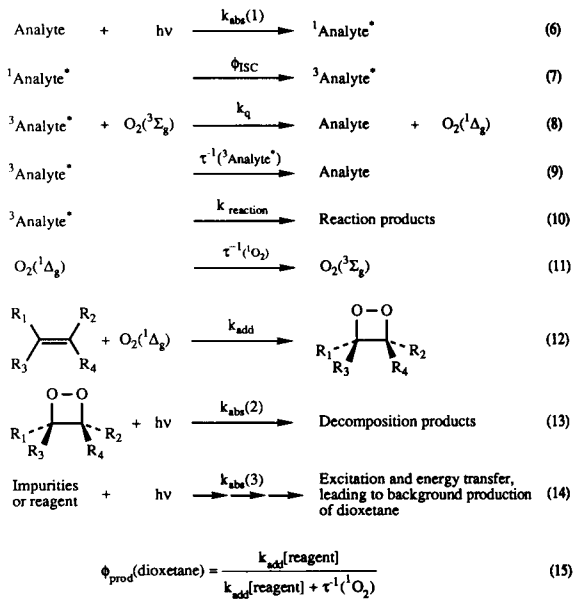

Scheme 2.

2. Theoretical aspects

2.1. Dioxetane CL

Thermally induced decomposition of the dioxetane leading to CL as described in Scheme 1 is the actual detection process. In the CLC system all reactions of Scheme 1 should take place inside the cell compartment of the CL detector, while the residence time is only about 2 s [2]. Therefore, the reactions of Scheme 1 have to be fast as well as efficient. This condition is only met for reaction (1) if the dioxetane is rather unstable, and/or if the temperature is high enough.

Raising the detector cell temperature to values higher than 70°C, a temperature previously applied [1,2], is generally not appropriate since boiling of the eluents and creation of gas bubbles in the detector cell should be prevented. Variation

of the dioxetane stability is therefore the only remaining parameter.

For DEDO, having a half life of about 60 s at 70°C [5,6], it can be calculated that only 2.3% of reaction (1) takes place within the cell compartment of the detector; its chemi-excitation efficiency is 100% [5] (giving one molecule of triplet excited ethylformate for each molecule of dioxetane decomposing). A dioxetane, with a ten times shorter half life at 70°C, would give a ten-fold increase of the percentage of CL within the cell compartment, provided that it would still be sufficiently stable at room temperature to allow spatial separation of the photochemical processes and the CL process. However the number of applicable dioxetanes is limited by the choice of the singlet oxygen reagent, which has to meet specific requirements. For this reason only dioxetanes bearing simple alkoxy substituents can be considered. It should be noted that dioxetanes with alkylamino- or dialkylamino substituents can not be used, since they are far too unstable at room temperature [6–8]. For most dioxetanes bearing alkoxy substituents there is generally little difference with the stability of DEDO [6,9–11]. Both *cis*-1,4,5,6-tetraoxabicyclo[4.2.0]octane (*p*-dioxene-dioxetane) and *cis*-1,3,4,5-tetraoxabicyclo[3.2.0]heptane (1,3-dioxole-dioxetane) are about equally stable as DEDO [10,11], while the stability of 3,3,4,4-tetramethoxy-1,2-dioxetane is even higher [10]. Decomposition activation parameters for 3-ethoxy-1,2-dioxetane (EDO), the product of singlet oxygen addition to ethyl vinyl ether (EVE), are not known. Based on sterical considerations [6,9], this dioxetane might be less stable than DEDO so that improvement of the CL yield in the detector cell might be attained. The CL yield is also determined by the chemi-excitation yield upon decomposition of the dioxetane, so that an overall improvement is only obtained if this is not significantly lower for EDO than for DEDO [5].

Instead of the thermally induced process, detection based on chemical triggering of dioxetane luminescence [12–15] might be considered. Since such an approach would impose many new conditions on the entire experimental system [16] it is outside the scope of the present paper.

Reactions (2) to (5) take place momentarily and do not influence the location of the CL emission. Since the reactions (2) and (5) finally lead to a CL signal, the highest signal is obtained if reaction (2) competes favourably with reactions (3) and (4), and reaction (5) with the radiationless decay of the fluorophore. The overall CL efficiency is the product of these two efficiencies. It is known from the literature that the highest k_{TS} rate constants for the spin forbidden reaction (2) are obtained for the fluorophore 9,10-dibromoanthracene (DBA) and its sulfonated analog, 9,10-dibromoanthracene-2-sulfonate (DBAS) [17,18]. Efficiencies of energy transfer to and fluorescence from these two compounds are almost identical [18]. The only significant difference between DBA and DBAS is their solubility [18], DBA being the fluorophore of choice in a normal-phase system and DBAS in a reversed-phase system.

To summarize this section it is concluded that only by applying a less stable dioxetane than DEDO some improvement might be expected for the CL process. Further optimization of the other variables governing the detection process opens little perspective.

2.2. Generation of singlet oxygen and production of dioxetane

More improvement can be expected from optimization of the photochemical processes, since detection limits in the CLC system are generally determined by background luminescence originating from dioxetane produced in side-reactions, rather than by inefficiencies of the CL process. An overview of the reactions that take place in the photochemical reactor is presented in Scheme 2. Apart from constructive dioxetane formation, there are also photoinduced reactions that do not contribute to the production of dioxetane, or even have a destructive effect on produced dioxetane. The highest sensitivity for a specific analyte is obtained if the constructive reaction pathways (reactions (6), (7), (8) and (12)) are efficient, whereas the non-constructive reactions (reactions (9) and (14)) and destructive pathways (reaction (13) and sometimes (10)) are absent, or at least

have a low efficiency. Reaction (10) is not necessarily destructive, since the reaction products may give efficient photoinduced production of singlet oxygen, thus indirectly contributing to the constructive production of dioxetane.

Below, the reaction pathways of Scheme 2 are related to experimental variables, that can be freely changed, revealing possibilities for optimization of the system.

The singlet oxygen reagent

Since addition of singlet oxygen to the substituted ethylenic compound, selectively giving a dioxetane product (reaction (12)), is in competition with the decay of singlet oxygen (reaction (11)), the efficiency for production of dioxetane is given by Eq. (15) (in the steady-state approximation). This equation implies that the efficiency is high if the inverse of the lifetime of singlet oxygen ($\tau^{-1}(^1O_2)$) is small compared to the product of the rate constant of reaction (12) and the reagent concentration (k_{add}[reagent]).

The lifetime of singlet oxygen in solution is determined by the solvent used [19] and ranges from about 1 μs in water to more than 1 ms in perfluorinated solvents [19]. In eluents utilized in CLC it is generally no longer than about 60 μs and can be as short as 1 μs, so that $\tau^{-1}(^1O_2)$ ranges from 1.7×10^4 to 1.0×10^6 s^{-1}. Thus efficient dioxetane production is realized if k_{add}[reagent] has at least the same value.

As has been outlined in preceding papers, for spectroscopic reasons the reagent has to be a simple substituted ethylenic compound and k_{add} will depend mainly on the number and the nature of the substituents [6,19]. The rate constant increases with the electron donating ability of the substituents and to some extend with their number. For DEE it is about 5×10^7 l mol^{-1} s^{-1} in polar solvents [6], so that concentrations in the order of 10^{-2} M are expected to give reasonable efficiencies of dioxetane production. For a reagent with a low reaction rate constant it follows from Eq. (15) that a high reagent concentration is required. Nevertheless, if such an inefficient reagent can be readily obtained in large amounts at a low cost its use might be preferred.

In this paper the commercially available reagent EVE will be applied as an alternative to DEE. For EVE, k_{add} is only about 3×10^4 l mol^{-1} s^{-1} in polar solvents [6], so that concentrations of more than 10 mol l^{-1} are expected to give similar efficiencies of dioxetane production as obtained with DEE. Reagents like *p*-dioxene and 1,3-dioxole (vide infra), having k_{add} values only about two and one decade lower than DEE respectively [11], are not commercially available. Furthermore, as they give dioxetanes with stabilities similar to DEDO [10,11] they are less appropriate.

Besides it should be noted that a high efficiency of dioxetane production does not necessarily imply a low detection limit, since the background luminescence is also proportional to this efficiency.

The irradiation window

Evidently, the photoinduced processes, reactions (6), (13) and (14), will only take place if the wavelengths of irradiation match the absorption spectrum of the compounds concerned, i.e., the analyte, the dioxetane, the reagent and possible impurities. The absorption spectrum of a simple dioxetane exhibits a maximum at short wavelengths, but extends to wavelengths as long as 380 nm [5,6]. As a result, only for analytes with an absorption spectrum extending to wavelengths longer than 380 nm, the constructive process initiated by reaction (6) can occur independent of the destructive process of reaction (13). In practice however various relevant analytes absorb at relatively short wavelengths. As a result, photoinduced dioxetane decomposition can generally not be avoided, but only minimized by masking the part of the spectrum of the excitation source that is not essential for excitation of the analytes.

Even after minimizing impurities present in solvents and reagents by thorough distillation, the background creating reaction (14) can occur and can only be reduced by irradiating at long wavelengths [20]. A more serious source of background arises if the singlet oxygen reagent itself, being present at a relatively high concentration, absorbs radiation. It is therefore crucial to select reagents like DEE and EVE which only absorb in

the deep UV. Reagents bearing large unsaturated substituents have absorption spectra extending over a wide range of wavelengths and are therefore excluded.

Irradiation time

Once an analyte has passed through the reactions (6), (7) and (8) it is restored in its ground state. The analyte can therefore complete this cycle many times if the irradiation time is sufficiently long, so that a chemical multiplication of the signal will be realized. Unfortunately the same holds for the background creating reaction (14) and, even more seriously, the destructive reaction (13). However, reaction (13) will only become important once a substantial amount of dioxetane has been produced. Thus, at a distinct irradiation time a balance between the production and the decomposition of the dioxetane will be reached. Since the production efficiency of the dioxetane depends on the analyte under consideration, the optimum irradiation time may differ from analyte to analyte.

Possible photochemical decomposition of the analyte, reaction (10), may enlarge this analyte influence. If the reaction products formed do not give rise to photoinduced generation of singlet oxygen, reaction (10) will only withdraw analyte from the constructive pathway, leading to an early balance between production and destruction and a low dioxetane concentration. On the contrary, if the reaction products do give rise to efficient sensitized generation of singlet oxygen, this may lead to a balance at relatively long irradiation times and a high dioxetane concentration.

Irradiation efficiency

The irradiation efficiency will influence the reactions (6), (13) and (14) in a similar way as the irradiation time. It is therefore expected that a more efficient irradiation will have the same effect as a longer irradiation time.

The irradiation efficiency can be raised by improving light collimation and by applying a more intense irradiation source. It should be noted that caution must be taken in comparing the results, if spectra of the irradiation sources are distinctly different.

The analyte

Obviously, also the analyte is a variable in the system under concern. In the present study the attention is confined to the class of polychlorinated biphenyls (PCBs). PCBs have been extensively used for a large number of purposes during the first half of this century. Their outstanding thermal stability, their resistance to oxidation as well as to many chemical agents and their excellent dielectric properties have made PCBs interesting compounds for use as dielectric fluids, hydraulic and other industrial fluids, fire retardants and plasticizers [21,22]. However it was not realised until 1966, when PCBs were first reported in environmental samples [23], that these lipophilic and toxic compounds had become a major environmental problem.

The photochemistry of PCBs has drawn considerable attention [21,24–28], in view of the possible environmental breakdown of PCBs by ultraviolet light in the solar spectrum. From these studies it is known that PCBs give efficient intersystem-crossing to the triplet state (close to 100%) [24,27], while their triplet characteristics [21,24] and photoinduced reactivity [21,24–26] are very diverse, depending on the number and localization of the chlorine substituents as well as the solvent used. It is appropriate to divide the PCBs into two main groups, differing with respect to the freedom of rotation around the central carbon–carbon bond connecting the two phenyl rings. The first group consists of PCBs bearing chlorine substituents on the 2,2',6, and/or 6' position, *ortho* to the central bond. Because of steric effects these PCBs can not easily adapt to a planar conformation and are therefore referred to as non-planar PCBs. Since the lowest excited electronic states (singlet as well as triplet) of biphenyls are preferably planar [29–31], the following characteristics can be readily conceived: the absorption spectra of non-planar PCBs are shifted to short wavelengths, the triplet state has a relatively short lifetime and the reactivity from the triplet state is high, as compared to PCBs that can adapt to a planar conformation (the second group, generally referred to as planar PCBs) [21,24–26].

The most toxic PCBs, i.e., PCB 77, 126 and

169 [32,33], are planar. Their concentrations in environmental samples however can be as much as three orders of magnitude lower as compared to the non-planar PCBs [33]. With the detection method under concern both the differences in absorption spectra and the differences in excited state characteristics might be useful to realize increased detectability of planar PCBs compared to non-planar PCBs. Taking into account that CLC systems for separation of planar PCBs from non-planar ones have recently been strongly improved [34], this may lead to extended significance of CLC separation with on-line detection of toxic PCBs, complementary to some commonly used techniques, LC clean-up followed by GC analysis [22,35,36].

3. Experimental

3.1. Equipment

For convenience, three aspects of the experimental set-up are described separately, viz., the chromatographic part, the photochemical reactor part and the CL detector part (see Fig. 1).

The chromatographic part

The chromatographic part is composed of a Model 300 solvent pump (Gynkotek, Munich), an analytical column and a laboratory-made six-port injection valve (Free University, Amsterdam), equipped with a 20-μl injection loop. Chromatograms are recorded on a Model BD12 recorder (Kipp and Zonen, Delft).

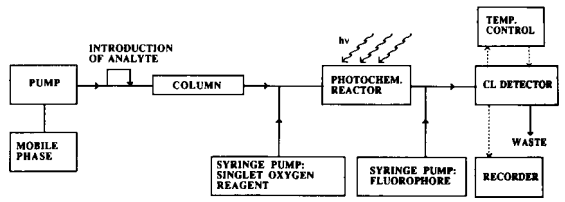

Fig. 1. Experimental set-up for photoinduced oxygenation of DEE with CL detection in a CLC system.

A laboratory-made analytical column (Free University, Amsterdam), 14 cm × 3.1 mm, packed with 5-μm RoSil C18HL particles (Alltech, Breda) is used if the system is operated with reversed-phase eluents and a Cosmosil PYE 5 analytical column (Nacalai Tesque, Kyoto, obtained from Promochem (Wesel)), 25 cm × 4.6 mm, packed with 5-μm particles containing a 2-(1-pyrenyl)ethyldimethylsilated stationary phase is applied if the system is operated with normal-phase eluents. The 20-μl injection loop is exchanged for a 100-μl injection loop for the analysis of the planar toxic PCBs 77, 126 and 169.

The photochemical reactor part

The original photochemical reactor [2] (photochemical reactor 1) consists of a Model 93110 (90-W, 25 mm arc length) medium-pressure mercury lamp (Philips, Eindhoven), mounted with a laboratory-made cylindrical quartz filter cuvette (9 mm path length) (Free University, Amsterdam).

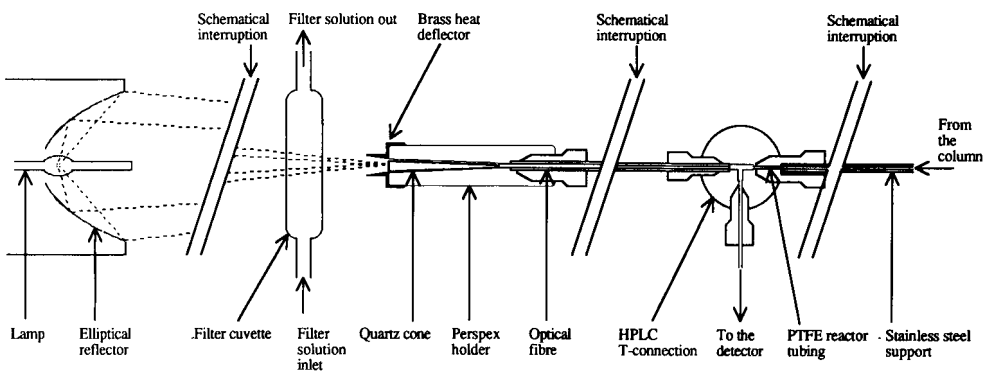

Fig. 2. Photochemical reactor 2. The real length of the total reactor, from the beginning of the reactor tubing (right side) to the front of the lamp housing (left side), on an optical rail is 65 to 85 cm depending on the length of reactor tubing used.

Filter solutions are pumped round, through the filter cuvette and a water cooler, with a Model 1022 centrifugal pump (Eheim, Berlin). The polytetrafluoroethylene (PTFE) reactor tubing (Eriks, Alkmaar), i.d. 0.33 mm, o.d. 0.73 mm, is knitted around the filter cuvette (diameter 5.7 cm), to reduce band broadening. The tubing is 1.0 to 10.0 m in length, providing reaction times ranging from 15 s to 2 min 33 s at flow rates of 0.34 to 0.59 ml min^{-1}.

The new photochemical reactor (Fig. 2) (photochemical reactor 2) consists of a Model USH-I02D (100 W, compact arc) high-pressure mercury lamp (USHIO, Tokyo), placed in a Model A1010 Arc Lamp Housing (Photon Technology International, Brunswick, NJ, obtained from Optilas (Alphen a/d Rijn)) equipped with an $f/4.5$ elliptical reflector. The focal point is located at about 280 mm from the front of the lamp housing and measures only about 3 mm in diameter. The lamp is focused onto a laboratory made quartz cone (length 30 mm, diameter 3.1 mm at the base and 0.61 mm at the top; top and base are polished) (Free University, Amsterdam), which is held axially on top of an optical fibre (core 0.8 mm), inside a perspex holder mounted with a brass heat shield. Light falling on the base of the quartz cone is forced into the optical fibre. The opposite end of the optical fibre is placed in a HPLC Valco T-connection, 1.0 mm core (Alltech). On the side opposing the optical fibre the PTFE reactor tubing (Eriks), i.d. 0.33 mm, o.d. 0.73 mm, is connected and held axially in line with the fibre by means of a stainless steel support. The tubing is 5.0 to 50 cm in length, providing reaction times ranging from 0.5 to 7.5 s at flow rates of 0.34 to 0.59 ml min^{-1}.

The singlet oxygen reagent, DEE or EVE, is added to the main flow, directly after the column (Fig. 1), with a Model 140A dual syringe solvent delivery system (Applied Biosystems, Ramsey, NJ) at a flow rate of 0.09 ml min^{-1}.

The CL detector part

The CL detector part consists of a Model 980 fluorescence detector (Applied Biosystems) with the lamp turned off and with a 25-μl detector cell installed. The stainless-steel bar containing the cell compartment is adapted with a thermocouple and a thermocoaxial electrical heater. The temperature is controlled with a laboratory-made electronic temperature programmer (Free University, Amsterdam) at 70.0 ± 0.1°C. Boiling and creation of bubbles inside the detector cell are avoided by operating the detector at about 4.5 bar backpressure.

For comparison with UV absorption detection, the CL detector is exchanged for a Model 20 UV–visible variable-wavelength detector (Carlo Erba, Milan).

The fluorophore, DBAS if the system is operated with reversed-phase eluents and DBA if the system is operated with normal-phase eluents, is added directly after the photochemical reactor (Fig. 1) with a laboratory-made syringe pump (Free University, Amsterdam) at a flow rate of 0.2 ml min^{-1}.

3.2. Chemicals and reagents

DEE (1,2-diethoxyethene) was prepared as described by Baganz et al. [37] and purified by double distillation prior to use. EVE (ethyl vinyl ether) was supplied by Merck (Darmstadt) and was purified by single distillation. Fresh solutions of these singlet oxygen reagents in acetonitrile, methanol or hexane, at optimized concentrations (vide supra), were made every two or three days.

DBA (9,10-dibromoanthracene) was purchased from Aldrich (Brussels) and used as obtained. DBAS (9,10-dibromanthracene-2-sulfonate, sodium salt) was prepared from DBA as described by Catalani et al. [18] and purified by recrystallization from water. Fresh solutions, 5.0×10^{-3} M in toluene (DBA) and 2.0×10^{-3} M in methanol (DBAS), were made every one or two months.

Anthracene and rose bengal were obtained from Aldrich. Crystalline PCBs 3, 10, 15, 52, 69 and the PCB mixture aroclor 1242 (IUPAC numbers according to Ballschmitter and Zell [38]) were purchased from Analabs (North Haven, CT) and Monsanto (St. Louis, MI) (PCB 3). Stock standard solutions were prepared (every 1 or 2 months) in eluent and stored at 4°C in the dark. PCBs 77, 122, 126 and 169, 99% purity dissolved

in cyclohexane, were obtained from Promochem (Wessel). Herring oil was supplied as a gift by the Swedish Environmental Protection Agency (Solna).

Acetonitrile and *n*-hexane were purchased from Westburg (Leusden) and methanol from J.T. Baker (Deventer); all solvents were LC grade. *n*-Hexane was distilled prior to use. Milli-Q water was prepared by ultrafiltration using a Milli-Q system (Millipore, Bedford, MA). Potassium iodide, sodium hydroxide, nickel sulfate, anhydrous sodium sulfate, acetic acid and sulfuric acid were supplied by J.T. Baker. Sulfuric acid was washed two times with 20 ml *n*-hexane before use. Silica gel 60 (70–230 mesh ASTM) was purchased from Merck and Alumina B super I from ICN Biomedicals (Eschwege). Silica and alumina were activated for 24 h at 140 and 200°C, respectively.

Filter solutions were made in deionized water. They will be referred to in the text as follows: $\lambda \geq 240$ nm is 40% (w/v) acetic acid and $\lambda \geq 260$ nm is 1.2% (w/v) potassium iodide in 0.5 M sodium hydroxide. In normal-phase, when the PYE column was used, 0.2 g l^{-1} DMADP (2,7-dimethyl-3,6-diazacyclohepta-2,6-diene perchlorate) and 50 g l^{-1} nickel sulfate were added to the filter solutions. These additives absorb radiation in the wavelength region from 290 to 410 nm. Shielding this part of the irradiation window is needed, since small amounts of a pyrene derivative bleeding off the column give rise to a high CL background, induced by absorption by the pyrene derivative in the indicated wavelength region. DMADP was synthesized according to Schwarzenbach and Lutz [39].

3.3. Procedures

Chromatographic conditions

Analyses were performed in an isocratic CLC system. The mobile phase, acetonitrile–water (80 + 20, v/v) in reversed-phase and *n*-hexane in normal-phase, is delivered at 0.25 ml min^{-1}. Only the analyses of the PCBs 77, 126 and 169 in herring oil were performed in normal-phase at a flow rate of 0.5 ml min^{-1} (combined with a doubled singlet oxygen reagent delivering flow rate and a doubled fluorophore delivering flow rate); the length of the PTFE reactor tubing was doubled too (5.0 m), giving an irradiation time of about 40 s.

Sample preparation

The herring oil sample was pretreated according to the procedure of Leonards et al. [33]. 0.5 g of herring oil was dissolved in 10 ml hexane. The mixture was shaken with 20 ml of concentrated sulfuric acid (70%). The organic layer was separated, concentrated to 2 ml under nitrogen and washed with 2 ml of distilled water. After drying over anhydrous sodium sulfate the organic layer was further concentrated to 0.5 ml. Subsequently this fraction was cleaned on a multi-layer column containing (from top to bottom): 1 cm anhydrous sodium sulfate, 5% water-deactivated basic alumina (2 g), 1 cm anhydrous sodium sulfate and 0.5% water-deactivated silica (3 g). The column was pre-eluted with 10 ml of *n*-hexane. Consecutively, the sample was placed on top of the column and eluted with *n*-hexane. The 8 to 25 ml fraction was collected, evaporated to 50 μl and finally injected in the LC system.

4. Results and discussion

Below the experimental variables outlined in the theoretical part will be evaluated. A distinction is made between variables concerning the CL detector and variables concerning the photochemical reactor. Subsequently the detection limits of some PCBs are compared and the application of the system to the analyses of toxic planar PCBs in herring oil is examined.

4.1. CL detector conditions

The only parameter to be varied (in the detector) is the dioxetane structure. Applying EVE as singlet oxygen reagent leads to EDO as the dioxetane giving CL in the detector cell. This dioxetane is less substituted and therefore expected to be less stable than DEDO [6,9], so that a larger percentage of the CL process will take place inside the detector cell. Thermal decomposition of EDO produces ethylformate and formalde-

hyde. One of these decomposition products can be generated in an excited electronic state. The chemi-excitation yield for this process however, which may or may not be significantly less favourable than for DEDO (approaching 100% [5]), will also have effect on the absolute CL intensity.

We have compared the overall efficiencies of DEDO and EDO for two model analytes (9-acetylanthracene and rose bengal). Photochemical reactor effects on the absolute CL signal intensity were eliminated as completely as possible. One irradiation filter (1 cm, 1.2% potassium iodide in 0.5 M NaOH) was used to shield the DEE and EVE absorption spectra completely from the lamp spectrum. Under these circumstances, since the absorption spectra of simple dioxetanes are alike [6], photodecomposition is expected to be similar for both DEDO and EDO. Both reagents were applied at a concentration giving an efficiency of singlet oxygen capture of at least 80% (1×10^{-2} M for DEE and 3×10^{-1} M for EVE (vide supra)). Furthermore, identical eluent compositions (acetonitrile–water, 90 + 10, v/v) were used.

The resulting CL peak intensities, for DEDO and EDO, are similar though not identical. Applying EVE (giving EDO) the CL signal intensity for 9-acetylanthracene is 5 times lower and for rose bengal 2 times lower, as compared to the signal intensities obtained applying DEE (giving DEDO).

The results indicate that the overall effect of the rate of dioxetane decomposition, the chemi-excitation efficiency and the energy transfer processes is in favour of DEDO. The difference however is sufficiently small to make EDO an interesting alternative in view of the fact that EVE is far more easily available.

4.2. Photochemical reactor conditions

The reagent

As outlined above, singlet oxygen reagents with a low k_{add} can be appropriate if they are applicable at sufficiently high concentrations. It should be realized that apart from structural effects of the reagent, the solvent may also have some influence on the reaction rate constant.

We have studied the singlet oxygen capture efficiency as a function of solvent and reagent concentration for DEE and EVE, which are closely related, but have nevertheless strongly different k_{add} values. For EVE in acetone k_{add} is over three orders of magnitude lower than for DEE [40].

The singlet oxygen capture efficiencies for DEE and EVE were monitored by measuring the

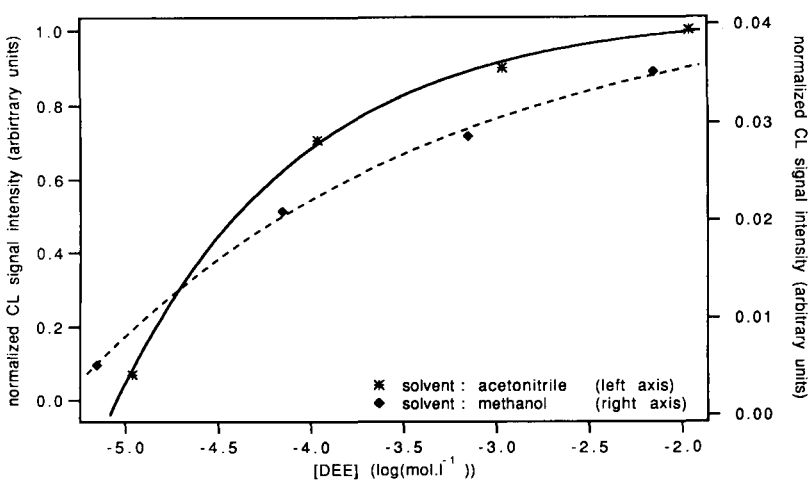

Fig. 3. Influence of singlet oxygen reagent concentration on the CL peak intensity for DEE in a reversed-phase system. The eluents are pure acetonitrile and pure methanol. The CL intensities are normalized to the situation applying DEE in acetonitrile.

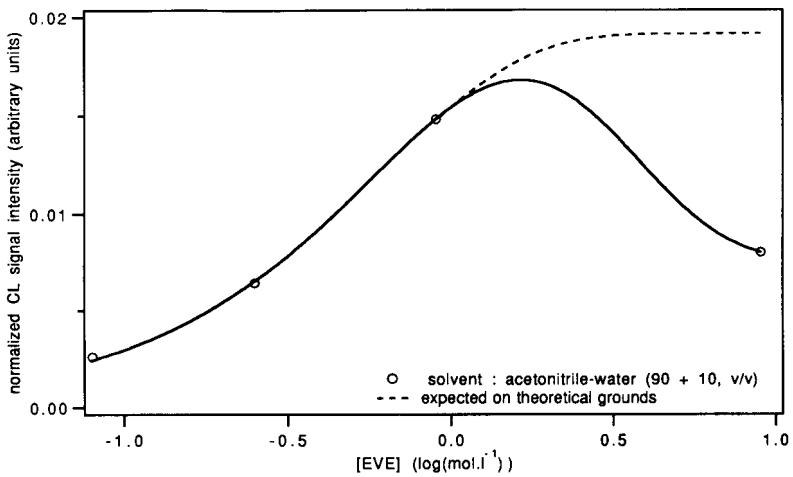

Fig. 4. Influence of singlet oxygen reagent concentration on the CL peak intensity for EVE in a reversed-phase system (acetonitrile–water, 90 + 10 (v/v)). The CL intensities are normalized to the situation applying DEE in acetonitrile.

relative CL peak intensities for injection of 10^{-7} M anthracene in the analytical system of Fig. 1, using different solvents and various reagent concentrations.

The results are visualized in Figs. 3–5. It is clear from Fig. 3 that for DEE in polar solvents (methanol and acetonitrile), the singlet oxygen capture efficiency does hardly increase for concentrations higher than 10^{-3} M. However the maximum CL peak intensities in acetonitrile and methanol differ considerably; in methanol it is about 25-fold lower. This is probably due to a difference in dioxetane stability in hydroxylic solvents as compared to non-hydroxylic solvents, as reported previously [2].

In view of its low k_{add}, for EVE in acetonitrile–water (90 + 10, v/v) the maximum efficiency would be expected at concentrations as high as 10 M (i.e., three orders of magnitude higher than for DEE in polar solvents). Indeed it can be seen from Fig. 4 that the relative peak intensity is rising with the EVE concentration.

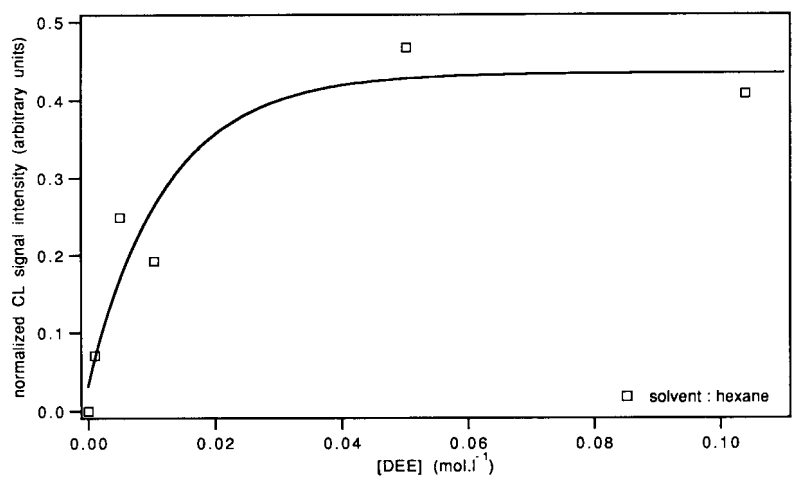

Fig. 5. Influence of singlet oxygen reagent concentration on the CL peak intensity for DEE in a normal-phase system (*n*-hexane). The CL intensities are normalized to the situation applying DEE in acetonitrile.

However, at concentrations higher than about 1 M the efficiency is decreasing again, presumably as a result of high concentration phenomena like aggregation. The absolute CL peak intensity is much lower than for DEE in acetonitrile, but compared to DEE in a hydroxylic solvent (methanol, Fig. 3) the difference is only about a factor two, which is in agreement with the relative CL signal intensities obtained for DEDO and EDO in acetonitrile–water (90 + 10, v/v).

In normal-phase (non-polar) solvents for DEE a clear decrease in singlet oxygen capture efficiency is seen (Fig. 5), compared to the situation in reversed-phase: the maximum efficiency is approached for DEE concentrations at about 5×10^{-2} M, more than ten times higher than required in reversed-phase solvents. The difference in absolute CL peak intensity, as compared to the situation using DEE in acetonitrile (both non-hydroxylic solvents), is relatively small (only a factor of about 0.5). For EVE in a normal-phase system the CL peak intensities are almost an order of magnitude lower than in reversed-phase; the influence of concentration was not studied.

It is concluded that, for reversed-phase systems, a reagent with a low reaction rate constant for addition of singlet oxygen used at a relatively high concentration, can still give effective singlet oxygen capture. In practice a 0.3 M EVE concentration was utilized, giving limits of detection close to those obtained for DEE.

The influence of the solvent is obvious: for both DEE and EVE k_{add} is higher in reversed-phase systems. In practice DEE was applied at a concentration of about 10^{-2} M in both reversed-phase and normal-phase solvents. Using higher concentrations in normal-phase does not give sufficient improvement (background level and noise also increase with enhanced singlet oxygen capture efficiency) in view of the extra costs associated with five to ten times more reagent consumption.

Irradiation window

The singlet oxygen reagent should not absorb radiation in the photochemical reactor (Scheme 2, reaction (14)), since this would give rise to generation of singlet oxygen, leading to autoxidation. The absorption spectra of DEE and EVE are shown in Fig. 6. It is clear that for EVE a wider part of the lamp spectrum is available for irradiation of analytes than for DEE. Especially the part of the spectrum between about 260 and 240 nm, available for EVE but not for DEE, might be of considerable importance to detect analytes absorbing exclusively in the deep UV. To mask the reagent absorption, a 4 M acetic acid irradiation filter was used in combination with

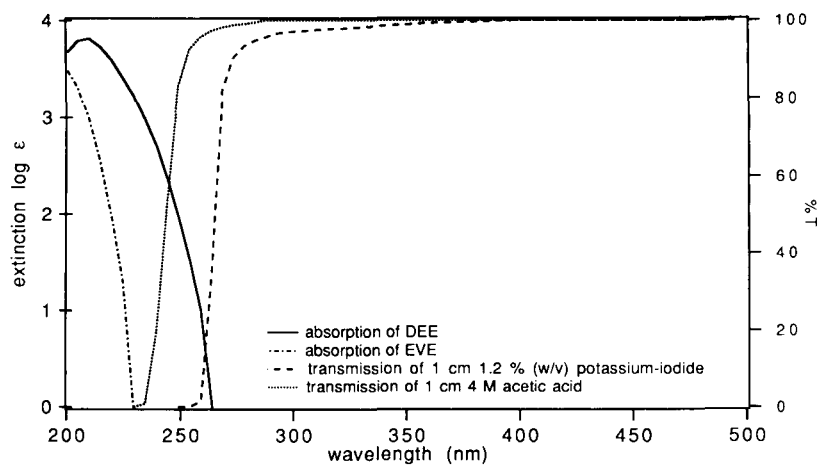

Fig. 6. Absorption spectrum of DEE and EVE and transmittance of the filter solutions (4 M acetic acid and 1.2% potassium iodide in 0.5 M NaOH) in the 9-mm cuvette.

EVE and a 1.2% (w/v) potassium iodide irradiation filter in combination with DEE (Fig. 6), unless specified otherwise.

For analytes, absorbing hardly any radiation at wavelengths longer than 260 nm, indeed some improvement in detectability is observed if EVE instead of DEE is used. However applying DEE with $\lambda \geq 240$ nm (acetic acid filter), thus allowing some auto-oxidation, also resulted in a better detectability for these analytes. For analytes, with an absorption spectrum clearly extending to wavelengths longer than 260 nm, short wavelength excitation is not appropriate; apparently photoinduced decomposition of the produced dioxetane (Scheme 2, reaction (13)) is enhanced more than photoinduced generation of singlet oxygen.

It is therefore concluded that the effect of changing the irradiation window is strongly analyte dependent.

Irradiation time

If only the analyte absorbs radiation (Scheme 2, reaction (6)) and no processes other than quenching of the analyte triplet by oxygen and addition of singlet oxygen to the reagent would occur, the CL signal would theoretically rise with irradiation time until the reagent has been completely consumed. In practice however the analyte will be subjected to photochemical reactions (Scheme 2, reaction (10)) and, as shown in a previous paper [20], the dioxetane to photoinduced decomposition (Scheme 2, reaction (13)). Apart from these photochemical aspects, band broadening (though minimized by knitting of the reactor) will have an effect on peak heights, if the residence time in the reactor is too long, especially for fast eluting compounds. As a result an optimum will be reached at a finite irradiation time.

Influence of irradiation time was studied for EVE and DEE in both normal-phase and reversed-phase, utilizing some PCBs. In normal-phase using DEE indeed the CL peak intensities rise with irradiation time until a maximum is reached. At prolonged irradiation the intensities decrease again. The irradiation time corresponding to the maximum depends on the individual PCB concerned. For the PCBs 3 and 15 (4-mono- and 4,4'-dichlorobiphenyl, respectively) the maximum is reached in about 50 s, whereas for the PCBs 10 and 69 (2,6-di- and 2,3',4,6-tetrachlorobiphenyl, respectively) it is observed after irradiation times about twice as long.

The differences between the individual PCBs are even more obvious for the signal-to-background ratio observed, since both the background and the signal are subjected to building-up and

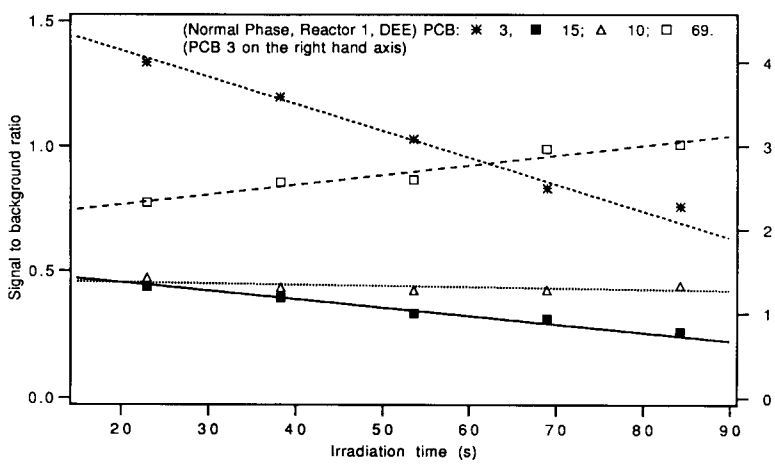

Fig. 7. Influence of irradiation time on signal to background ratio for four PCBs (1.0×10^{-6} M PCB 3, 1.0×10^{-7} M PCB 15, 1.0×10^{-5} M PCB 10 and 1.0×10^{-5} M PCB 69 injected) in a normal – phase system (mobile phase *n*-hexane), applying DEE as the singlet oxygen reagent.

decomposition of dioxetane. For this ratio the PCB reactivity is the only variable.

From Fig. 7 it can be seen that for DEE in normal-phase the signal-to-background ratios for the PCBs measured show different trends with increasing irradiation time. For PCB 69 it increases with irradiation time, whereas it is almost constant for PCB 10 and decreases for the PCBs 3 and 15.

A stronger distinction was obtained in a reversed-phase system applying DEE (Fig. 8). The curves for PCBs 3 and 15 slowly rise at short irradiation times, followed by a significant decline. The PCBs 10 and 69 on the other hand reveal continuously rising signal-to-background ratios.

It is noted that the PCBs 10 and 69 belong to the group of non-planar PCBs, whereas PCBs 3 and 15 are planar. Differences in signal-to-noise ratio as a function of irradiation time might therefore be correlated to differences in triplet state reactivities and lifetimes for these two groups.

In non-polar solvents (normal-phase, hexane) the major reaction pathway for PCBs from the excited triplet state is exchange of chlorine substituents for hydrogen of the solvent [24–26]. This exchange process can be more than an order of magnitude faster for non-planar PCBs than for planar PCBs [24]; exchange of the ortho chlorine substituents, releasing steric hindrance, is preferred [24]. In oxygenated solutions, as is the case in our system, these radical processes will also lead to radical chain oxygenation of the PCBs [24], finally giving rise to complete photobleaching. For the planar PCBs these routes lead to a situation where photoinduced generation of singlet oxygen does no longer occur. In contrast, for the non-planar PCBs, since exchange of *ortho*-chlorine substituents is preferred to exchange of the other chlorine substituents, in the first stage planar PCBs might be formed. As will be outlined below, the efficiencies for photoinduced generation of singlet oxygen are up to two orders of magnitude higher for planar PCBs than for the non-planar ones (see *Limits of detection*). This implies that if for instance only one percent of a non-planar PCB is converted into a planar one this may lead to a signal similar to the original signal of the non-planar PCB. Therefore it can be imagined that the signal-to-background ratio remains constant over a much longer irradiation time. Photoinduced loss of chlorine substituents might therefore explain the different behaviors of the PCBs 3 and 15 compared to the PCBs 10 and 69.

The photochemistry of PCBs in polar solvents, especially water, is more complicated [25,26].

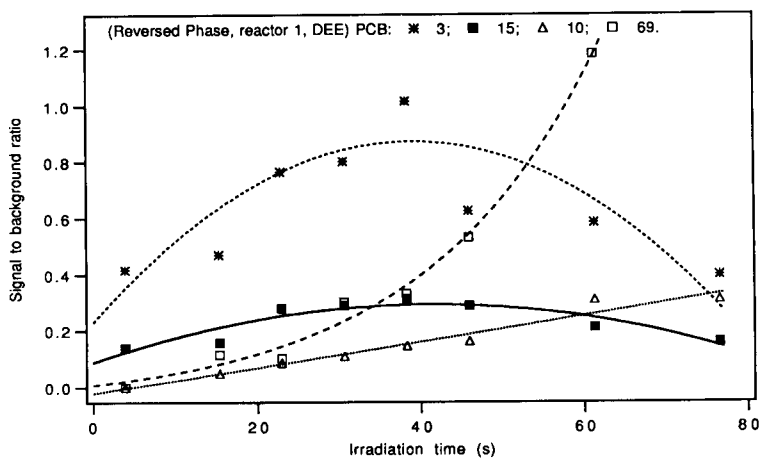

Fig. 8. Influence of irradiation time on signal to background ratio for four PCBs (1.0×10^{-6} M PCB 3, 1.0×10^{-7} M PCB 15, 1.0×10^{-5} M PCB 10 and 1.0×10^{-5} M PCB 69 injected) in a reversed-phase system (mobile phase acetonitrile–water (80 + 20, v/v)), applying DEE as the singlet oxygen reagent.

Again the non-planar PCBs react much faster than the planar PCBs, but the pathways can be completely different from those in non-polar solvents. In methanol the main route for reaction is still through homolytic cleavage of the carbon chlorine bonds [24], but in acetonitrile–water mixtures (or pure water) the reaction pathways are mainly heterolytic in nature [25,26]. Furthermore it is found that oxygen quenches the reaction, but does not give rise to significant oxidation of the PCBs [26], so that photobleaching of the PCBs will not be as fast as in non-polar solvents. The solvent composition in our system (reversed-phase, acetonitrile–water (80 + 20, v/v)) is closely related to that studied by Orvis et al. [26] and Moore and Pagni [25]. In these investigations mainly the formation of hydroxybiphenyls was observed. For non-planar PCBs this may lead to many secondary photoproducts with less sterically strained triplet excited states [41]. The influence of irradiation time on the signal-to-background ratio in reversed-phase for the PCBs 10 and 69 may therefore be explained by assuming fast photohydrolysis to products giving enhanced singlet oxygen sensitization, while photobleaching through oxygenation is not very fast. Photohydrolysis of the PCBs 3 and 15 will be relatively slow. This might explain why their signal-to-background ratios are not strongly influenced by the irradiation time.

In both solvent compositions examined above, DEE was applied. For EVE such a high reagent concentration is required that it might influence the photoinduced reactivity of the PCBs. The signal-to-background ratios as a function of irradiation time for EVE in the same reversed-phase system are shown in Fig. 9. From a comparison with Fig. 8 it is clear that only for PCB 15 the relation has changed significantly. The overall trend, a different dependence for non-planar and planar PCBs, is the same.

For another non-planar PCB, PCB 52 (2,2′,5,5′-tetrachlorobiphenyl), the effect of irradiation time on signal-to-background ratio was less conclusive. In reversed-phase (acetonitrile–water (80 + 20, v/v)) the signal-to-background ratio increases with irradiation time, like observed for the other non-planar PCBs. However, in normal-phase (*n*-hexane) it decreases with almost a factor of two as the irradiation time is prolongated from 20 to 90 s, a behaviour which is more similar to that of the planar PCBs.

It is concluded that in general there is a significant difference in photochemical reactivity between planar and non-planar PCBs. The behaviour of an individual PCB is not easily pre-

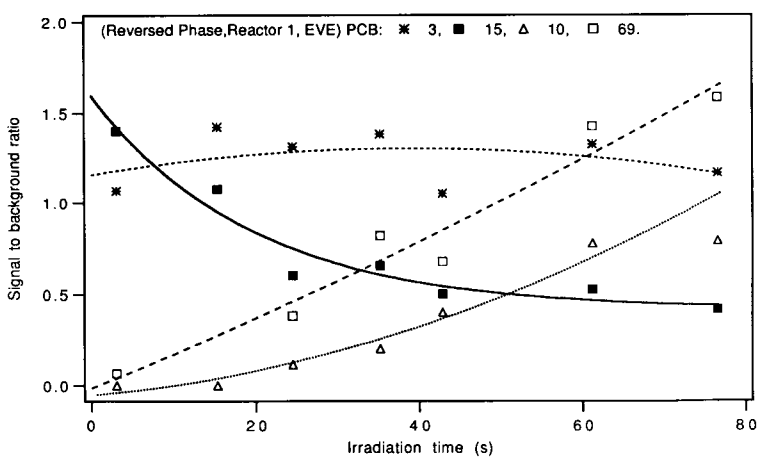

Fig. 9. Influence of irradiation time on signal to background ratio for four PCBs (8.0×10^{-6} M PCB 3, 7.5×10^{-6} M PCB 15, 2.6×10^{-5} M PCB 10 and 5.3×10^{-5} M PCB 69 injected) in a reversed-phase system (mobile phase acetonitrile–water (80 + 20, v/v)), applying EVE as the singlet oxygen reagent.

dictable; it depends on the precise chemical structure and the solvent composition applied.

Effect of irradiation efficiency

The photochemical reactor used in the experiments described above consists of a medium pressure mercury light source mounted with a quartz filter cuvette and a PTFE reactor. This kind of reactor has been applied in many LC systems [42], despite of the fact that its light collection is rather inefficient.

We have constructed a reactor (denoted as photochemical reactor 2) with a much more efficient collection of light (see Fig. 2). Almost all the light emitted from the high pressure mercury source is axially focussed into the PTFE reactor tubing. As a result high CL peak intensities are reached for relatively short irradiation times (the PTFE reactor tubing was never longer than 50 cm, corresponding to an irradiation time of about 8 s).

Influences of irradiation time on absolute CL peak intensities, signal-to-background ratios or detection limits are however less pronounced, applying photochemical reactor 2, than with the original reactor. This is probably due to the fact that the light intensity decreases gradually along the axis of the reactor tubing, due to losses at the tubing surface, scatter and absorption. Considering the fact that the photochemical processes in the reactor part where the irradiation is most intense will contribute most to the generation of the dioxetane, dioxetane produced at an earlier stage (see Fig. 2) will probably add only little to the total amount of dioxetane.

Absolute signal intensities, for the analytes rose-bengal and anthracene, are found to change linearly with lamp power over the range of 73 to 95 Watt, indicating that, for photochemical reactor 2, lamp power is a more important variable than irradiation time.

In Fig. 10 the chromatograms of an aroclor 1242 commercial PCB mixture, obtained with photochemical reactor 2 at an irradiation time of 3 s and with the original reactor at 15, 31 and 77 s, are compared. Relative peak intensities for photochemical reactor 2 correspond most reasonably to those obtained for an irradiation time of about 15 s in the original reactor, indicating that photochemical reactor 2 gives similar results at a shorter time scale.

4.3. Application to the analyses of PCBs

Detection limits

Chromatographic detection limits for a number of PCBs, obtained at optimized irradiation times and excitation filters are presented in Table 1. For comparison, the detection limits obtained with UV–visible absorption detection, at opti-

Table 1
Detection limits (mol l^{-1}) for the PCBs 3, 15, 10, 69 and 52, obtained with chemiluminescence detection under various conditions, applying optimized irradiation times and excitation filters

Experimental conditions					
Reactor type	2 [a]	1 [b]	1 [c]	1 [d]	1 [e]
Reagent	DEE [f]	DEE [g]	DEE [g]	EVE [f]	EVE [f]
Eluent	Normal phase	Normal phase	Reversed phase	Normal phase	Reversed phase
Units	mol l^{-1}	mol l^{-1}	mol l^{-1}	mol l^{-1}	mol l^{-1}
PCB	Detection limit (mol l^{-1})				
3	3.2×10^{-8}	2.2×10^{-8}	1.5×10^{-7}	3.2×10^{-6}	2.0×10^{-7}
15	6.6×10^{-8}	2.1×10^{-8}	4.8×10^{-8}	1.1×10^{-5}	4.0×10^{-7}
10	4.7×10^{-7}	2.0×10^{-6}	2.2×10^{-5}	$> 1.1 \times 10^{-4}$	5.0×10^{-6}
69	3.0×10^{-6}	1.0×10^{-6}	4.1×10^{-6}	1.7×10^{-4}	2.0×10^{-6}
52	1.9×10^{-7}	1.3×10^{-7}	1.7×10^{-6}	1.3×10^{-5}	2.0×10^{-6}

[a] Irradiation time 1 s, [b] irradiation time 40 s, [c] irradiation time 30 s, [d] irradiation time 35 s, [e] irradiation time 23 s, [f] $\lambda \geq 240$ nm, [g] $\lambda \geq 260$ nm.

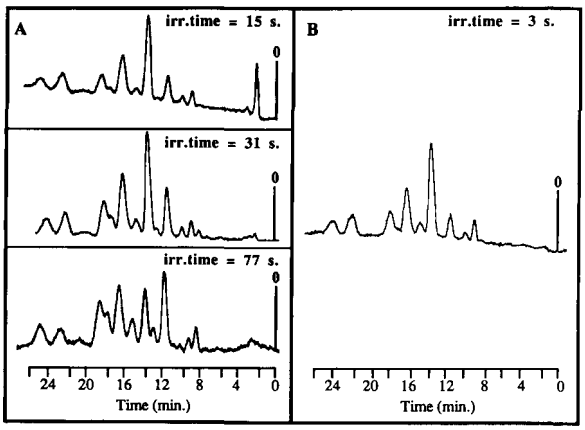

Fig. 10. Chromatograms of a commercial PCB mixture (aroclor 1242) in a reversed-phase system (acetonitrile–water (80 +20, v/v)), applying DEE (1.0×10^{-2} M in acetonitrile) as the singlet oxygen reagent at various irradiation times with both the photochemical reactors 1 and 2. A: photochemical reactor 1 at 15, 31 and 77 s irradiation time (concentrations 16.8, 8.4 and 8.4 mg l^{-1} injected respectively). B: photochemical reactor 2 (95 W) at 3 s irradiation time (concentration 33.5 mg l^{-1} injected).

mum wavelengths longer as well as shorter than 260 nm, were measured in reversed-phase LC, see Table 2. The LC parameters in Table 2 are identical to the reversed-phase parameters in Table 1; only the addition of the singlet oxygen reagent and the fluorophore are omitted.

The planar PCBs have lower detection limits than the non-planar ones both in UV absorption and in CL detection. This is partially due to a difference in absorptivity, which is higher for the planar PCBs than for the non-planar PCBs. The mutual difference between the detection limits obtained for the planar and the non-planar PCBs is however much more pronounced if CL detection is applied. Apparently the efficiency of generation of singlet oxygen for the planar PCBs is much higher. Since the efficiencies of intersystem crossing have been shown to be similar for both classes of PCBs [24], the efficiency of singlet oxygen generation is probably connected to the triplet state lifetime of the PCBs, which is indeed much longer for the planar than for the non-planar ones [24,43,44].

Table 2
Detection limits (mol l^{-1}) for the PCBs 3, 15, 10, 69 and 52, obtained with UV–visible absorption detection in a reversed-phase LC system, at optimized wavelengths > 260 nm and < 260 nm

PCB	Detection limit (mol l^{-1})	
	$\lambda < 260$ nm [a]	$\lambda > 260$ nm [b]
3	8.0×10^{-8}	8.0×10^{-8}
15	7.5×10^{-8}	1.0×10^{-7}
10	5.0×10^{-7}	2.0×10^{-6}
69	2.0×10^{-7}	1.0×10^{-6}
52	7.5×10^{-8}	4.0×10^{-7}

[a] PCB 3 at 234 nm; 15 at 257 nm; 10, 69 and 52 at 230 nm.
[b] At 274 nm for all PCBs.

The gap between the detection limits obtained for planar and non-planar PCBs, interesting from a selectivity point of view, is influenced by the practical circumstances utilized in CL detection. Though the experimental variables will not be totally independent, some general trends can be outlined.

The lowest detection limits are obtained with the original reactor using DEE as the reagent in a normal-phase system; the original reactor is slightly better than reactor 2, apart from PCB 10. For the planar PCBs these detection limits are about a factor of four lower than obtained with UV–visible absorption detection, in agreement with the enhancement factor obtained by Shellum and Birks [4] for PCB 15 in reversed phase. For the non-planar PCBs on the other hand, absorption detection is a little more sensitive than CL detection at short wavelength (< 260 nm) and about equally sensitive at relatively long wavelengths (> 260 nm).

The best selectivity between non-planar and planar PCBs is obtained in a reversed-phase system using DEE as the reagent. In this situation the detection limits for the non-planar PCBs are two to three orders of magnitude higher than for the planar ones. Compared to UV–visible absorption detection this represents a gain in selectivity of at least an order of magnitude, depending on the specific PCB concerned. This improvement is mainly caused by an increase in the detection limits of the non-planar PCBs, whereas the detection limits of the planar PCBs remain essentially unchanged. For the PCBs 15 (planar) and 10 (non-planar), both containing two chorine

substituents, there is even a gain in selectivity of almost two orders of magnitude, as compared to UV–visible absorption detection, regardless of the wavelength used.

Applying EVE does only result in significant changes for the normal-phase system, giving detection limits higher by at least two orders of magnitude for all PCBs. Applying EVE in a reversed-phase system does also result in increased detection limits, compared to DEE, but changes are less pronounced. Only for the PCBs 10 and 15 the detection limits are significantly different, giving a higher detection limit for the planar and a lower detection limit for the non-planar one.

Below, the normal-phase system utilizing DEE and photochemical reactor 1, being most sensitive to planar PCBs, is further evaluated for application to the analyses of the PCBs 77, 126 and 169.

Detection of the toxic PCBs 77, 126 and 169 in a complex matrix

Monitoring environmental PCB contamination is of great importance, since these contaminants are believed to form a serious threat to many wildlife species [33]. This threat is most serious for top-predators, since PCBs are very lipophilic and tend to bioaccumulate [33,45].

The analysis in these monitoring studies are generally done by means of gas chromatographic (GC) separation with electron capture detection (ECD) or mass spectrometric (MS) detection, with either electron impact ionization (EI), or negative-ion chemical ionization (NCI) [22,35,36,46]. Because of the complexity of the matrices concerned (generally soil samples, or organs and tissues) a thorough sample pretreatment is needed [22,30,32], which is not directly compatible with GC [22].

Significant improvement and simplification has been achieved by utilizing a CLC cleanup step [22,35,36,46]. Nevertheless, detection limits referring to the concentration in the CLC injection loop, preceding the GC analyses, are still relatively high. Sufficiently low values, a little less than 0.01 ppb, are only obtained with NCI-MS detection [46], whereas detection limits measured with ECD and EI-MS can be as high as 1 ppb or more [22,36].

Unfortunately, GC detection methods provide little difference in response for the PCB congeners, while the PCBs that are most dangerous based on toxic equivalents [33] (the planar PCBs 77, 126 and 169, possessing PCDD (Poly-Chloro-Dibenzo-Dioxine) like toxicity) are generally present at about three decades lower concentrations than most of the non-planar congeners [32,46]. Even with the high separating power of GC techniques, analyses of the PCBs 77, 126 and 169 are therefore extremely difficult. An interesting option is the use of a selective stationary phase in the CLC cleanup to separate the PCBs 77, 126 and 169 from the other PCBs [34]. Therefore CLC can be gaining importance in the analyses of PCBs. It is interesting to examine whether CL detection based on photoinduced generation of singlet oxygen, being far more sensitive to planar PCBs than to non-planar PCBs, can offer the desired selectivity and sensitivity.

Normal-phase LC with a PYE analytical column and reactor type 1 with DEE as the singlet oxygen reagent was applied, to obtain both good separation and most sensitive detection of planar PCBs. The detection limits obtained for the PCBs 77, 126, 169 and 122 are shown in Table 3, together with the associated UV–visible absorption detection data. It is clear that the detection limits for the planar PCBs measured with CL detection are more favourable. Detection limits are comparable to those found with ECD and EI-MS detection, referring to the concentrations in the LC system preceding GC analysis (MS-NCI

Table 3
Detection limits for the PCBs 77, 126 and 169 in a normal-phase LC system with a PYE analytical column, obtained with UV–visible absorption detection at 254 nm and chemiluminescence detection, applying DEE as the singlet oxygen reagent, photochemical reactor type 1 at an irradiation time of 40 s and $\lambda \geq 240$ nm

PCB	Detection limit			
	UV–visible absorption		Chemiluminescence	
	mol l^{-1}	ppb	mol l^{-1}	ppb
77	1.6×10^{-8}	4.5	2.5×10^{-9}	0.7
126	2.9×10^{-8}	9.7	4.8×10^{-9}	1.6
169	3.1×10^{-8}	11.2	9.1×10^{-9}	3.3
122	4.3×10^{-9}	1.4	4.3×10^{-9}	1.4

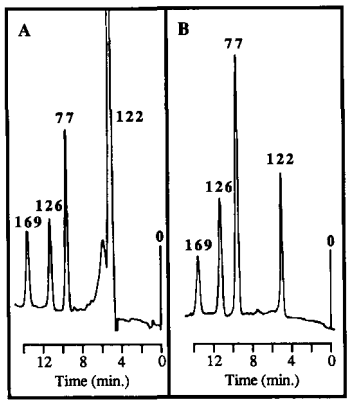

Fig. 11. Chromatograms of an academic mixture of four PCBs (77, 126, 169 and 122; 150, 150, 150 and 165 ppb injected, respectively) in normal-phase (*n*-hexane), using a PYE column. (A) UV absorption detection at 254 nm. (B) CL detection applying DEE (1.0×10^{-2} M) as the singlet oxygen reagent and an irradiation time of 40 s in photochemical reactor 1.

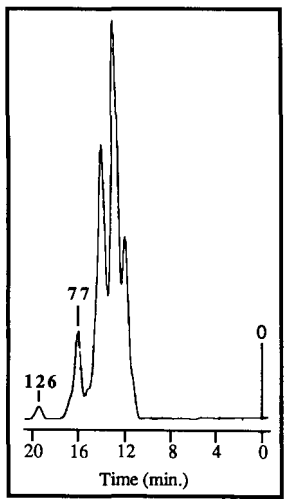

Fig. 12. Chromatogram (CL detection) of a commercial PCB mixture (aroclor 1242, 8.06 mg l^{-1} in *n*-hexane injected) in a normal-phase system (*n*-hexane), using a PYE analytical column and DEE (1.0×10^{-2} M in *n*-hexane) as the singlet oxygen reagent. The irradiation time is 40 s.

detection limits are evidently better). PCB 122 (2′,3,3′,4,5-pentachlorobiphenyl) is a PCB containing only one ortho chlorine substituent (mono-*ortho* PCB). These PCBs show characteristics in between planar and non-planar PCB. Clearly the detection limit for PCB 122 is low in both CL and UV–visible absorption detection. However, contrary to the PCBs 77, 126 and 169, there is no improvement on applying CL detection compared to UV–visible absorption detection.

The selectivity of the present method for the PCBs 77, 126 and 169 is illustrated by the chromatograms in Fig. 11. Obviously the PCBs 77 and 126 and to some extend PCB 169 show an im-

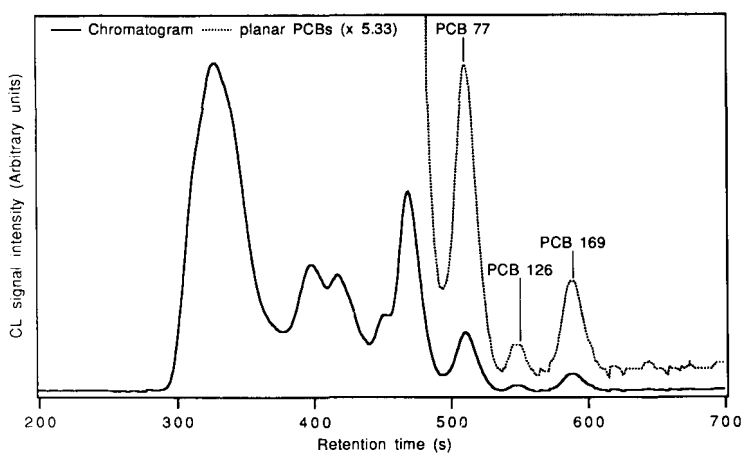

Fig. 13. Chromatogram (CL detection) of a pretreated herring oil sample, additionally spiked with PCBs (total PCB concentrations are about 30 ppb in the herring oil sample for each of the PCBs 77, 126 and 169) in a normal-phase system (*n*-hexane), using a PYE analytical column and DEE (1.0×10^{-2} M in *n*-hexane) as the singlet oxygen reagent. The irradiation time is 40 s.

provement in signal-to-noise ratio, clearly illustrated by their peak heights relative to that for PCB 122.

The enhanced selectivity is more pronounced for the analyses of planar toxic PCBs in a commercial PCB mixture. Aroclor 1242 contains about 0.5 mass percent of PCB 77 [47–49] and only about 2×10^{-3} mass percent of PCB 126 [48]. Nevertheless both PCBs can be clearly seen in the chromatogram of Fig. 12. The remaining peaks in this chromatogram may result from the other planar PCBs in aroclor 1242, PCBs 15, 35 and 37 [49], present at mass percentages of 1.5, 0.1 and 0.3, respectively, and/or from some of the non-planar PCBs present at far higher mass percentages (up to almost 8 percent for PCB 8 [49]).

Finally we have applied the CL detection method to the analysis of PCBs in a complex matrix. A sample of 0.5 g of herring oil, spiked with each of the PCBs 77, 126 and 169 to individual concentrations of about 30 ppb, was pretreated as outlined in the experimental part and analysed in a normal-phase CLC system adapted with a PYE analytical column and connected to the CL detection system. The resulting chromatogram is shown in Fig. 13. The peaks for the PCBs 77, 126 and 169 are all well above the detection limit. Thus, a significant improvement, compared to PCB analysis with CLC and simple UV detection has been realized, although for practical applications additional effort will be required; for instance the concentrations of PCBs 77, 126 and 169 in real samples can be less than 1 ppb [33].

5. Conclusions

The results discussed above indicate that dioxetane CL detection in CLC based on photosensitized on-line generation of singlet oxygen offers interesting applicabilities.

The use of the detection method can be extended to normal-phase CLC systems. Furthermore, instead of DEE, which needs to be synthesized, the reagent EVE, which is commercially available, can be utilized. In reversed-phase these reagents provide similar results.

With the introduction of a new photochemical reactor (photochemical reactor 2), irradiation times can be reduced, so that band broadening is minimized and analysis times are reduced to those of existing CLC detection methods.

The optimum settings of experimental parameters, like irradiation window and irradiation time, are analyte dependent. They offer possibilities to enhance selectivity. This is shown to be of considerable interest in the analysis of PCBs.

Presumably as a result of different photochemical behaviour, the detection method offers some inherent selectivity in the analysis of PCBs; planar PCBs provide much lower detection limits than non-planar ones. As a result CLC analysis may become an interesting technique for the detection of the toxic PCBs 77, 126 and 169.

Acknowledgments

The authors are indebted to P.E.G. Leonards (Institute of Environmental Studies, Free University), for the use of the PYE column and the herring oil sample.

References

[1] H.A.G. Niederländer, F.W. Engelaer, C. Gooijer and N.H. Velthorst, in P.E. Stanley and L.J. Kricka (Eds.), Bioluminescence and Chemiluminescence Current Status, Wiley, Chichester, 1991, p. 227.
[2] H.A.G. Niederländer, W. van Assema, F.W. Engelaer, C. Gooijer and N.H. Velthorst, Anal. Chim. Acta, 255 (1991) 395.
[3] C.L. Shellum and J.W. Birks, in J.W. Birks (Ed.), Chemiluminescence and Photochemical Reaction Detection in Chromatography, VCH, New York, 1989, p. 231.
[4] C.L. Shellum and J.W. Birks, Anal. Chem., 59 (1987) 1834.
[5] T. Wilson and A.P. Schaap, J. Am. Chem. Soc., 93 (1971) 4126.
[6] P.D. Bartlett and M.E. Landis, in H.H. Wasserman and R.W. Murray (Eds.), Singlet Oxygen (Organic Chemistry, Vol. 40), Academic Press, New York, 1979, p. 243.
[7] H. Nakamura and T. Goto, Photochem. Photobiol., 30 (1979) 27.
[8] C.S. Foote, A.A. Dzakpasu and J.W.P. Lin, Tetrahedron Lett., 14 (1975) 1247.

[9] J.C. Hummelen, Ph.D. Thesis, Groningen, Netherlands, 1985, p. 168.
[10] T. Wilson, D.E. Golan, M.S. Harris and A.L. Baumstark, J. Am. Chem. Soc., 98 (1976) 1086.
[11] A.P. Schaap, Tetrahedron Lett., 21 (1971) 1757.
[12] A.P. Schaap, M.D. Sandison and R.S. Handley, Tetrahedron Lett., 28 (1987) 1159.
[13] A.P. Schaap, T.S. Chen, R.S. Handley, R. de Silva and B.P. Giri, Tetrahedron Lett., 28 (1987) 1155.
[14] A.P. Schaap, R.S. Handley and B.P. Giri, Tetrahedron Lett., 28 (1987) 935.
[15] S. Beck and H. Köster, Anal. Chem., 62 (1990) 2258.
[16] H. Niederländer, Ph.D. Thesis, Amsterdam, Netherlands, in preparation.
[17] W. Adam, in W. Adam and G. Cilento (Eds.), Chemical and Biological Generation of Excited States, Academic Press, New York, 1982, p. 115.
[18] L.H. Catalani, T. Wilson and E.J.H. Bechara, Photochem. Photobiol., 45 (1987) 273.
[19] B.M. Monroe, in A.A. Frimer (Ed.), Singlet Oxygen, Vol. I (physical-chemical aspects), CRC Press, Boca Raton, FL, 1985, p. 177.
[20] H.A.G. Niederländer, M.M. de Jong, C. Gooijer and N.H. Velthorst, Anal. Chim. Acta, 290 (1994) 201.
[21] O. Hutzinger, S. Safe and V. Zitko, The Chemistry of PCB (Chap. 6; photodegradation of chlorobiphenyls), CRC Press, Boca Raton, Florida, 1974, p. 119.
[22] H. Hyvönen, T. Auvinen and M.L. Riekkola, J. Microcol. Sep., 4 (1992) 123.
[23] S. Jensen, New Scientist, 32 (1966) 612.
[24] L.O. Ruzo, M.J. Zabik and R.D. Scheutz, J. Am. Chem. Soc., 96 (1974) 3809.
[25] T. Moore and R.M. Pagni, J. Org. Chem., 52 (1987) 770.
[26] J. Orvis, J. Weiss and R.M. Pagni, J. Org. Chem., 56 (1991) 1851.
[27] S. Hashimoto and J.K. Thomas, J. Photochem. Photobiol. A: Chem., 55 (1991) 377.
[28] Y. Mao and J.K. Thomas, J. Chem. Soc., Faraday Trans., 88 (1992) 3079.
[29] F. Negri and M.Z. Zgierski, J. Chem. Phys., 97 (1992) 7124.
[30] E.C. Lim and Y.H. Li, J. Chem. Phys., 52 (1970) 6416.
[31] P.J. Wagner, J. Am. Chem. Soc., 89 (1967) 2820.
[32] V.A. Mc Farland and J.U. Clarke, Environ. Health Persp., 81 (1989) 225.
[33] P.E.G. Leonards, B. van Hattum, W.P. Cofino and U.A.Th. Brinkman, Environ. Toxicol. Chem., 13 (1993).
[34] P. Haglund, L. Asplund, U. Järnberg and B. Jansson, J. Chrom., 507 (1990) 389.
[35] F.A. Maris, E. Noroozian, R.R. Otten, R.C.J.M. van Dijck, G.J. de Jong and U.A.Th. Brinkman, J. High Resolut Chromatogr. Chromatogr. Commun., 11 (1988) 197.
[36] H. Siren, H. Hyvönen, M. Saarinen, S. Rovio and M.L. Riekkola, Chromatographia, 34 (1992) 421.
[37] H. Baganz, K. Praefcke and J. Rost, Chem. Ber., 96 (1963) 2657.
[38] K. Ballschmitter and M. Zell, Fresenius' Z. Anal. Chem., 302 (1980) 20.
[39] G. Schwartzenbach and K. Lutz, Beilstein, second supplement, IX-40, p. 1139.
[40] A.P. Schaap and K.A. Zaklika, in H.H. Wasserman and R.W. Murray (Eds.), Singlet Oxygen (Organic Chemistry, Vol. 40), Academic Press, New York, 1979, p. 173.
[41] M. Saraka, G. Dauphin and P. Boule, Chemosphere, 18 (1989) 1391.
[42] J.R. Poulsen and J.W. Birks, in J.W. Birks (Ed.), Chemiluminescence and Photochemical Reaction Detection in Chromatography, VCH, New York, 1989, p. 149.
[43] J.J. Donkerbroek, N.J.R. van Eikema-Hommes, C. Gooijer, N.H. Velthorst and R.W. Frei, Chromatographia, 15 (1982) 218.
[44] J.J. Donkerbroek, N.J.R. van Eikema-Hommes, C. Gooijer, N.H. Velthorst and R.W. Frei, J. Chromatogr., 255 (1983) 581.
[45] O. Hutzinger, S. Safe and V. Zitko, The Chemistry of PCB (Chap. 1: introduction), CRC Press, Boca Raton, FL, 1974, p. 1.
[46] H. Bagheri, P.E.G. Leonards, R.T. Ghijsen and U.A.Th. Brinkman, Int. J. Environ. Anal. Chem., 50 (1993) 257.
[47] J.C. Duinker, D.E. Schultz and G. Petrick, Anal. Chem., 60 (1988) 478.
[48] N. Kannan, S. Tanabe, T. Wakimoto and R. Tatsukawa, J. Assoc. Off. Anal. Chem., 70 (1987) 451.
[49] D.E. Schultz, G. Petrick and J.C. Duinker, Environ. Sci. Technol., 23 (1989) 852.

ELSEVIER

Analytica Chimica Acta 297 (1994) 369–376

ANALYTICA CHIMICA ACTA

Three-column system for preconcentration and speciation determination of trace metals in natural waters

Michael Groschner *, Pierre Appriou

URA CNRS 322, Faculté des Sciences de Brest, 6 Avenue le Gorgeu, 29275 Brest Cedex, France

Received 2 November 1993; revised manuscript received 25 April 1994

Abstract

A three-column system consisting of a combination of C_{18} reversed phase, Dowex anion-exchange resin and the chelating resin Chelamine is described. This method permits the simultaneous preconcentration and differentiation between neutral hydrophobic organic metal complexes, anionic complexes and the "free ion" concentration of the transition metals in water samples with complex matrices. General operating conditions were established by numerous experiments with model substances. The sample analyses can be made without any previous treatment and hence the pre-established natural equilibria are unadulterated. The method was used in the investigation of several fresh-water and sea-water samples for the determination of Cu^{2+}, Cd^{2+}, Pb^{2+} and Mn^{2+} and showed excellent reproducibility.

Keywords: Ion chromatography; Preconcentration; Speciation; Trace metals; Waters

1. Introduction

The determination of trace metals such as Cu, Pb, Cd and Mn is becoming increasingly important because of the increased interest in environmental pollution. These metals tend to be complexed by organic and inorganic ligands in natural waters, which in turn affects both their chemical reactivity and biological availability. When the concentration of these trace metals is low, even with increased instrumental sensitivity, direct determination of their concentrations becomes difficult because of the interacting matrix of a complex medium such as sea water. Consequently, a preconcentration and matrix elimination step is usually required and provided, for example, by a liquid–solid extraction using a chelating resin such as Chelex 100, as described by numerous workers [1–5]. Although Chelex resin is able to preconcentrate trace metals, some severe disadvantages arise such as loss of some trace elements (Mn) during the washing step, the need for well defined pH conditions or poor selectivity. Because of these problems, a commercial chelating resin, Chelamine, based on a pentamine ligand (1,4,7,10,13-pentaazatridecane or tetrene) grafted on an organic polymer, was examined and described by Blain et al. [6]. This resin permits

* Corresponding author.

SSDI 0003-2670(94)00228-E

matrix elimination and preconcentration of Cd, Cu, Ni, Pb and Zn in a wide pH range (5.5–8) with a high degree of selectivity for the transition metals relative to the alkali and alkaline earth elements. For this reason, Chelamine seems to be suitable as the basis of a system including several columns that will permit the simultaneous preconcentration and separation of different metal species.

A two-column ion-exchange system with Chelex 100 and AG MP1 macroporous anion-exchange resin has already been described by Liu and Ingle [7]. However, this arrangement does not seem to be very suitable for the study of metal speciation determination as the Chelex resin works in the pH range 4–5.5, requiring a buffer, which will finally lead to an imbalance of the pre-established natural conditions. Lewis and Landing [8] used a three-column ion-exchange sequence for the analysis of Black Sea water. The first column collected colloidal particles (metal sulfides), the second acted as an anion exchanger and the third as a chelating cation-exchange resin. As the use of anion exchangers for the study of sea water is limited because of the high chloride ion concentration and the authors used the pH-dependent resin Chelex 100 in addition to TSK–8-hydroxyquinoline, their speciation results have to be treated in caution.

Mills and Quinn [9,10] used C_{18} reversed phase for isolating copper–organic complexes from sea water and the chelating resin Chelex 100 for the determination of the total metal content. The use of C_{18} reversed phase was subsequently described by numerous workers for several applications: investigation of liquid chromatography (LC) for the determination of copper(II)–amino acid complexes in sea water [11], determination and preconcentration of Cu and Cd metal–organic complexes [12,13] and differentiation between metal–EDTA complexes and organic complexes [14]. Preconcentration systems for trace metal in sea water using LC have been reported [15–17], but even with this approach only the total metal content is obtained without any indication of speciation or metal complexation.

Dowex anion-exchange resin was used by Vanderdeelen [18] to separate metal–EDTA complexes. As further described by Burba [27], this resin has excellent capacities for the preconcentration of anionic trace metals.

This paper proposes a combination of C_{18} reversed phase, Dowex anion-exchange resin and Chelamine chelating resin. This method permits the simultaneous preconcentration and differentiation between neutral hydrophobic organic–metal complexes, anionic complexes and the "free ion" concentration of the transition metals in natural waters, but also can be extended to other aqueous liquids with complex matrices, e.g., biological fluids.

As each column has precise operating conditions and also limitations, which are discussed in Section 3, a general operating range was established from numerous experiments with model substances and tried on several fresh-water and sea-water samples.

2. Experimental

2.1. Reagents

All aqueous solutions were prepared with deionized water obtained from a Milli-Ro/Milli-Q apparatus (Millipore). The chelating resin Metalfix Chelamine was purchased from Fluka, the anion-exchange resin Dowex 1-X8 (100–200 mesh) from Aldrich and the C_{18} phase (Bond Elut LRC columns) from Analytichem International. The reagents and ligands used as model substances, e.g., EDTA, nitrilotriacetic acid (NTA), tryptophan, 8-hydroxyquinoline and fulvic acid, were purchased from several sources. Nitric acid and ammonia solution for elution and regeneration of the resins were made from ultra-pure reagents (Merck) and deionized water. The metal standards and spikes were prepared from commercial standard solutions.

2.2. Apparatus

A Perkin-Elmer Zeeman 3030 instrument for electrothermal atomic absorption spectrometry (ETAAS) equipped with an AS 60 autosampler was used. All pH measurements were made with

an Orion Research 501 digital ionanalyser. The acidic eluates were stored in PTFE tubes which were previously cleaned by soaking in hydrochloric acid overnight and rinsed with deionized water. All procedures were carried out under a laminar flow-hood.

2.3. Column procedure

Columns loaded with Chelamine were prepared as described by Blain et al. [6]. A 1.2-g amount of wet resin was packed into columns purchased from Bio-Rad and successively rinsed with 10 ml of water, 10 ml of 2 M HNO_3, 10 ml of water, 10 ml of water containing 600 μl of 2 M ammonia solution and finally 30 ml of water (adjustment to near neutral). A 1-g of Dowex wet resin was packed into the same type of columns (Bio-Rad) and successively rinsed with 10 ml of 2 M HNO_3 and 20 ml of deionized water as a precleaning step. Bond Elut LRC C_{18} columns were ready for use but nevertheless were previously rinsed with 5 ml of 2 M HNO_3 and 10 ml of deionized water. Before processing the samples, the C_{18} reversed phase was wetted with methanol and rinsed with water. The assemblages of the two preconcentration systems C_{18}–Chelamine and C_{18}–Dowex–Chelamine are shown in Fig. 1.

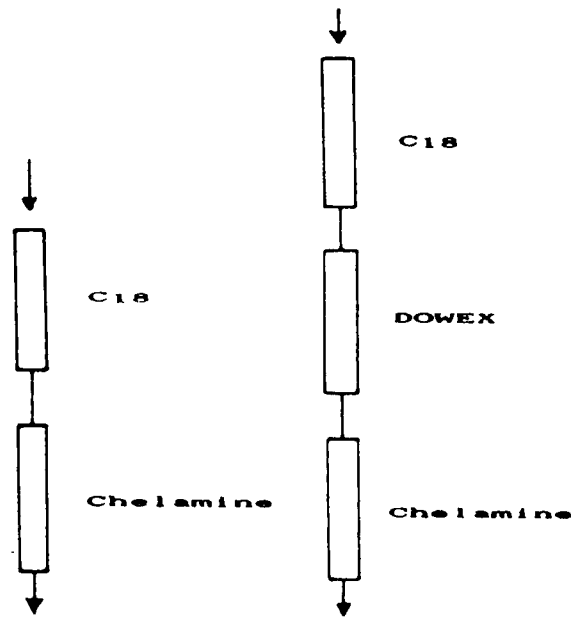

Fig. 1. C_{18}–Chelamine and C_{18}–Dowex–Chelamine preconcentration systems.

All natural water samples were filtered (Millipore Type HA 0.45 μm filter) and processed without any further treatment. As the aim of this work was the development of a three-column system, we did not take account of colloidally bound metals by carrying out experiments on digested, filtered samples, as this would destroy the pre-established natural equilibria, or of the suspended solids content which was discarded after filtration.

The spiked aqueous solutions were buffered to pH $\approx$ 8 by adding 2 M borate buffer solution. The samples were passed under gravity flow according to the simplified column fitting and therefore the flow-rate was limited to 0.2–0.3 ml min^{-1} by the slow speed through, the C_{18} columns. As the method was applied here to samples of river, sewage and and sea water from a trading port, samples in which trace metal concentrations are expected to be higher than in open ocean waters, sample volumes of only 40–210 ml were processed. The time needed is then still acceptable for avoiding serious variations of the samples from losses of metals by adsorption on the container walls or changes in speciation due to biological activity. However, this low flow-rate could be a serious limitation if the method is applied to open ocean samples. Blain et al. [6], who studied the influence of flow-rate on the recovery efficiencies of Chelamine for Cu and Mn, mentioned that copper can be totally recovered whereas Mn showed a 75% recovery at a flow-rate of 1 ml min^{-1}. Both metals were quantitatively recovered at 0.3 ml min^{-1}.

Analysis with C_{18} can be done much faster and Mills and Quinn [9,10] used a flow-rate of 12–15 ml min^{-1}. For Dowex a 100% recovery was still obtained at 1 ml min^{-1} for a Cu–EDTA complex. The speed of the method is then essentially limited by the third column (Chelamine) and we are currently trying to obtain other chelating systems that are not subject to this problem.

After the preconcentration step, the columns were separated, rinsed with water (20 ml) and eluted with 4 ml of 2 M HNO_3, the eluates being recovered in PTFE tubes.

2.4. Breakthrough properties and capacity

The breakthrough properties and the capacity of the resin Chelamine were well described by Blain et al. [6]. The capacity was found to be 1 mmol g^{-1} for copper. We examined the breakthrough property of the Dowex resin by processing a 1-l volume (without salinity) of 0.2 mmol l^{-1} $(CuEDTA)^{2-}$ complex at a flow-rate of 1 ml min^{-1}, 102 μmol g^{-1} of the complex was retained until column breakthrough started.

For C_{18} it is more difficult to give a general uptake capacity, as the properties will largely depend on the structure and the hydrophobic character of the adsorbed molecule. Reports of the use of C_{18} [5,9,10,14] made no mention of these properties, indicating that they apparently did not exceed the uptake capacities with the working sample volumes used. We examined the breakthrough behavior of our C_{18} cartridges (Bond Elut LRC) by passing 1 l of a solution containing 10 mg Cu and 0.4 mol of tryptophan. With the assumption that a $Cu(Trypt)_2$ complex is formed, 0.04 mmol of this complex can be retained by a cartridge (200 mg of resin) before breakthrough starts.

2.5. Model solutions and spikes

For the preparation of the model solutions, 30 ml of deionized water were spiked with 50 μl of 1 mg l^{-1} copper standard solution complexed by different ligands (EDTA, tryptophan, etc). The complexed standard solutions were previously prepared by shaking copper sulfate standard solution with a slight stoichiometric excess of ligand. For the determination of spike recoveries in fresh and sea water, the same procedure was used. The pH of the model solutions was adjusted to 8.

The blanks of the model solutions were checked by passing the same volume without spikes. The blanks for the various columns were determined in the acidic eluates after the precleaning and neutralization steps and are given in Table 1.

Table 1
Blanks after precleaning step

Metal	Blank (ng) [a]		
	C_{18}	Dowex	Chelamine
Cu	0.84 ± 0.20	1.10 ± 0.20	2.12 ± 0.52
Pb	< 0.02	< 0.02	0.76 ± 0.28
Cd	0.28 ± 0.12	0.10 ± 0.04	0.12 ± 0.08
Mn	1.36 ± 0.04	0.12 ± 0.08	0.88 ± 0.68

[a] Means and confidence intervals (three determinations).

Table 2
Recoveries for Cu complexes with different ligands

Ligand	Recovery (%) [a]	
	C_{18}	Dowex
Fulvic acid	94.6 ± 4.0	35 ± 7
8-Hydroxyquinoline	99.5 ± 0.5	5.5 ± 3.5
Tryptophan	103 ± 2	9.5 ± 1.5
NTA	101.4 ± 0.4	11.5 ± 6.5
EDTA	< 1%	98.8 ± 1.3

[a] Means and confidence intervals (three determinations). Metal ion concentration, 2.6×10^{-8} mol l^{-1}; ligand concentration, 8×10^{-8} mol l^{-1}; matrix, deionized water.

3. Results and discussion

The results obtained after passing the model solutions show that the three-column scheme is suitable for the preconcentration and simultaneous speciation determination of neutral organic metal complexes, anionic complexes and "free ion" concentrations of transition metals in aqueous solutions. The model investigations were carried out only with copper complexes. As the behaviour of complexes with respect to the C_{18} and Dowex resins will be dominated by the ligand rather than by the bivalent metal ions, it can probably be assumed that the selectively characteristics of the columns can be transferred to other transition metals. The different recoveries of copper–ligand complexes in deionized water for C_{18} reversed phase and Dowex are given in Table 2. The metal concentration in the spiked

samples was 2.6×10^{-8} mol l^{-1} and the different ligands tested were present in a stoichiometric excess at 8×10^{-8} mol l^{-1}, the complexes having been previously formed at higher concentration. The trials were first carried out on the individual columns (Table 2) and double-checked with the sequential column scheme, which yielded the same results. The cations examined (Cu^{2+}, Pb^{2+}, Mn^{2+}, Cd^{2+}) were also processed as "organic free" solutions (deionized water without ligand addition) at the same concentrations and no significant uptake by C_{18} or Dowex was noted (recovery $\ll 0.5\%$). For saline water ($S = 35‰$) higher ligand concentrations were used (0.01 mmol) to avoid complex decomposition due to cation interactions. These trials were carried out only with the C_{18} reversed phase (Dowex resin was not used for sea-water analysis) and confirmed the results in Table 2.

As the complexation capability of Chelamine is able to destroy even strong complexes such as $(CuEDTA)^{2-}$ ($98.4 \pm 1.4\%$ recovery), this resin seems to be a reliable trap for transition metal compounds passing through the two previous columns.

3.1. C_{18} reversed phase

As shown in Table 2, the model substances represented by copper complexed by fulvic acid, 8-hydroxyquinoline and NTA are retained by C_{18} reversed phase with high yields, which apportions the greatest fraction of neutral hydrophobic transition metal complexes to the first column of the preconcentration system. Consequently, it can be stated that this column will generally be able to preconcentrate metals complexed by humic substances, amino acids, aromatic ligands and even small organic ligands forming neutral complexes (NTA). As already described by Shunda and Hanson [14] and confirmed by our results, EDTA complexes of the form MY^{2-} are not retained by C_{18} reversed phase. Conversely, NTA forms neutral complexes at the given pH (ca. 8) and is extracted by C_{18} for this reason. Uncomplexed metal ions M^{2+} and inorganic charged complexes will pass through the C_{18} phase.

Further speciation of the adsorbed complexes could be achieved by sequential elution with water–methanol mixtures and subsequent rinsing with 2 M nitric acid [13], but was not studied here.

3.2. Dowex

With a good recovery for $(CuEDTA)^{2-}$ spikes in fresh-water, the strong anion-exchange resin Dowex 1-X8 tends to be an ideal phase for retaining anionic complexes. Although this resin shows a rather poor collection efficiency for copper complexes with fulvic acid, 8-hydroxyquinoline, tryptophan and NTA, this does not diminish its usefulness for the preconcentration system as these kinds of complexes are already taken up by C_{18}.

However, with increasing salinity, chloride ions start to compete with the dissolved anionic complexes, leading to a rapid decrease in spike recoveries. As shown by further experiments, preloaded Cu–EDTA complex can be totally eluted by 10 g l^{-1} NaCl solution when the exchange capacity of the resin is overwhelmed. For this reason, it is advisable to exclude Dowex anion resin for metal speciation determination when the salinity of the water sample exceeds 2–3‰.

Lewis and Landing [8], using DEAE anion-exchange resin, found the same conclusion for metal–organic complexes in sea water. They, however, described its use for preconcentrating anionic metal–sulfide complexes in 22‰ salinity waters. We have checked this assertion for our Dowex resin only by some incidental trials and found that metal–sulfide complexes are really able to complete with Cl^- ions even in 35‰ salinity water with up to 90% recovery. However, the C_{18} reversed phase was also able to retain a few percent of these complexes (ca. 13% in fresh water, ca. 30% in sea water), probably because of the existence of some polysulfide chains which are adsorbed on the lipophilic groups of this phase. The higher recovery in 35‰ salinity water can be seen as a result of neutralization of some anionic polysulfide chains by major cations, which is favourable for adsorption on the C_{18} phase. As the determination of metal sulfides was not the purpose of this study, we did not investigate it

more deeply. For this work we did not use Dowex for sea-water samples, but this resin combined with C_{18} and Chelamine may be also a useful tool for the analysis of anoxic waters.

3.3. Chelamine

The properties of the chelating resin Chelamine have been described in detail by Blain et al. [6] and this work showed that this phase is ideal for most requirements as the final column in our preconcentration system. Chelamine retains Cd, Cu, Zn, Pb and Mn in the pH range 5–8 and therefore will remove these metals from most natural waters with excellent efficiencies. Consequently, natural samples can be analysed without any previous treatment such as acidification or buffering (which would have been necessary with Chelex 100), hence the determination of the pre-established natural equilibria is unaffected.

However, care must be taken when passing spiked samples prepared with distilled water without buffer. As the resin has strongly basic groups, precipitation of hydroxides will probably occur in the micro-environment of the resin surface owing to a local increase in the pH, leading to a decrease in recoveries to around 50%. After the buffering of these samples the results reported by Blain et al. [6] were obtained. However, natural waters are sufficiently buffered by their dissolved salts, as shown by spike recoveries (98.8 $\pm$ 3.3%) in both fresh- and sea-water samples.

As further described by Blain et al. [19], the discrimination of polyamines against the major sea-water cations (Na^+, Ca^{2+}, Mg^{2+}) is better than that of Chelex and 8-hydroxyquinoline used by Lewis and Landing [8].

As already noted above, our investigation showed the capability of this resin to destroy even the strong EDTA complexes.

3.4. Natural water samples

As the primary aim of this work was the development and examination of a preconcentration and speciation system, natural water analysis was carried out to show the reproducibility and limits of this method with complex samples rather than to give a detailed description of established chemical equilibria and reaction mechanisms. However, attention must be paid to generally known and reported conditions when determining the accuracy of the method.

In Table 3, the results for natural samples are given and show the good reproducibility of the analysis. There are no noticeable losses of trace metals during column processing as the recovery of the total metal content of the three columns was 98.6% compared with the same samples preconcentrated using only Chelamine. As shown by Blain et al. [6] and double-checked by passing spiked sea- and fresh-water samples, Chelamine collects Cd, Cu, Mn and Pb with nearly quantitative efficiency.

Samples AI and AII were fresh-water samples taken from a brooklet near a pig-breeding facility (AI) and at a distance of a few hundred metres below a small swamp, BI and BII originated from two different settling tanks of a sewage purification plant and S (sea-water sample) was taken from the trading port of Brest (France).

For the sea-water sample (S) we did not use Dowex resin for the reasons mentioned above. Musani et al. [20] examined the interaction of Cd and Pb ions with humic acid isolated from marine sediments. They used high-voltage paper electrophoresis in model solutions of 100, 30 and 10% sea water to simulate estuarine conditions. The behaviour of Cd and Pb in our sea-water and fresh-water samples shows good agreement with the results of Musani et al. [20]. Their investigations with sea-water models showed that nearly the whole of Pb exists as an uncharged complex whereas Cd yields only a cationic zone. With decreasing salinity the situation becomes different and Pb complexes coexist in two forms, neutral and cationic complexes, and Cd shows the beginning of the formation of uncharged complexes. As stated, Cd is generally less bound by humic acids. Comparing these fact the result for samples AI, AII and S, we noted that in the sea water sample (S) virtually all of the Pb was extracted as a hydriphobic neutral organic complex by C_{18} whereas Cd passed through this column and was retained by Chelamine. For the fresh-water samples AI and AII ca. 8% of Cd was

retained by C_{18} but nearly 20–25% of the Pb passed through this phase.

Capodaglio [21], who studied the surface waters of the Eastern North Pacific ocean, found that the organically complexed lead fraction contributes a significant portion of the total (48–50%) and the "free" lead fraction represents 1.4% of the total concentration. Bruland [22] estimated that 67% of Cd is complexed with organic ligands in the surface waters of the North Pacific. Both workers used differential-pulse anodic stripping voltametry. Their results are not in agreement with those of Musani et al., but it should be noted that they analysed open ocean sea waters whereas Musani et al. studied model solutions to simulate estuarine conditions where metal and ligand concentrations are much higher.

The method described in this paper is different. It does not mean that a metal ion is not complexed if it is not taken up by the C_{18} phase, as has been noted above, for example EDTA and charged small organic complexes will pass through this column. In sea-water analysis this method gives the rate of metal complexation with ligands sufficiently hydrophobic to be retained by the C_{18} phase. Geringa et al. [23], who studied metal complexation in the water phase of incubated marine slurries, also stated this. They found that more than 99% of dissolved copper is organically complexed. This is in good agreement with the results of Van den Berg [24,25] and of Coale and Bruland [26]. Geringa et al. noted further that copper complexation determined with the C_{18} phase is much less than the total extent of complexed species. For Cd they noted a negligible complexation according to Musani et al. [20], but Bruland [22] obtained different results for open-ocean sea water, as mentioned above.

As also noted in earlier work by Mills and Quinn [9,10], Cu tends to coexist in two forms: as complexes being retained by C_{18} and as species passing through this phase. As both groups had

Table 3
Results for natural water samples

Sample [a]	Metal ion	Concentration ($\mu g\ l^{-1}$) [b]		
		C_{18}	Dowex	Chelamine
AI	Cu	0.36 ± 0.03	0.30 ± 0.01	0.03 ± 0.01
	Pb	0.042 ± 0.003	0.008 ± 0.003	< 0.002
	Cd	0.002 ± 0.001	0.018 ± 0.001	0.007 ± 0.003
	Mn	0.13 ± 0.02	0.02 ± 0.01	0.420 ± 0.001
AII	Cu	0.13 ± 0.01	0.15 ± 0.01	0.030 ± 0.005
	Pb	0.021 ± 0.003 [c]	0.008 ± 0.003	0.006 ± 0.003
	Cd	0.004 ± 0.001 [c]	0.032 ± 0.003	0.016 ± 0.002
	Mn	0.10 ± 0.01	0.060 ± 0.001	1.48 ± 0.07
BI	Cu	0.93 ± 0.07	0.66 ± 0.01	0.10 ± 0.02
	Pb	0.20 ± 0.02	0.27 ± 0.02	0.04 ± 0.02
	Cd	< 0.001	0.045 ± 0.010	< 0.001
BII	Cu	0.89 ± 0.07	1.23 ± 0.03	0.09 ± 0.03
	Pb	0.20 ± 0.02	0.140 ± 0.005	< 0.01
	Cd	< 0.001	0.06 ± 0.008	< 0.001
S	Cu	0.410 ± 0.005		0.66 ± 0.02
	Pb	0.150 ± 0.005		< 0.005
	Cd	< 0.001		0.088 ± 0.007
	Mn	0.038 ± 0.001		2.03 ± 0.07

[a] AI and AII = fresh water taken from a brooklet; BI and BII = sewage samples; S = sea water taken from the trading port of Brest. Sample volumes and preconcentration factors: AI and AII, 180 ml, factor 45; BI and BII, 40 ml, factor 11.3; S, 210 ml, factor 52.5.

[b] Means and confidence intervals (three determinations).

[c] Only two determinations because of sample contamination.

to use two different methods for examinating the Cu equilibrium, our system is an improvement as it permits this analysis in only on step.

In fresh-water analysis, the utilization of Dowex resin allows a more precise speciation than in sea water. Most of the Cu, Pb and Cd in fresh water but also in sewage samples (BI, BII) passing through the C_{18} phase were retained by the Dowex resin and only a few percent of these ions were found in the final Chelamine column, which indicates that anionic complexation is fairly high. Mn, in contrast, was weakly retained by Dowex and the main content was found in the Chelamine extract. However, in both sea and freshwater Mn was found to be complexed also by hydrophobic organic ligands as it was retained by C_{18}.

4. Conclusion

The three-column preconcentration system for fresh-water samples and the two-column system for sea-water samples show very good reproducibility even in complex media. This method gives a different and additional aspect to the already reported procedures for the examination of transition metal speciation in natural conditions, as differentiation between the hydrophobic, anionic and "free" metal composition becomes possible. This system permits one-step preconcentration and speciation determination of transition metals, which hitherto could only be achieved by a time-consuming comparison of several methods.

Acknowledgements

This work was supported by a graduate fellowship awarded to Michael Groschner by the CIES of France in cooperation with the Service Culturel de l'Ambassade de France in Vienna.

References

[1] H.M. Kingston, I.L. Barnes, T.J. Brady and T.C. Rains, Anal. Chem., 50 (1978) 2064.
[2] A.J. Paulson, Anal. Chem., 58 (1986) 183.
[3] S.C. Pai, Anal. Chim. Acta, 211 (1988) 271.
[4] A. Siriraks and H.M. Kingston, Anal. Chem., 62 (1990) 1185.
[5] F. Baffi, A.M. Cardinale and R. Bruzzone, Anal. Chim. Acta, 270 (1992) 79.
[6] S. Blain, P. Appriou and H. Handel, Anal. Chim. Acta, 272 (1993) 91.
[7] Y. Liu and J.D. Ingle, Anal. Chem., 61 (1989) 525.
[8] B.L. Lewis and W.M. Landing, Mar. Chem., 40 (1992) 105.
[9] G.L. Mills and J.G. Quinn, Mar. Chem., 10 (1981) 93.
[10] G.L. Mills and J.G. Quinn, Mar. Chem., 15 (1984) 151.
[11] F. Baffi, M.C. Ianni, A.M. Cardinale, E. Magi and R. Frache, Anal. Chim. Acta, 260 (1992) 99.
[12] Z.S. Liu and S.D. Huong, Anal. Chim. Acta, 267 (1992) 31.
[13] G.L. Mills, A.K. Hanson and J.G. Quinn, Mar. Chem., 11 (1982) 355.
[14] W.G. Sunda and A.K. Hanson, Limnol. Oceanogr., 32 (1987) 537.
[15] L.C. Azeredo, R.E. Sturgeon and A.J. Curtius Spectrochimica Acta, Part B, 48 (1993) 91.
[16] S. Comber, Analyst, 118 (1993) 505.
[17] O.J. Challenger, S.J. Hill and P. Jones, J. Chromatogr., 639 (1993) 197.
[18] J. Vanderdeelen, Anal. Chim. Acta, 49 (1970) 364.
[19] S. Blain, P. Appriou and H. Handel, Analyst, 116 (1991) 815.
[20] Lj. Musani, P. Valenta, H.W. Nürnberg, Z. Konrad and M. Branica, Estuarine Coastal Mar. Sci., II (1980) 639.
[21] G. Capodaglio, Mar. Chem., 29 (1990) 221.
[22] K.W. Bruland, Limnol. Oceanogr., 37 (1992) 1008.
[23] L.J.A. Gerringa, J. Van der Meer and G. Cauwet, Mar. Chem., 36 (1991) 51.
[24] C.M.G. Van den Berg, Mar. Chem., 11 (1982) 307.
[25] C.M.G. Van den Berg, Mar. Chem., 15 (1984) 1.
[26] K.H. Coale and K.W. Bruland, Limnol. Oceanogr., 33 (1988) 1084.
[27] P. Burba, Fresenius' J. Anal. Chem., 341 (1991) 709.

ELSEVIER

Analytica Chimica Acta 297 (1994) 377–386

ANALYTICA CHIMICA ACTA

Chromatographic surfaces prepared from lyso phosphatidylcholine ligands

D. Rhee, R. Markovich, W.G. Chae, X. Qiu, C. Pidgeon *

Department of Medicinal Chemistry, School of Pharmacy, Purdue University, West Lafayette, IN 47907, USA

Received 17 March 1994; revised manuscript received 23 May 1994

Abstract

A chromatographic surface was prepared by immobilizing 1-*O*-(11-carboxyl)undecyl-2-*O*-methyl-*sn*-3-glycerophosphocholine on silica propylamine (loading 127 μmole/g of silica) at a monolayer density. This chromatographic surface is denoted as ^{ether}IAM.PC; this bonded phase is one type of immobilized artificial membrane (IAM) chromatography surface. ^{ether}IAM.PC was endcapped with (1) both decanoic anhydride and propionic anhydride (^{ether}IAM.PC$^{C10/C3}$); or (2) both dodecanoic cyclic anhydride and propionic anhydride (^{ether}IAM.PC$^{C13COOH/C3}$). This latter IAM surface contains carboxyl groups at the interface of the immobilized membrane. ^{ether}IAM.PC columns were evaluated as liquid chromatographic supports using amphetamine analogs under isocratic conditions. After perfusing ^{ether}IAM.PC$^{C13COOH/C3}$ with 50,000 column volumes at pH conditions between pH 2 and pH 8.5, the capacity factors, k', of amphetamine analogs on ^{ether}IAM.PC$^{C13COOH/C3}$ column decreased only 6% of the initial value, whereas ^{ether}IAM.PC$^{C10/C3}$ showed this stability only at the low pH.

Keywords: Liquid chromatography; Immobilized artificial membranes (IAMs); Lyso phosphatidylcholine; Solid phase adsorption synthesis; Lipids

1. Introduction

Immobilized artificial membrane (IAM) chromatography surfaces are prepared by immobilizing analogs of cell membrane lipids on solid surfaces. Cell membrane lipids are amphipathic and contain a polar headgroup and nonpolar fatty acids. IAM chromatographic surfaces were initially described a few years ago [1–5] and several applications for IAM technology are available [6–9]. IAM applications include the purification of several membrane proteins [6,7], the prediction of solute transport across human skin [8], and a method to obtain binding constants of ligands to functional enzymes immobilized on IAM surfaces [1]. All of these earlier studies used IAM surfaces that were prepared by immobilizing double chain phosphatidylcholine (PC) ligands on silica propylamine. For these earlier studies, both of the fatty acid chains of the PC ligands were linked to the glycerol backbone through ester bonds.

Because esters are intrinsically less stable than ether bonds, we prepared PC ligands containing fatty acids linked to the glycerol backbone by ether bonds to improve the stability of the surfaces. In addition to having an ether link between the alkyl chain and the glycerol backbone, the ether PC analogs contain only a single fatty acid group linked to the glycerol backbone instead of two fatty acids. IAMs prepared from single chain PC analogs spontaneously solvate in aqueous media; whereas, IAMs prepared from double chain PCs

* Corresponding author.

SSDI 0003-2670(94)00260-S

do not solvate. Thus IAM surfaces prepared from these single chain phospholipids are more hydrophilic surfaces compared to IAM surfaces prepared from the double chain PC analogs. We have recently performed NMR studies of IAMs prepared from the single chain phosphatidylcholine ligands described in this report [10–12]. This report describes the synthesis of the single chain PC ligand and the bonding strategy used for immobilizing the ligand on silica propylamine surfaces. Preliminary results on the stability of the immobilized ligands are also given.

One of the most interesting applications of the ^{ether}IAM surfaces prepared in this report is in the prediction of drug binding to liposomes, and predicting drug transport through membranes. Our recent studies have demonstrated that ^{ether}IAMs are more convenient models for drug binding and drug transport than all established methods including octanol–water partition coefficients, liposomes, reversed phase liquid chromatographic (LC) columns, Caco-2 cells, and in situ rat intestinal models [8]. Since the main barrier to drug transport is usually a cell membrane, it is not surprising that IAMs are a good model for drug transport. However, from a structural point of view, immobilized single chain ether phospholipids are unrelated to fluid (non-bonded) diacylated phospholipids and it was therefore unexpected that ^{ether}IAM.PC would be able to predict the binding of drugs to fluid membranes. This application of IAMs is in progress and the method will be described in a separate publication along with the mechanism of drug binding to ^{ether}IAMs.

2. Experimental

2.1. Chemicals and reagents

All chemicals were analytical-reagent grade unless stated otherwise. Choline *p*-toluenesulfonate salts were obtained from Sigma (St. Louis, MO) and dried over P_2O_5 for 18 h prior to use. Phosphorus oxychlorides were purchased from Aldrich (Milwaukee, WI) and used as received. Alcohol-free chloroform was purchased as sure-seal bottles from Aldrich. IAM.PC$^{C10/C3}$ used for solid-phase adsorption synthesis was purchased from Regis (Morton Grove, IL). IAM.PC$^{C10/C3}$ is a stable chromatographic matrix that exhibits little or no phospholipid leaching when bathed in organic solvents that are used to facilitate many different chemical reactions. IAM.PC$^{C10/C3}$ is an IAM surface prepared from immobilizing a double chain PC analog. Silica propylamine (12 μm, 300 Å) was purchased from Regis. Several amphetamine analogs were used to test the chromatography of the IAM surfaces; the amphetamine analogs were mescaline, escaline, proscaline, isoproscaline, and buscaline, and they were synthesized by Dr. Nichols in the Department of Medicinal Chemistry. Decanoyl cyclic anhydride was synthesized as described [5]. All reactions were monitored on silica gel 60F 254 thin layer chromatography (TLC) plates purchased from Merck (Darmstadt). Detection methods for TLC were either short-wavelength ultraviolet light, 50% aqueous sulfuric acid solution, Phospray, or ninhydrin.

2.2. NMR spectroscopy

^{1}H NMR spectra were recorded on a Varian VXR-500 spectrometer. For NMR analysis, the compounds were dissolved in D_2O obtained from Aldrich. All ^{1}H NMR spectra were obtained by accumulating 16 scans at 500 MHz and a spectral width of 6000 Hz. Chemical shifts were referenced to HOD (4.67 ppm).

2.3. FTIR spectroscopy

A Nicolet SXC 20 Fourier transform infrared (FTIR) spectrophotometer was used for quantitative measurement of silica-bonded phase. Infrared spectra were obtained using IAM particles pressed into a thin wafer with the microscope in the reflectance mode. Complete details of this technique have been described [13]. We have used this method extensively to characterize many other membrane lipids bonded to silica propylamine [14].

2.4. Elemental analysis

Elemental analysis was performed on a Perkin-Elmer PE 240 in the Microanalysis Laboratory at Purdue University.

2.5. Column packing

^{ether}IAM.PC columns were packed with a Shandon column packer purchased from Keystone Scientific

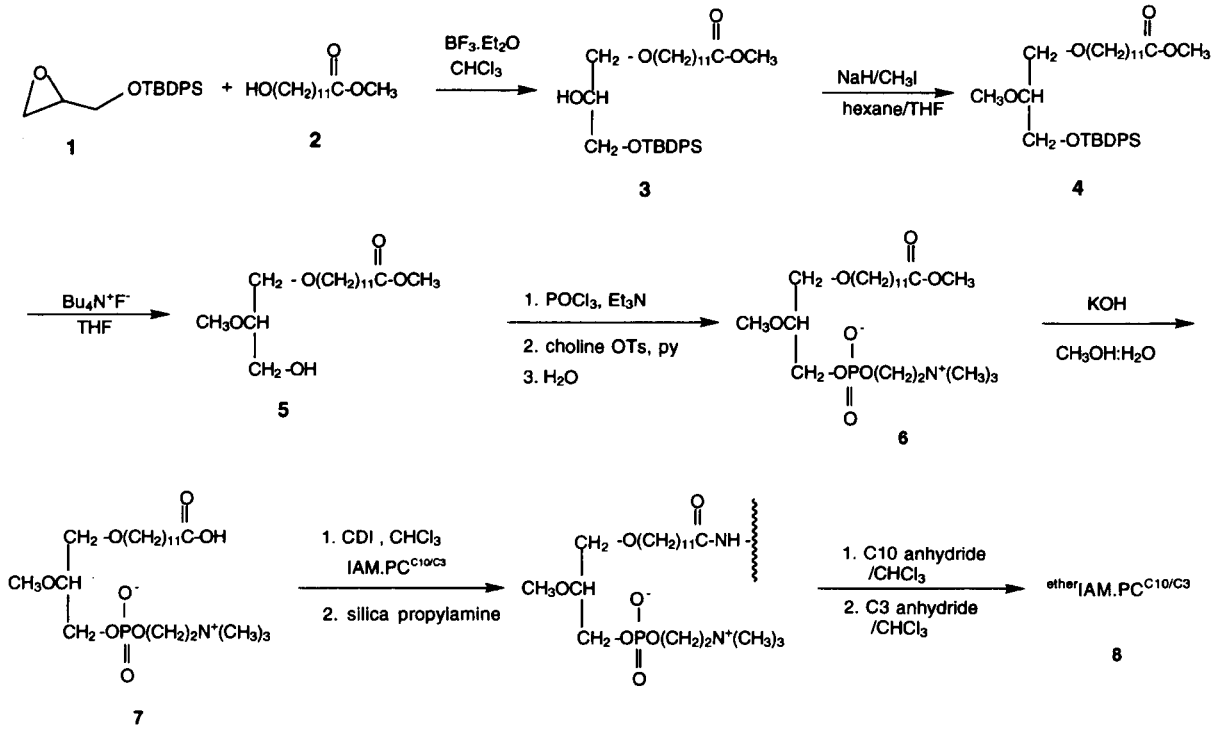

Scheme 1. Synthetic route for preparing ^{ether}IAM.PC$^{C10/C3}$.

(State College, PA). Wet-fill methods were chosen for packing the ^{ether}IAM.PC columns. ^{ether}IAM.PC slurries in acetone (10%, w/v) were packed in 3 cm × 4.6 mm i.d. columns by the down-flow method [15,16].

2.6. LC conditions

A 3 cm × 4.6 mm i.d. IAM column with a void volume or column volume (V_0) of 410 μl was used for all analyses and the amphetamine analogs were detected at 210 nm. The injection volume was always 20 μl of the amphetamine solution (0.1 μg/μl) and the flow rate was either 1 ml/min or 2 ml/min. The buffered aqueous mobile phase contained 0.1 M ammonium phosphate that was pH adjusted using concentrated ammonium hydroxide or phosphoric acid. Chromatograms were obtained using a Rainin LC pumping system interfaced with a Knauer Model 87 detector and a Shimadzu integrator. Other chromatographic conditions are given in the figure legends.

2.7. Synthesis

Scheme 1 shows (i) the synthetic pathway used to prepare the desired single chain ether PC ligand **7** and (ii) the immobilization of the PC ligand to prepare ^{ether}IAM.PC$^{C10/C3}$. The synthesis of 1-*O*-(11-carboxymethyl)-undecyl-2-*O*-methyl-rac-glycerol (**5**) was performed as described [17]. The synthesis of the remaining compounds **6** and **7** is described below.

2.8. 1-O-(11-carboxymethyl)undecyl-2-O-methyl-sn-3-glycerophosphocholine (6)

To a solution of triethylamine (2.52 ml, 0.018 mole) and phosphorous oxychloride (1.6 ml, 0.018 mole) in 120 ml of alcohol-free $CHCl_3$ cooled to 0°C by an ice bath, a solution containing 4.7 g of **5** (0.015 mole) in 120 ml of alcohol-free $CHCl_3$ was slowly added (over 30 min). The reaction mixture was then warmed to room temperature. After stirring another 30 min, choline tosylate (6.11 g, 0.0222 mole) and pyridine (11.69 ml, 0.1479 mole) were added. The reaction mixture was then stirred for 20 h at room temperature. The reaction was quenched with 6.8 ml of water and stirred for 30 min. The solvent was removed under vacuum and the residue was dissolved in 100 ml of dichloromethane–toluene (1:1, v/v), filtered, and concentrated under vacuum. The residue was dissolved in 60 ml of

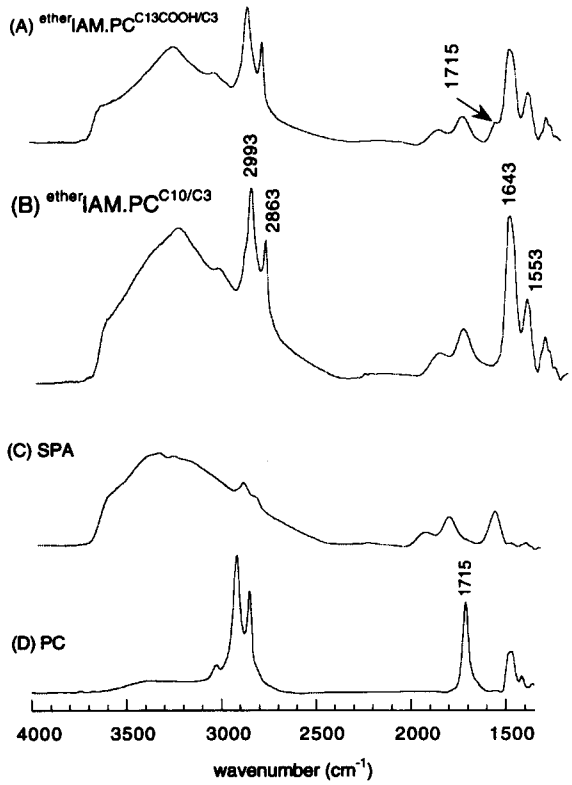

Fig. 1. Infrared spectra of ^{ether}IAM.PC$^{C13COOH/C3}$ (A), phospholipid **7** bonded to SPA (B, ^{ether}IAM.PC$^{C10/C3}$), silica propylamine (C) and phospholipid **7** (D). The characteristic IR band corresponding to the free carboxyl group of phospholipid **7** is at 1715 cm^{-1}. After immobilization of phoshpolipid **7**, this carboxyl band is converted into amide I and amide II bands at 1643 cm^{-1} and 1553 cm^{-1} respectively as shown in the ^{ether}IAM.PC$^{C10/C3}$ spectra (B). As shown in (A), the infrared spectrum of ^{ether}IAM.PC$^{C13COOH/C3}$ shows a band at 1715 cm^{-1} corresponding to the free carboxyl groups on the IAM surface. These carboxyl groups are not present in the IR spectra of ^{ether}IAM.PC$^{C10/C3}$.

tetrahydrofuran (THF)–H_2O (9:1, v/v) and chromatographed on an AG 501-X8 D column using THF–H_2O (9:1, v/v). Then fractions (20×15 ml) were collected. The fractions containing **6** were pooled and the solvent was evaporated to concentrate the crude product. This crude product was applied to a column of silica packed in $CHCl_3$. Elution with $CHCl_3$–MeOH–H_2O (65:35:4, v/v/v) yielded 4.74 g (66%) of **6** as a white solid. TLC ($CHCl_3$–MeOH–H_2O, 65:25:4) R_F 0.36. IR (CaF_2, neat) 3026.0, 2917.3, 2850.8, 1737.3, 1467.3, 1059.4, 1251.7, 1092.2. ^{1}H NMR (500 MHz, D_2O) δ 4.16 (br s, 2 H, $P(O)(O^-)OCH_2$), 3.88 (m, 1 H, CH_2OP), 3.74 (m, 1 H, CH_2OP), 3.54 (s, 3 H, $COOCH_3$), 3.49–3.52 (m, 4 H, $CH_2N^+(CH_3)_3$, OCH_2CH), 3.38–3.43 (m, 3 H, CH_2OCH_2), 3.32 (s, 3 H, $CHOCH_3$), 3.08 (s, 9 H, $N^+(CH_3)_3$), 2.22 (t, 2 H, J=7.5 Hz, $(CH_2)_{10}CH_2CO_2$), 1.44 (m, 4 H, OCH_2CH_2-$(CH_2)_7CH_2CH_2CO_2$), 1.14 (br s, 14 H, $(CH_2)_7$). FAB-MS m/z: 484 (MH^+).

2.9. 1-O-(11-carboxyl)undecyl-2-O-methyl-sn-3-glycerophosphocholine (7)

A MeOH–H_2O (48:6.8, v/v) solution of **6** (4.74 g, 0.0098 mole) and KOH (2.988 g) was stirred at room temperature for 2 h. At this time, 5 ml of H_2O was added to the reaction mixture followed by acidification to pH 3 using formic acid. This mixed solvent of the reaction was dried under vacuum to leave ~5 ml of H_2O. The crude product was desalted by a C_{18} reversed-phase column by loading the acidified product on the C_{18} column, washing with 500 ml of H_2O, and then eluting the product with MeOH. Fractions (~250 ml) were collected and checked for phosphate using Phospray; the column was eluted with MeOH until no Phospray positive spots were detected by TLC. After removing the solvent under vacuum, 4.17 g (91%) of **7** were obtained as a white solid. Compound **7** is PC ω-carboxyl ligand that is suitable for immobilization on many different surfaces. TLC ($CHCl_3$–MeOH–H_2O, 65:25:4) R_F 0.32. IR (CaF_2, neat) 3026.0, 2921.8, 2851.7, 1708.3, 1466.7, 1056.8, 1241.8, 1087.7. ^{1}H NMR (500 MHz, D_2O) δ 4.14 (br s, 2 H, $P(O)(O^-)OCH_2$), 3.87 (m, 1 H, CH_2OP), 3.73 (m, 1 H, CH_2OP), 3.47–3.53 (m, 4 H, $CH_2N^+(CH_3)_3$, OCH_2CH), 3.34–3.42 (m, 3 H, $(CH_2)_{10}CH_2OCH_2$), 3.30 (s, 3 H, $CHOCH_3$), 3.07 (s, 9 H, $N^+(CH_3)_3$), 2.20 (t, 2 H, J=7.5 Hz, $(CH_2)_{10}CH_2CO_2$), 1.42 (m, 4 H, $OCH_2CH_2(CH_2)_7CH_2CH_2CO_2$), 1.14 (br s, 14 H, $(CH_2)_7$). FAB-MS m/z: 470 (MH^+).

2.10. Immobilization of 7 on silica propylamine

A solution of **7** (100 mg, 0.213 mmol) in 0.5 ml of MeOH was adsorbed to 300 mg of IAM.PC$^{C10/C3}$ powder. This is the first step in performing a solid phase adsorption synthesis using IAM surfaces and it is the most critical step for successful activation of the PC ω-carboxyl ligand **7** with CDI. This adsorption step was described in detail [14,18] during the immobilization

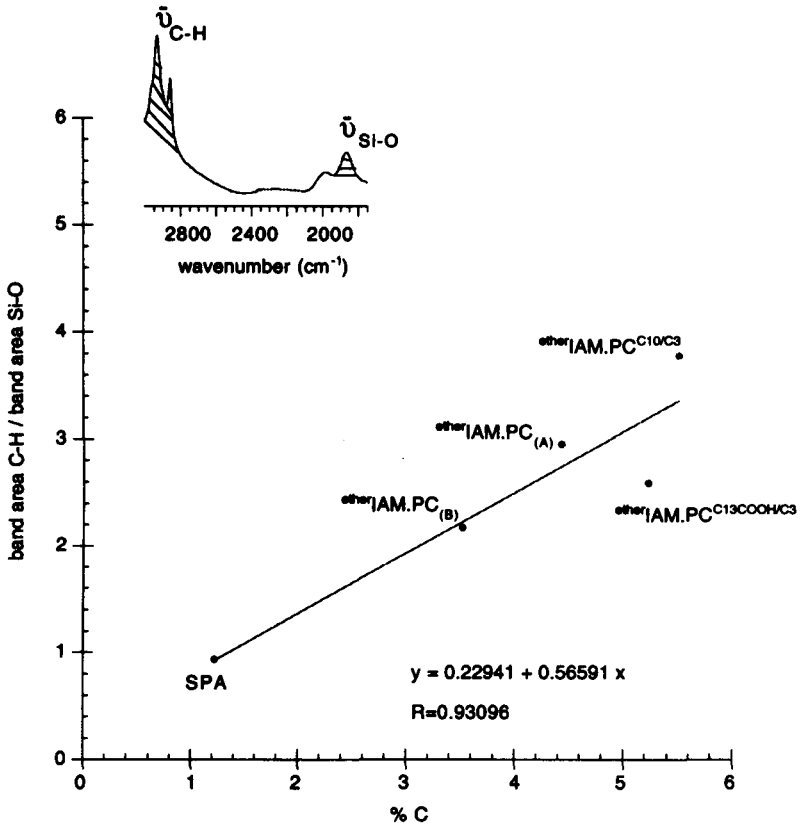

Fig. 2. Correlation between IR analysis and elemental analysis in quantitating the hydrocarbon content of IAM bonded phases. ^{ether}IAM.PC$_{(A)}$ was used for making ^{ether}IAM.PC$^{C10/C3}$ and ^{ether}IAM.PC$_{(B)}$ was used for making ^{ether}IAM.PC$^{C13COOH/C3}$. Complete details for this assay are available [15].

of several ω-carboxyl phospholipid ligands. The MeOH was completely removed by vacuum evaporation. The dried IAM.PC$^{C10/C3}$ chromatographic packing material containing **7** noncovalently adsorbed to the surface was suspended in 10 ml of alcohol-free $CHCl_3$. CDI (41.40 mg, 0.256 mmol) was added to the suspension, and then the suspension was stirred at room temperature for 2 h, filtered through a sintered glass 15F funnel, and washed with 5 ml of alcohol-free $CHCl_3$. TLC developed in $CHCl_3$–MeOH–H_2O (65:25:4, v/v/v) showed that lysolipid **7** (R_F 0.22) was almost completely converted to the phospholipid-imidazolide (R_F 0.37). The combined filtrates were directly added to a 10 ml $CHCl_3$ suspension of silica propylamine (SPA) (1 g) and stirred for 18 h at room temperature. The silica suspension was filtered through a sintered glass 30F funnel, washed with $CHCl_3$, MeOH, and acetone and dried under vacuum. The immobilization was repeated and thus there were two different lots of ^{ether}IAM.PC; one was denoted as ^{ether}IAM.PC$_{(A)}$ and the other one as ^{ether}IAM.PC$_{(B)}$. Elemental analysis of this ^{ether}IAM.PC$_{(A)}$ surface gave C 4.43% and H 0.96% and that of ^{ether}IAM.PC$_{(B)}$ gave C 3.52% and H 0.78%. Elemental analysis of the silica propylamine starting material gave C 1.22% and H 0.93%.

2.11. *Endcapping of ^{ether}IAM.PC*

The residual amines always remain on the SPA surface after bonding compound **7** and these residual amines were end-capped using alkyl anhydride. Thus ^{ether}IAM.PC was suspended in 10 ml of alcohol-free $CHCl_3$ containing decanoic anhydride (0.5 ml, 1.46 mmol) for 18 h at room temperature. The silica was filtered through a sintered glass 15F funnel, washed with $CHCl_3$, THF, CH_2Cl_2, MeOH, and acetone, and dried at 40°C under vacuum to obtain ^{ether}IAM.PC^{C10}

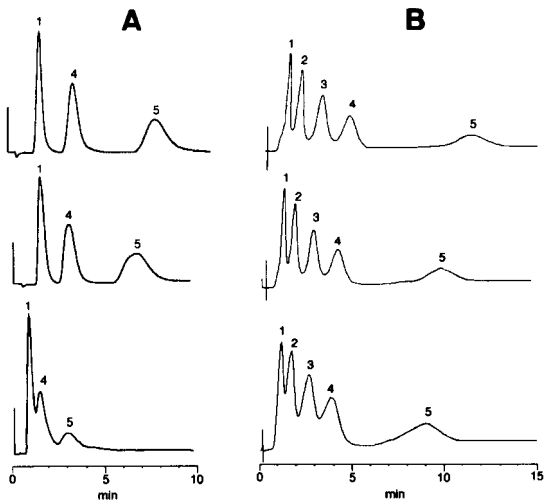

Fig. 3. Isocratic separation of amphetamine analogs on ^{ether}IAM.PC$^{C10/C3}$ (A) and ^{ether}IAM.PC$^{C13COOH/C3}$ (B) columns perfused with acidic and basic mobile phases. All chromatograms were obtained using a pH 7.3 aqueous buffer as mobile phase. The eluting peaks correspond to mescaline (1), escaline (2), isoproscaline (3), proscaline (4), and buscaline (5). The upper chromatograms show the elution profile from an unused column that was equilibrated with pH 7.3 buffer. The middle chromatogram shows the elution profile after perfusing this column with 40,000 column volumes of acidic mobile phase between pH 2–7 and then reequilibrating the column back to pH 7.3 for analysis of retention time. The lower chromatogram shows the amphetamine elution profile after perfusing 10,000 column volumes at pH 8.5 through the IAM column previously challenged with 40,000 column volumes of acidic mobile phase.

(**8a**). The superscript C10 denotes that the surface was endcapped with a C10 alkyl chain. A second endcapping step was performed by stirring the IAM packing material in 10 ml of alcohol-free $CHCl_3$ containing propionic anhydride (0.5 ml, 3.84 mmol) for 18 h at room temperature. The completely endcapped ^{ether}IAM.PC$^{C10/C3}$ chromatographic packing material **8b** was filtered, washed, and dried as described above. Elemental analysis of ^{ether}IAM.PC$^{C10/C3}$ gave C 5.52% and H 1.11%.

2.12. Synthesis of ^{ether}IAM.PC$^{C13COOH/C3}$

^{ether}IAM.PC$^{C13COOH/C3}$ was prepared by endcapping ^{ether}IAM.PC with dodecanoic cyclic anhydride instead of the linear decanoic anhydride. Dodecanoic cyclic anhydride is a large ring cyclic anhydride and ring opening during endcapping results in a carboxyl group at the IAM membrane surface. After endcapping ^{ether}IAM.PC with dodecanoic cyclic anhydride, this surface was end-capped with propionic anhydride as described above. Elemental analysis of ^{ether}IAM.PC$^{C13COOH/C3}$ gave C 5.23% and H 1.01%.

2.13. Stability test

The pH stability of both the ^{ether}IAM.PC$^{C10/C3}$ and the ^{ether}IAM.PC$^{C13COOH/C3}$ chromatographic surfaces were evaluated using amphetamine analogs as test compounds. All retention times of the amphetamine analogs were measured on ^{ether}IAM.PC$^{C10/C3}$ and ^{ether}IAM.PC$^{C13COOH/C3}$ columns at pH 7.3. Thus for the pH stability studies of the IAM surfaces, columns perfused at low pH were re-equilibrated to pH 7.3 for measuring the retention times of the test analytes and then the columns were re-perfused at low pH. Changes in retention times at pH 7.3 were thus used to evaluate the pH stability of the IAM phases. The test conditions involved perfusing 10,000 column volumes (i.e., 10,000 column volumes × 0.46 ml/column volume = 4600 ml) of mobile phase through the IAM column at several different solution pH conditions. The following pH values were used: pH 7.3, pH 5.0, pH 3.0, pH 2.0, and pH 8.5. The capacity factors for the test compounds were calculated using

$$k' = \frac{t_m - t_o}{t_o} \quad (1)$$

where t_m is the retention time in minutes of the test compound and t_o is the retention time of an unretained compound. Retention times were measured in triplicate.

3. Results and discussion

The PC ω-carboxyl ligand **7** is insoluble in $CHCl_3$, THF, ether, benzene, ethyl acetate, toluene, hexane, and acetone. Reacting **7** with CDI could not be done in solution and therefore CDI activation was performed using the solid phase adsorption synthetic procedure developed in our laboratory. The solid phase adsorption synthesis method obviates the need to use aprotic solvents like dimethylsulfoxide (DMSO) and dimethylformamide (DMF) to cosolubilize polar reactants (like **7**) with nonpolar reactants (like CDI). The general strategy is to merely dissolve the polar reactant in protic

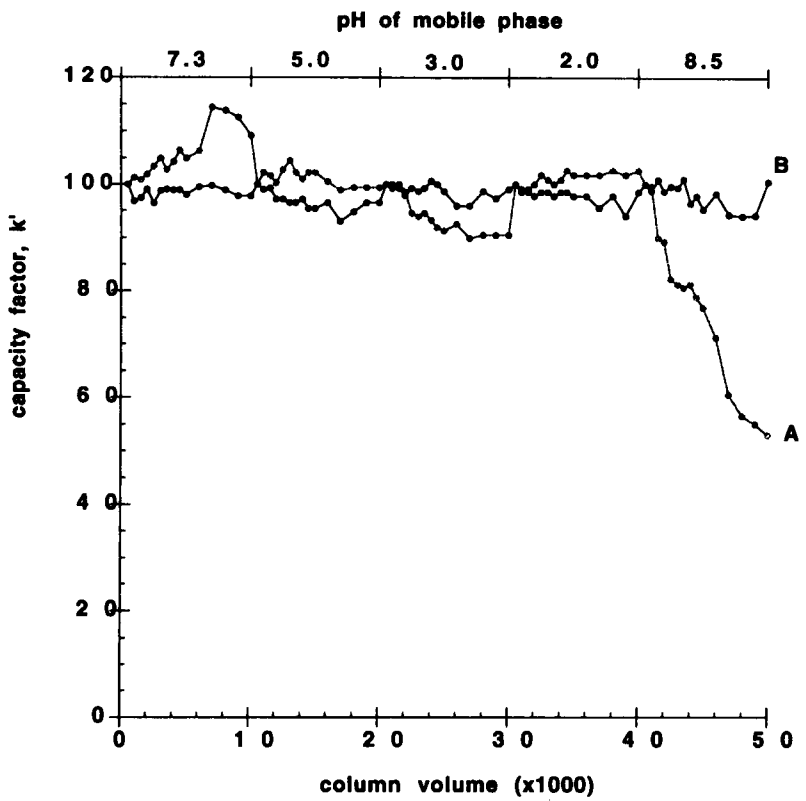

Fig. 4. Stability of ^{ether}IAM.PC$^{C10/C3}$ (A) and ^{ether}IAM.PC$^{C13COOH/C3}$ (B) when challenged with acidic and basic mobile phases. Capacity factors were measured at pH 7.3 as described in the legend of Fig. 3 and also in the Experimental section.

solvent as MeOH and use this solution to load the polar reactant onto the IAM chromatographic surface. After removing MeOH, the chromatographic IAM packing material, containing the polar component adsorbed to the surface is suspended in organic solvent containing the soluble reactants and/or other coupling reagents. We have extensively used the solid phase adsorption method for preparing phospholipids.

Because compound 7 is the polar reactant and CDI is nonpolar, a solution of PC ω-carboxyl 7 (100 mg, 0.213 mmol) in 0.5 ml of MeOH was adsorbed onto 300 mg of IAM.PC$^{C10/C3}$ solid phase. The MeOH was removed (for 16 h at 40°C under vacuum) and then a solution of 41.40 mg of CDI (0.256 mmol) in 10 ml of alcohol-free $CHCl_3$ was used to suspend the IAM.PC$^{C10/C3}$ packing material and initiate the chemical reaction. The suspension was stirred at room temperature for 2 h, filtered, and washed with 20 ml of $CHCl_3$ to obtain imidazolide of phospholipid 7. The IAM.PC$^{C10/C3}$ surface was washed with 20 ml of MeOH to recover unreacted 7 that is insoluble in $CHCl_3$. The convenient recovery of unreacted starting material using the solid phase adsorption synthesis method is a significant advantage over using DMSO to perform the reaction.

When the solid phase synthesis was performed with octadecyl silane reversed-phase surfaces, the CDI activation of 7 was only ~50% completed after 24 h. When phospholipid 7 was stirred in $CHCl_3$ and CDI, only trace amounts of product formed. Thus both the high yields (>95%) and the convenience afforded by solid phase adsorption synthesis using IAM material makes this procedure very useful for coupling polar compounds with nonpolar compounds.

The ^{ether}IAM.PC surface was prepared by reacting the imidazolide of phospholipid 7 with silica propylamine for 18–24 h. Based on both elemental analysis and FTIR analysis of the surface, 127 μmol or 60 mg of lysolipid 7 was bonded per g of SPA (Table 1). ^{ether}IAM.PC is bright blue when sprayed with Phospray

Table 1
Chemical analysis of ^{ether}IAM.PC surface

Surfaces	%C[a]	($\bar{\nu}$C–H/$\bar{\nu}$Si–O) band area [b]	Ligand density (μmol) [c]	%Coverage of amines
Silica propylamine	1.22	0.93	350	
^{ether}IAM.PC	4.43	2.95	127	36.2
^{ether}IAM.PC^{C10}	5.09 [d]	3.45	28	8.0
^{ether}IAM.PC$^{C10/C3}$	5.52	3.78	60	17.1

[a]The %C values were measured from elemental analysis.
[b]The ($\bar{\nu}$C–H/$\bar{\nu}$Si–O) band areas were measured from FTIR analysis.
[c]The ligand density was calculated from;

$$\Delta\%C = \frac{xCm}{(1+x)} \times 10^6 (\mu\text{mol})$$

where, x is the ligand density, $\Delta\%C$ is the net carbon gain from elemental analysis, and Cm is the carbon content per PL molecule.
[d]Obtained from Fig. 1.

that indicates a high surface density of phospholipids, but this surface is ninhydrin positive indicating that residual amines remain on the floor of the ^{ether}IAM.PC surface. FTIR analysis of the surface indicated that ~36.2% of the silica propylamines were reacted. Consequently ^{ether}IAM.PC was endcapped with decanoic anhydride to form ^{ether}IAM.PC^{C10} that was still slightly ninhydrin positive. FTIR analysis indicated that the hydrocarbon content increased 0.5 so that ~50% of the residual amines remained. Thus ^{ether}IAM.PC^{C10} was further endcapped with propionic anhydride to form ^{ether}IAM.PC$^{C10/C3}$ that was ninhydrin negative. Infrared analysis indicated that ~30% of the unreacted silica propyl amines are not accessible to the bonding ligands. In other words, 30% of the residual amines reside in small crevices in the silica surface; the ω-carboxyl PC ligands can not enter the small crevices. Small crevices in the silica matrix used to prepared IAMs have been extensively discussed [14]. ^{ether}IAM.PC$^{C10/C3}$ thus has no residual amines, a high density of immobilized ligands and the silica floor is chemically neutral compared to IAM.PC bonded phases.

During our earlier studies we prepared IAMs from double chain PC carboxyl ligands instead of single chain PC carboxyl ligands that are described in this report. After endcapping, IAMs prepared from double chain PC analogs do not solvate in aqueous media. However, ^{ether}IAM.PC$^{C10/C3}$ is a completely endcapped IAM prepared from a single chain PC analog that spontaneously wets when suspended in aqueous media. This ability of aqueous media to solvate the IAM surface is significant regarding the ability of the IAM surface to emulate artificial membranes. Liposomes are artificial membranes prepared in aqueous media and the liposome surface is hydrophilic.

^{ether}IAM.PC$^{C10/C3}$ and ^{ether}IAM.PC$^{C13COOH/C3}$ were analyzed by FTIR reflectance microscopy (Fig. 1). The main purpose of the IR analysis was to (i) confirm covalent bonding (i.e., amide bond formation) of the single chain PC ligand to silica propylamine and (ii) confirm the presence of surface carboxyls on the ^{ether}IAM.PC$^{C13COOH/C3}$ surface. In Fig. 1, the amide I and amide II bands at 1643 cm^{-1} and 1553 cm^{-1} respectively, confirm the presence of an amide link, i.e., the formation of a covalent bond between the ω-carboxyl PC ligand and the silica surface amines. Fig. 1 also clearly shows the intense carbonyl band at 1715 cm^{-1} indicating ^{ether}IAM.PC$^{C13COOH/C3}$ surface contains free carboxyl groups on the membrane surfaces. The IR spectra of silica propylamine particles before and after coupling with the single chain PC ω-carboxyl ligand show intense bands at 2993 cm^{-1} and 2863 cm^{-1} which are due to the alkyl chains of the immobilized PC ligands. These bands can be sued to quantitate the amount of PC immobilized (Fig. 2).

The chromatographic profile of amphetamine analogs on ^{ether}IAM.PC$^{C10/C3}$ and ^{ether}IAM.PC$^{C13COOH/C3}$ perfused at several pH conditions is shown in Fig. 3. There is little change in the retention times of the test solutes after perfusion of 40,000 column volumes of low pH mobile phase through the ^{ether}IAM.PC$^{C10/C3}$ column. However, after perfusing 10,000 column volumes of pH 8.5 mobile phase through the

Table 2
Summary of mobile phase effects in ^{ether}IAM.PC$^{C10/C3}$ LC columns[a]

		V_e	V'_R	k'
Escaline	A	1,77	1.36	3.27
	B	1.63	1.22	2.93
	C	0.88	0.56	1.78
Proscaline	A	3.64	3.23	7.78
	B	3.2	2.78	6.71
	C	1.49	1.17	3.70
Buscaline	A	8.23	7.82	18.82
	B	7.02	6.61	15.92
	C	3.00	2.68	8.46

[a]Values of A, B, C were obtained as same conditions as Fig. 3; (A) 1st injection, (B) after perfusing 40,000 column volume under acidic conditions, and (C) after perfusing B followed by 10,000 column volume at pH 8.5.

^{ether}IAM.PC$^{C10/C3}$ column, the ^{ether}IAM.PC$^{C10/C3}$ LC column exhibited significantly decreased resolution of the test compounds. Thus at low pH mobile phase conditions, k' of the amphetamine analogs decreased only 15%; whereas, at basic pH conditions, the k' decreased 50% (compare middle and lower spectra in Fig. 3). Table 2 summarizes elution volumes (V_e), adjusted retention volumes (V'_R), and capacity factors (k') for each test compound subjected to chromatography on ^{ether}IAM.PC$^{C10/C3}$ surfaces.

Amphetamine chromatography using ^{ether}IAM.PC$^{C13COOH/C3}$ surfaces (Fig. 3B) was obtained under identical conditions as those on ^{ether}IAM.PC$^{C10/C3}$ surfaces (Fig. 3A). As shown in Fig. 3B, acid stability of both columns is similar but the ^{ether}IAM.PC$^{C13COOH/C3}$ column is much more stable at elevated pH conditions compared to the stability of ^{ether}IAM.PC$^{C10/C3}$ at elevated pH conditions. This is clearly shown by comparing the elution profiles for each column (compare the bottom chromatograms in Fig. 3). The k' values for amphetamine decreased by only 6% after perfusing 10,000 column volumes of pH 8.5 through ^{ether}IAM.PC$^{C13COOH/C3}$, whereas on the ^{ether}IAM.PC$^{C10/C3}$ column, the k' decreased by ~50% under identical conditions.

Table 3 summarizes V_e, V'_R and k' values for each test compound for chromatography on ^{ether}IAM.PC$^{C13COOH/C3}$. Fig. 4 shows a typical plot of the pH dependence of capacity factor for ^{ether}IAM.PC$^{C10/C3}$ (Fig. 4A) and ^{ether}IAM.PC$^{C13COOH/C3}$ (Fig. 4B). The stability of the acidic IAM surface, ^{ether}IAM.PC$^{C13COOH/C3}$, to elevated pH is apparent as no change in capacity factor was observed (Fig. 4B).

Table 3
Summary of mobile phase effects in ^{ether}IAM.PC$^{C13COOH/C3}$ LC columns[a]

		V_e	V'_R	k'
Mescaline	A	2.40	2.00	5.00
	B	2.30	1.90	4.75
	C	2.30	1.90	4.75
Escaline	A	3.78	3.38	8.45
	B	3.55	3.15	7.88
	C	3.43	3.03	7.58
Isoproscaline	A	6.26	5.86	14.64
	B	5.68	5.28	13.2
	C	5.32	4.92	12.28
Proscaline	A	9.48	9.08	22.70
	B	8.32	7.92	19.8
	C	7.67	7.27	18.18
Buscaline	A	24.00	23.60	59.00
	B	20.32	19.92	49.80
	C	17.79	17.39	43.48

[a]Values of A, B, C were obtained as same conditions as Fig. 3; (A) 1st injection, (B) after perfusing 40,000 column volume under acidic conditions, and (C) after perfusing B followed by 10,000 column volume at pH 8.5.

Acknowledgements

We are very grateful for the support from Eli Lilly and Company. This work was also supported by NSF (CTS 9214794), NIH (AI 33031), and Regis Chemical Company (2R446M3022-02).

References

[1] C. Pidgeon, C. Marcus and F. Alvarez, in J.W. Kelly and T.O. Baldwin (Eds.), Applications of Enzymes in Biotechnology, Plenum Press, New York, 1991.
[2] C. Pidgeon, U.S. Pat., 4,931 (1990) 498.
[3] C. Pidgeon, Enz. Microb. Technol., 12 (1990) 149.
[4] C. Pidgeon, U.S. Pat., 4,927 (1990) 879.
[5] C. Pidgeon and U.V. Venkatarum, Anal. Biochem., 176, (1989) 36.
[6] W.G. Chae, C. Luo, D. Rhee, C.R. Lombardo, P. Low and C. Pidgeon, N.H. Fischer, M.B. Isman and H.A. Stafford (Eds.), Modern Phytochemical Methods, Plenum Press, New York, 1991.

[7] S. Otto, C. Marcus, C. Pidgeon and C. Jefcoate, Endocrinology, 129 (1991) 970.
[8] F.M. Alvarez, C.B. Bottom, C. Prashant and C. Pidgeon, Immobilized Artificial Membrane Chromatography Prediction of Drug Transport across Biological Barriers, Plenum Press, New York, 1993; C. Pidgeon et al., unpublished results
[9] R.J. Markovich, X. Qiu, D.E. Nichols, C. Pidgeon, B. Invergo and F.M. Alvarez, Anal. Chem., 63 (1991) 1851.
[10] X. Qiu and C. Pidgeon, J. Phys. Chem., 97 (1993) 12399.
[11] X. Qiu, D. Rhee and C. Pidgeon, Preparation of Lipid Membranes for use in Separation Science: IAM Chromatography, in U.J. Krull and D.P. Nikolelic (Eds.), Biophysics of Organized Lipid Membranes for Applications in Chemical Analysis, Plenum Press, New York, 1994.
[12] S. Ong, X. Qiu and C. Pidgeon, J. Phys. Chem., (1994) in press.
[13] R.J. Markovich, J.M. Stevens and C. Pidgeon, Anal. Biochem., 182 (1989) 237.
[14] S. Ong, S.J. Cai, C. Bernal, D. Rhee, X. Qiu and C. Pidgeon, Anal. Chem., 66 (1994) 782.
[15] R.E. Majors, Anal. Chem., 44 (1972) 1722.
[16] J.J. Kirkland, J. Chromatogr. Sci., 9 (1971) 206.
[17] X. Qiu, S. Ong, C. Bernal, D. Rhee and C. Pidgeon, J. Org. Chem., 59 (1993) 537.
[18] C. Pidgeon, R. Markovich, M. Liu, T. Holzer, R. Novak and K. Keyer, J. Biol. Chem., 268 (1993) 7773.

ELSEVIER

Analytica Chimica Acta 297 (1994) 387–403

ANALYTICA CHIMICA ACTA

Automated detection of methanol vapour by open path Fourier transform infrared spectrometry

Arjun S. Bangalore [a], Gary W. Small [a,*], Roger J. Combs [b], Robert B. Knapp [b], Robert T. Kroutil [b]

[a] *Center for Intelligent Chemical Instrumentation, Department of Chemistry, Clippinger Laboratories, Ohio University, Athens, OH 45701-2979, USA*

[b] *U.S. Army Edgewood Research, Development and Engineering Center, Aberdeen Proving Ground, MD 21010-5423, USA*

Received 17 January 1994; revised manuscript received 19 May 1994

Abstract

Signal processing techniques are developed to detect the presence of methanol vapour in an open path Fourier transform infrared (FTIR) measurement. An automated detection algorithm is implemented through the direct application of digital filtering and pattern recognition methods to short segments of FTIR interferograms. To test the data analysis methodology, a pollutant source of methanol vapour is simulated by the use of open air active bistatic, passive terrestrial, and passive laboratory spectrometer configurations. Approximately 30,000 interferograms collected from these experiments are used in optimizing and testing the digital filtering and pattern recognition techniques. Interferogram segment lengths ranging from 40 to 150 points are evaluated, along with different segment starting positions and filter bandpass widths. Interferogram segments as short as 40 points (0.01 cm optical retardation) are found to yield detection percentages approaching 100%. These results are achieved while maintaining an extremely low rate of false detections (0.5%).

Keywords: Infrared spectrometry; Fourier transform; Automated detection of methanol vapour; Open path FTIR spectrometry

1. Introduction

Open path Fourier transform infrared (FTIR) spectrometry is a technique of increasing importance for the remote detection of airborne pollutants [1]. A potential new application for this technology is the measurement of products formed through incomplete combustion of oxygenated automotive fuels. These fuels are finding increasing use in major cities due to their attractive properties in reducing smog production [2,3].

One combustion product of interest is methanol. Assessing the environmental impact of methanol production during combustion requires methodology to identify and quantitate methanol in the atmosphere [4]. The purpose of this study is to assess the feasibility of open path FTIR spectrometry for use in detecting methanol vapour.

Traditional open path FTIR measurements require a reference spectrum of the infrared background present in the field of view of the spectrometer for use in removing background features from sample spectra [1,5]. This background spectrum is an emission profile with contributions from the infrared radiation source, the intervening atmosphere, and the instrumental response

* Corresponding author.

SSDI 0003-2670(94)00246-I

function of the spectrometer [6]. The normal variation of meterological conditions and the possible use of an ambient temperature infrared source often preclude the collection of a stable (i.e., representative) background spectrum, however.

Recent work in our laboratories has focused on overcoming this limitation through the use of a novel strategy for removing contributions from the infrared background without a separate background spectral measurement [6,7]. This approach is based on a combination of digital filtering and pattern recognition techniques applied directly to short segments of interferogram data collected by the spectrometer. The digital filtering step isolates in the interferogram those frequencies pertaining to a spectral band of the target analyte, while the pattern recognition step attempts to use the filtered interferogram signal as a signature in determining the presence or absence of the target analyte. Previous studies have demonstrated the effectiveness of this methodology in eliminating contributions from the infrared background as well as from the adjacent spectral bands of interfering compounds [8,9].

In previous work, this interferogram-based data analysis approach has proven effective in detecting SF_6, acetone, 2-butanone, CCl_3F (Freon 11), and CCl_2F_2 (Freon 12) [6–9]. The detection of each of these compounds was performed through the use of a single narrow spectral band in the region of 800–1200 cm^{-1}. The wide (full-width at half-height (FWHH) $\approx 69\ cm^{-1}$) C–O stretching band of methanol at 1034 cm^{-1} presents a fundamentally different spectral signature for use in testing the interferogram-based analysis [10]. This band is wider than those used previously, and it exhibits a different band contour due to the presence of the RQP branches arising from changes in rotational state coupled to the vibrational transition. An important consideration in applying the interferogram-based methodology to the detection of methanol is the impact of this difference in band width and band contour on the analysis. Furthermore, the use of a short interferogram segment for the detection eliminates the high resolution rotational fine structure of the methanol spectrum often used in traditional gas-phase infrared analyses. Demonstrating the ability to detect methanol vapour without high resolution spectral information is another important goal of this work.

To allow these issues to be addressed, a pool of approximately 30,000 FTIR interferograms was assembled based on three different spectrometer configurations. This set of interferogram data was used to optimize and test the interferogram-based methanol detection and to study key experimental variables involved in the analysis. Through this work, this paper assesses the overall feasibility of open path FTIR spectrometry to implement automated detections of methanol vapour sources.

2. Experimental

2.1. Instrumentation

This investigation employed the Midac Outfielder FTIR emission spectrometer (Unit 120) with a Newtonian telescope and a remote infrared source (Midac, Irvine, CA). The spectrometer has a 6° field of view (FOV) which is reduced to approximately 0.3° through the use of the telescope. This allows the FOV to be filled with the infrared source for a 100 m path distance between the source and spectrometer. The 2000 cm^2 aperture metal paraboloid of the infrared source collimates the 1550 K radiation from a silicon carbide heater element. The spectrometer employs a Hg:Cd:Te infrared detector designed to respond over the spectral range of 800 to 1400 cm^{-1}.

In this study, the interferometer mirror velocity used was 2.454 ± 0.005 mm/s [11]. The spectrometer was interfaced to a Dell System 486P/50 IBM PC compatible computer (Dell Computer, Austin, TX) operating under MS-DOS (Microsoft, Redmond, WA). Data acquisition was performed with the MIDCOL software package [12]. Interferogram points were collected at every eighth zero crossing of the helium neon (HeNe) reference laser, resulting in a maximum spectral frequency of 1975 cm^{-1}. A total of 1024 sampled interferogram points permitted calculation of spectra with a point spacing of approximately 4 cm^{-1}.

2.2. Methods

Interferogram data were acquired with three spectrometer configurations [8]. These spectrometer configurations are presented schematically in Fig. 1, and are termed active bistatic, passive terrestrial, and passive laboratory. In the active bistatic configuration, the infrared source was positioned approximately 30 m

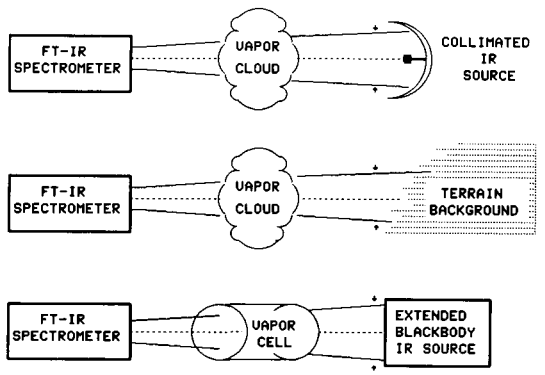

Fig. 1. FTIR spectrometer configurations for data collection: (A) active bistatic, (B) passive terrestrial, and (C) passive laboratory.

from the spectrometer. The source was operated at temperatures significantly lower than 1550 K (12 V) by placing lower voltages of 1, 2, 6, and 8 V across the heater element. For a significant reduction in the infrared source voltage (i.e., radiance), the resulting spectral response becomes similar to that of the passive terrestrial configuration.

The passive terrestrial configuration replaces the infrared source with an ambient background terrain radiance. The radiance difference between the ambient background and sample vapour is often small. This small radiance difference is usually the controlling vapour detection parameter. Spectral vapour detection with a FTIR spectrometer requires a radiance difference between the vapour and the infrared background source [6]. For the active bistatic and passive terrestrial spectrometer configurations, reagent grade methanol (Oriole Brand chemicals, Warner-Graham, Baltimore, MD) was disseminated by static evaporation. Some of the data were also collected while acetone and 2-butanone were released. No attempts were made to measure the concentrations of any of the compounds present in the open path measurements.

The passive laboratory configuration simulates the conditions of the passive terrestrial measurements in a controlled laboratory environment. In this experiment, the telescope was removed from the optical train and an ambient temperature vapour cell was used to contain the methanol sample. The cell had a 62 cm^2 aperture and 8.2 cm path length.

Various aqueous solution mixtures of methanol were evaporated into the vapour cell. The solutions were prepared by mixing spectral grade methanol (Fisher, Pittsburgh, PA) and deionized water. The aqueous alcohol dilution factors ranged from 1/2 to 1/64 corresponding to approximate methanol vapour pressures from 72.7 to 4.1 Torr at 25°C [13]. Assuming ideal gas behaviour and taking into consideration the 8.2 cm path length of the gas cell, the products of concentration and path length for the methanol samples ranged from 7181 to 405 ppm-m. The units of ppm-m are used here for consistency with the standard reporting practices for open path measurements. Table 1 shows the number of interferograms collected with the various dilution factors as a function of the near ambient blackbody temperature. The relatively low methanol vapour pressures produced spectra with band contours quite similar to those obtained from the passive terrestrial measurements.

A 4 × 4-inch extended blackbody (Model SR-80, CI Systems, Agoura, CA) was used to obtain an adjustable infrared temperature source from 5 to 50°C. The blackbody supplies a NIST traceable infrared source accurate to ± 0.03°C and precise to ± 0.01°C. A HeNe laser was used to align the optical train of the FTIR spectrometer, vapour cell, and extended blackbody by use of multiple reflections from the beamsplitter of the interferometer. Separation distances of components along the optical path were approximately 6 cm between spectrometer and cell, and 11 cm between cell and blackbody. These distances ensured that the 62 cm^2 vapour cell aperture was within the spectrometer FOV and that only the 4 × 4-inch extended blackbody was viewed by the spectrometer.

2.3. Data analysis

All computer processing of the interferogram data was completed on a Silicon Graphics 4D/460 R3000 computer using the Irix operating system, version 4.0.5. (Silicon Graphics, Mountain View, CA) The computer included 128 megabytes of main memory, 5 gigabytes of disk storage, and 6 CPU processors. All of the data analysis software was written in Fortran 77. The software was compiled with version 3.4.1 of the Silicon Graphics Fortran 77 compiler with optimization level 3 being used. Fourier transform and multiple linear regression computations performed as part of the digital filter design work made use of subroutines from the IMSL package (IMSL, Houston, TX).

Table 1
Experimental parameters for passive laboratory data set

Blackbody temperature (°C)	Dilution factor					
	1/2	1/4	1/8	1/16	1/32	1/64
Training set						
50	16[a] (32[b])	16 (32)	16 (31)	16 (32)	16 (32)	144 (160)
45	16 (32)	16 (32)	16 (32)	16 (32)	16 (32)	16 (32)
40						114 (128)
35	16 (32)	16 (32)	16 (32)	16 (32)	16 (32)	13 (32)
30	16 (32)	16 (32)	16 (32)	16 (32)	144 (160)	
28				64 (128)		
27				64 (128)		
26	14 (32)	12 (32)	16 (32)	55 (128)		
25		12 (32)				
22			16 (32)			
20	13 (32)	16 (32)			70 (128)	
15	16 (32)	16 (32)	16 (33)	16 (32)	16 (32)	
10	16 (32)	16 (33)	16 (33)	16 (32)	16 (32)	66 (161)
5						89 (128)
Prediction set						
40	16 (32)	16 (32)	16 (32)	16 (32)	16 (32)	13 (32)
28	16 (32)	16 (32)	16 (32)	16 (32)	263 (128)	
26.5				33 (128)		
25.5				58 (128)		
22		16 (32)				
20			16 (32)		16 (32)	
15	16 (32)				266 (128)	
5		19 (32)	17 (32)	16 (32)	16 (32)	16 (32)

[a]Number of methanol-containing interferograms collected.
[b]Number of background interferograms collected.

2.4. Assembly of data

Laboratory data collected under simulated remote sensing conditions were analyzed separately from the field data. Both data sets have methanol-containing and background interferograms. The classification of each interferogram as methanol-containing or not was performed by Fourier processing the interferogram to obtain the single-beam spectrum and subtracting a background spectrum known to contain no methanol features. If clear evidence of a methanol spectral band was observed, the corresponding interferogram was judged methanol-containing. Interferograms not meeting this criterion were classified as backgrounds. Some interferograms could not be judged with confidence. These interferograms were removed completely from the analysis.

Each of the data sets was sub-divided into training and prediction data sets. The training data set was used to optimize the digital filtering and pattern recognition components of the interferogram-based data analysis. The prediction data set was withheld from these computations and was used as an independent test set for determining the rate of positive and missed detections, as well as the rate of false detections.

The training and prediction sets for both the laboratory and the field data were assembled using different procedures. For the laboratory data, the training and prediction sets were assembled by use of 24 data files that contained a total of 5914 interferograms. Each file contained several sets of interferograms. As indicated in Table 1, each set was collected under specific conditions of source temperature and methanol concentration. Alternate data sets in each file were included in

Table 2
Description of methanol laboratory data

Set	Methanol-Containing interferograms	Background interferograms	Total
Training set	1402	2467	3869
Prediction set	925	1120	2045
Total	2327	3587	5914

the training set. The remaining sets were included in the prediction data set. This procedure ensured that different spectral backgrounds and methanol signal strengths were present in the training and prediction sets. Table 2 summarizes the training and prediction data sets formed from the laboratory data.

For the field data, a procedure developed by Carpenter and Small [14] was used for the selection of optimal training and prediction sets. The training and prediction sets were mutually exclusive. The full field data set had 62 data files containing a total of 30,772 interferograms. Table 3 summarizes the training and prediction sets selected from the pool of field data. The distribution of interferograms from the active bistatic and passive terrestrial spectrometer configurations is also indicated in Table 3.

3. Discussion and results

In an open path FTIR measurement, the spectral bands of any infrared-active species present are superimposed on the infrared background emission detected by the spectrometer. The success of any automated detection scheme for a target analyte such as methanol is determined by the degree to which the spectral signature of the analyte can be extracted from the other information present.

In this study, the C–O stretching vibration centered at 1034 cm^{-1} was used as a characteristic spectral signature for the detection of methanol. The literature band position of 1034 cm^{-1} agrees with our experimental determination of 1035 cm^{-1}. The absorption is relatively strong, with a peak absorption coefficient of 25 cm^{-1} atm^{-1} [3]. As noted previously, the FWHH of the band is approximately 69 cm^{-1}, and it exhibits an RQP band shape formed by the superposition of vibrational and rotational transitions. The contour of this band is observed in the absorbance spectra displayed in Fig. 2A and B, although the rotational fine structure normally observed in gas-phase methanol spectra is missing due to the limited spectral resolution. The Q-branch of the band is indicated by an arrow in each spectrum. The displayed spectra were obtained by Fourier processing interferogram data collected by the spectrometer. For the data collection, the spectrometer was operated in the active bistatic configuration at two different source radiances (6–8.1 and 2 V). The Fourier processing step included Mertz phase correction and triangular apodization. The computed single-beam spectra were ratioed to a similarly processed background spectrum, and the resulting transmittance values were converted to absorbance to produce spectra with units familiar to the laboratory spectroscopist.

An inspection of the spectra in Fig. 2 reveals that both absorption and emission spectral features are observed and that a wide range of band intensities are encountered. In absorbance units (AU), absorption transitions are observed as positive spectral features, while emissions occur as negative features. The peak intensity of the strong absorption feature in Fig. 2A is approximately 0.3 AU, while the weak emission band in Fig. 2B has a peak intensity of approximately −0.006 AU. Clearly, an effective detection scheme for methanol must be able to extract both absorption and emission signals across a large range of band intensi-

Table 3
Description of methanol field data

Set	Methanol-containing interferograms		Background interferograms		Total
	Total	Active/passive	Total	Active/passive	
Training set	1228	685/543	6000	2179/3821	7228
Prediction set	615	181/434	22929	6026/16903	23544
Total	1843	866/977	28929	8205/20724	30772

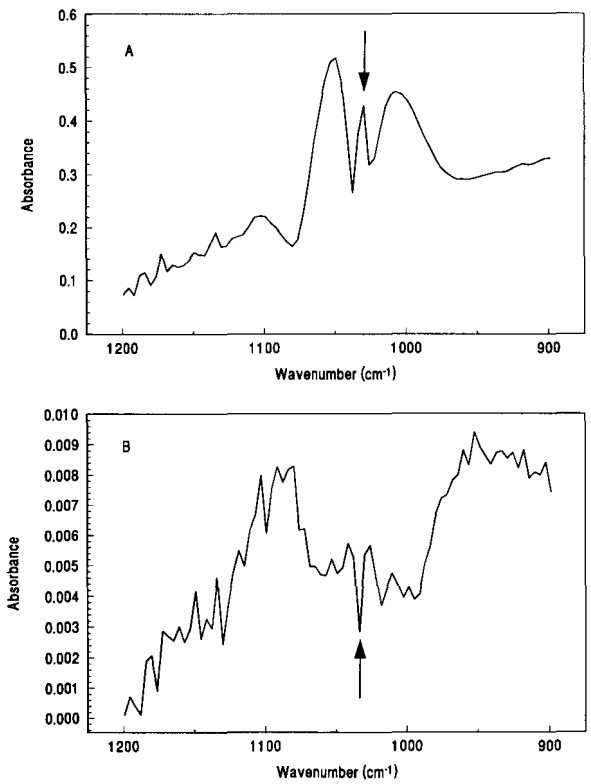

Fig. 2. Remote sensing absorbance spectra of methanol collected by a commercial Midac FTIR instrument (field data): (A) strong absorption spectrum, (B) weak emission spectrum. The arrows denote the Q-branch of the methanol C–O stretch.

ties. In addition, the detection must be performed in the presence of significant baseline variation in the computed spectra. Baseline variation is caused by a mismatch between the sample and background spectra that are ratioed. This mismatch results from a change in the infrared background emission between the two measurements. Baseline variation of the type observed in Fig. 2 is often encountered even when spectra collected consecutively are ratioed.

3.1. Overview of data analysis methodology

The data analysis methodology used in this work was developed to overcome the problems in extracting analyte spectral signals that were illustrated in Fig. 2. The approach is based on the direct application of digital filtering and pattern recognition methods to analyze short segments of FTIR interferograms.

The digital filtering step is designed to extract only those frequencies from the interferogram that are associated with the targeted spectral band of the analyte (e.g., the 1035 cm^{-1} C–O stretching band of methanol). The interferogram is reduced to a superposition of a series of sinusoidal waveforms corresponding to the specific frequencies that are passed by the digital filter. The digital filter bandpass is defined in the spectral domain and suitable filter design methods are used to construct an interferogram-domain filter with the same frequency response.

In the interferogram-based analysis, no separate measurement of the infrared background is required, thereby eliminating all of the issues discussed above regarding the match between background and sample measurements. Since no background measurement is used, an alternate method must be employed to remove signatures from the data that are not related to methanol. Signatures at spectral frequencies outside the region of 1035 cm^{-1} are removed by the filter. Background signatures within the filter bandpass are removed by windowing the interferogram to select an appropriate segment for use in the analysis.

The windowing procedure can be understood by considering that the interferogram, after digital filtering, is reduced to contain only information about the spectral features that lie within the frequency bandpass of the filter. These features have different widths and thus, their waveform representations in the interferogram damp at different rates. The infrared background can be considered as a wide spectral feature that, through the application of the filter, has been truncated to the same width as the filter bandpass. The interferogram representation of this wide feature will damp faster than the corresponding representation of the analyte band. Thus, beyond some point in the interferogram, the interferogram representation of the infrared background will have damped nearly to zero while the information describing narrow spectral features remains. The information describing the narrow spectral bands consists of contributions from the analyte band, as well as nearby bands associated with any interfering compounds present. Therefore, judicious choice of the interferogram segment allows much of the infrared background information to be removed.

The pattern recognition step implements an automated method to determine if the interferogram signature extracted by the digital filter actually

corresponds to the target analyte rather than to some interfering species. The position of the spectral band within the digital filter bandpass and the shape of the band are both reflected in the profile of the filtered interferogram segment. The pattern recognition step allows the intensity and shape of the interferogram segment to be used in deciding if the analyte is present.

3.2. Digital filter design

The implementation of a digital filter in the interferogram domain requires the evaluation of the convolution of the interferogram and the interferogram-domain representation of the filter frequency response function. This filter representation is termed the impulse response of the filter. The impulse response and frequency response are Fourier transform pairs. Various strategies can be employed to approximate the convolution. The method employed in this study is an implementation of a finite impulse response (FIR) digital filter with time-dependent coefficients [15]. Separate FIR filters are used in approximating the convolution at each interferogram point. This filter design scheme has been termed a finite impulse response matrix (FIRM) filter due to the matrix of individual filters required. The application of the FIRM filter can be represented as

$$X'_j = \sum_{i=j-100}^{j} h_{i,j} X_i \qquad (1)$$

where the intensity of point j in the filtered interferogram, X'_j, is computed from a sum of terms. Each term in the sum is based on the intensities of specific points in the unfiltered interferogram, relative to point j (the X_i), and a set of filter coefficients, $h_{i,j}$. The $h_{i,j}$ values approximate the impulse response of the filter. The presence of the subscript, j, on the $h_{i,j}$ term reflects the time-dependent (i.e., interferogram-point dependent) nature of the FIRM filter. The impulse response matrix defined by the $h_{i,j}$ contains non-zero values for only those X_i that have been determined significant in approximating the convolution. The FIRM filter design employs regression analysis techniques to compute the $h_{i,j}$ and to determine the significance of the X_i. A statistical F test at the 99.99% level is used in the regression to determine which X_i are included. For the filters generated to extract methanol signals, the number of non-zero filter terms varied over the range of 24–30.

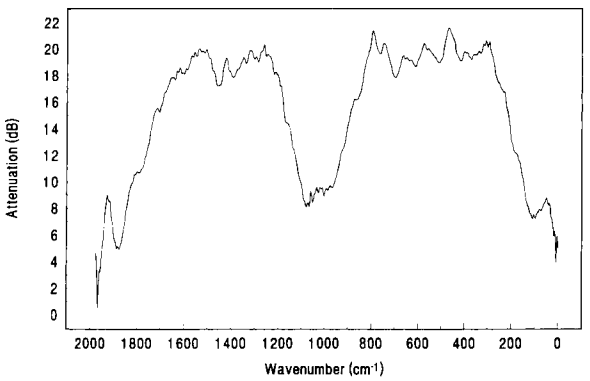

Fig. 3. Frequency response of the digital bandpass filter centered at the methanol absorption band (1035 cm^{-1}). The FWHH of the passband is approximately 250 cm^{-1}.

Previous work has demonstrated that no sacrifice in filter performance results from this reduction in filter size through the use of significance testing [15].

Fig. 3 is a composite bandpass of one of the FIRM filters generated in this study. The attenuation of the filter is plotted in units of decibels (dB). The filter bandpass is centered at 1035 cm^{-1}, and the FWHH of the bandpass is approximately 250 cm^{-1}. The attenuation of the filter outside of the bandpass is approximately 18 dB except at the edges of the frequency range. The decrease in attenuation here is a characteristic of the FIRM filter generation method. The filter design does not demand high attenuation in spectral regions where the infrared detector generates little signal.

Fig. 4 displays the results obtained by applying this filter to two interferogram segments. Fig. 4A plots points 25–174 (relative to the centerburst) in an unfiltered interferogram collected with no methanol in the instrument FOV, while Fig. 4C plots this interferogram segment after application of the filter whose bandpass is displayed in Fig. 3. Figs. 4B and 4D are the corresponding plots of the same segment of an interferogram whose corresponding single-beam spectrum shows clear evidence of a methanol absorption band. The two unfiltered interferogram segments in Figs. 4A and 4B are visually highly similar. However, Figs. 4C and 4D show a clear difference between the two segments. By isolating the frequencies in the region of the methanol band, the presence of the methanol absorption is now clearly observed in the interferogram segment. Furthermore, the characteristic shape of the methanol spec-

tral band is encoded in the beat pattern of the filtered interferogram.

3.3. Pattern recognition methodology

Application of the FIRM filter to an interferogram segment of p points produces a filtered intensity value for each point in the segment. Taken together, these filtered intensities can be considered as a p-dimensional vector that characterizes the interferogram. The tip of the vector identifies a point in a p-dimensional data space, where the coordinate axes correspond to the intensities of specific points in the filtered interferogram. If the filter is effective in extracting the interferogram-domain representation of the methanol spectral feature, then the data space constructed from a set of filtered interferogram segments should contain separate clusters of points corresponding to methanol-containing and background interferograms.

Fig. 5 allows this clustering to be visualized for the 7228 interferograms in the training set of field data. Principal components analysis (PCA) [16] was applied to 60-point filtered interferogram segments in order to compute two-dimensional views of the data that approximate the interpoint relationships existing in the full 60-dimensional space. Fig. 5 is a plot of the projections of the 7228 60-dimensional points onto the first and second principal components of the data. The first two principal components explain 92% of the variance in the 60-dimensional data. Interferograms with known methanol signatures are plotted as squares, while background interferograms are plotted as triangles. Clustering of the methanol-containing and background containing interferograms is clearly observed.

While techniques such as PCA can be used to visualize the relationships that exist in a multidimensional data space, pattern classification techniques are required in order to make a yes/no decision regarding the presence of the analyte signature in any arbitrary filtered interferogram. Among the various classification methods available, piecewise linear discriminant analysis (PLDA) [17] has been found effective in

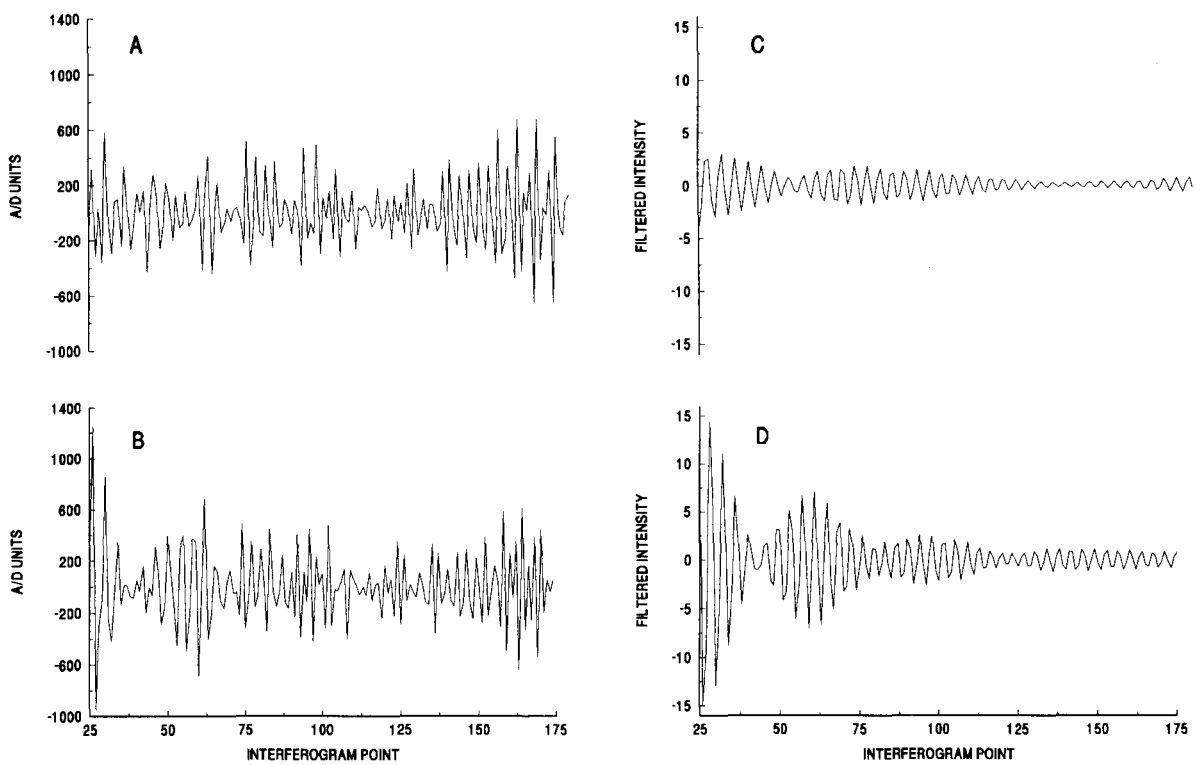

Fig. 4. Filtered and unfiltered interferogram segments (points 25–174 relative to the interferogram centerburst): (A) unfiltered background interferogram, (B) unfiltered methanol interferogram, (C) filtered background interferogram, and (D) filtered methanol interferogram.

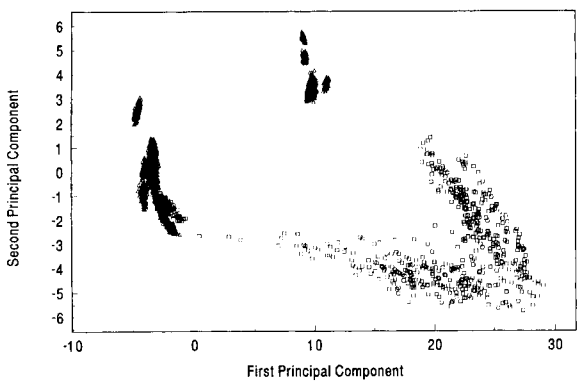

Fig. 5. Principal components score plot displaying the projections of the 7228 filtered interferogram segments in the training data set. Scores along the first and second principal components are displayed. Methanol-containing interferograms are plotted as squares while background interferograms are plotted as triangles.

determining analyte signatures in filtered interferogram segments. This approach is based on the construction of separating surfaces or discriminants in the data space that define regions of space occupied by points belonging to specific categories of data. Through the construction of these separating surfaces, unknown points can be classified or assigned membership in one of the data categories simply by computing the orientation of the point relative to the discriminants. PLDA employs multiple linear hyperplanar surfaces to approximate a nonlinear separating surface between the data categories. For the methanol detection in the laboratory and field data, surfaces defined by two and three discriminants, respectively, were required to achieve a maximum percentage of correct classifications of the training data set.

In the present analysis, two data categories are present, corresponding to filtered interferogram segments with and without methanol signatures. Given the training set of p-dimensional filtered interferogram segments, numerical optimization methods are used to move the separating surfaces into an optimal orientation in the data space. Optimal positioning of the discriminants results in the correct classification of the maximum number of training set interferograms. This study employed Simplex optimization to achieve an optimal placement of the discriminants. For the laboratory and field data sets, a total of 8000 and 18,000 iterations of the Simplex procedure were required, respectively, in order to achieve the best discriminant placement possible. Once the discriminants have been positioned, any p-dimensional filtered interferogram segment can be classified as either methanol-containing or non-methanol based on the calculation of its discriminant score. The discriminant score is a threshold value computed by application of the piecewise linear discriminant to the filtered interferogram segment. Discriminant scores greater than zero indicate that the interferogram segment is judged to contain a methanol signature, based on the orientation of the vector representation of the segment relative to the previously computed separating surface. The magnitude of the discriminant score indicates the distance to the surface.

3.4. *Overview of parameter optimization for methanol detection*

The data analysis concepts described above were applied to the design of an automated detection scheme for methanol. The parameters optimized in this study were interferogram segment size, segment location, and filter bandwidth. Throughout the work, the position of the filter bandpass was held constant at 1035 cm^{-1}, the experimentally determined center of the targeted spectral feature of methanol.

The importance of the three parameters studied is illustrated in Fig. 6. Figs. 6A and 6B are synthetic Gaussian-shaped spectral bands with FWHH values of 69 and 11 cm^{-1}, respectively. The bands in Figs. 6A and 6B are designed to approximate the widths of the entire methanol band at 1035 cm^{-1} and the S–F stretching band of SF_6 at 940 cm^{-1}. SF_6 is a test compound used in pollution monitoring that has been studied extensively with our data analysis methodology [6,7]. No attempt was made to construct a replica of the RQP band shape of the methanol C–O stretch. The Gaussian function in Fig. 6A simply matches the width of the overall band. Figs. 6C and 6D are segments of the interferograms obtained by inverse Fourier transforming the spectra in Figs. 6A and 6B, respectively. These interferograms represent the analyte signals that the data analysis methodology is attempting to extract.

An inspection of Fig. 6 reveals three key points regarding the importance of interferogram segment size, segment location, and filter bandwidth. First, the optimal interferogram segment (i.e. segment size and location) is directly dependent on the width of the analyte band. For a wide spectral feature such as the

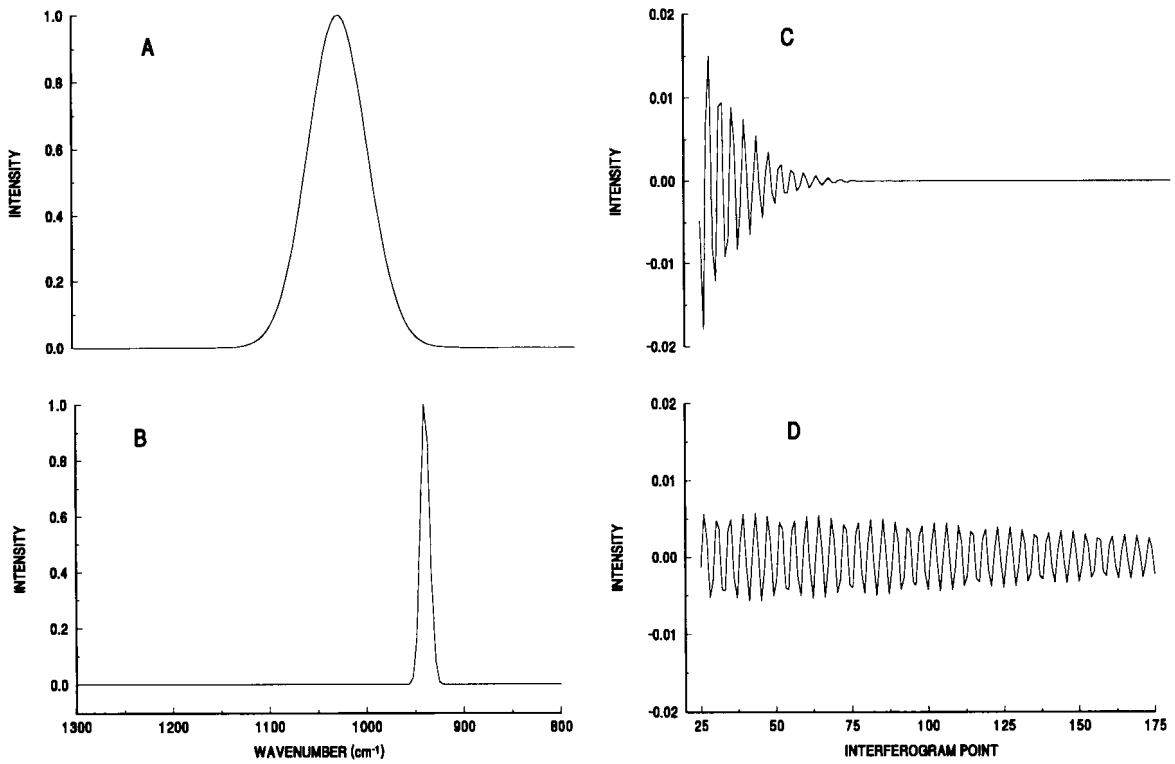

Fig. 6. Synthetic spectra and corresponding interferograms: (A) Gaussian spectrum approximating the width of the methanol band at 1035 cm^{-1}, (B) Gaussian spectrum approximating the absorption band of SF_6 at 940 cm^{-1}, (C) interferogram segment corresponding to Fig. 6A, (D) interferogram segment corresponding to Fig. 6B.

C–O stretching band of methanol, the corresponding interferogram information is compressed into a short segment near the centerburst. The interferogram signal corresponding to the significantly narrower SF_6 band is spread over a much larger segment. This suggests that, relative to SF_6, a shorter interferogram segment can be used to extract methanol information. For completeness, an inspection of Fig. 4D reveals that the interferogram information corresponding to the actual methanol band is spread over a larger region than that depicted in the synthetic interferogram of Fig. 6C. This is due to the presence of the narrow Q-branch (FWHH ≈ 6 cm^{-1}) in the actual methanol spectrum. The information corresponding to this narrow feature is still present at a larger distance from the centerburst than the information corresponding to the wider P- and R-branches.

Second, even though the synthetic SF_6 and methanol spectral bands have the same peak intensity, a significantly greater methanol signal is observed in the interferogram. The intensity of the interferogram signal is clearly related to the area of the band rather than the peak intensity. This suggests that interferogram-based detections of wide spectral features should be significantly easier than the corresponding detections of narrow features. Assuming a detector-noise limiting measurement, the signal-to-noise ratio in the interferogram is highest in the region of the centerburst. This provides an additional advantage for the detection of interferogram information corresponding to wide spectral features.

The third key point to consider is the effect of the filter bandpass width on the optimal interferogram segment. As noted previously, the application of the filter serves to truncate the infrared background emission to the same width as the filter bandpass. The interferogram representation of the background is a damping sinusoidal waveform whose amplitude is related to the infrared intensity reaching the detector. This background interferogram signal obscures the lower ampli-

tude signal due to the analyte spectral band. Thus, as noted above, the interferogram segment used for the detection must be selected from a region in which the background signal has effectively damped to zero. Thus, an interaction clearly exists between the interferogram segment used for the analyte detection and the width of the filter bandpass. The design of an optimal detection scheme must therefore include a study of this interaction.

3.5. Selection of interferogram segment size and segment location

Preliminary studies were performed to determine the optimal segment size of the interferogram containing methanol information and the optimal width of the digital filter bandpass. As noted above, the methanol information in the interferogram is concentrated close to the centerburst. Interferogram segment sizes used in the present analysis were 40, 60, 76, 100, and 150 points. The optimal segment size was found to be a 150-point segment with the starting point being 25 and the ending point being 174 points away from the centerburst. This is the same segment plotted in Figs. 4 and 6. Below point 25, it was very difficult to generate well-performing FIRM filters, as the intensity in the interferogram varies non-linearly near the centerburst. The linear model of Eq. 1 was found to be inadequate in this region. Above point 175, the interferograms did not contain any useful analyte information. Further investigations were restricted to using segments between 25 and 174 points.

The segment location defines the starting and ending points of the interferogram segment used. For the 40-point segment size, nine different segment locations were used. The locations were points 25/64, 35/74, 45/84, 55/94, 65/104, 75/114, 85/124, 95/134, and 105/144. The numerator denotes the starting point and the denominator denotes the ending point of the segment, relative to the centerburst. For the 60-point segment, the seven segment locations used were 25/84, 35/94, 45/104, 55/114, 65/124, 75/134, and 85/144. For the 75 and 100-point segment sizes, five segment locations were used with starting points being 25, 38, 50, 62, and 75. For the 150-point segment size, only one segment (25/174) was possible.

Given the large width of the methanol band, it was expected that the bandpass filters with larger widths would exhibit better performance. Narrow bandpass filters would suppress analyte information while very wide filters would pass frequencies outside the analyte band of interest. After initial studies, 14 digital bandpass filters having a Gaussian shape, centered at 1035 cm^{-1}, and with FWHH values ranging from 164 to 287 cm^{-1} were generated. These FWHH values were estimated from the actual filter frequency responses such as that displayed in Fig. 3. Filter widths less than 164 cm^{-1} were not investigated due to the inability of the FIRM filter design methodology to generate filters that operate near the centerburst and have narrow bandpass widths.

3.6. Pattern recognition training and prediction results

The data analysis results exhibit better filter performance for the laboratory data than for the field data. Two discriminants were needed to classify all methanol-containing patterns in the training set of laboratory data while three discriminants were needed for classification of the maximum number of methanol-containing patterns in the field data training set. The pattern recognition results will be discussed separately for each segment size.

3.7. 40-point segments

The pattern recognition performance for a given digital filter and interferogram segment was judged by considering the percentage of methanol-containing patterns classified correctly. For the training data set of laboratory data, this value was greater than 96%. The performance was not sensitive to either segment location or filter width. The performance with the separate prediction data was also greater than 96% for the first five segments from the centerburst. For these five segments, the performance was insensitive to the segment location and the filter width. For three of the four remaining segments, which were more remote from the centerburst, the performance degraded.

For the field data, Figs. 7A and 7B show the training and prediction performance, respectively, as a function of filter width. Five representative 40-point segments are displayed. The training performance varied between 50 and 100%. The best performance was found for segment 25/64 and was almost insensitive to filter

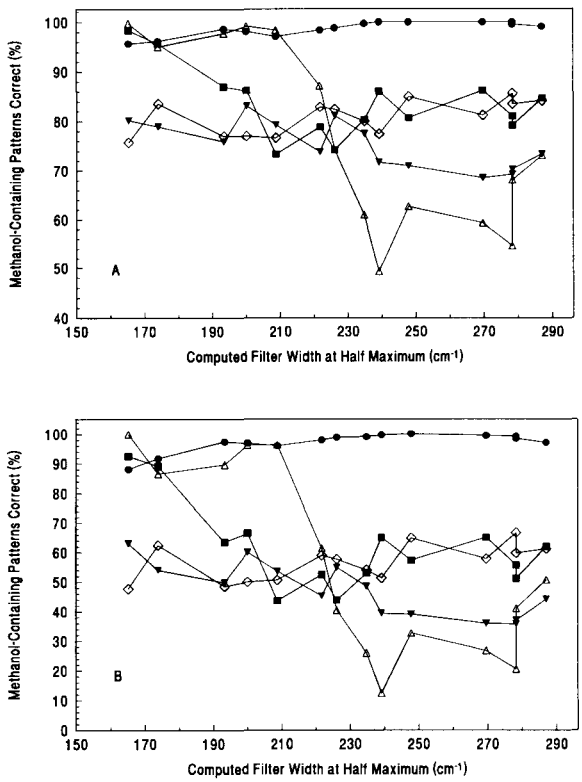

Fig. 7. Comparative performance of digital bandpass filters for 40-point segments. Segment locations are (●) 25/64, (△) 45/84, (■) 65/104, (◇) 85/124, and (▼) 105/144: (A) training performance, (B) prediction performance.

width. For other segments, the performance degraded and was sensitive to both segment location and filter width. In the prediction results for segment 25/64, the performance for the filters with width 193 cm^{-1} and above was best. The performance was found to be sensitive to the segment location and the filter width for other segments. The performance generally degraded for segments located farther from the centerburst.

3.8. 60-point segments

The training performance of the filters for the laboratory data was greater than 97% and almost insensitive to the segment location and the filter width. The prediction performance for the laboratory data was greater than 96% except in one case. In most of the cases it was 100%. Figs. 8A and 8B show the training and prediction performance of filters for the field data. The training performance varied between 65–100%. The performance for segment 25/84 was the best (>95%). For the other segments, the performance was dependent on both the segment location and the filter width. For the prediction data, the performance varied between 45–100% and was best for segment 25/84 and for wide filters (≥ 193 cm^{-1} FWHH). For the other segments, the performance was sensitive to both the segment location and the filter width. Generally, the performance degraded for segment locations remote from the centerburst. However, for certain combinations of the segment location and the filter width, the performance was comparable to the best results. The range of variation in performance for both the training and the prediction was much less for the 60-point segments compared to the 40-point segments.

3.9. 76-point segments

The performance of filters for both the training and the prediction of the laboratory data was greater than

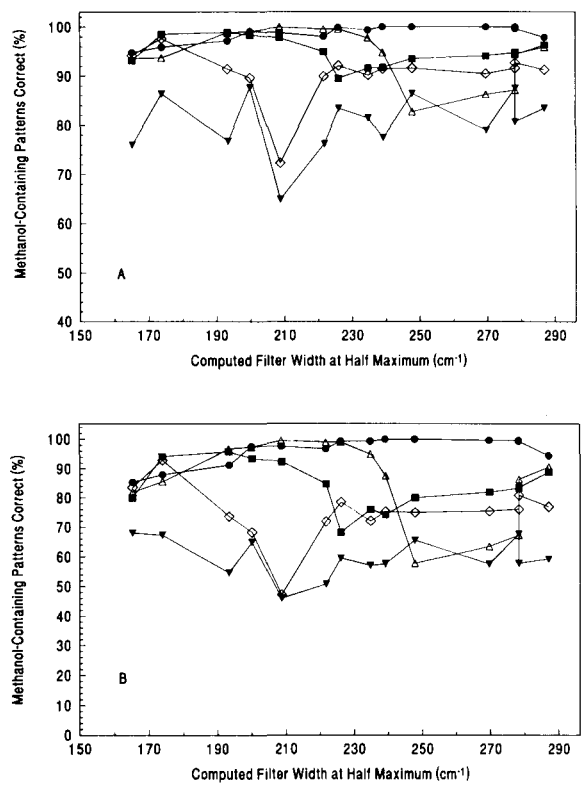

Fig. 8. Comparative performance of digital bandpass filters for 60-point segments. Segment locations are (●) 25/84, (△) 35/94, (■) 45/104, (◇) 65/124, and (▼) 85/144: (A) training performance, (B) prediction performance.

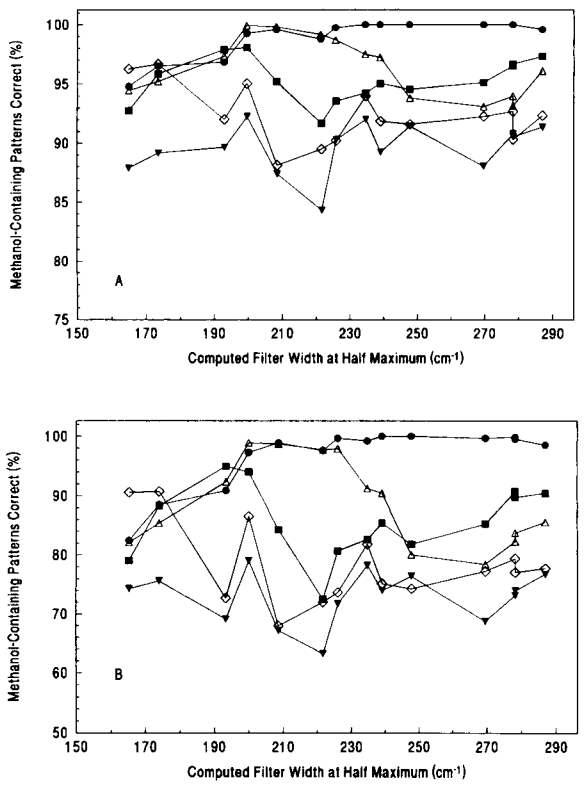

Fig. 9. Comparative performance of digital bandpass filters for 76-point segments. Segment locations are (●) 25/100, (△) 38/113, (■) 50/125, (◇) 62/137, and (▼) 75/150: (A) training performance, (B) prediction performance.

98% and was almost insensitive to both the segment location and the digital filter bandpass width. Figs. 9A and 9B show the training and prediction performance of the filters for the field data. The best performance was observed for segment 25/100 and for filters with widths ≥ 208 cm^{-1}. For the other 75-point segments, the performance was sensitive to both the segment location and the filter width and degraded as the segment location became more remote from the centerburst. The prediction performance varied between 60–100%. It was best for the segment 25/100 and for the filters with a bandpass width greater than 209 cm^{-1}. As with other segment sizes, the performance was sensitive to the segment location and the filter width and degraded as the segment location used was located farther from the centerburst. For both the training and the prediction set, the range of variation in performance was reduced as compared to the 40- and 60-point segments.

3.10. 100-point segments

Both the training and the prediction performances for the laboratory data were greater than 99% and were insensitive to both the segment location and the filter width. Figs. 10A and 10B display the training and prediction performance of the filters for the field data. The training performance was better than that for the 40, 60, and 75-point segments and varied between 85–100%. The best performance was for segment 25/124 and for the filters with width ≥ 209 cm^{-1}. The performance degraded for the other segment locations and also became sensitive to the filter width. Generally, the performance became worse for segment locations that were located farther from the centerburst. As before, the prediction performance was best for segment 25/124 and for filters with widths ≥ 193 cm^{-1}. For other segments, the performance was more sensitive to the segment location and the filter width. The range of variation was between 65–100%.

3.11. 150-point segments

The training and the prediction performances for both the laboratory and the field data for segment 25/174 were almost insensitive to the filter width. The performance was greater than 99% and in most cases it was 100%.

3.12. Evaluation of results

Overall, the training and the prediction performances (reflected by the percentage of methanol-containing patterns correctly classified) for the filters using laboratory data were comparable. However, for the field data the training performance was generally better than the prediction performance. The better performance in the prediction of the laboratory data as compared to that of the field data can be attributed to the fact that the training set of field data was not a global data set and thus did not contain all of the possible types of background interferograms. The performance for both the training and the prediction results improved as the segment length increased for both the laboratory and the field data. This is clearly seen in Figs. 7–10 for the field data. The percentage of methanol-containing patterns correctly classified increased gradually from the 40-point to the 100-point segments. This observation

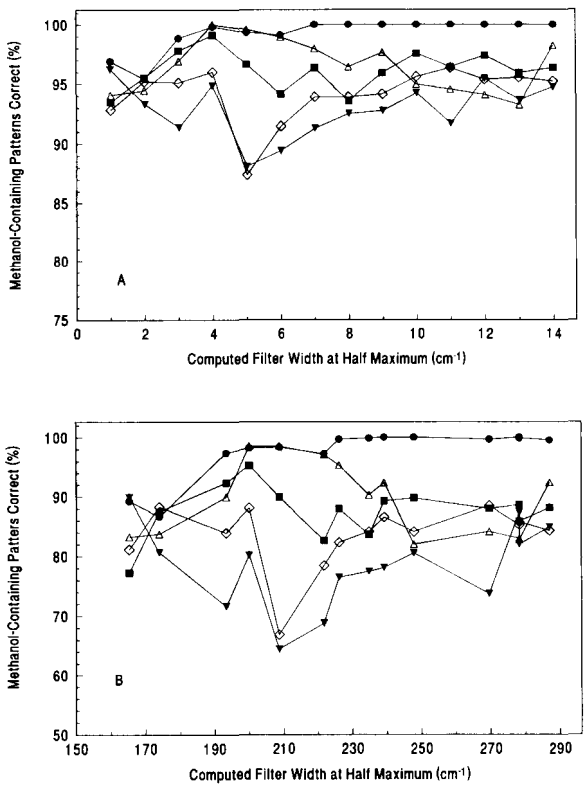

Fig. 10. Comparative performance of digital bandpass filters for 100-point segments. Segment locations are (●) 25/124, (△) 38/137, (■) 50/149, (◇) 62/161, and (▼) 75/174: (A) training performance, (B) prediction performance.

is attributed to the fact that methanol information increased from the 40-point segments to the 150-point segments and that a longer interferogram profile was available to the pattern recognition method for use in recognizing the methanol signature. This result can be understood by inspecting the filtered interferogram segments displayed in Figs. 4C and 4D. While the information in the first 40 points of the filtered segment provides the greatest discrimination between the methanol-containing (Fig. 4D) and background (Fig. 4C) interferograms, discriminating information is still clearly present out to point 174.

Within each segment size, the performance generally decreased as the segment used was located farther from the interferogram centerburst. This effect can also be seen in Figs. 7–10. As indicated in the discussion of Fig. 6, since the methanol spectral band is wide, the methanol features in the interferogram are concentrated near the centerburst. Therefore, as the segment location is moved farther from the centerburst, the segments contain less methanol information and the classification performance is degraded. It is also seen from Figs. 7–10 that the classification performance was sensitive to the width of the bandpass filter. The performance was generally more sensitive to the filter width as the segment location became more remote from the centerburst. For the laboratory data, the performance was comparatively less sensitive to the segment size, the segment location, and the filter bandpass width.

An inspection of Figs. 7–10 also indicates that for the data employed here, the choice of interferogram segment position and length is more important than the choice of filter width. For the optimal segments, only slight variation in performance is noted over the filter widths studied. To put this result in the proper perspective, however, it should be emphasized that the purpose of filtering is to reject the interferogram signals corresponding to spectral features of widths similar to the analyte band, but located at frequencies lying outside the filter bandpass. For the particular data used in this work, the frequency selectivity provided by the filtering was not critical due to the lack of spectral interferences at nearby frequencies. For example, some of the field data contained spectral signals due to acetone and 2-butanone. However, the bands for acetone and 2-butanone that are nearest to the 1035 cm^{-1} methanol C–O stretch are located at 1217 and 1175 cm^{-1}, respectively.

The best results obtained for both the laboratory data and the field data are summarized in Tables 4 and 5. These results confirm the observation that the methanol information is present closer to the centerburst. Missed detections, which is the percentage of methanol-containing patterns misclassified, are negligible for the laboratory data while it is zero in most of the cases for the field data. False detections, which is the percentage of background patterns misclassified as methanol-containing patterns, are less than 1% for the laboratory data. For the field data, the rate of false detections is less than 1% for about 80% of the cases. For the remaining 20% of the cases, the false detections varied between 1 and 2%. As indicated in Table 5, for segments of various lengths starting at point 25, the major improvement obtained with increasing segment length is a reduction in the rate of false detections. This can be attributed simply to a larger signal being available

Table 4
Pattern recognition results for laboratory data

Segment		Filter FWHM[a] (cm^{-1})	Training results		Prediction results			
Size	Location		Methanol Containing (%)	Missed Detection (%)	Methanol Containing (%)	Missed Detection (%)	False Detection (%)	Total Percentage
40	35/74	226	99.93 (1401)[b]	0.07 (1)[b]	99.46 (920)[c]	0.54 (5)[c]	0.36 (4)[d]	99.36 (2032)[e]
60	25/84	156	99.79 (1399)	0.21 (3)	100.00 (925)	0.00 (0)	0.36 (4)	99.80 (2041)
76	25/100	200	100.00 (1402)	0.00 (0)	100.00 (925)	0.00 (0)	0.45 (5)	99.76 (2040)
100	25/124	200	100.00 (1402)	0.00 (0)	100.00 (925)	0.00 (0)	0.36 (4)	99.80 (2041)
150	25/174	200	100.00 (1402)	0.00 (0)	100.00 (925)	0.00 (0)	0.45 (5)	99.76 (2040)

[a]Full width at half maximum of bandpass digital filter.
[b]Number of interferograms out of 1402 total.
[c]Number of interferograms out of 925 total.
[d]Number of interferograms out of 1120 total.
[e]Number of interferograms out of 2045 total.

for use in discriminating weak methanol signatures from those of backgrounds. The very small decrease in false detections obtained by increasing the segment from 100 to 150 points (0.14% vs. 0.15%) suggests that a point of diminishing returns is reached at a segment size of approximately 100 points.

For the field data, Fig. 11 shows the correlation between the training and the prediction results for all segment sizes, segment locations, and filter widths. It is evident from the figure that high performance in the training procedure correlates with high performance in the prediction. Poorly trained discriminants did not perform well in the prediction.

Fig. 12 shows a sample result obtained by the application of the methanol digital filter and the pattern recognition procedure to a subset of the field data prediction set containing the weakest methanol signals. Plotted in the figure are the discriminant scores for each interferogram. As noted previously, discriminant scores greater than zero indicate that the interferogram segment is judged to contain a methanol signature. The prediction data set used in generating the figure contained 2996 interferograms that were taken from thirteen different data files. The first 609 interferograms in the data set were known to contain methanol. The remaining 2387 interferograms were collected under

Table 5
Pattern recognition results for field data

Segment		Actual FWHM[a] (cm^{-1})	Training result		Prediction result			
Size	Location		Methanol Containing(%)	Missed Detection (%)	Methanol Containing (%)	Missed Detection (%)	False Detection (%)	Total Percentage
40	25/64	247	100.00 (1228)[b]	0.00	100.00 (615)[c]	0.00	0.34 (78)[d]	99.67 (23466)[e]
60	25/84	247	100.00 (1228)	0.00	100.00 (615)	0.00	0.23 (52)	99.78 (23492)
76	25/100	247	100.00 (1228)	0.00	100.00 (615)	0.00	0.23 (52)	99.77 (23490)
100	25/124	239	100.00 (1228)	0.00	100.00 (615)	0.00	0.15 (34)	99.86 (23511)
150	25/174	226	100.00 (1228)	0.00	100.00 (615)	0.00	0.14 (32)	99.86 (23511)

[a]Full width at half maximum of bandpass digital filters.
[b]Number of interferograms out of 1228 total.
[c]Number of interferograms out of 615 total.
[d]Number of interferograms out of 22929 total.
[e]Number of interferograms out of 30772 total.

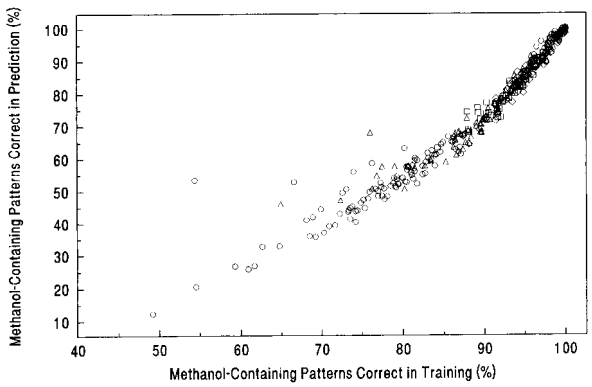

Fig. 11. Correlation between training and prediction results of methanol-containing interferograms of field data for (○) 40, (△) 60, (□) 76, (◇) 100, and (▽) 150 point segments.

varying background conditions. Interferograms shown between numbers 1605 and 2650 had acetone present in the FOV of the spectrometer to serve as a test of the ability of the methodology to reject signals from a potential spectral interference.

This figure indicates that the digital filtering/pattern recognition technique gave positive discriminant scores for each of the first 609 interferograms. Most of the other discriminant scores with interferograms containing no methanol in the test data set were negative in value. A few of the discriminant scores were slightly above the discriminant score threshold. All positive discriminant scores in the interferograms greater than interferogram 609 are regarded as false detections.

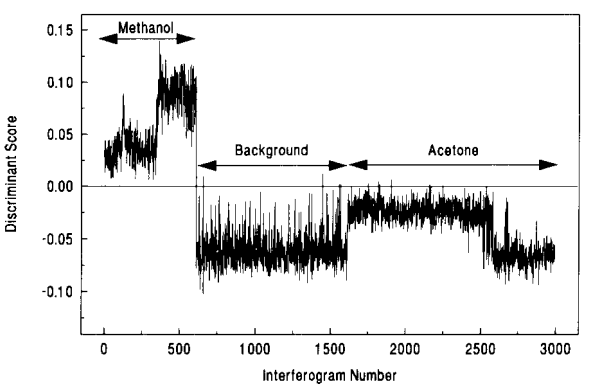

Fig. 12. Discriminant score plot for a subset of the prediction set. Interferograms 1–609 contain methanol while interferograms 610–2996 do not contain methanol. Discriminant scores greater than 0.0 indicate interferograms classified as methanol-containing by the piecewise linear discriminant method.

These discriminant values were all very close to the zero threshold value which indicated that the confidence in discrimination of these interferograms was not very strong. The acetone-containing interferograms between 1605 and 2650 showed very few false detections which gives further indication that the piecewise linear discriminants are selective for methanol vapour.

4. Conclusions

The results presented indicate that it is possible to perform a highly accurate and automated detection of atmospheric pollutants such as methanol by implementing a data analysis procedure based on short segments of interferograms. This methodology does not require a stable infrared background or any type of background measurement. The results observed in the detection of methanol are generally superior to those that we have obtained previously with other test compounds such as SF_6. The use of a wide spectral feature such as the C–O stretching band of methanol is observed to enhance the interferogram-based approach due to concentration of the methanol information in the interferogram to a narrow region near the centerburst. Furthermore, the unique contour of the methanol absorption band provides additional discriminating information in the interferogram due to the establishment of a characteristic beat pattern.

It is also important to note that the methanol detection has been achieved without the collection of the high resolution rotational fine structure often considered necessary for discriminating the gas-phase spectra of small molecules. The combination of windowing the interferogram and applying bandpass digital filtering allows a frequency-selective analysis to be implemented with a short interferogram segment. Only compounds with spectral signatures of the same frequency and width as the analyte band will interfere with this analysis. While further testing will be required to establish the applicability of this approach to a measurement environment in which a large number of potential interferents are present, the results presented here suggest that excellent selectivity is present in the interferogram-based analysis.

It is estimated that the performance of the digital filtering and pattern recognition methodology could be improved by the use of a more global training set with

additional types of infrared backgrounds. Further improvements in a methanol detection scheme may require an improved method of generating digital filters for use with interferogram points located near the centerburst. Such improvements may require non-linear terms in Eq. 1. This is a current area of study in our laboratories.

The results presented here focused on the qualitative detection (i.e., presence or absence) of methanol vapour. However, the known concentrations of the laboratory data used in this work allow a rough estimate to be made regarding the limit of detection of methanol achievable with our interferogram-based detection scheme. The 405 ppm-m methanol sample could be recognized in single-scan interferograms corresponding to a temperature difference (ΔT) of 15°C between the sample cell and the blackbody source. Path lengths and ΔT values can be orders of magnitude higher in actual open path measurements, leading to improved sensitivity. In addition, if the sample is present in the spectrometer FOV in a fairly static manner, additional benefits in sensitivity may be obtained by signal averaging the interferogram. For reference purposes, the methanol present in the exhaust of a methanol-burning engine has been measured at 1470 ppm [2]. While no specifications have been established for an automated methanol monitor, our results suggest that open path FTIR spectrometry is a viable technique for atmospheric monitoring of methanol vapour.

Finally, an ideal methanol sensor would have the ability to make a quantitative estimate of methanol concentration. Preliminary work suggests that the filtered interferogram data also contains quantitative information. The development of techniques to extract this quantitative information from filtered interferogram signals is also an area of current research in our laboratories.

Acknowledgements

Funding for this work was provided by the Department of the Army. Portions of this work were presentedat the 25th American Chemical Society Central Regional Meeting, Pittsburgh, PA, October, 1993.

References

[1] R.M. Hammaker, W.G. Fateley, C.T. Chaffin, T.C. Marshall, M.D. Tucker, V.D. Makepeace and J.M. Poholarz, Appl. Spectrosc., 47 (1993) 1471.
[2] P.L. Hanst and E.R. Stephens, Spectroscopy, 4 (9) (1989) 33.
[3] P.L. Hanst, N.W. Wong and J. Bragin, Atmos. Environ., 16 (1982) 969.
[4] H.B. Singh and P.B. Zimmerman, in J.O. Nriagu (Ed.), Gaseous Pollutants: Characterization and Cycling, Wiley-Interscience, New York, 1992, Chap. 5.
[5] P.L. Hanst, Spectroscopy, 8 (9) (1993) 44.
[6] R.T. Kroutil, J.T. Ditillo and G.W. Small, in H. Meuzelaar (Ed.), Computer-Enhanced Analytical Spectroscopy, Plenum, New York, 1990, Chap. 4.
[7] G.W. Small, T.F. Kaltenbach and R.T. Kroutil, Trends Anal. Chem., 10 (1991) 149.
[8] R.T. Kroutil, R.J. Combs, R.B. Knapp and G.W. Small, Proceedings of the 9th International Conference on Fourier Transform Spectroscopy, SPIE, Bellingham, WA, 1994, pp. 24–31.
[9] G.W. Small and A.S. Barber, Chemom. Intell. Lab. Syst., 15 (1992) 203.
[10] G. Herzberg, Molecular Spectra and Molecular Structure: II. Infrared and Raman Spectra of Polyatomic Molecules, Van Nostrand Reinhold, New York, 1945, p. 335.
[11] R.J. Combs, R.B. Knapp and P.E. Field, Anal. Instrum., 21 (1993) 163.
[12] R.T. Kroutil, M. Housky and G.W. Small, Spectroscopy, 9(2) (1994) 41.
[13] E. Hala, L. Wichterle, J. Polak and T. Boublik, Vapour Liquid Equilibrium Data at Normal Pressures, Pergamon, London, 1968, pp. 104–111.
[14] S.E. Carpenter and G.W. Small, Anal. Chim. Acta, 249 (1991) 305.
[15] G.W. Small, A.C. Harms, R.T. Kroutil, J.T. Ditillo and W.R. Loerop, Anal. Chem., 62 (1990) 1768.
[16] E.R. Malinowski, Factor Analysis in Chemistry, Wiley-Interscience, New York, 2nd edn., 1991, pp. 49–58.
[17] T.F. Kaltenbach and G.W. Small, Anal. Chem., 63 (1991) 936.

ELSEVIER

Analytica Chimica Acta 297 (1994) 405–416

ANALYTICA CHIMICA ACTA

Calibration transfer across near-infrared spectrometric instruments using Shenk's algorithm: effects of different standardisation samples

E. Bouveresse [a], D.L. Massart [a,*], P. Dardenne [b]

[a] *ChemoAC, Pharmaceutical institute, Vrije Universiteit Brussel, Laarbeeklaan 103, B-1090 Brussels, Belgium*

[b] *Station de Haute Belgique, Rue de Serpont 100, B-6800 Libramont-Chevigny, Belgium*

Received 19 April 1994; revised manuscript received 24 May 1994

Abstract

In this paper, transfer of calibration models between near-infrared spectrometric instruments using three different standardisation sets is described. The first set contains samples which are very similar to the agricultural samples from three different sets to be analysed, the second set contains generic standards, and the third one contains pure organic and inorganic chemicals. To test the accuracy of each standardisation, root mean square errors and correlation coefficients are computed before and after standardisation. To test the predictive ability, standard error of prediction for the three different prediction sets are also computed before and after standardisation. For standardisation, Shenk's algorithm is used: a description of this algorithm is given.

Keywords: Infrared spectrometry; Calibration models; Shenk's algorithm

1. Introduction

Standardisation

Several problems due to poor instrument performances and a need for all calibrations have recently surfaced in spectroscopy. They concern standardisation, i.e. the possibility to transfer the calibration from one system to another.

The first of the encountered problems is the transfer of a calibration model across two different instruments. If the instrumental response of a first system differs from that which would have been obtained with a second system (this can be due to many reasons such as different sources, different optical systems, different detectors, etc.), the calibration model built on the first system and applied to the second one will give erroneous results. Multivariate instrument standardisation enables to correct the differences between instruments, and avoids to use time-consuming complete recalibration procedures, and to transport recalibration samples from one place to another.

The second problem is the calibration transfer from an instrument to itself over a period of time. The instrumental responses from a single instrument over a period of time can be subject to important fluctuations such as temperature variations [1], wavelength shifts, linear or non-linear drifts, etc. If such fluctuations occur between the calibration procedure and the analysis procedure of unknown samples, or if the instrument needs to be repaired because of technical problems, this could lead to erroneous results. Multivariate instrument standar-

* Corresponding author.

SSDI 0003-2670(94)00237-G

disation enables to correct these fluctuations over time, without repeating the whole recalibration.

Standardisation methods: two different approaches

In order to transfer a calibration model, several standardisation methods have been suggested. The two different approaches used to transfer the calibration across NIR instruments are the following ones:

The first approach consists of trying to transfer the spectra obtained with the secondary system to the primary system, and applying the calibration model built on the primary instrument to these modified spectra. Different methods such as direct standardisation[2], piecewise direct standardisation [2,3], and Shenk's method follow this approach [4,5].

The second approach consists of building a calibration model on a primary system, trying to transfer it to a secondary system, and applying this modified calibration model to the spectra obtained on the secondary instrument. This approach was developed by Forina et al. [6,7].

In this paper, only Shenk's method has been studied. This method is widely applied to transfer calibration between NIR instruments, when results coming from different instruments have to be compared (Quality-control nets)

It should be noted that the method used to correct these instrumental responses, and still applied today in several places, is a very simple method based on bias and slope correction of the model built on the "master" instrument. Some samples were measured on the "slave" instrument, the spectra obtained and the calibration model built on the "master" was used to compute the values to be predicted. Then, the values obtained with the model built on the "master" instrument applied to the spectra measured on the "master" instrument are regressed on those values: a linear model is computed, correcting the values found with the "slave" spectra to the right values obtained with the "master" spectra. The combination of this simple linear model with the calibration model gives a modified calibration model which gives the right values (obtained from wet chemistry) from spectra obtained on the "slave" instrument.

Standardisation samples

Three different sets of samples are involved: the first is the calibration set, the samples of which are used to build a calibration model on the "master" instrument. To transfer calibration models between instruments, two other sets of samples are used:

Samples from the standardisation set are measured on the two instruments to compute the standardisation parameters.

Samples from the prediction set are measured in the "slave" instrument, and the spectra obtained are transferred on the "master" instrument with the standardisation parameters computed with the standardisation set. Then, those transferred spectra and the calibration model built with the calibration set are used to predict the studied variables.

Beside the standardisation method, the selection of the samples used to compute the transfer parameters appears to be very important, and this problem has received very little attention in the literature. Two different approaches are possible, and the choice between these two approaches depends on different practical reasons.

The first possibility is to select the "best" subset samples from the set to be predicted (only measured on the "slave" instrument), to remeasure this set on the "master" instrument, and to compute the transfer parameters with this subset. The main advantage of this method is that the samples used for standardisation are very representative for those used for prediction, and standardisation can be successfully applied [2,3]. This approach has the following practical limitations:

The samples have to be measured on both instruments. If the composition of those samples changes over time, and if the instruments are very far from each other, this can lead to serious problems.

For each type of product to be predicted, one needs a subset of samples. If the number of different products to be analysed is very high, many different subsets have to be remeasured on the "master" instrument.

The second possibility is to use samples not coming from the prediction set, but of a similar nature. These standardisation samples are measured on the two different instruments to compute the standardisation parameters, but all samples of the prediction set are measured only at one place. This method enables to standardise spectra from samples, which are not measurable on both instruments for whatever reason. Nevertheless, a drawback of this method is that it uses samples of the same nature as those used in the prediction set, and these samples can change over time.

In this paper, this second possibility and also a third approach are studied: in this third approach, standardisation is performed with the use of more stable samples (generic standards) which are completely different from the studied samples. This approach should be very helpful to overcome the problems of stability, and should be applicable to samples from different natures. The type and the number of these generic standards should be well chosen, not to lose information during the transfer of spectra. For example, if one wants these standards to be applicable to samples with very different NIR spectra, the spectra of these generic standards should probably cover a larger range of optical density, in order to contain all possible linear and non-linear variations in the optical density (O.D.) field where the measured spectra are located.

In this article therefore, different types of standardisation samples are tested:

30 standardisation cells, made of different agronomic products.

6 standardisation cells, which contain 6 different inert standards.

12 standardisation cells, which contain organic and inorganic pure products.

Interlaboratory experiment

Since 1987, the Station de Haute Belgique (SHB, Libramont, Belgium) has been running a network of NIRS instruments, in order to analyze cereals and forages [8]. The software developed by ISI (InfraSoft International, Port Mathilda, USA), which involves Shenk's algorithm for standardisation, is the key of this network. Recently, the idea of an European Network has surfaced from participants of QUEST (food quality established by spectroscopic techniques), which is a concerted action subsidized by the CEC in the framework of the general FLAIR program (Food-Linked Agro-Industrial Research).

The standardisation and prediction sets were measured by three participants of QUEST (referred to as DA, SP, UK), and by the Station de Haute Belgique (referred to as SHB).

2. Theory: Shenk's method

Shenk's patented [5] method is based on two main steps: wavelength index correction, followed by spectral intensity correction. These two corrections are stored in a standardisation file, which is used to transfer spectra from one "slave" to one "master" instrument. The main advantage is that the software based on this method can be directly linked to NIR spectrometers, and can use raw data obtained on those spectrometers.

The main steps of this method are graphically described in Fig. 1a–e, and the following notations are used: **Xs** = matrix which contains spectra of the standardisation samples measured on the "slave" instrument; **Xm** = matrix which contains spectra of the standardisation samples measured on the "master" instrument; $X_{.i}$ = ith column of the **X** matrix (it corresponds to the responses of all samples at the ith wavelength); $X_{j.}$ = jth row of the **X** matrix (it corresponds to the spectrum of the jth sample); Nw = number of wavelengths; Ns = number of samples; $N = Ns \cdot Nw$ = number of measurements in one **X** matrix.

2.1. Mathematical treatment

Step 1

All spectra from the standardisation set are transformed by a first derivative mathematical treatment. Those spectra will be used for wavelength adjustment (steps 2 to 4).

2.2. Wavelength index correction

Step 2 (see Fig. 1a)

For each "master" instrument wavelength (i), a spectral window ($i-w$,$i+w$) of neighbouring wavelengths on the "slave" instrument is chosen, the correlations between $Xm_{.i}$ and each $Xs_{.k}$ (k from $i-w$ to $i+w$) are computed, and the "slave" instrument wavelength from this window (m), for which the absorptions $Xs_{.m}$ are most highly correlated with those measured on the "master" instrument $Xm_{.i}$ is found.

Step 3 (see Fig. 1b)

To obtain a more precise estimation of the wavelength at which the correlation is maximum, one fits a quadratic model to the wavelength with the highest correlation (m), and its two neighbouring wavelengths ($m-1$ and $m+1$):

$$\text{Correlation} = a + b \cdot i + c \cdot i^2 \quad (1)$$

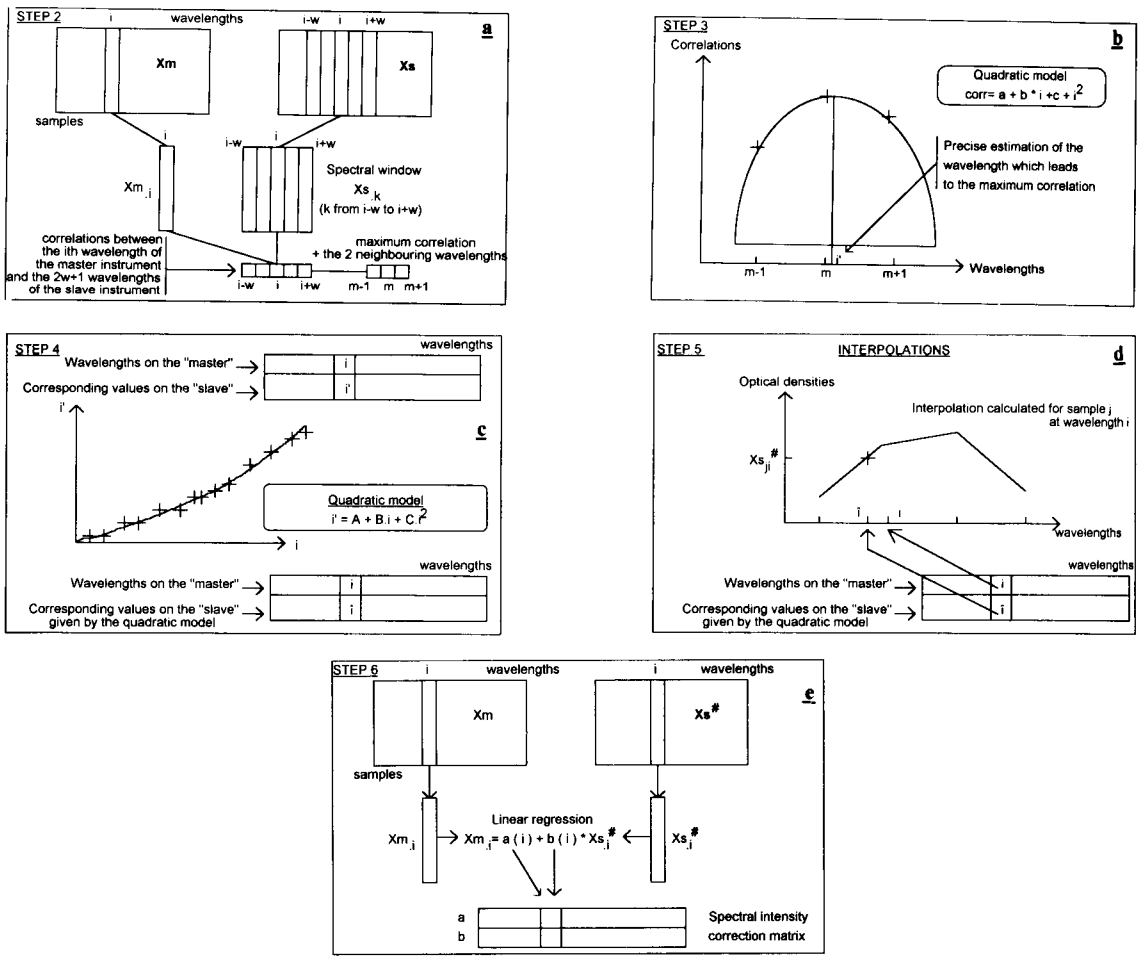

Fig. 1. Graphical description of Shenk's method (steps 2 to 6). a = step 2; b = step 3; c = step 4; d = step 5; e = step 6.

The different locations of the quadratic models obtained for each spectral "master" instrument wavelength are considered as the "slave" wavelengths (i'), that best match the corresponding master wavelengths (i).

Step 4 (see Fig. 1c)

A new quadratic model is fitted relating "master" wavelengths to their matching "slave" wavelengths ("slave" position)

$$i' = A + B \cdot i + C \cdot i^2 \qquad (2)$$

and definitive values for the "slave" wavelength ($\hat{i}$) corresponding to a "master" wavelength (i) are obtained.

2.3. Spectral intensity correction

In steps 5 to 8, the spectra without any mathematical treatment (and not the first derivative spectra) are used.

Step 5 (see Fig. 1d)

Interpolations are performed to compute the responses of the spectra measured on the "slave" instrument at the wavelengths suggested by the quadratic model ($\hat{i}$). The **Xs** matrix after interpolation will be referred to as $\mathbf{Xs}^{\#}$.

for $i = 1$ to Nw, (3)

$\mathrm{Xs}^{\#}_{,i} = \mathrm{Xs}_{,\hat{i}}$ (computed by interpolation)

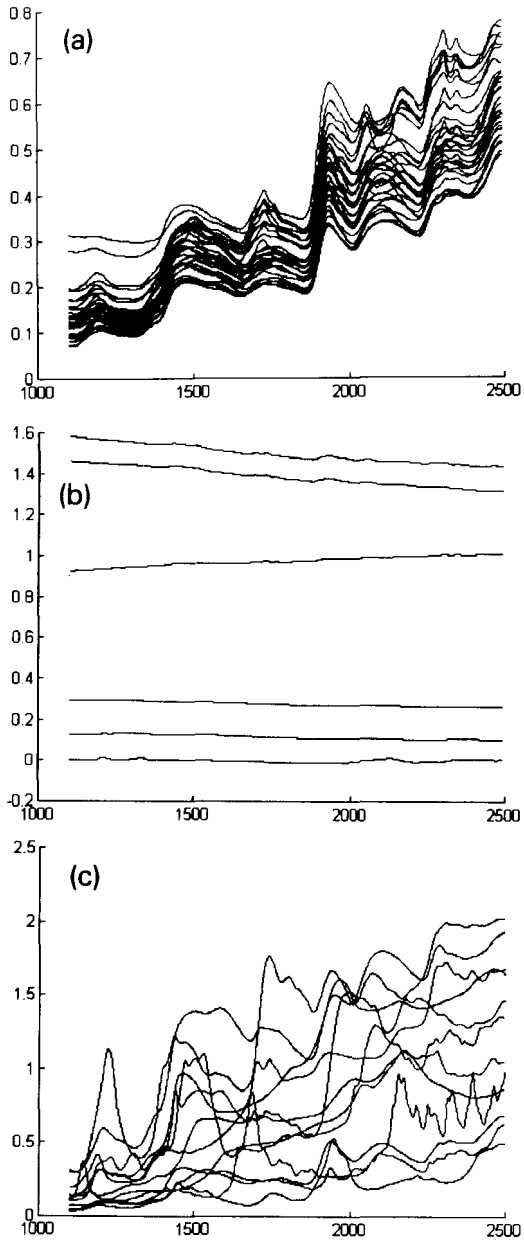

Fig. 2. Spectra of the 3 standardization sets. a = STD1 set: 30 cells with agronomic samples; b = STD2 set: 6 generic standards; c = STD3 set: 12 cells with pure organic and inorganic chemicals.

Step 6 (see Fig. 1e)

Spectral intensity correction is obtained by linear regression of the responses of the "slave" instrument at each shifted wavelength $Xs_{,i}^{\#}$ on the response of the "master" instrument at the corresponding wavelength $Xm_{,i}$.

$$Xm_{,i} = a(i) + b(i) \cdot Xs_{,i}^{\#} \quad (4)$$

where intercept (a) and slope (b) are computed for each wavelength i.

Step 7

Wavelength by wavelength, the response of the "slave" instrument is then adjusted with the corresponding regression coefficients.

$$Xstd_{,i} = a(i) + b(i) \cdot Xs_{,i}^{\#} \quad (5)$$

where **Xstd** is the **Xs** matrix after standardisation.

Step 8

The wavelength index and spectral intensity correction factors are stored in a standardisation file.

2.4. Transfer of spectra

Each spectrum obtained with the "slave" instrument can be standardised by using the standardisation file of step 8. To obtain the standardised spectra, the "slave" instrument wavelengths are shifted with the quadratic model given by Eq. 2, in order to obtain the calculated wavelength values. Interpolations are performed to compute the responses of the spectra measured on the "slave" instrument at the wavelengths suggested by the quadratic model. Finally, these "slave" instrument responses are corrected wavelength by wavelength with the regression coefficients of the spectral intensity correction matrix computed in step 6.

3. Experimental

NIRS instruments

The measurements are made on different spectrometers. The NIRSystem 6500 monochromator of SHB is referred to as the "master" instrument; The NIRSystem 5000 monochromators of UK, DA and SP will be referred to as the "slave" instruments. Before making the measurements, the instruments have been checked up and set up according to the diagnostic procedure of ISI's software: noise level, detector response and wavelength accuracy [9].

Table 1
(a) Name and composition of the standardization and prediction sets

Set name	Description
STD1	30 sealed cups with agronomic products (ISI standardization set)
STD2	6 generic standards (4 from Labsphere + 2 made by SHB)
STD3	12 sealed cups with pure organic and inorganic products
HE	6 grass samples
MA	6 corn samples
CO	17 colza samples

(b) Studied variables for each agronomic samples

Agronomic samples	Studied variables
HE	Proteins, cellulose
MA	Proteins, cellulose
CO	Proteins, fat

Standardisation samples

Three different types of standardisation samples were tested:

30 standardisation cells, made of different agronomic products by InfraSoft International (ISI, Port Mathilda, USA). These cells contain dried powders of different products such as grass, corn, wheat, colza, etc.... This standardisation set will be referred to as STD1.

6 standardisation cells, which contain different standards: 4 standards made by Labsphere, INC. (North Sutton, USA), and 2 made in the Station de Haute Belgique (Libramont, Belgium). These standards have very flat NIR spectra, but they cover a larger range of O.D. than the former 30 samples. This standardisation set will be referred to as STD2.

12 standardisation cells, made by the Station de Haute Belgique (Libramont, Belgium). These cells contain different pure products (urea, glyceride, butyric acid, polyethylene, ammonium carbonate, starch, naphthalene, lactose, saccharose, calcium sulfate, citric acid, oxalic acid). These products have NIR spectra which cover a larger range of O.D. than the former 30 samples. This standardisation set will be referred to as STD3.

Sample measurements

Before being measured by each "slave" system, the samples were measured once in SHB. The measurements consist of 6 different sets of samples (see Table 1a). The STD1, STD2, and STD3 sets contain standardisation samples, and the HE, MA, and CO sets contain agronomic samples (HE = grass, MA = corn, CO = rapeseed) used as the prediction set. The studied variables for all agronomic samples are summarized in Table 1b.

For each sample, two spectra are measured to check the repeatabilities. From these duplicates, the mean spectra are calculated. These are used in the calculations. Trimming of spectra obtained with 6500 NIRSystems is done, to obtain the same wavelength range (1100–2498 nm, step 2 nm) as the spectra obtained with NIRSystems 5000. Spectra of each standardisation set are plotted in Figs. 2a to 2c, and spectra of each prediction set are plotted in Figs. 3a to 3c.

Software

Pretreatment of spectra, determinations of standardisation files, transfers of spectra, and statistical calculations are performed with ISI's software. Graphical displays and further treatments of the results are performed in Matlab 4.0. Conversion of data from ISI's software to MATLAB and vice versa are performed by programs in QBASIC.

Calibration on the master instrument

For each set of agronomic samples, a calibration model is built on the "master" instrument in SHB. The calibration equations obtained are used to estimate the values of the studied variables given in Table 1b.

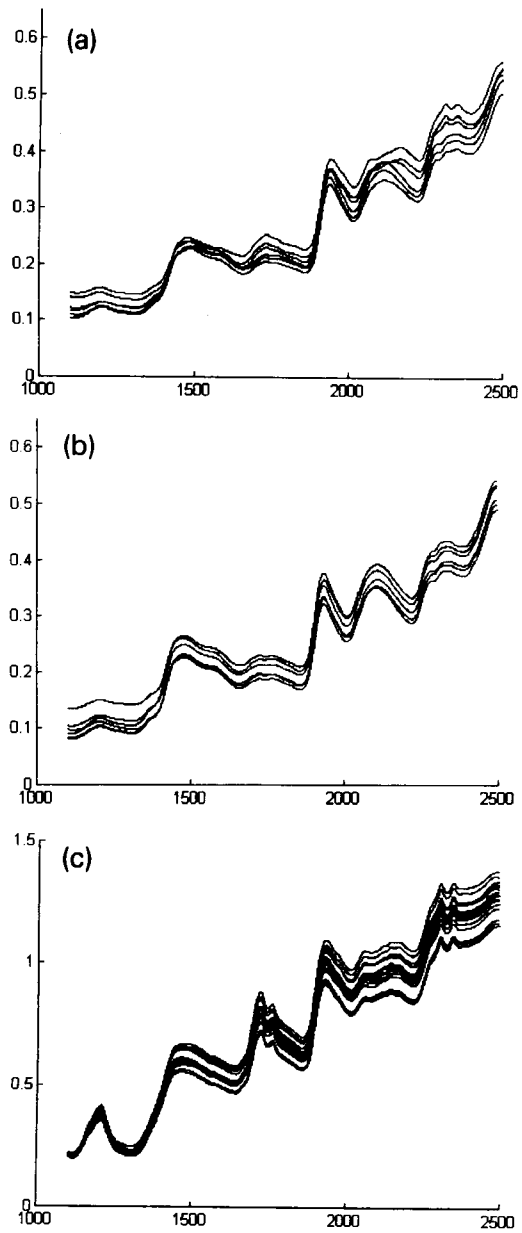

Fig. 3. Spectra of the 3 prediction sets. a = HE set: 6 grass samples; b = MA set: 6 corn samples; c = CO set: 17 colza samples.

Details about those calibration models are given in Table 2.

Standardisation

The root mean square errors RMSE (Eq. 6), the root mean square errors corrected for bias RMSE(c) (Eq. 7) and the determination coefficients R^2 (Eq. 8) between non-standardised spectra obtained on the "slave" instruments and spectra obtained on the "master" instrument are computed.

$$\mathrm{RMSE} = \frac{\sqrt{\sum_{i=1}^{Nw}\sum_{j=1}^{Ns}(Xm_{ji} - Xs_{ji})^2}}{\sqrt{N}} \tag{6}$$

$$\mathrm{RMSE(c)} = \frac{\sqrt{\sum_{i=1}^{Nw}\sum_{j=1}^{Ns}(Xm_{ji} - Xs_{ji})^2 - \left[\sum_{i=1}^{Nw}\sum_{j=1}^{Ns}(Xm_{ji} - Xs_{ji})\right]^2 / N}}{\sqrt{N-1}} \tag{7}$$

$$R^2 = \frac{\left(\sum_{i=1}^{Nw}\sum_{j=1}^{Ns}(Xm_{ji}\cdot Xs_{ji})^2 - \sum_{i=1}^{Nw}\sum_{j=1}^{Ns}(Xm_{ji})\cdot\sum_{i=1}^{Nw}\sum_{j=1}^{Ns}(Xs_{ji})/N\right)/(N-1)}{(S_m \cdot S_s)} \tag{8}$$

where S_m and S_s are the standard deviations computed with all the values obtained on the "master" and on the "slave" instrument.

With the calibration equations built on the "master" instrument, prediction for the different variables is calculated with the non-standardised spectra, and standard errors of prediction SEP (Eq. 9) are computed. In the literature, SEP gives usually the differences between computed values and reference values. In this paper, the SEP has a quite different meaning: in this case, the reference values used are the values obtained with the spectra measured on the "master" instrument. In other words, SEP gives the differences between values computed with spectra obtained on the "slave" instrument (standardised or not), and values computed with spectra obtained on the "master" instrument.

Table 2
Calibration models: numbers of samples involved, means of the values obtained, Standard error of calibration (SEC), and determination coefficient

Variables	Set	Number of samples	Mean	SEC	R^2
Proteins	HE	564	15.56	0.85	0.98
Cellulose	HE	563	26.21	1.27	0.96
Proteins	MA	482	7.78	0.43	0.90
Cellulose	MA	449	20.70	1.04	0.93
Proteins	CO	382	22.47	0.56	0.94
Fat	CO	354	45.85	0.73	0.91

Table 3
Root mean square errors (microlog) for each prediction set and for each "slave" instrument

		Before	STD1	STD2	STD2′	STD3
UK	HE	5779	6579	7279	6740	9429
	MA	6174	7618	8394	7848	11199
	CO	6513	11126	10599	9332	8187
SP	HE	8737	1460	5395	5875	10484
	MA	8435	1169	5439	5898	11130
	CO	14004	9148	12349	12428	11292
DA	HE	4043	2659	6664	6948	13693
	MA	3703	1957	6164	6119	14786
	CO	10660	9437	15974	16255	17913

Table 4
Root mean square errors corrected for bias (microlog) for each prediction set and for each "slave" instrument. (*) indicates acceptable RMSE(c) values

		Before	STD1	STD2	STD2′	STD3
UK	HE	5306	4457	4966	4619	6072
	MA	4867	4113	4590	4213	6331
	CO	5300	6274	8164	7315	7830
SP	HE	2157	453*	5738	4451	3663
	MA	2115	508*	4231	4503	5873
	CO	7053	5575	4314	7333	6551
DA	HE	3518	1770*	5237	4923	8316
	MA	3583	1748*	5601	5144	9037
	CO	7676	6301	11844	9695	10538

Table 5
Determination coefficients between spectra obtained on the "master" instrument and spectra obtained on the "slave" one, before and after standardization

		Before	STD1	STD2	STD2′	STD3
UK	HE	0.9982	0.9998	0.9984	0.9985	0.9984
	MA	0.9982	0.9998	0.9984	0.9986	0.9984
	CO	0.9998	0.9998	0.9997	0.9997	0.9997
SP	HE	0.9999	1.0000	0.9997	0.9999	0.9994
	MA	0.9999	1.0000	0.9996	0.9998	0.9992
	CO	0.9996	0.9999	0.9995	0.9997	0.9999
DA	HE	0.9996	0.9998	0.9987	0.9992	0.9982
	MA	0.9995	0.9999	0.9984	0.9991	0.9982
	CO	0.9999	0.9999	0.9988	0.9993	0.9998

$$\mathrm{SEP} = \frac{\sqrt{\Sigma (Y_m - Y_{pred})^2}}{\sqrt{Ns}} \qquad (9)$$

where Y_m are the values of the variables to be predicted (e.g., concentrations), obtained with the spectra measured on the "master" instrument, where Y_{pred} are the values of the variables to be predicted, obtained with the "spectra" measured on the "slave" instrument, with or without standardisation.

Four different standardisations are computed: the first three involve the complete method of Shenk and one of the three sets of standardisation samples, and the last one involves the STD2 set of standardisation samples, and Shenk's method without the wavelength adjustment (this standardisation will be referred to as STD2′). This is due to the fact that this wavelength adjustment uses derivative spectra, and in the case of the samples of the STD2 set, which have very flat NIR spectra, derivative spectra will not contain any information.

After all standardisation files are computed, RMSE, RMSE(c), and determination coefficients (R^2) between standardised spectra and spectra obtained on the "master" instrument are computed. With the calibration equations built on the "master" instrument, prediction for the same variables is calculated with the standardised spectra, and standard errors of prediction (SEP) are calculated and compared to those obtained with the non-standardised spectra.

4. Results and discussion

Before we describe the results, it should be noted that all the instruments are 5000 and 6500 NIRSystems and therefore very similar. The results and the conclusions should be interpreted in that context. It is probable that transfer between more different instruments would lead to other conclusions.

The results concerning RMSE, RMSE(c), and correlation coefficients between spectra obtained in SHB and spectra obtained in UK, SP, DA (non-standardised and standardised with the 4 different sets) are summarized in Tables 3, 4 and 5. The values with star in Table 4 are acceptable RMSE(c) values for standardised spectra (values under 2000 μlog).

To test the predictive ability, SEP are given for each test set (HE, MA, CO) measured in UK, SP, and DA (Tables 6–8). SEC obtained on the master instrument are given for comparison. The SEP obtained should be smaller than half the corresponding SEC: if SEP is

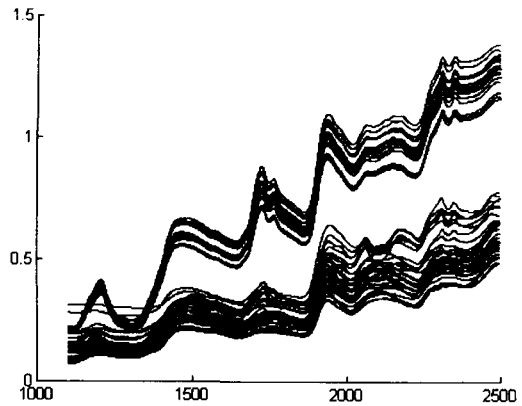

Fig. 4. Comparison between the CO and STD1 sets.

larger or of the same order of magnitude, standardisation is not useful.

Standardisation with the 30 agronomic samples gives the best results: this must be due to the fact that the 30 samples are of the same nature as the samples to be predicted, and that the 30 spectra have a similar optical density (O.D.) range as the HE and MA spectra. Fig. 4 shows that the CO spectra are in a different O.D. range compared to the 30 standardisation samples. The bad results obtained with CO samples can be explained by the different natures of the samples, but can also be due to the fact that one is measuring in different O.D. ranges. This was in fact the reason for trying to use generic standards, which cover a wider O.D. range.

Standardisation with STD2′ gives results, which are not as good as those obtained with STD1; RMSE(c) and R^2 coefficients are not good, SEP are average.

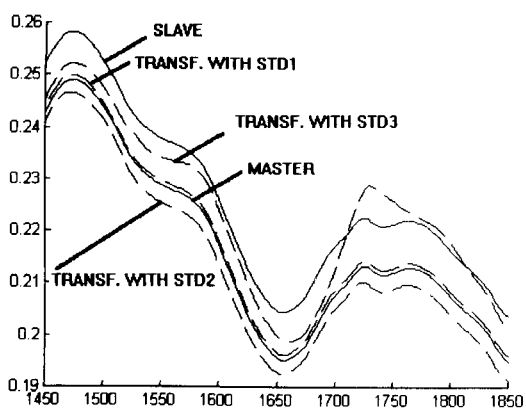

Fig. 5. Comparison of the spectra of one corn sample (MA set) obtained with the "master" instrument, with the "slave" instrument, and transfered with one of the three STD sets.

Standardisation with the STD2 set gives results which show only small differences with the STD2′ set. This proves that wavelength shifts between those NIR-Systems are very small.

Standardisation with the STD3 set gives bad results: spectra after standardisation are often more different than before.

Fig. 5 represents a zoomed part of spectra from one sample of the MA set in order to show how similar the standardised spectra are to the spectra obtained on the "master" instrument.

Figs. 6a and 6b show the mean of the differences and the standard deviation of the differences between spectra obtained in SHB and in SP for the MA, HE, CO and STD1 sets. Those two figures show that the mean and the standard deviation of the differences between SHB and SP for CO and STD1 are very different. This could be due to the different O.D. ranges of the two sets. The comparison of MA and HE with STD1 seems to confirm this assumption: thus, the mean and the standard deviation of the spectra from MA, HE, and STD1 are very close together, and those three sets are exactly in the same O.D. range. This could explain the results obtained in Tables 3, 4 and 5. Differences between spectra from one instrument to another seem to depend on the O.D. range, where the spectra are located.

Figs. 7 and 8 show the mean of the differences and the standard deviation of the differences between spectra obtained in SHB and in SP for the MA, HE, CO and STD2 sets (Fig. 7a–b), and for the MA, HE, CO and STD3 set (Fig. 8a–b). The curves corresponding to the STD2 and STD3 sets are very far from those of the HE, MA, and CO sets, and standardisations with STD2 and

Table 6
(a) Standard errors of prediction (proteins) for the HE set

	SEC	Before	Std1	Std2	Std2′	Std3
UK	0.85	0.66	0.21	0.35	0.45	1.18
SP	0.85	0.37	0.14	0.73	0.69	1.68
DA	0.85	0.53	0.45	1.38	0.47	3.87

(b) Standard errors of prediction (cellulose) for the HE set

	SEC	Before	Std1	Std2	Std2′	Std3
UK	1.27	0.45	0.21	0.93	0.48	7.07
SP	1.27	1.17	0.35	1.02	0.52	0.85
DA	1.27	0.49	0.34	0.82	0.95	1.16

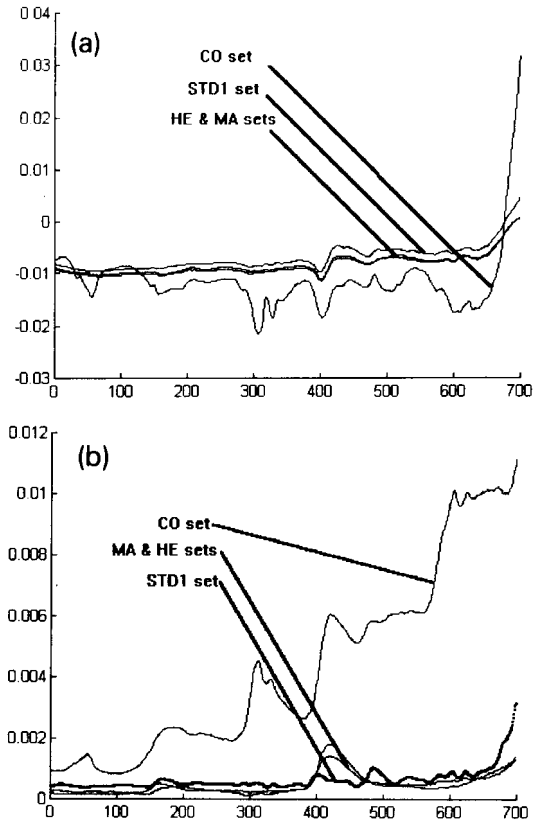

Fig. 6. Mean and standard deviation of the differences between spectra obtained in SP and in SHB for the samples of the MA, HE, CO, and STD1 sets. a = Mean; b = standard deviation.

STD3 do not give good results, as indicated in Tables 3, 4 and 5.

In other words, if one computes differences between instrumental responses of two systems with standardisation samples located in one O.D. range, and if those differences are then used to standardise spectra located in a second O.D. range different from the former, the results obtained will not be acceptable. Differences between spectra obtained on two different instruments depend probably on the O.D. ranges, where the spectra are located.

When standardisation samples are in the same O.D. range as the samples to be predicted, the standardisation parameters computed should give good results. Nevertheless, some unexpected problems might appear: in Fig. 6a, the curve corresponding to the STD1 set is quite the same as those of the MA and HE sets, but it is shifted to the top: this means that spectra of the STD1 set showed smaller differences than samples of the MA and HE sets. It should be noticed that this systematic bias (it does not depend on the wavelength) influences the RMSE, which is significantly larger than the RMSE(c). However, the standard errors of prediction after standardisation with the STD1 set are not influenced by this bias, because the calibration models developed to predict the studied values involve first derivative spectra, which removes constant shifts in absorbency. However in some NIR applications, one uses the raw spectra to build the calibration model. In this case, the bias would give erroneous prediction values.

The presence of this bias proves that attention should be paid to the standardisation samples chosen, and although the standardisation and prediction samples are of the same nature, some unexpected differences might appear.

To explain the presence of this bias, some hypotheses can be advanced:

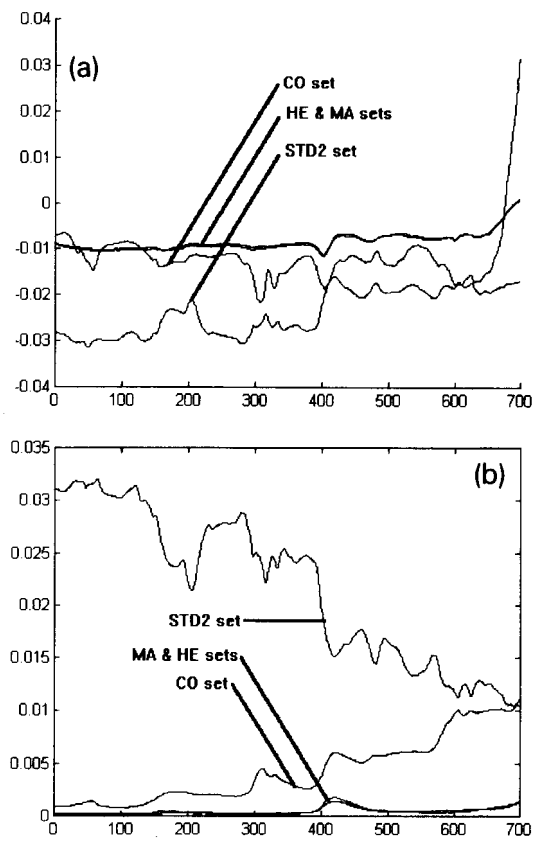

Fig. 7. Mean and standard deviation of the differences between spectra obtained in SP and in SHB for the samples of the MA, HE, CO, and STD2 sets. a = Mean; b = standard deviation.

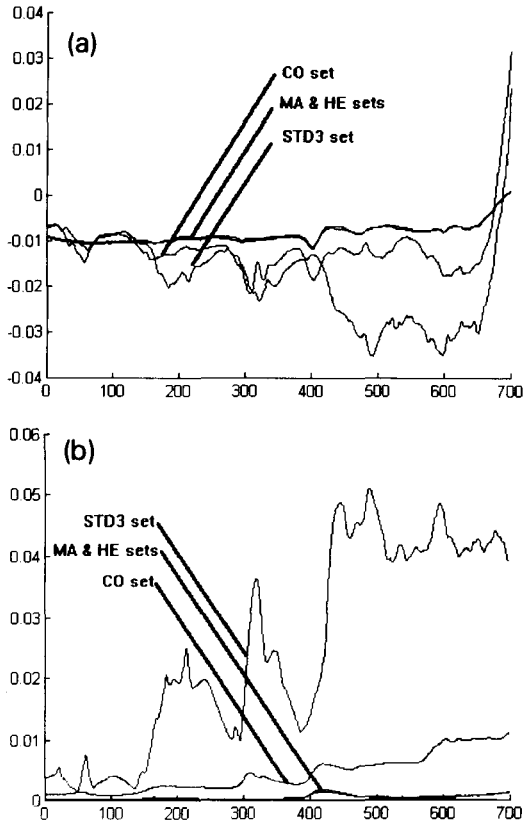

Fig. 8. Mean and standard deviation of the differences between spectra obtained in SP and in SHB for the samples of the MA, HE, CO, and STD3 sets. a = Mean; b = standard deviation.

hypothesis 1: different evolutions of the products over time (different modifications of their compositions).

hypothesis 2: different contributions of the cells used (the cells used from standardisation set and prediction set are not exactly the same).

hypothesis 3: temperature variations between measurements of the standardisation and prediction set.

The last hypothesis is improbable, because the time required for each analysis is very short (a few seconds for each sample), and because all sets are analysed one after the other: in this case, such an important shift is almost impossible.

To explain the presence of the bias, hypothesis 1, hypothesis 2, or a combination of those two seems to be more suitable, than hypothesis 3. There is probably a modification of the amount of water in the samples to be predicted between the measurements made in SHB and in SP. Thus, Fig. 6a shows some fluctuations

Table 7
(a) Standard errors of prediction (proteins) for the MA set

	SEC	Before	Std1	Std2	Std2′	Std3
UK	0.43	0.40	0.12	0.95	0.04	1.24
SP	0.43	0.23	0.10	0.89	0.14	5.71
DA	0.43	0.39	0.22	1.58	0.69	7.65

(b) Standard errors of prediction (cellulose) for the MA set

	SEC	Before	Std1	Std2	Std2′	Std3
UK	1.04	0.47	0.30	0.38	0.60	2.89
SP	1.04	0.74	0.15	0.85	0.38	2.45
DA	1.04	0.92	0.33	1.22	0.61	1.72

Table 8
(a) Standard errors of prediction (proteins) for the CO set

	SEC	Before	Std1	Std2	Std2′	Std3
UK	0.56	0.97	1.33	0.37	0.15	0.99
SP	0.56	0.95	1.08	2.65	1.13	1.20
DA	0.56	0.51	1.23	4.23	2.08	1.93

(b) Standard errors of prediction (fat) for the CO set

	SEC	Before	Std1	Std2	Std2′	Std3
UK	0.73	1.30	0.64	1.14	0.74	6.79
SP	0.73	0.64	1.41	0.52	1.06	4.16
DA	0.73	0.54	0.95	2.15	1.20	5.54

of the bias between standardisation and prediction samples. Moreover, Fig. 6b shows humps at 1900–2000 nm for the spectra to be predicted, but no hump for the standardisation samples is present. In fact, those different origins of the amount of water are probably due to the fact, that standardisation samples are in cells, but prediction samples are in normal cups (they are more sensitive to external variations). As can be seen here, different evolutions of the samples do not lead to a constant bias, but to local variations at particular wavelengths. This remark shows that hypothesis 2 seems to be improbable to explain the origin of the bias.

5. Conclusions

Differences between spectra obtained on two different instruments depend probably on the O.D. ranges,

where the spectra are located. If the standardisation samples used to correct differences between instruments are very different from the samples of the prediction set, and particularly if the differences between "master" and "slave" instruments in the same spectral region are different in the standardisation set compared to the prediction set, this could lead to poor predictions.

It appears that one needs standardisation samples which cover exactly the same O.D. range as the prediction samples. In this case, the best standardisation set used to standardise spectra from one prediction set should be the prediction set itself, or a representative subset of it. Another possibility could also be to find standardisation samples which cover exactly the same range for each spectral region, but to know in which region they are, one needs to remeasure some samples on the "master" instrument to compute the differences. If some samples have to be remeasured, standardisation with subset selection seems to be a better choice.

If we decide that products very similar to the prediction samples (e.g., grass samples to predict other grass samples) can be used for standardisation without any remeasure of prediction samples on the "master" instrument, some problems might appear: in this paper, it is shown that a systematic bias can surface, although the products used in the two sets (standardisation and prediction) are very similar. If possible to remeasure some samples on the "master" instrument, this is to be recommended. In that case, as said higher, standardisation with subset selection has to be applied, since no systematic unexpected difference between standardisation and prediction sets will occur with this method.

In case of standardisation samples different from those used for prediction, a good compromise has to be found, between too similar standardisation samples (which could only be applicable for the prediction of particular samples) and too different standardisation samples (which could lead to bad standardisations).

Acknowledgements

We would like to thank I. Murray (SAC Aberdeen, UK), A. Garrido-Varo (Escuela Tecnica Superior de Ingenieros Agronomos y de Montes, Cordoba, Spain) and L.K. Sørensen (Steins Laboratorium, Albertslund, Denmark), participants of QUEST, for NIRS measurements.

References

[1] Y. Wang and B.R. Kowalski, Anal. Chem., 65 (1993) 1301.
[2] Y. Wang, D.J. Veltkamp and B.R. Kowalski, Anal. Chem., 63 (1991) 2750.
[3] Y. Wang, M.J. Lysaght and B.R. Kowalski, Anal. Chem., 64 (1992) 562.
[4] J.S. Shenk and M.O. Westerhaus, Crop Sci., 31 (1991) 1694.
[5] J.S. Shenk, M.O. Westerhaus, U.S. Pat., 4866644, Sept 12 (1989).
[6] M. Forina, C. Armanino and R. Giangiacomo, in Hildrum, Isaksson, Naes, Tandberg (Eds.), Near Infrared Spectroscopy, Ellis Horwood, Chichester, 1992.
[7] M. Forina, G. Drava, C. Armanino, R. Boggia, S. Lanteri, R. Leardi, Chemom. Intell. Lab. Syst., in press
[8] P. Dardenne, R. Biston, in R. Biston and N. Bartiaux-Thill (Eds.), Proc. Third International Conference on Near Infrared Spectroscopy, Agric. Res. Centre Publ., Belgium, 1991, p. 655.
[9] J.S. Shenk, in R. Biston and N. Bartiaux-Thill (Eds.), Proc. Third International Conference on Near Infrared Spectroscopy, Agric. Res. Centre Publ., Belgium, 1991, p. 649.

ELSEVIER

Analytica Chimica Acta 297 (1994) 417–425

ANALYTICA CHIMICA ACTA

Possibilities for graphic representation of multifactor simplex optimisation

A. Lopez Molinero

Analytical Chemistry Department, Faculty of Sciences, University of Zaragoza, 50009 Zaragoza, Spain.

Received 10 November 1993; revised manuscript received 6 May 1994

Abstract

The progress of a multifactor simplex optimisation algorithm has been plotted in a visual mode, after a reduction in the number of factors using the statistic principal component analysis method. The effectiveness of the proposed graphic representation has been evaluated when applied to simplex previously published optimisation methods such as: colorimetric determination of cholesterol, flow-injection spectrophotometric determination of promethazine and synthesis of an industrial pyrazolone. The procedure has also been applied to develop new experimental analytical methods like the determination of arsenic trichloride by inductively coupled plasma atomic emission spectrometry.

Keywords: Principal component analysis; Graphic representation; Multifactor simplex optimisation

1. Introduction

The simplex method is a general procedure for optimisation of mathematical functions. A deduced alternative that has been widely accepted by analytical chemists [1,2] was devised by Spendley et al. [3] and modified by Nelder and Mead [4]. This useful algorithm is known as the modified simplex method (MSM). The method is based on a direct sequential search procedure and works with the displacement of a geometric figure, defined by a number of points equal to one more than the number of variables in the optimisation process, and is carried out according to a set of logical rules, consisting of reflection, expansion, contraction and massive contraction of the geometric figure. The efficiency and simplicity of this modification have been fundamental for its general application to develop new analytical methods, in particular in atomic spectroscopy [5–8]

The simplex optimisation process can be substantially understood by mapping the progress of the procedure. Application of this technique, however, is only possible when the response function depends on one or two factors.

In this article, the ability of a multifactor simplex modified algorithm to converge to the optimum is visualised. The procedure is based on mapping the progress of the simplex over the surface response. The initial variables of the simplex are reduced to two new factors, using the principal component analysis (PCA) method. The factors involved are the first principal component (PC1) and the second principal component (PC2) vectors. If the response is superimposed over the plane defined by PC1 and PC2, a two-dimen-

0003-2670/94/$07.00
SSDI 0003-2670(94)00227-D

sional graph is obtained, representing the search for the optimum in a multifactor simplex.

This response surface determination strategy produces information describing not only the variable coordinates for the optimum but also makes it possible to obtain more information about a system than is obtained by simplex search.

2. Experimental

PCA was applied using the commercial software package Systat 2.0 (Systat Program Version 2.0) running on an Apple Macintosh LC.

The modified simplex method was programmed using BASIC, a language according to the theory of Nelder and Mead [4]. It runs on an IBM PC-AT microcomputer.

2.1. Factors reduction procedure

The experimental vertices, obtained from applying the modified simplex algorithm to an optimisation experience, are evaluated by PCA. From this study, the number of variables can be reduced to two new factors that are the eigenvectors of the correlation matrix of the original data. Working with this matrix a more general result is obtained and the differences of the original data are normalised. The eigenvectors are PC1 and

Table 1
Experimental data of the simplex optimisation for the cholesterol determination according to Ref. [9] and results of the PCA

Experimental vertices of the simplex				Response Tot. Res	New-reduced-vertices		Denomination Vertex
Var. A	Var. B	Var. D	Var. E		Factor 1	Factor 2	
8.300	25.000	25.000	50.000	47.800	−1.754	−1.950	A
23.800	35.900	35.900	57.300	72.400	−1.353	−1.387	B
11.900	71.300	35.900	57.300	88.600	−0.894	0.380	C
11.900	35.900	71.300	57.300	95.600	0.241	−0.952	D
11.900	35.900	35.900	80.900	91.500	−0.085	−1.536	E
21.500	64.500	64.500	76.400	94.900	0.708	0.202	F
4.800	67.900	67.900	78.600	90.900	1.336	0.435	G
9.600	59.900	59.900	74.000	95.500	0.693	−0.027	H
15.600	26.900	79.900	87.000	92.200	1.671	−1.531	I
17.500	57.700	101.900	66.500	0.000	1.741	0.381	J
13.300	41.400	52.400	70.100	95.300	0.070	−0.999	K
12.500	74.000	44.200	51.900	99.200	−0.812	0.647	L
11.000	97.600	26.300	34.400	56.200	−2.054	1.737	M
16.700	84.000	39.200	78.900	90.200	0.085	0.863	N
13.100	47.900	63.300	62.700	95.800	0.203	−0.499	O
20.600	54.000	52.300	56.600	89.600	−0.606	−0.299	P
12.300	58.400	58.000	69.600	97.500	0.367	−0.095	Q
16.500	81.100	62.600	60.300	97.800	0.165	1.130	R
5.800	66.200	49.500	45.900	90.100	−0.749	0.388	S
17.500	65.000	60.800	68.800	96.800	0.349	0.253	T
16.200	91.300	49.500	62.600	96.700	−0.167	1.464	U
18.800	73.900	71.300	78.700	96.100	1.168	0.730	W
14.200	74.000	50.900	58.600	93.000	−0.323	0.667	X

Eigenvalues (higher than 1.0)		Rotated loadings (Varimax)			Percent of total variance explained	
Num. 1	Num. 2	Variable	Factor 1	Factor 2	Factor 1	Factor 2
1.681	1.014	Var. A	0.122	0.013	36.713	25.636
		Var. B	−0.104	0.984		
		Var. D	0.890	0.041		
		Var. E	0.807	−0.236		

PC2, the first and second principal component, respectively. The scores of the first two principal components are obtained for all the experimental vertices and these are the new coordinates of the vertices. That is, each vertex of the simplex previously defined by n variables, is redefined by only two new variables or factors (the scores).

2.2. Graphic presentation

The simplex optimisation search for n factors can be plotted in a three-dimensional graph when the response is plotted versus the two new variables (PC1 and PC2). Alternatively, the contour plot of the response versus the two new variables can be obtained. This latter has been selected in this work, and so characteristic map figures or iso-response contour diagrams will be shown. The map-figures are obtained using the graphic module of the Systat 2.0 package, which uses spline fits.

3. Results and discussion

The proposed method for two-dimensional graphic representation of the simplex optimisation search has been applied to four samples of the bibliography.

The first case we have considered is the colorimetric determination of cholesterol in blood serum according to Ref. [9].

Morgan and Deming have evaluated the potential of the modified simplex method for the determination of total cholesterol in blood serum carried out following the procedure of Carr and Drekter [10]. In this method the absorbance, measured at 630 nm, is a function of five factors. Factorial designs, however, have been previously used to evaluate the relative significance of the factors, and only four of the five factors (A, solvent; B, dehydrating reagent; D, color reagent and E, color development time) were chosen as having the most significant effects on the response function.

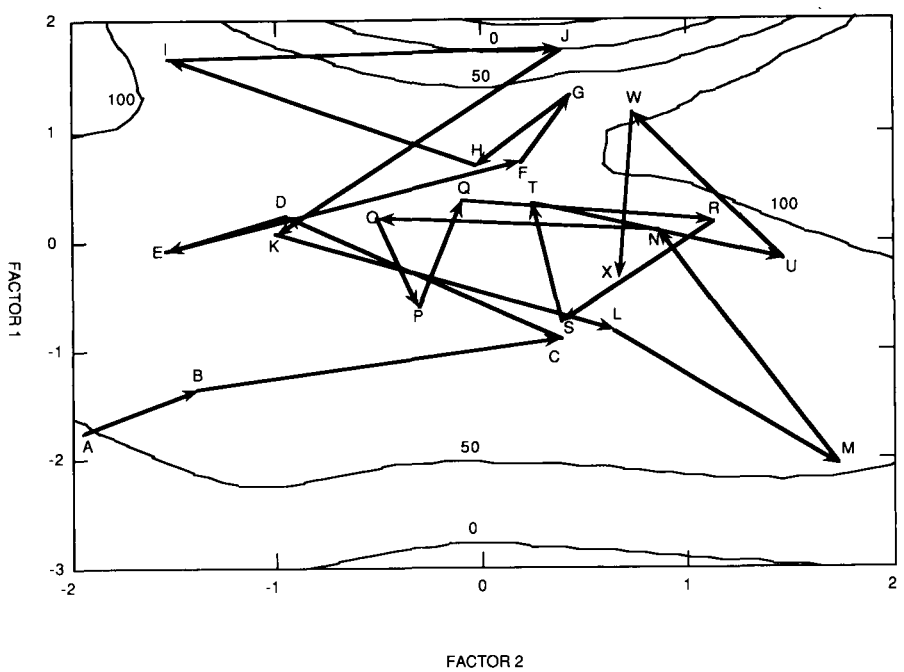

Fig. 1. Evolution of the response for cholesterol determination during the search of the fourth-dimensional simplex when plotted in contour map.

The experimental vertices obtained from the application of the modified simplex optimisation [9] are shown in Table 1.

When PCA is applied to this experiment, two important facts are obtained:

(i) The experimental variables are reduced to two new factors (vectors PC1 and PC2). In the example considered, the redefined variables retain 36.7 and 25.6%, respectively, in the initial variance of the data. The experimental vertices of the simplex can now be redefined by the values of the scores on PC1 and PC2 presented in Table 1.

(ii) The relative significance of the initial *n*-variables on the response can also be evaluated by the loadings or correlation coefficient between the factors and the stated component. Therefore, in the first principal component, the factors D and E give the highest loadings with 0.890 and 0.807, respectively. The second principal component is highly influenced by factor B, with a loading of 0.984.

In Fig. 1 the evolution of the 4-factors experimental simplex can be followed through the progress of the new vertices (i.e., from vertex A to vertex X). The vertices are superimposed on a contour map, which represents the iso-response curves of the function.

The observations of the results of this procedure (reduction in the number of variables and graphic representation) permit us to reach the following conclusions for the example considered:

(i) The optimum direction for the simplex

Table 2
Experimental data of the simplex optimisation for the determination of promethazine hydrochloride reported in Ref. [11] and results of the PCA

Experimental vertices of the simplex				Response Absorbance	New-reduced-vertices		Denomination Vertex
Coil length	Flow rate	$[H_2SO_4]$	[Ce(IV)]		Factor 1	Factor 2	
45.000	4.100	0.100	0.357	0.168	−0.867	−2.468	A
87.000	4.231	0.264	2.310	0.360	−0.028	1.442	B
55.000	4.231	0.264	8.500	0.462	−0.891	−1.019	C
55.000	4.231	0.794	2.310	0.384	1.388	−0.654	D
55.000	4.655	0.264	2.310	0.384	−1.789	0.129	E
81.000	4.574	0.694	7.350	0.312	0.212	2.417	F
68.000	4.408	0.485	4.930	0.401	−0.178	0.674	G
72.000	4.306	0.358	3.430	0.447	−0.208	0.562	H
67.000	4.334	0.393	3.840	0.465	−0.265	0.282	I
64.000	4.507	0.100	6.420	0.453	−2.030	0.334	J
63.000	4.460	0.219	5.710	0.462	−1.435	0.209	K
71.000	4.100	0.406	8.790	0.378	0.267	0.200	L
63.000	4.250	0.511	5.350	0.504	0.266	−0.159	M
62.000	4.146	0.657	5.170	0.507	1.097	−0.420	N
74.000	4.437	0.662	0.728	0.180	0.712	1.328	O
60.000	4.289	0.376	6.400	0.534	−0.450	−0.385	P
58.000	4.311	0.525	6.790	0.537	−0.017	−0.345	Q
65.000	4.100	0.681	6.400	0.534	1.305	−0.275	R
66.000	4.100	0.720	6.580	0.498	1.456	−0.159	S
58.000	4.100	0.589	6.580	0.504	0.837	−0.911	T
60.000	4.166	0.567	6.230	0.534	0.618	−0.583	U

Eigenvalues (higher than 1.0)		Rotated loadings (Varimax)			Percent of total variance explained	
Num. 1	Num. 2		Factor 1	Factor 2	Factor 1	Factor 2
1.371	1.184	Coil length	0.183	0.892	30.437	29.880
		Flow rate	−0.615	0.602		
		$[H_2SO_4]$	0.896	0.194		
		[Ce(IV)]	0.065	0.015		

search is easily determined. The first steps provide a fast direction for convergence to optimum, but during the last steps the convergence is slow.

(ii) The nature of the optimum is obtained. The vertex L is located near the maximum (not local maximum) of the domain studied.

(iii) We can visualise two regions of maximum response (value 100), one characterised by high values of Factor 1 and low values of Factor 2 and another by high values of Factor 1 and Factor 2.

Sultan and Suliman [11] have published the application of super modified simplex optimisation to the flow-injection spectrophotometric determination of promethazine hydrochloride in drug formulations. The method involves the use of Ce(IV) to oxidize promethazine in sulphuric acid media to yield a reddish coloured compound. Its absorbance at 515 nm was monitored. Keeping the sample loop size constant at 110 μl, the other variables such as reaction coil length of the FIA mounting, cerium(IV) concentration, sulphuric acid concentration and flow rate parameters, were optimised.

The progress of the simplex can be seen from the values in Table 2. After application of the PCA method to the coordinates of the experiments, the four initial variables are reduced to two new factors (PC1 and PC2). The first and second principal component retain 30.4 and 29.9%, respectively, in the initial variance of the data.

Sulphuric acid concentration has a great influence on the first principal component, with a loading factor of 0.896, and over the second principal component the reaction coil length has the greatest influence, with a loading factor of 0.892.

Table 2 also offers the coordinates of the experimental vertices, redefined by the scores of PC1 and PC2 vectors. Their graphic representation (see Fig. 2) over the iso-response contour lines (iso-response contour map) shows certain interesting trends of the simplex search.

The simplex searches from the initial point: vertex A to vertex U. First, the progress is fast and is directed to a maximum at the response value of 0.5. This maximum is located next to

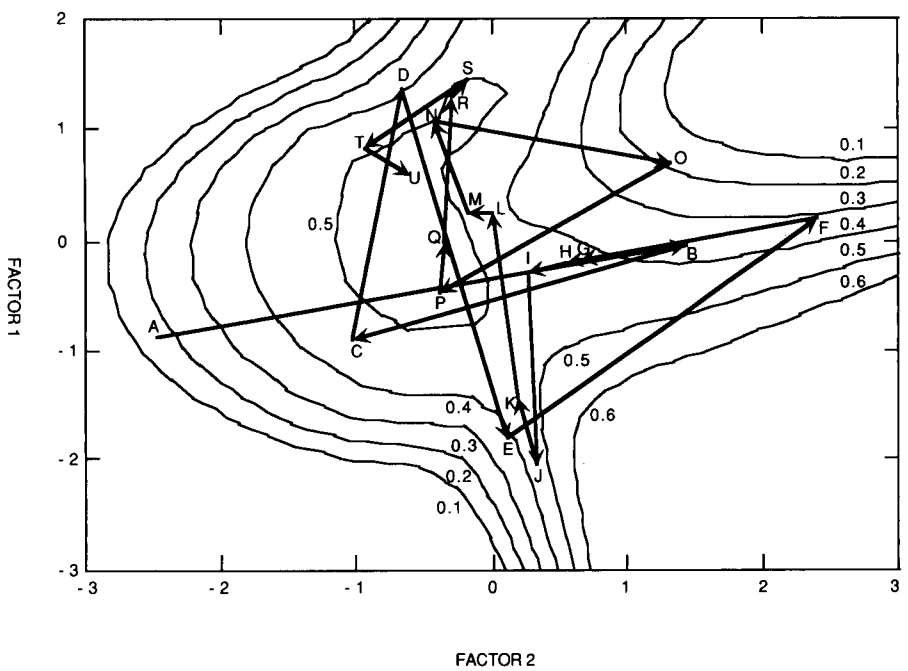

Fig. 2. Contour diagram for the evolution of the response during the search for the fourth-dimensional simplex of the promethazine hydrochloride determination.

values of 0.0, for Factor 1 and Factor 2. However, this seems a local maximum, and an exploration of the region with positives values for PC2 (from 0.7 to 3) and negatives for PC1 (from −0.3 to −3) can provide useful information (higher values of the response).

From this experiment we can conclude that a maximum has been located but the simplex also indicates the presence of a maximum at other values of variables, for instance, at greater reaction coil length than the one used.

Lazaro et al. [12] have studied the optimisation of the synthesis of an industrial pyrazolone. The yield of the reaction depends on time of methanolysis (factor Time 1); temperature of the second step of reaction (factor Temperat); time of reaction of the third step (factor Time 3); temperature of the prior reaction (factor Temper 4); volume of acetic acid (factor Cataliz.) and chlorohydrate to *p*-nitroaniline molar ratio (factor Ratio mol).

In Table 3 the coordinates of the experiments obtained from reference data are given.

Application of PCA to the previous data found six new variables, which retain each 16.7% of the initial variance of the data. The factor Time 1, therefore, most influences PC1 with a loading of 0.972, and the factor Temperat most influences PC2 with a loading of 0.987, and so on.

The results of the simplex progress from vertex A to vertex L given in Fig. 3 indicate that the yield increases towards positive values of PC1 (as the reaction time increases) and towards moderate positive values of PC2 (as the Temperat factor increases).

This is a particular example where the initial variables are not interconnected, and it is not possible to reduce the initial set of variables. This is confirmed by the correlation matrix of the original data, which presents very low values of correlation coefficients between variables. In this matrix the highest correlation coefficient is 0.300.

Table 3
Experimental data of the simplex optimisation for synthesis of an industrial pyrazolone reported in Ref. [12] and results of the PCA

Experimental vertices of the simplex						Response Yield	New-reduced-vertices		Denomination Vertex
Time 1	Temperat.	Time 3	Temper. 4	Cataliz.	Ratio mol		Factor 1	Factor 2	
30.000	45.000	15.000	51.000	0.000	1.600	76.000	−1.110	−0.573	A
156.000	48.000	21.000	48.000	20.000	1.500	93.000	2.409	0.248	B
57.000	58.000	21.000	48.000	20.000	1.500	60.000	−0.338	2.340	C
57.000	48.000	42.000	48.000	20.000	1.500	87.000	−0.855	0.167	D
57.000	48.000	21.000	37.000	20.000	1.500	80.000	−0.888	0.217	E
57.000	48.000	21.000	48.000	90.000	1.500	50.000	−0.433	−0.202	F
57.000	48.000	21.000	48.000	20.000	1.150	66.000	−0.414	−0.038	G
71.000	50.000	24.000	46.000	2.000	1.450	76.000	−0.171	0.652	H
86.000	38.000	27.000	45.000	7.000	1.400	78.000	0.022	−2.043	I
95.000	44.000	21.000	44.000	2.500	1.830	68.000	0.361	−0.515	J
86.000	45.000	27.000	45.000	6.800	1.660	75.000	0.073	−0.372	K
142.000	47.000	39.000	39.000	25.000	1.400	95.000	1.344	0.118	L

Eigenvalues (higher than 1.0)		Rotated loadings (Varimax)			Percent of total variance explained	
Num. 1	Num. 2	Variable	Factor 1	Factor 2	Factor 1	Factor 2
1.735	1.343	Time 1	0.972	−0.075	16.676	16.649
		Temperat.	−0.072	0.987		
		Time 3	0.149	−0.040		
		Temper. 4	−0.159	0.064		
		Cataliz.	−0.022	0.101		
		Mol. ratio	0.021	−0.064		

Chlorides of certain elements are gaseous. Those compounds constitute a new alternative for gaseous sample introduction in atomic spectroscopy. Therefore, the reaction of arsenic(III) with chloride ions in strong sulphuric acidic media has been recently reported [13]. The subsequent volatile chloride generated has been swept to an inductively coupled plasma (ICP) spectrometer and arsenic has been determined. The experimental variables for arsenic trichloride determination by ICP-atomic emission spectrometry (AES) have been optimised by the MSM method.

The arsenic emission signal to background signal ratio has been optimised as a function of the following factors: HCl concentration (HCl factor); H_2SO_4 concentration (H_2SO_4 factor); the flow of the acids (factor Ac. Flow) and the carrier gas flow (factor Gas Flow).

Table 4 shows the vertices, obtained from the four-factors simplex optimisation, for the analytical determination of arsenic and the values of the vertices in the new coordinates are also gathered. The study of this optimisation by PCA shows that the two new variables, PC1 and PC2, explain 40.3 and 25.4% of the initial variance, respectively. PC1 is correlated with the factors Gas flow and Acid flow, which presents a loading of 0.928 and 0.853, respectively. PC2 is influenced by HCl and H_2SO_4 concentration, with a loading of 0.971 and 0.851, respectively.

The simplex evolution can be seen in Fig. 4, from point A up to point S. Interesting conclusions can be deduced for this example. First, the optimisation progresses slowly to point F. From here, the evolution is towards the optimum. Two maxima are found, one in front of the other. The first one is characterised by low PC2 values and the second by positive values (i.e., for high and

Table 4
Experimental data of the simplex optimisation of arsenic chloride determination by ICP-AES and results of the PCA

Experimental vertices of the simplex				Response	New-reduced-vertices		Denomination
[HCl]	[H_2SO_4]	Acid flow	Gas flow	Em. signal	Factor 1	Factor 2	Vertex
50.000	50.000	4.000	0.500	0.000	−1.061	−0.604	A
50.000	10.000	8.000	0.500	3.200	−0.478	−1.716	B
50.000	80.000	4.000	1.000	0.000	−0.870	−0.839	C
66.700	80.000	4.000	1.000	4.000	−0.858	0.254	D
66.700	10.000	4.000	1.000	4.833	−1.090	−0.090	E
10.000	10.000	4.000	0.500	4.100	−1.603	2.020	F
83.300	10.000	6.000	1.000	7.625	−0.496	0.857	G
66.700	10.000	6.000	1.000	5.889	−0.509	−0.236	H
66.700	80.000	6.000	1.500	10.500	0.261	0.184	I
50.000	90.000	7.000	2.000	8.500	0.962	−0.996	J
66.700	95.000	7.000	2.000	10.750	0.916	0.031	K
66.700	90.000	10.000	2.000	15.000	1.845	−0.245	L
66.700	90.000	7.000	2.000	14.500	0.974	0.097	M
66.700	90.000	7.000	2.000	22.500	0.974	0.097	N
83.300	95.000	7.000	2.000	19.000	0.928	1.125	O
50.000	10.000	7.000	2.000	23.500	0.846	−1.128	P
10.000	10.000	7.000	2.000	14.600	0.883	2.153	Q
66.700	10.000	5.000	0.800	17.600	−1.014	−0.186	R
50.000	90.000	4.000	1.350	19.000	−0.609	−0.860	S

Eigenvalues (higher than 1.0)		Rotated loadings (Varimax)			Percent of total variance explained	
Num. 1	Num. 2	Variable	Factor 1	Factor 2	Factor 1	Factor 2
1.864	1.215	Gas flow	0.928	0.103	40.256	25.367
		Acid flow	0.853	−0.091		
		HCl	0.012	0.971		
		H_2SO_4	0.143	0.232		

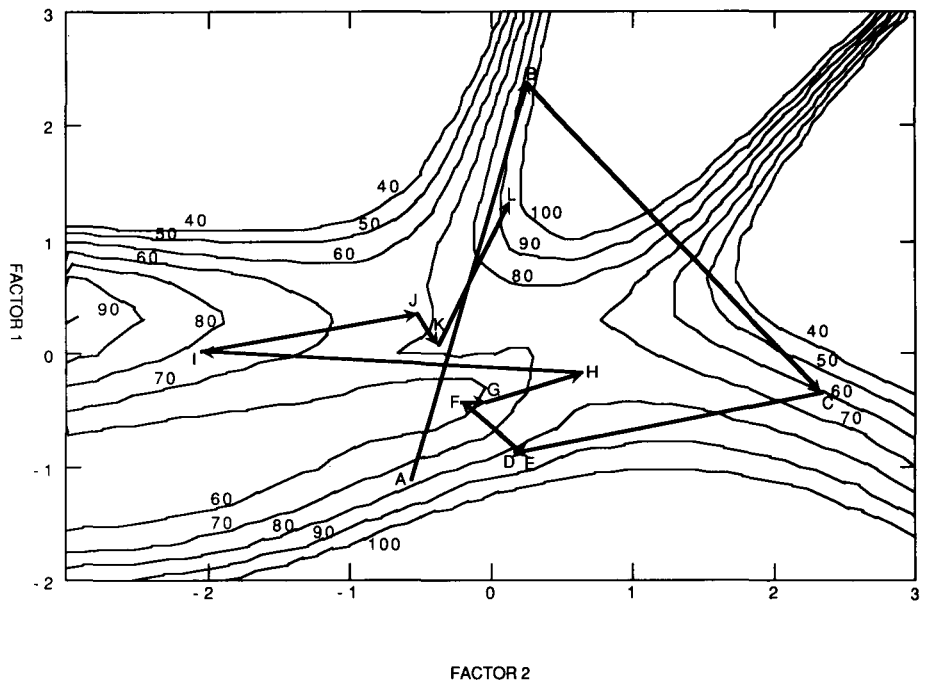

Fig. 3. Contour diagram for the evolution of the response during the progress of the sixth-dimensional simplex of the synthesis of an industrial pyrazolone.

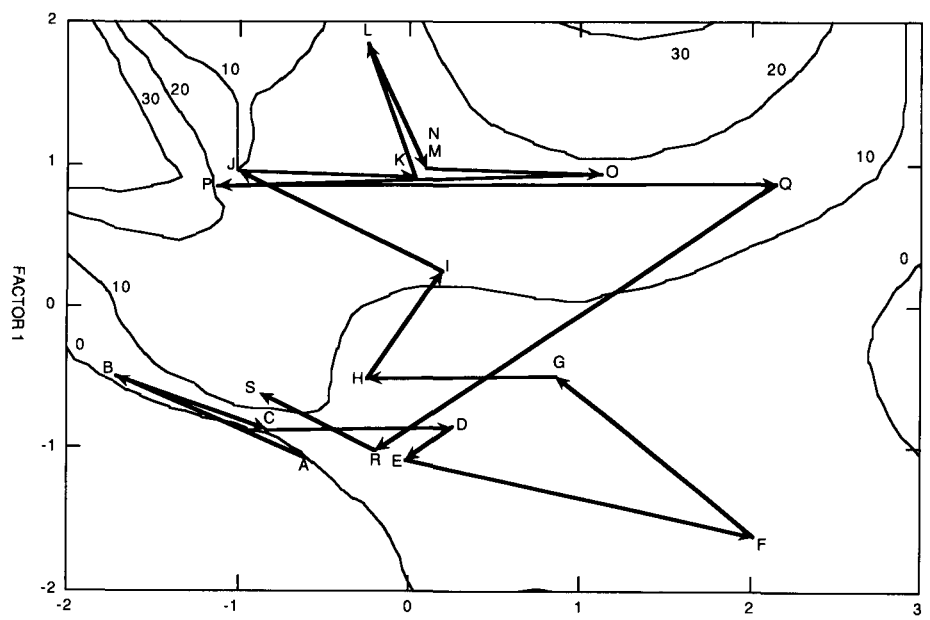

Fig. 4. Contour diagram for the evolution of the response during the progress of the fourth-dimensional simplex, of arsenic chloride determination by ICP-AES.

low HCl acid concentration). This duality is explained experimentally because the HCl concentration enrichment produces more arsenic trichloride volatilization, but also because the background signal is increased.

4. Conclusions

The graphic representation of the progress of the *n*-dimensional simplex algorithm, in only two dimensions and over the iso-response contour diagram, is possible if the initial *n*-variables are reduced to two new factors. This is done by applying PCA. This strategy provides more information than is obtained by simplex search. In the cases considered, the simplex evolution has been shown very clearly. The final step was observed more easily and the influences of the variables were detected.

Acknowledgments

This work has been financed by project PB90/0590 of DIGICYT (Spanish Education and Science Department). The authors thank professors J.I. Garcia, F. Laborda and E. Castells for helpful discussion of the paper.

References

[1] S.D. Brown, R.S. Bear and T.B. Blank, Anal. Chem., 64 (1992) 22R.
[2] F.H. Walters, L.R. Parker, S.L. Morgan and S.N. Deming, Sequential Simplex Optimisation, CRC Press, Boca Raton, FL, 1991.
[3] W. Spendley, G.R. Hext and F.R. Himsworth, Technometrics, 4 (1962) 441.
[4] J.A. Nelder and R. Mead, Comput. J., 7 (1965) 308.
[5] L. Ebdon, M.R. Cave and D.J. Mowthorpe, Anal. Chim. Acta, 115 (1980) 179.
[6] J. Sneddon, Spectroscopy International, 2 (1990) 42.
[7] L.A. Yarbo and S.N. Deming, Anal. Chim. Acta, 73 (1974) 391.
[8] S.M. Sultan and F.E. Suliman, Analyst, 118 (1993) 573.
[9] S.L. Morgan and S.N. Deming, Anal. Chem., 46 (1974) 1170.
[10] J.J. Carr and I.J. Drekter, Clin. Chem., 2 (1956) 353.
[11] S.M. Sultan and F.E. Suliman, Anal. Sci., 8 (1992) 841.
[12] R. Lazaro, P. Bouchet and R. Jacquier, Bull. Soc. Chim., 11–12 (1977) 1171.
[13] A. Lopez Molinero, C. Rubio and J.R. Castillo, 1993 European Winter Conference on Plasma Spectrochemistry, Granada, 1993.

ELSEVIER

Analytica Chimica Acta 297 (1994) 427–435

ANALYTICA CHIMICA ACTA

Synergetic adsorption of the copper–phenanthroline–tributylphosphate complex at a mercury drop electrode

I. Čuljak, M. Mlakar *, M. Branica

Center for Marine Research Zagreb, Rudjer Bošković Institute, POB 1016, 41001 Zagreb, Croatia

Received 28 January 1994; revised manuscript received 9 May 1994

Abstract

In the framework of electrochemical investigations on the synergetic adsorption of mixed ligand complexes at the mercury drop electrode, a cathodic stripping voltammetric method for the determination of copper(II) as mixed ligand complex with 1,10-phenanthroline (Phen) and tributylphosphate (TBP) in aqueous solutions was examined. The measurements were based on the accumulation of the copper–phenanthroline complex on the mercury drop surface covered with a layer of TBP molecules. The copper reduction response is strongly enhanced due to the formation of a mixed complex which is very hydrophobic and, therefore, strongly adsorbs at the electrode surface. The effect of various parameters (pH, metal and ligand concentrations, time and potential of accumulation) on the reduction process is examined. The voltammetric procedure was then applied to the detection of copper in natural water samples.

Keywords: Stripping voltammetry; Copper–phenanthroline–tributylphosphate complex; Mixed ligands

1. Introduction

Synergy as a term was used for the first time in solvent extraction to describe a manifold enhancement of the uranium extraction from aqueous solution by dialkylphosphoric acid in an organic phase with a neutral organophosphorus compound [1]. The basic condition for the synergetic effect is a substitution of the remaining water molecules from the coordination sphere of a central metal ion with a neutral donor molecule making it in that way very hydrophobic. From an electrochemical point of view, the organic phase can be very successfully replaced by the hydrophobic mercury drop electrode surface and the effect is called synergetic adsorption [2–4]. The phenomenon was established in experiments with uranyl ion and confirmed with molybdenum [5] and palladium [6] mixed ligand complexes.

A conventional method for the determination of copper is anodic stripping voltammetry either by a mercury drop electrode or a thin film mercury electrode as working electrodes [7–10]. Recently, cathodic stripping voltammetric proce-

* Corresponding author.

SSDI 0003-2670(94)00225-B

dures based on the accumulation of copper(II) complexes with organic ligands [11–15], are developed. The present investigations are based on the formation of a mixed ligand complex of copper with 1,10-phenanthroline (Phen) and tributylphosphate (TBP) at the electrode surface. A strongly adsorbed complex enabled determination of low copper concentrations in aqueous solutions as well as in some natural water samples.

2. Experimental

2.1. Equipment

Voltammetric measurements (linear sweep, cyclic, differential pulse and square-wave) were performed with a PAR 384B polarographic analyzer (Princeton Applied Research) and with a PAR 273 potentiostat/galvanostat both connected to a Hewlett-Packard Model 9816S technical computer. The systems were controlled by a software program as described earlier [16].

pH measurements were performed with an Orion Research pH meter and EA 920 expandable ion analyzer. Measurements were performed in an EA 875-20 conventional electroanalytical cell (50 ml) with a corresponding universal cap (Metrohm, Herisau). The working electrode was a hanging mercury drop electrode (HMDE) (Metrohm), the reference electrode was an Ag/AgCl electrode filled with saturated NaCl and the counter electrode was a platinum wire. Stirring of the solutions during the accumulation was performed with a "turbo" stirrer constructed in our laboratory, with a maximum speed of 4000 rotations min^{-1}.

2.2. Reagents

All solutions were prepared from analytical-reagent grade chemicals. A stock solution of Cu(II) was prepared by dissolution of an appropriate amount of $Cu(NO_3)_2$ (Merck) salt in bidistilled water and acidified with nitric acid to pH about 2. A supporting electrolyte was 0.55 mol/l NaCl. pH of the solutions was adjusted with Suprapur hydrochloric acid or sodium hydroxide (both Merck).

2.3. Procedure

Prior to the measurements, the solutions were deaerated in the polarographic cell for 20 min with extra pure nitrogen. pH of the solutions was adjusted to about 9.5 by the addition of sodium hydroxide. The copper(II) ion was accumulated on the HMDE at the potential of −0.3 V while the solution was stirred (about 1000 rpm). After the accumulation and a rest period of 10 s, the voltammograms were recorded at a scan rate of 50 mV/s, in a negative direction. The copper reduction peak in the presence of ligands was recorded between −0.6 and −0.7 V.

3. Results and discussion

3.1. The influence of phenanthroline and TBP on the copper redox process

Cu(II) ion in 0.55 mol/l NaCl at pH of about 3 reduces in two steps. The first one, at the potential close to the dissolution of mercury, corresponds to the reduction of Cu(II) to Cu(I) ion and the second one at −0.15 V, corresponds to the reduction of Cu(I) to Cu–amalgam. In the region of higher pH values those two peaks disappear and at pH about 5 at −0.5 V a very broad peak is recorded probably as a response to a copper hydroxide reduction.

By the addition of 1,10-phenanthroline (Phen) to the chloride solution of copper(II) ion two reduction peaks appear at various potentials depending strongly on the pH of the solution. When the solution is acidic those two reduction peaks are close to the potentials of the copper reduction process in chloride solution without other ligands [17]. In the neutral region, that is between pH 6 and 8, those two peaks appear at completely different potentials [15]. The first one, corresponding to the reduction of the Cu(I)–phenanthroline complex at about −0.4 V and the second one, corresponding to the reduction of Cu(II)–phen complex at the potential about −0.6

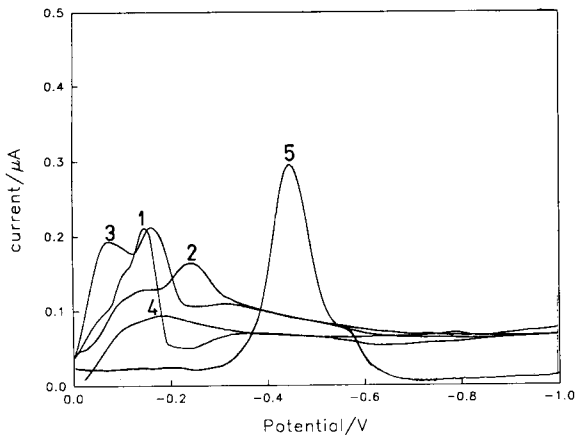

Fig. 1. Linear scan voltammetry of: (1) 10^{-5} mol/l TBP; (2) 10^{-5} mol/l TBP+2×10^{-6} mol/l Phen; (3) 10^{-5} mol/l TBP+10^{-7} mol/l Cu(II); (4) 10^{-7} mol/l Cu(II)+2×10^{-6} mol/l Phen; (5) 10^{-7} mol/l Cu(II)+2×10^{-6} mol/l Phen+10^{-5} mol/l TBP; pH 9.5; $t_{acc}=60$ s; $E_{acc}=0.0$ V; $v=50$ mV/s.

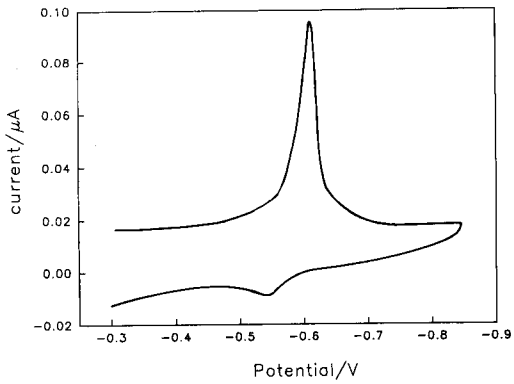

Fig. 2. Cyclic voltammogram of 10^{-7} mol/l Cu+2×10^{-6} mol/l Phen+10^{-5} mol/l TBP at pH 9.5 in 0.55 mol/l NaCl; $t_{acc}=30$ s; $E_{acc}=-0.3$ V; $v=50$ mV/s.

V. Both copper complexes with phenanthroline are strongly adsorbed at the electrode surface and the maximum current is obtained when accumulation was performed at a potential between 0.0 and −0.1 V. Copper(II) ion in the presence of 1,10-phenanthroline at pH > 8.5 gives no reduction response on linear scan voltammograms (Fig. 1, curve 4).

The copper(II) ion reduction process in the presence of tributylphosphate is completely inhibited (Fig. 1, curve 3). That is caused by the fact that the free Cu(II) ion does not form complex with TBP and its reduction should take place through the layer of adsorbed TBP molecules.

When copper(II) ion is present in the chloride solution together with both ligands, phenanthroline and TBP at pH about 9.5, after the accumulation time of 60 s, a new, very pronounced reduction peak appears on linear scan voltammograms at the potential about −0.6 V (Fig. 1, curve 5). On cyclic voltammograms a reduction current was registered on the cathodic side, but on the anodic side only response to the relaxation of the strongly adsorbed copper mixed complex from the electrode surface was recorded (Fig. 2). Performing the second scan on the same drop, no response on either side of the cyclic voltammogram was recorded. Such a behaviour is caused by the copper mixed ligand complex desorption from the electrode surface and its successive irreversible dissociation.

The reduction peak of copper–phen–TBP complex is very sensitive to changes of the pH in the solution, as well as on the concentration of copper(II) and both ligands. Furthermore, the reduction peak is strongly affected with the accu-

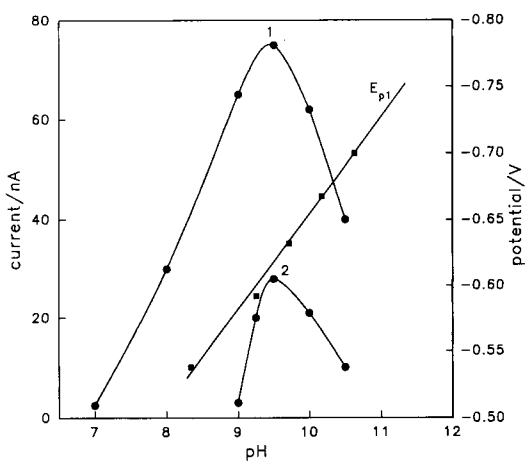

Fig. 3. LS reduction current and potential dependence on pH in the presence of: (1) 10^{-7} mol/l Cu(II); (2) 5×10^{-8} mol/l Cu(II); and 2×10^{-6} mol/l Phen and 10^{-5} mol/l TBP at pH = 9.5; $t_{acc}=3$ min; $E_{acc}=-0.3$ V; $v=50$ mV/s.

mulation time and potential, temperature and scan rate.

3.2. Effect of pH

As already mentioned the copper–phen–TBP complex reduction peak is strongly dependent on pH of the solution and appears in a rather narrow pH region. The reduction peak of the copper mixed ligand complex with a copper(II) ion concentration of 10^{-7} mol/l and a deposition period of 3 min at −0.3 V, is recorded on linear scan voltammograms in the pH region from about 7 to about 10.5, with a maximum value at pH 9.5 (Fig. 3, curve 1). In the same time through that pH range the peak potential E_p moves linearly in the negative direction with the a slope of 52 mV/pH unit. When the copper concentration was 5×10^{-8} mol/l the pH range in which the reduction peak appears is much more narrow (Fig. 3, curve 2), the copper mixed ligand complex reduction peak being recorded only in the pH range from 9.1 to 10.2.

The cause of this behaviour of the Cu–phen–TBP complex, as well as the Cu–phen complex, was assumed to originate from the calculated distribution of copper(II) ions with pH in the chloride solutions. As it was already mentioned, the reduction process of the Cu–phen complex is recorded in the pH range between 6 and 8.5. That is in good agreement with the calculated pH region in which Cu–phen complex forms. The complex is obviously formed between free copper ion and phenanthroline. The stoichiometry of the Cu–phen complex is most probably Cu:phen = 1:2, according to the theoretical distributions calculated form the stability constants. In pH region above 7.5, the copper–phen–TBP complex begins to form and its reduction process is recorded. According to the theoretical distributions it is likely to presume that the copper mixed ligand complex is not formed with free copper(II) ions, but with $Cu(OH)_2$ species. Therefore, the appearance of the mixed ligand species in the rather narrow pH range (between 9 and 10.5) can be explained by the calculated distribution of copper ion in the aqueous solutions of various pH. The mixed ligand complex reaches its maximum at the pH of maximum $Cu(OH)_2$ fraction (about 9.5) in calculated distributions, and slowly disappears in pH region in which $Cu(OH)_3^-$ begins to form. That is also in agreement with the theoretical presumption that the synergy in the extractions can be realised only when the complex with the first, chelating ligand is neutral and only as such can be synergetically extracted (adsorbed) with the second neutral ligand [18]. Therefore, the Cu^{2+} charge is neutralized by two hydroxide ions and copper hydroxide is then complexed with neutral phenanthroline molecules giving a neutral chelate complex. According to the theoretical distributions calculated from the stability constants the stoichiometry of the complex is probably $Cu(OH)_2phen_2$. Such a complex is then complexed with TBP molecules at the mercury drop electrode surface giving the mixed ligand complex $Cu(OH)_2Phen_2TBP$, but only in the pH range in which $Cu(OH)_2$ species is present in the solution. The copper–phen–TBP complex reduction response completely vanishes at pH 10.5.

3.3. Effect of ligand concentration

The dependence of the copper–phen–TBP reduction current and potential on the 1,10-phenanthroline concentration with two different copper concentrations is shown in Fig. 4. The peak height increases with phenanthroline concentration in the range from 10^{-7} to about 2×10^{-6} mol/l with a copper concentration of 5×10^{-8} mol/l. Further enhancement of phenanthroline concentration causes a decrease of the reduction current. With a copper concentration of 4×10^{-7} mol/l the reduction current increases until the phenanthroline concentration of 4×10^{-6} mol/l is reached and then slowly decreases with further increase of phenanthroline concentration. It is evident that with lower copper concentrations in the solution and, therefore, lower copper concentrations at the electrode surface the competition with the phenanthroline molecules is present, so inhibition of the mixed ligand complex reduction process takes place due to the excess of ligand in the solution. With higher concentrations of the copper(II) ion there is no competition with the phenanthroline molecules,

and only a slight inhibition of the mixed ligand complex reduction process is registered due to the saturation of the electrode surface with the complex molecules.

In the concentration range in which the peak current increases the peak potential moves to the negative values due to the stabilisation of the adsorbed mixed complex layer at the electrode surface. In the range of the electrode surface saturation the reduction potential shifts only slightly towards negative values.

The influence of TBP concentration on the peak current and potential is shown in Fig. 5. With the copper concentration of 5×10^{-8} mol/l the peak current rapidly increases in the TBP concentration range from 1×10^{-6} to 5×10^{-6} mol/l and then, at higher TBP concentrations (until 2×10^{-5} mol/l), rapidly decreases. Such a behaviour is caused probably by the competition of copper mixed ligand complex with TBP molecules for the electrode surface. With the copper concentration of 4×10^{-7} mol/l the maximum reduction current was obtained with the TBP concentration 2×10^{-5} mol/l. After that concentration of TBP the complex reduction current slowly decreases due to the saturation of the electrode surface with copper mixed ligand complex and in that way inhibition of the electrode process.

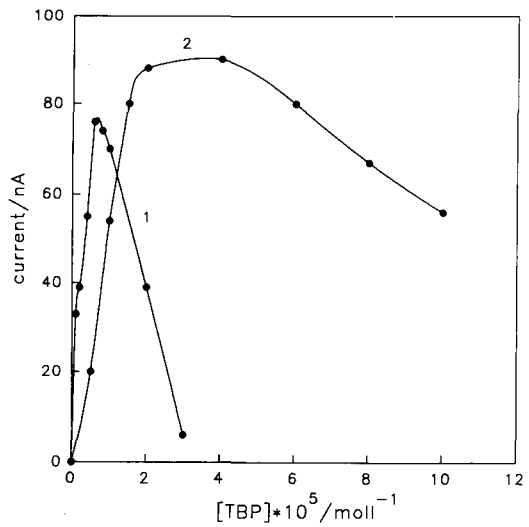

Fig. 5. LS reduction current dependence on TBP concentration in the presence of: (1) 5×10^{-8} mol/l Cu(II); (2) 4×10^{-7} mol/l Cu(II) and 2×10^{-6} mol/l Phen at pH 9.5; $t_{acc} = 3$ min; $E_{acc} = -0.3$ V; $v = 50$ mV/s.

The peak potential in the same time remains almost at the same value (about −0.680 V vs. Ag/AgCl).

3.4. Effect of the accumulation potential

The dependence of the stripping peak current on the preconcentration potential was examined over the range 0.0 to −0.45 V in 0.55 mol/l NaCl (Fig. 6). A maximum reduction current was obtained with a deposition potential of −0.3 V. By the accumulation at more positive potentials the reduction peak is much smaller probably due to the fact that the TBP molecules are adsorbed at the electrode surface at the potential of about −0.2 V. Therefore, the adsorption of the copper mixed complex can be accomplished when the layer of TBP molecules is stabilized at the electrode surface, i.e., at the potentials more negative than −0.2 V. When deposition is performed at the potentials more negative then −0.4 V the reduction current again sharply decreases. The reason is probably the fact that the complex is formed only at the electrode surface and that at

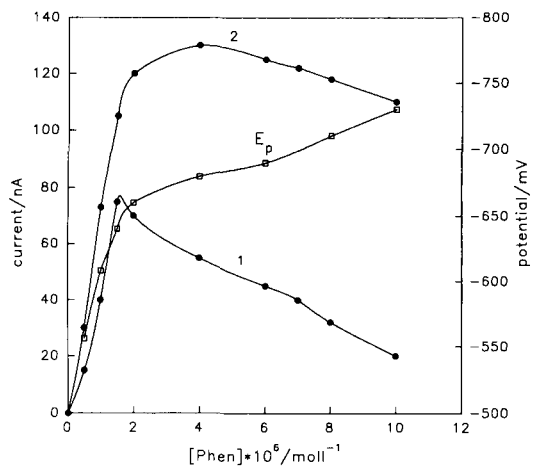

Fig. 4. LS reduction current and potential dependence on phenanthroline concentration in the presence of: (1) 5×10^{-8} mol/l Cu(II); (2) 4×10^{-7} mol/l Cu(II) and 10^{-5} mol/l TBP at pH 9.5; $t_{acc} = 3$ min; $E_{acc} = -0.3$ V; $v = 50$ mV/s.

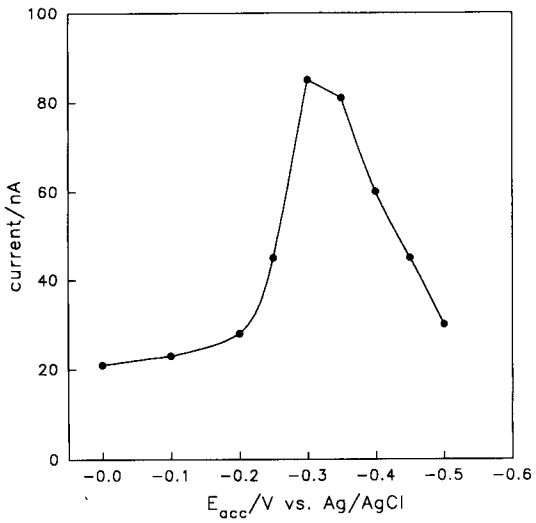

Fig. 6. LS reduction current dependence on the accumulation potential in the presence of 5×10^{-8} mol/l Cu (II), 10^{-5} mol/l TBP and 2×10^{-6} mol/l Phen at pH 9.5; $t_{acc} = 3$ min; $v = 50$ mV/s.

potentials more negative than −0.4 V copper(II), which diffuses towards the electrode, is reduced before the complexation can take place.

The dependence of the peak potential on the accumulation period shows the curve which is similar to the i_p/E_{acc} curve, meaning that the potential of the copper–phen–TBP reduction peak is most negative when deposition is performed at −0.3 V. That is obviously caused by the fact that the copper–phen–TBP complex is most stable when accumulation is performed at −0.3 V.

3.5. Effect of the accumulation time

The dependence of the mixed copper complex reduction current on the accumulation time with various Cu(II) concentrations in the range from 10^{-9} to 10^{-7} mol/l, with constant phenanthroline (2×10^{-6} mol/l) and TBP (1×10^{-5} mol/l) concentration, constant pH 9.5 and accumulation potential of −0.3 V, was examined by three different voltammetric techniques: linear scan, differential pulse and square-wave voltammetry. In Fig. 7 the reduction current dependence on the deposition time with various copper concentrations measured by liner scan voltammetry is shown. In the range of copper concentrations between 1×10^{-8} to 3×10^{-8} mol/l the dependence is linear until an accumulation time of 20 min. In the range of copper(II) concentrations between 5×10^{-8} and 10^{-7} mol/l for deposition times longer than 10 min the reduction current reaches a plateau. When the copper concentration is above 10^{-7} mol/l for an accumulation time of 3 min the reduction current reaches a maximum and then begins to decrease. For a concentration of copper(II) of 4×10^{-7} mol/l the reduction current after an accumulation period longer than 10 min drops to a zero value.

A similar relationship between reduction current and deposition time with various copper concentrations was obtained in measurements by differential pulse voltammetry, only for a concentration range of copper(II) ion between 1×10^{-9} and 2×10^{-8} mol/l the current was about two times higher (Fig. 8). That allows us to make measurements of copper(II) concentrations which were one order of magnitude lower.

In Fig. 9 is shown the dependence of the reduction current on the accumulation time measured by square-wave voltammetry. The satura-

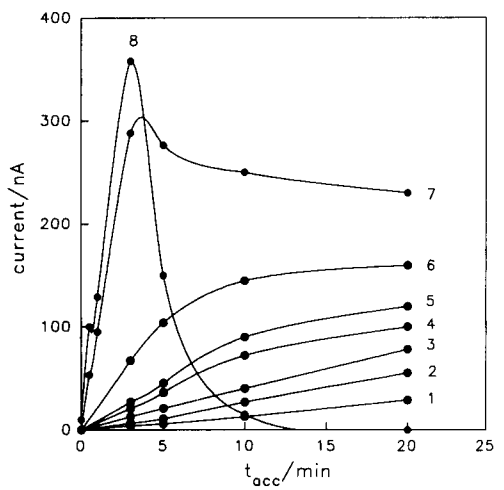

Fig. 7. LSV reduction current dependence on the accumulation time in the presence of: (1) 10^{-8}; (2) 2×10^{-8}; (3) 3.5×10^{-8}; (4) 5×10^{-8}; (5) 7×10^{-8}; (6) 10^{-7}; (7) 2×10^{-7}; (8) 4×10^{-7} mol/l Cu(II), 10^{-5} mol/l TBP and 2×10^{-6} mol/l Phen at pH 9.4; $E_{acc} = -0.3$ V; $v = 50$ mV/s.

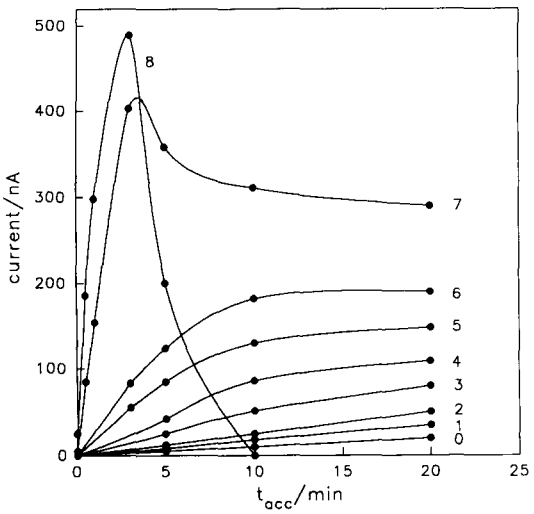

Fig. 8. DPV reduction current dependence on the accumulation time in the presence of: (0) 10^{-9}; (1) 5×10^{-9}; (2) 10^{-8}; (3) 2×10^{-8}; (4) 5×10^{-8}; (5) 7×10^{-8}; (6) 10^{-7}; (7) 2×10^{-7}; (8) 4×10^{-7} mol/l Cu(II), 10^{-5} mol/l TBP and 2×10^{-6} mol/l Phen at pH 9.5; $E_{acc} = -0.3$ V; square-wave amplitude, $a = 0.04$ V.

tion of the electrode surface is observed at shorter accumulation periods. The linearity is detected only in the copper concentration range between

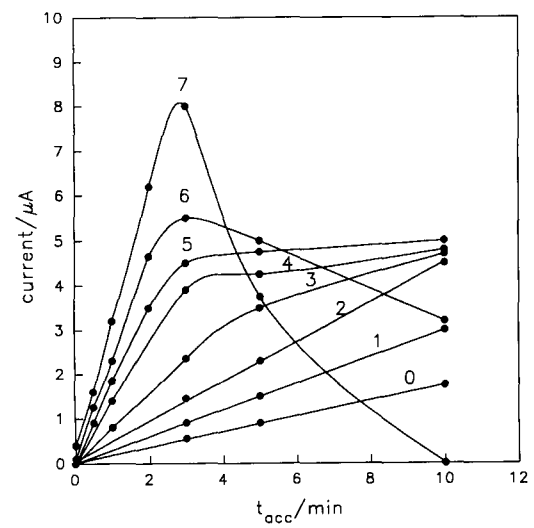

Fig. 9. SWV reduction current dependence on the accumulation time in the presence of : (0) 10^{-9}; (1) 5×10^{-9}; (2) 10^{-8}; (3) 2×10^{-8}; (4) 5×10^{-8}; (5) 10^{-7}; (6) 2×10^{-7}; (7) 4×10^{-7} mol/l Cu(II) and 10^{-5} mol/l TBP and 2×10^{-6} mol/l Phen at pH 9.5; $E_{acc} = -0.3$ V; $f = 120$ s^{-1}; $a = 0.04$ V.

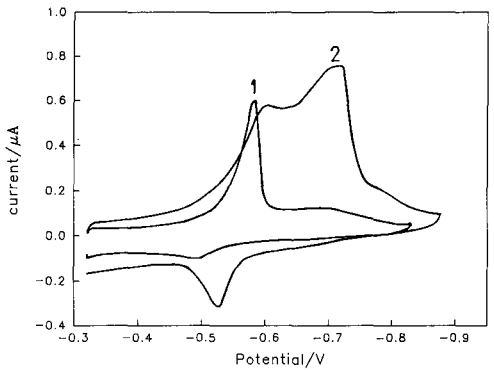

Fig. 10. Cyclic voltammogram of 5×10^{-7} mol/l Cu(II) in the presence of 10^{-5} mol/l TBP and 2×10^{-6} mol/l Phen at pH 9.4; $E_{acc} = -0.3$ V; $v = 50$ mV/s; t_{acc}: (1) 3 min; (2) 20 min.

10^{-9} and 10^{-8} mol/l. Furthermore, it must be pointed out that the currents are about two orders of magnitude larger than in measurements by linear scan and differential pulse voltammetry.

In the copper(II) concentration range higher than 10^{-7} mol/l for the accumulation periods longer then 3 min the electrode surface is completely covered with the copper mixed ligand complex so the reduction current begins to decrease due to the inhibition of the reduction process. It must be pointed out that in the copper(II) concentration range $\geq 10^{-7}$ mol/l for accumulation times longer than 3 min, that is in the range where the first reduction peak begins to decrease, a second reduction peak appears at about -0.75 V (Fig. 10). As the deposition period is longer the second peak is bigger and is shifted to more negative potentials while the first one slowly decreases. That can be explained by the formation of a second or a differently oriented layer of adsorbed copper–phen–TBP molecules. In cyclic voltammetry on the anodic scan a pronounced peak is recorded, which was connected with the relaxation process of larger amount of adsorbed molecules.

The electrode surface coverage by the copper–phen–TBP complex at the copper(II) concentration level of 5×10^{-8} mol/l and the accumulation time of 5 min was evaluated to amount to $(1.10 \pm 0.02)\times10^{-10}$ mol/cm^2.

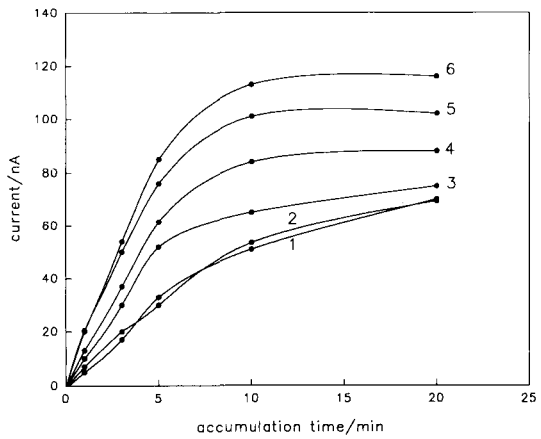

Fig. 11. LS reduction current dependence on the accumulation time in the presence of 5×10^{-8} mol/l Cu(II), 10^{-5} mol/l TBP and 2×10^{-6} mol/l Phen at pH 9.5 at various temperatures: (1) 5; (2) 10; (3) 20; (4) 30; (5) 40; (6) 50°C; $E_{acc} = -0.3$ V.

3.6. Temperature dependence

Temperature is an important parameter in adsorption experiments. Measurements were performed by linear scan voltammetry with a copper(II) concentration of 5×10^{-8} mol/l, varying both the temperature, in the range from 0 to 50°C, and the accumulation time (1 to 20 min) (Fig. 11). It was found that the adsorption is strongest with the temperature of 50°C and weakest when temperature of the solution was about 0°C, what is opposite from what was expected. Temperature effects of the adsorbed copper mixed ligand complex can be explained by the results of Zhou et al. [19] obtained with the adsorption of humic acids. They categorized it as an endotherm and possibly chemisorption process. Therefore, the temperature enhancement will favour this chemical reaction and consequently the chemisorption process of the copper mixed ligand complex. Furthermore, the factor which can indirectly influence such a behaviour of the copper mixed ligand complex is the lower solubility of TBP in water and its greater adsorbability at the electrode surface at higher temperatures [20].

3.7. Nature of surface active substances

The influence of different kinds of surfactants (cationic, anionic or non-ionic) on the reduction response of the Cu–phen–TBP system was examined. The organic surfactants are likely to interfere due to the competition for the electrode surface. The addition of sodium dodecyl sulphate (SDS) of about 10^{-5} mol/l, decreased the Cu–phen–TBP reduction peak with approximately 5%. The mixed ligand complex reduction current decreased about 15% on the addition of 230 μg/l of Triton X-100. *N*-Dodecyl pyridinium chloride suppressed the reduction peak at a concentration level of about 10^{-4} mol/l for about 8%. Therefore, the destruction of organic surfactants by UV irradiation is recommended when analyzing natural water samples with a high content of organic matter.

3.8. Analytical application

The synergetic adsorption method for copper(II) determination via its mixed ligand complex with 1,10-phenanthroline and TBP was found to be suitable for the natural water samples of lower carbonate content. The method involves a pH adjustment of the sample to 9.5. At that pH level carbonate precipitation occurs, so the difficulties in the copper(II) determination arise. Nevertheless, in the samples of lower salinity, that is in the samples taken from the river Raša estuary (Istrian region, North Adriatic sea), Cu(II) concentrations were determined successfully. Samples were taken from three different locations in the estuary. The salinity was found to amount to 5, 8 and 15‰ and the copper(II) concentrations detected amount to $(1.6 \pm 0.3)\times10^{-9}$, $(1.3 \pm 0.2)\times10^{-9}$ and $(0.9 \pm 0.1)\times10^{-9}$ mol/l, respectively, with an accumulation time of 10 min at -0.3 V vs. Ag/AgCl.

Acknowledgments

The financial support of the Ministry of Science and Technology of the Republic of Croatia, under the Project 1-07-011, Physical Chemistry of

Trace Metals in Aquatic Systems, is gratefully acknowledged.

References

[1] J.M. Schmitt, reported by K. Brown, C.F. Coleman, D.C. Crouse and A.D. Ryan, USAEC ORNL-2346, 1957.
[2] M. Mlakar and M. Branica, J. Electroanal. Chem., 257 (1988) 269.
[3] M. Mlakar and M. Branica, Anal. Chim. Acta, 221 (1989) 279.
[4] M. Mlakar and M. Branica, Mar. Chem., 46 (1994) 61.
[5] Z. Zhao and Z. Gao, Electroanalysis, 1 (1989) 371.
[6] F. Quentel, C. Elleouet and C. Madec, Electroanalysis, 4 (1992) 707.
[7] A. Nelson and R.F.C. Mantoura, J. Electroanal. Chem., 164 (1984) 265.
[8] A. Nelson, Anal. Chim. Acta, 169 (1985) 287.
[9] G.M.P. Morrison, T.M. Florence and J.L. Stauber, Electroanalysis, 2 (1990) 9.
[10] M. Boussermart, L. Menargues and J.L. Stauber, Electroanalysis, 5 (1993) 125.
[11] U. Forsman, J. Electroanal. Chem., 122 (1981) 215.
[12] J.C. Moreira, R.D. Miller and A.G. Fogg, Electroanalysis, 3 (1991) 385.
[13] J. Zhao, D. Sun and W. Jin, Anal. Chim. Acta, 268 (1992) 293.
[14] A.G. Fogg, F.N. Ertas, J.C. Moreira and J. Barek, Anal. Chim. Acta, 278 (1993) 41.
[15] I. Čuljak, M. Mlakar and M. Branica, Electroanalysis, (1994) in press.
[16] I. Pižeta and M. Branica, J. Electroanal. Chem., 250 (1988) 293.
[17] K. Sugiyama and K. Aoki, J. Electroanal. Chem., 262 (1989) 211.
[18] H.M.N.H. Irving, Solvent Extraction Chemistry, North-Holland, Amsterdam, 1967, p. 91.
[19] J.L. Zhou, S. Rowland, R. Fauzi C. Mantoura and J. Brawen, Water Res., 28 (1994) 571.
[20] C.E. Higgins, W.H. Baldwin and B.A. Soldano, J. Phys. Chem., 63 (1959) 113.

ELSEVIER

Analytica Chimica Acta 297 (1994) 437–442

ANALYTICA CHIMICA ACTA

Substituted cobalt phthalocyanine complexes as carriers for nitrite-sensitive electrodes

Jun-Zhong Li, Xin-Yu Pang, Ru-Qin Yu *

Department of Chemistry & Chemical Engineering, Hunan University, Changsha 410082, China

Received 21 December 1993; revised manuscript received 21 April 1994

Abstract

A new poly(vinyl chloride) membrane electrode based on lipophilic 2,9,16,23-tetra-*tert*-butylphthalocyanine–cobalt is described which demonstrates excellent selectivity toward the nitrite ion. The resulting electrodes displayed a near-Nernstian response for nitrite in the concentration range 10^{-5}–0.1 M with the selectivity sequence nitrite > thiocyanate > iodide > perchlorate > bromide > nitrate > chloride. The UV/Vis spectra and a.c. impedance studies showed that the excellent selectivity for nitrite was related to the unique interaction between the central cobalt ion and nitrite.

Keywords: Ion selective electrodes; UV–Visible spectrophotometry; Carriers; Nitrite; Phthalocyanines; Poly(vinyl chloride)

1. Introduction

Anion-sensitive membrane electrodes based on ion exchangers such as lipophilic quaternary ammonium or phosphonium salts used to display classical Hofmeister behavior and the counter-anions in the membrane phase are dissociated from the mobile, lipophilic, positively charged sites. Thus, the selectivity is dictated by the relative solubility of individual anions in the solvent mediator (i.e. plasticizer) [1,2]. Recently, electrodes using plasticized poly(vinyl chloride) (PVC) membranes incorporating derivatives of vitamin B_{12}, Co(III), Sn(IV), Mo(IV) and Mn(III) porphyrin complexes and organometallic compounds have been reported, which showed a potentiometric anion-selectivity sequence deviated from the Hofmeister pattern [3–7]. These deviations resulted from the direct interaction between the central metal and the analyte ion and the steric effect associated with the structure of the porphyrin ring.

The conventional method for the determination of nitrite in the presence of nitrate is rather tedious [8,9]. Nitrite-sensitive electrodes with improved selectivity which can be used in analytical practice were reported by Simon and co-workers [3,10] using vitamin B_{12} derivatives as carriers. The compounds used by these authors were, unfortunately, rather difficult to synthesize. Metal

* Corresponding author.

SSDI 0003-2670(94)00239-I

phthalocyanines are a kind of extensively used dyes which can be obtained easily, and which have good chemical and thermal stability, with acid–base corrosion endurance. Recently, we have found that the membrane electrodes incorporating cobalt phthalocyanine derivatives are sensitive to nitrite species and the high electron density around the central cobalt atom favours the interaction between nitrite ion and the carrier incorporated in the membrane. This paper reports on the use of (2,9,16,23-tetra-*tert*-butylphthalocyanine)cobalt(II) and copper(II) as nitrite carriers for the preparation of PVC membrane electrodes.

2. Experimental

Reagents

Aqueous solutions were prepared with doubly distilled water and sodium salts of analytical purity. Tetrahydrofuran (THF), high-molecular-weight PVC, and the plasticizer dibutyl phthalate (DBP) were products of Shanghai Chemical Co. The synthesis of hexadecyltrioctylammonium iodide (HTOAI) was described elsewhere [11]. Chemicals used for the synthesis were chemically-pure or analytical-reagent grade.

Apparatus

Potentiometric and pH measurements were made with a Model PHS-10A digital ion analyzer (Xiaoshan). The cells used for millivolt measurements were of the following type:

$Hg–Hg_2Gl_2$ | KCl (satd.) ¦ sample solution || membrane ||0.01 M KCl | AgCl–Ag

The solutions were buffered with 0.01 mol l^{-1} phosphate and adjusted to the desired pH with H_2SO_4 or NaOH. Before use, the electrodes were conditioned in 0.01 mol l^{-1} $NaNO_2$ solution for 2 h. When not in use, the electrodes were stored in deionized water at room temperature and protected from ambient light to prevent any possible photodecomposition of the ionophores.

The membrane composition was 2.5% (m/m) ionophores, 31% (m/m) PVC and 66.5% (m/m) plasticizer (DBP). The PVC membrane electrodes were fabricated from various carriers and assembled according to Thomas and co-workers [12,13].

2.1. Determination of EMF response and selectivity of the electrodes

Anion selectivity coefficients, $\log K^{\mathrm{Pot}}_{NO_2^-,j^{z-}}$, were determined in 0.1 mol l^{-1} solutions of the corresponding sodium salts by the separate solution method [14]. The following equation was used to calculate $\log K^{\mathrm{Pot}}_{NO_2^-,j^{z-}}$,

$$\log K^{\mathrm{Pot}}_{NO_2^-,j^{z-}} = (E_2 - E_1)/S + \log[NO_2^-] - \log[j]^{1/z}$$

where E_2 is the electrode potential in 0.1 mol l^{-1} nitrite solution and E_1 is the potential of the electrode in a 0.1 mol l^{-1} solution of the interfering ion j^{z-}. The solutions were buffered at pH 3.50 ± 0.05 with 0.01 mol l^{-1} phosphate and H_2SO_4. The single-ion activities were calculated by using the extended Debye–Huckel equation.

A.c. impedance experiments

The a.c. impedance spectra of the electrode membrane containing (2,9,16,23-tetra-*tert*-butylphthalocyanine)Co(II) were recorded with a PAR M368-2 system (EG&G Princeton Applied Research) in 0.01 mol l^{-1} phosphate solutions adjusted to pH 3.50. The frequency range used was $10^5 - 10^{-2}$ Hz (at 15°C).

UV / Vis absorption spectra

Spectra of the chloroform phase obtained by shaking a solution of metal–phthalocyanine complexes in $CHCl_3$ with an aqueous 0.1 mol l^{-1} $NaNO_2$ for 30 min were recorded on a PE Lambda 17 spectrophotometer (Bodenseewerk Perkin-Elemer, Überlingen, Germany).

Syntheses

(2,9,16,23-tetra-tert-butylphthalocyanine)Co(II) (CoTTBPc, Fig. 1, I). The method of synthesis as described by Metz et al. [15] was modified as follows: 1.8 g (8.1 mmol) of 4-*tert*-butylphthalic acid [16], 2.9 g (48.5 mmol) of urea (water free), 235 mg (4.5 mmol) of ammonium chloride, 325

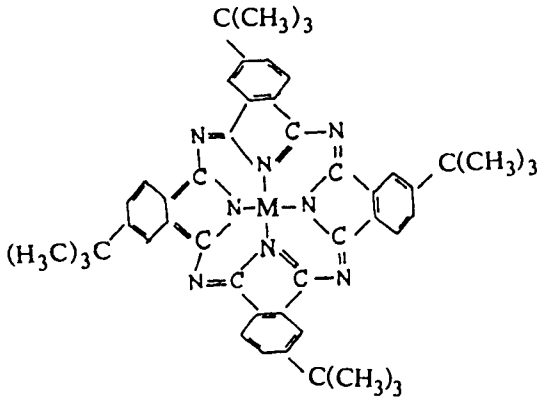

Fig. 1. Structures of the carriers studied. I: M = Co, II: M = Cu.

mg (2.5 mmol) of cobalt (II) chloride and 34 mg (0.03 mmol) of ammonium molybdate were powdered and mixed thoroughly, the mixture was heated to 180°C and kept for 30 min, then the temperature was increased to 200°C and kept for another 4 h. The crude product was boiled 2 h with 1 mol l^{-1} HCl, filtered and washed with water until the filtrate was neutral. The product was further purified by dissolving in $CHCl_3$, filtering and removing the solvent under reduced pressure to yield a blackish-blue solid. Analysis: calculated for $C_{48}H_{48}N_8Co$ (M_r = 795.86): C, 72.44; N, 6.07; N, 14.08; found: C, 71.35; H, 5.99; N, 13.85%.

(2,9,16,23-tetra-tert-butylphthalocyanine)Cu(II), (CuTTBPc, Fig. 1, II). The compound was synthesized in a similar way with use of cuprous chloride instead of cobalt chloride. Analysis: calculated for $C_{48}H_{48}N_8Cu$ (M_r = 800.48): C, 71.96; H, 6.00; N, 14.00; found: C, 70.98; H, 5.86; N, 14.37%.

3. Results and discussion

Response characteristics of the electrodes

Potentiometric response characteristics of the electrodes containing different carriers are shown in Fig. 2. The electrode incorporating CoTTBPc showed a near-Nernstian potentiometric response for 1×10^{-5}–0.1 mol l^{-1} nitrite with a slope of −57 mV per pNO_2 (15°C) in 0.01 mol l^{-1} phosphate buffer solution adjusted to pH 3.5. The time required for the electrode to reach 90% response depended mainly on the activity being measured: from high to lower nitrite activity, the response time was varied from several seconds up to 2 min. Potential readings for the electrode dipped alternatively into stirred solutions of 0.01 and 0.001 mol l^{-1} $NaNO_2$ showed a standard deviation of 0.8 mV over 2 h (n = 6). The potentiometric response characteristics of the electrode doped with CuTTBPc toward the nitrite ion were rather poor (see Fig. 2).

The potentiometric selectivity coefficients for membranes containing different carriers are shown in Table 1. The electrode doped with CoTTBPc displayed remarkable selectivity for nitrite over common anions tested. Virtually, all of these ions are more lipophilic than nitrite, and would be expected to interfere seriously with classical anion-exchanger type membranes. Surprisingly, the CuTTBPc-based electrode displayed a typical Hofmeister selectivity sequence in spite of its completely similar structure with CoTTBPc. This indicates that the remarkable selectivity of the CoTTBPc-based electrode toward the nitrite ion might be contributed to the unique

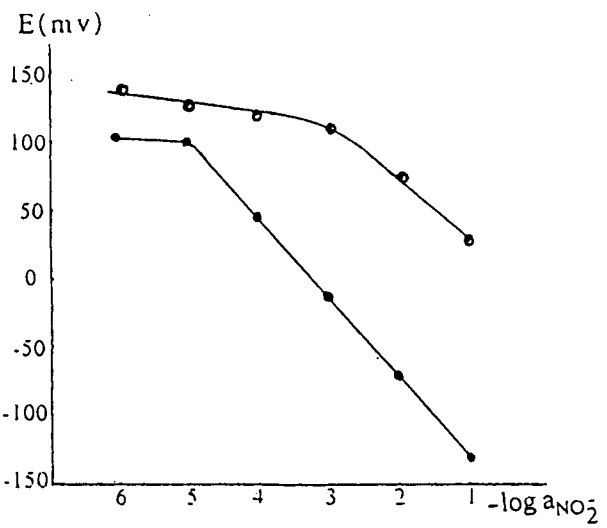

Fig. 2. Potentiometric response of the electrodes. (●) CoTTBPc; (○) CuTTBPc.

Table 1
Potentiometric selectivity coefficients of the electrodes

Anion	$\log K^{Pot}_{NO_2^-,anion}$	
	CoTTBPc	CoTTBPc [a]
Nitrite	0	0
Perchlorate	−1.62	−0.24
Thiocyanate	−1.04	−0.19
Iodide	−1.56	−0.21
Bromide	−2.89	−1.46
Nitrate	−3.05	−2.87
Chloride	−3.50	−3.00

[a] The membrane composition is 2.5% (m/m) ionophore, 66.5% (m/m) DBP, 31% (m/m) PVO and 2%mol HTOAI.

interaction between the central cobalt atom and nitrite species.

For nitrite-sensitive electrodes based on vitamin B_{12} derivatives, the improved selectivity of the electrodes toward nitrite was contributed to the specific exchange between the nitrite and the axial coordination anions of the compounds [10]. One notices that some metal phthalocyanines as a kind of semiconductor can absorb reversibly oxidative (electron-accepting) gases, and the conduction mechanism is thought to be hole conduction [17,18]. For the compound CoTTBPc, it was said that the oxygen adducts of the compound could be formed only in solution and could not be isolated. The complexation of oxygen which occurs in solution is reversible [15]. In this case, it is possible that the central cobalt is oxidized to the +3 state. Indeed, when some metal phthalocyanines are exposed to air, O_2^- can be detected on the surface of the complexes by X-ray photo-electron spectroscopic (XPS) measurements [19]. Under the experimental conditions of the presence of oxygen and low pH of the test solution, it is probable that part of the original central Co(II) will be oxidized to Co(III), and the carrier will in fact serve as a charged carrier, i.e., the response mechanism of the electrode is more or less similar to that of the electrode based on vitamin B_{12} derivatives. To test the response mechanism, small amounts of HTAOI (1–3 mol% as referred to the ionophore) were added to the membrane phase. In general, if the electrode is operating via a neutral carrier, the small amounts of lipophilic quaternary ammonium sites in the membrane phase will serve as counter cations stabilizing the formation of a negatively charged nitrite–Co(II)–phthalocyanine complex. In contrast, if the electrode is operating via a charged carrier mechanism, the addition of lipophilic quaternary ammonium sites will make the selectivity and response function worse. The selectivity coeffi-

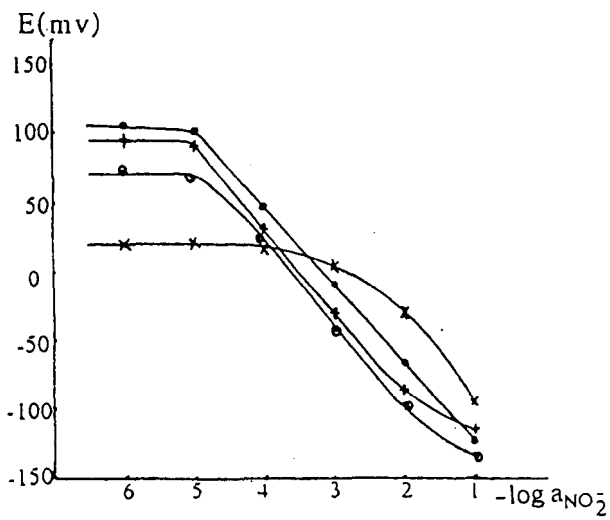

Fig. 3. Calibration curves of the electrode based on CoTTBPc at different pH values. (●) pH 3.5; (+) pH 4.5; (○) pH 5.5; (×) pH 6.5.

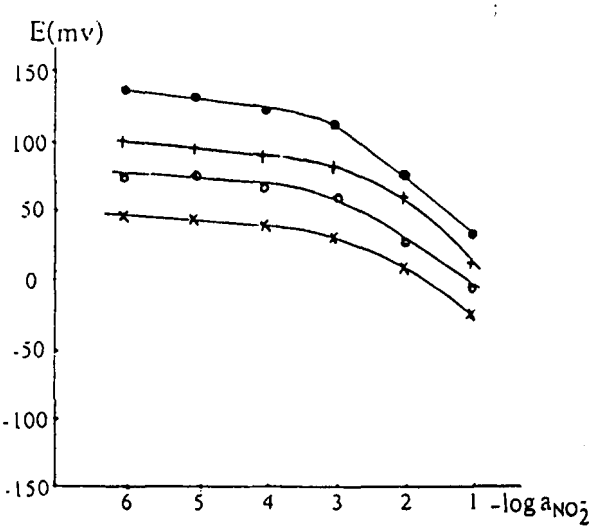

Fig. 4. Calibration curves of the electrode based on CuTTBPc at different pH values. (●) pH 3.5; (+) pH 4.5; (○) pH 5.5; (×) pH 6.5.

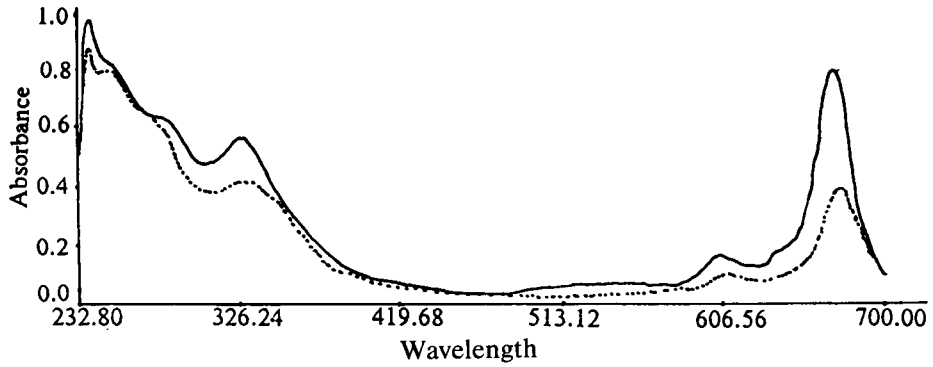

Fig. 5. UV/Vis absorption spectra of CoTTBPc in $CHCl_3$ (———) before and (- - - - -) after extraction with 0.1 mol l^{-1} aqueous $NaNO_2$, buffered with 0.01 mol l^{-1} phosphate, and adjusted to pH 3.5.

cients of the membrane incorporating 2% HTAOI are shown in Table 1. It is evident that the selectivity of the electrode toward nitrite is worse than that of the electrode without quaternary ammonium. On the other hand, the linear response range of the electrode toward nitrite is narrower (8×10^{-5}–0.1 mol l^{-1} nitrite). From these results it seems that the electrode is operating via a charged-carrier mechanism. This was further ascertained by the electrode doped with CuTTBPc, since Cu(II) cannot be oxidized and must serve as a neutral carrier. Indeed, the selectivity sequence of the CuTTBPc-based electrode fits the Hofmeister pattern perfectly.

In general, the anion-selective membrane electrodes based on organometallic complexes are sensitive to pH, for these metals can form oxides and hydroxides at moderate or high pH. On the other hand, the effective concentration of nitrite ion is influenced by pH. So it is important to study the effect of the solution pH on the properties of the nitrite-sensitive electrodes based on a metal phthalocyanine. Calibration curves of the electrode were obtained by using buffers in the pH range 3.5–6.5 (Figs. 3 and 4). As the pH increases, the starting potentials of the electrode were shifted toward more negative values. This behavior can be explained by an increased level of interference from OH^-. For the same reason, the electrodes showed a better response and extended linearity at lower pH values. It is interesting to notice that at pH 3.5, when about 40% nitrite species existed in the protonated form, the electrode showed a linear response toward the

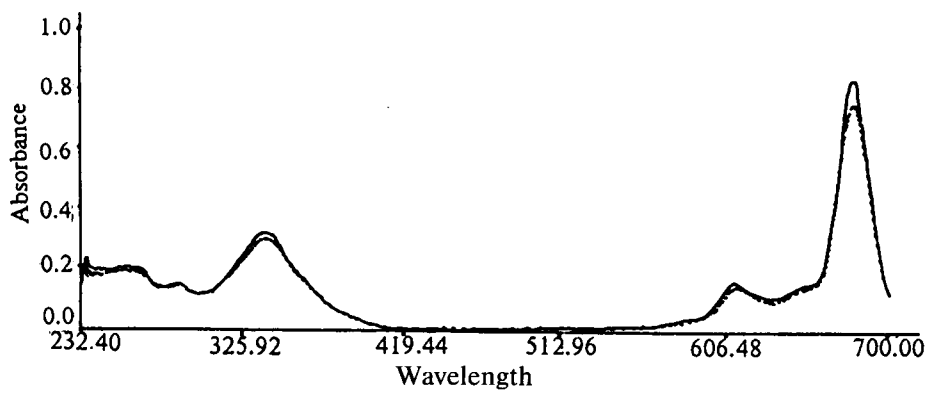

Fig. 6. UV/Vis absorption spectra of CuTTBPc in $CHCl_3$ (———) before and (- - - - -) after extraction with 0.1 mol l^{-1} aqueous $NaNO_2$, buffered with 0.01 mol l^{-1} phosphate, and adjusted to pH 3.5.

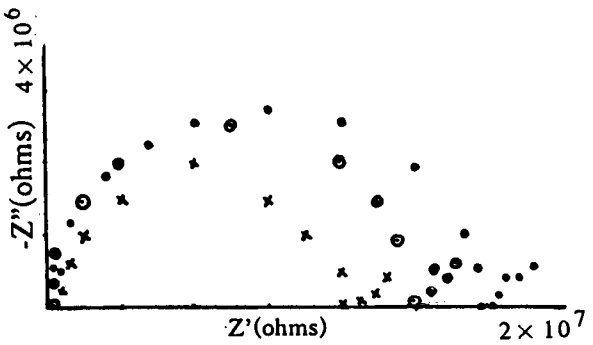

Fig. 7. Impedance plots of a membrane incorporating CoTTBPc after conditioning in (×) 10^{-1}, (⊙) 10^{-3} and (●) 10^{-5} mol l^{-1} $NaNO_2$ solutions for 2 h.

nitrite ion in a relatively wide concentration range (Fig. 3). It is evident that low pH values will favour the oxidation of CoTTBPc in the membrane phase to the charged form, but on the other hand it was shown that low pH values will favour the replacement of O_2^- of the oxygen adduct by anions such as F^-, NO_2^- and HCO_3^- [20]. Such a replacement reaction is not likely to occur for the case of copper(II) complexes, and the pH did not have a remarkable effect on the electrode based on CuTTBPc (Fig. 4).

It is possible to study the interaction between the central metal of the carrier and the nitrite species with UV/Vis spectroscopy. Fig. 5 shows the absorption spectra of CoTTBPc in $CHCl_3$. The UV/Vis spectrum of CoTTBPc in $CHCl_2$ treated with 0.1 mol l^{-1} $NaNO_2$ aqueous solution showed a minor change in the low-energy portion of the spectrum compared with that of CoTTBPc. It is probable that CoTTBPc possessed weak *d–d* transitions between the central cobalt atom and the nitrite species. The spectrum of CuTTBPc, on the other hand, was unchanged after treating with $NaNO_2$ aqueous solution (see Fig. 6). This observation seems to support the hypothesis that the potentiometric selectivity of the membrane was correlated with the unique coordination of nitrite species to CoTTBPc.

The a.c. impedance spectra of the membrane incorporating CoTTBPc were recorded after conditioning in $NaNO_2$ solutions for 2 h. Well-defined semicircles at high frequencies and Warburg impedance at low frequency intervals were observed (see Fig. 7). The bulk resistance increased with decreasing concentration of $NaNO_2$ aqueous solution this indicates that the transfer process of nitrite species across the PVC membrane was controlled by the diffusion process.

Acknowledgement

This work was supported by the National Science Foundation of China and Partially by the Laboratory of Electroanalytical Chemistry, Changchun Institute of Applied Chemistry, Academy of Science.

References

[1] M.A. Arnold and R.L. Arnold, Anal. Chem., 58 (1986) 84R–101R.
[2] Ru-Qin, Yu, Ion-Sel. Electr. Rev., 3 (1986) 153.
[3] P. Schulthess, D. Ammon, B. Krautler, C. Caderas, R. Stepanek and W. Simon, Anal. Chem., 57 (1985) 1397.
[4] N.A. Chaniotakis, A.M. Chasser, M.E. Meyerhoff and J.T. Groves, Anal. Chem., 60 (1988) 185.
[5] A. Hodinar and A. Tyo, Anal. Chem., 61 (1989) 1169.
[6] Q. Chang and M.E. Meyerhoff., Anal. Chim. Acta, 186 (1986) 81.
[7] S. Daunert, S. Wallace, A. Florido and G. Bachas, Anal. Chem., 63 (1991) 1676.
[8] B. Chaube, A.K. Baveja and V.K. Gupta, Talanta, 31 (1984) 391.
[9] C.H. Kiang, S.S. Kuan and G.G. Guibault, Anal. Chim. Acta, 80 (1975) 209.
[10] R. Stepanek, B. Krautler, P. Schulthess, D. Amman, B. Lindemann and W. Simon, Anal. Chim. Acta, 182 (1986) 83.
[11] Ru-Qin. Yu and S.S. Huang, Talanta, 30 (1983) 427.
[12] G.J. Moody, R.B. Oke and J.D.R. Thomas, Analyst, 95 (1970) 910.
[13] A. Graggs, G.J. Moody and J.D.R. Thomas, J. Chem. Educ., 51 (1974) 541.
[14] E. Pungor, K. Toth and A. Hrabeczy-Paall, Pure Appl. Chem., 51 (1979) 1973.
[15] J. Metz, O. Schneider and M. Hanack, Inorg. Chem., 23 (1984) 1067.
[16] M. Hanack, J. Metz and G. Pawlowski, Chem. Ber., 115 (1982) 2836.
[17] T.A. Jones and B. Bott, Sensors Actuators, 43 (1984) 5.
[18] P.B.M. Archer, A.V. Chadwick, J.J. Miaski, M. Tamiti and J.D. Wright, Sensors Actuators, 16 (1989) 379.
[19] J.D. Wright, Mater. Sci., 13 (1987) 295.
[20] E.I. Ochiai, Bioinorganic Chemistry, An Introduction, Allyn and Bacon, Boston, MA, 1977, pp. 195–196.

ELSEVIER

Analytica Chimica Acta 297 (1994) 443–451

ANALYTICA CHIMICA ACTA

Determination of trace amounts of selenium and tellurium in high-purity iron by electrothermal atomic absorption spectrometry after reductive coprecipitation with palladium using ascorbic acid

Tetsuya Ashino *, Kunio Takada, Kichinosuke Hirokawa

Institute for Materials Research, Tohoku University, Katahira 2-2-1, Sendai 980-77, Japan

Received 9 February 1994; revised manuscript received 13 May 1994

Abstract

Trace amounts of selenium and tellurium in high-purity iron were quantitatively separated by a reductive coprecipitation technique with palladium, and determined by electrothermal atomic absorption spectrometry. When ascorbic acid was used as reductant, selenium and tellurium could be simultaneously separated from large quantities of iron. The precipitate was dissolved in HNO_3 and HCl, then the sample solution was injected into a graphite furnace with ascorbic acid solution. The atomic absorbance of selenium was increased about 4 times, and the atomic absorbance of tellurium was increased about 3.5 times by the presence of palladium. The detection limits (3σ) of selenium and tellurium were 0.01_7 $\mu g\ g^{-1}$ and 0.01_1 $\mu g\ g^{-1}$, respectively.

Keywords: Atomic absorption spectrometry; Iron; Palladium; Selenium; Tellurium

1. Introduction

The characteristics of high purity metals have been widely investigated. In order to assess the purity, trace elements have to be determined. Selenium and tellurium contribute to the increased cutting capabilities of iron. Therefore, not only for the evaluation of the purity of high purity iron, but also for the control of selenium and tellurium contents in iron, a procedure has been developed. Trace amounts of selenium and tellurium have been determined by neutron activation analysis (NAA) [1,2], X-ray fluorescence analysis (XRF) [3,4], hydride generation atomic absorption spectrometry (hydride-AAS) [5,6] and electrothermal atomic absorption spectrometry (ET-AAS) [7,8]. ET-AAS is suitable for the determination of trace amounts of selenium and tellurium in a high purity iron, because both elements can be determined from a single sample by the same procedure, and special techniques are not needed. However, it may be necessary to separate and concentrate trace amounts of selenium and tellurium from iron, not only because

* Corresponding author.

SSDI 0003-2670(94)00226-C

the sensitivity of the determination of both selenium and tellurium by ET-AAS is not sufficient, but also because the sensitivity may be decreased by the presence of iron. Various coprecipitation methods for the separation and concentration of selenium and tellurium in several metals have been reported [9–11]. Gold, platinum, palladium and some other noble metal ions are suitable as carriers for reductive coprecipitation procedures since they can easily be reduced by various reductants. Palladium has been used as a matrix modifier for the determination of selenium and tellurium by ET-AAS [12,13]. Therefore, a highly sensitive determination of these metals is expected. In order to develop a procedure for a highly sensitive determination of trace amounts of selenium and tellurium in high purity iron, a reductive coprecipitation method using ascorbic acid with palladium and determination by ET-AAS were investigated and employed. A reductive coprecipitation method using only palladium as carrier for separation of selenium and tellurium in metals and solutions has not been reported. It is expected that trace amounts of selenium and tellurium are simultaneously separated from large quantities of iron by a single separation and that this method is very sensitive. The method is suitable for the analysis of a large number of samples.

2. Experimental

2.1. Apparatus

For the determination of selenium and tellurium, a Hitachi Z-9000 simultaneous multi-element atomic absorption spectrophotometer was used, and background was collected by the polarized Zeeman effect. A hollow cathode lamp (Hamamatsu Photonics) was used as light source. The operating conditions are listed in Table 1. For dissolution and coprecipitation of samples, an erlenmeyer flask with ground stopper (inner volume 200 ml) was used. For filtration, a membrane filter (Nuclepore Polycarbonate, pore size 0.2 μm, Coster Co.) was used. For the determination of palladium and selenium in the concentration range from 1 to 20 μg ml^{-1}, a Hitachi P-5200 dual monochromatic ICP emission analysis system was used, and the operating conditions are listed in Table 2.

Table 1
Instrumental and operating conditions of ET-AAS

Wavelength	Se, 196.0 nm
	Te, 214.3 nm
Lamp current	Se, 8.0 mA
	Te, 4.0 mA
Argon flow rate	
carrier gas	300 ml min^{-1}
interrupted gas	20 ml min^{-1}
Cuvette	Tube type
Injection volume	
sample	20 μl
ascorbic acid	10 μl
Temperature program	
drying	80–150°C, 30 s
ashing	150–1200°C, 30 s
	1200–1200°C, 30 s
atomizing	2600°C, 5 s
cleaning	3000°C, 10 s

2.2. Reagents

Selenium standard solution (1.00 μg ml^{-1}) was prepared by the following procedure: 100 mg of metallic selenium (99.999 + %, shot, Mitsuwa Chemicals) was dissolved in 10 ml of 7 M HNO_3, and diluted to 100 ml with water. It was diluted with water before use.

Tellurium standard solution (1.00 μg ml^{-1}) was prepared as follows: 100 mg of metallic tel-

Table 2
Instrument and operating condition of ICP-AES

	Spectrometer 1	Spectrometer 2
Slit width (μm)	30	30
Slit height (mm)	10	10
Observation height (mm)	15	15
Grating (grooves mm^{-1})	3600	1200
Rf power (kW)	1.0	
Plasma gas (l min^{-1})	12	
Nebulizer gas (l min^{-1})	0.45	
(kPa)	120	
Auxiliary gas (l min^{-1})	0.5	
Wavelength (nm)	Se I 196.026	
	Pd I 340.458	

lurium (99.99%, shot, Mitsuwa Chemicals) was dissolved in 10 ml of 7 M HNO_3, and diluted to 100 ml with water. It was diluted with water before use.

Palladium standard solution (3 mg ml^{-1} solution is used for calibration, 0.6 mg ml^{-1} solution is used for coprecipitation) was prepared by dissolving 300 mg of metallic palladium (99.9%, powder, Mitsuwa Chemicals) in 5 ml of HNO_3, and diluted to 100 ml with water. It was used for calibration. A 20-ml aliquot of the solution was diluted to 100 ml with water, and used for coprecipitation. Distilled water was used for all preparations of the standard and sample solution. All the reagents used were analytical-reagent grade.

2.3. Samples

High purity iron of Grade 1 iron powder (Johnson Matthey Materials Technology) was used. As reference sample we used Special low alloy steel SRM-364 (U.S. Department of Commerce, National Institute of Standards and Technology).

2.4. Procedures

Preparation of sample

1 g of the sample was weighed into an erlenmeyer flask. 5 ml of 14 M HNO_3, 5 ml of 12 M HCl and 5 ml of water were added, and the sample was dissolved on a heating plate. Subsequently, 10 ml of 18 M H_2SO_4 and 10 ml of 15 M H_3PO_4 were added, and the solution was heated to fumes. After cooling at room temperature, the solution was diluted with 80 ml of water. Then, 5 ml of 0.6 mg ml^{-1} palladium standard solution and 2 g of ascorbic acid were added, and the flask containing the solution was stoppered at room temperature for 0.5 h in case of selenium, and 3 h in case of tellurium. After standing, the precipitate was collected through a membrane filter. The collected precipitate was then immediately dissolved in 1.5 ml of 14 M HNO_3 and one drop (about 0.05 ml) of 12 M HCl at room temperature. Finally, the solution was exactly diluted to 10 ml with water. The blank was prepared by the same procedure as described above without the sample. The preconcentration factor is 10.

ET-AAS determination

20 μl of the sample solution or the blank solution was injected into a graphite furnace, immediately followed by the injection of 10 μl of 3% ascorbic acid solution. The atomic absorbance was measured under the conditions shown in Table 1.

Preparation of calibration solutions

0–15 ml of the selenium and/or tellurium standard solution were transferred into volumetric flasks, followed by addition of 5 ml of 3 mg ml^{-1} palladium standard solution, 7.5 ml of 14 M HNO_3 and five drops (about 0.25 ml) of 12 M HCl. Finally, the solutions were exactly diluted to 50 ml with water.

3. Results and discussion

3.1. Effects of iron on the determination of selenium and tellurium by ET-AAS

The effects of iron on the determination of selenium and tellurium by ET-AAS were examined, and the relationship between the concentration ratio (iron:selenium, iron:tellurium) and the atomic absorbance of selenium and/or tellurium is shown in Fig. 1. The employed method was as follows: to the solution containing 0.1 μg ml^{-1} selenium and/or tellurium iron was added in the concentration range from 0.1 μg ml^{-1} to 10 mg

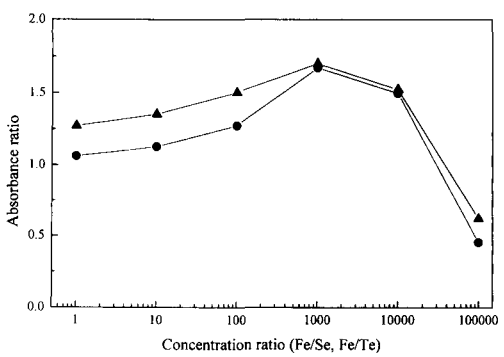

Fig. 1. The relationship between the concentration ratio (iron:selenium, iron:tellurium) and atomic absorbance: ●, selenium; ▲, tellurium; Se and Te = 0.1 μg ml^{-1}, atomic absorbance ratios are normalized to 1 when no iron is present.

ml^{-1} (1 to 1×10^5 times the concentration of both elements), and the atomic absorbance of selenium and/or tellurium was measured. It was found that for an iron concentration lower than 1000 times the concentration of selenium and tellurium, the atomic absorbance of both elements increased on addition of iron, but it decreased in the presence of iron for concentrations larger than 1000 times. In spite of the addition of palladium and ascorbic acid to the iron-containing solution, the same results were obtained. Therefore, for the determination of trace amounts of selenium and tellurium in high purity iron by ET-AAS, it is necessary to separate selenium and tellurium from iron.

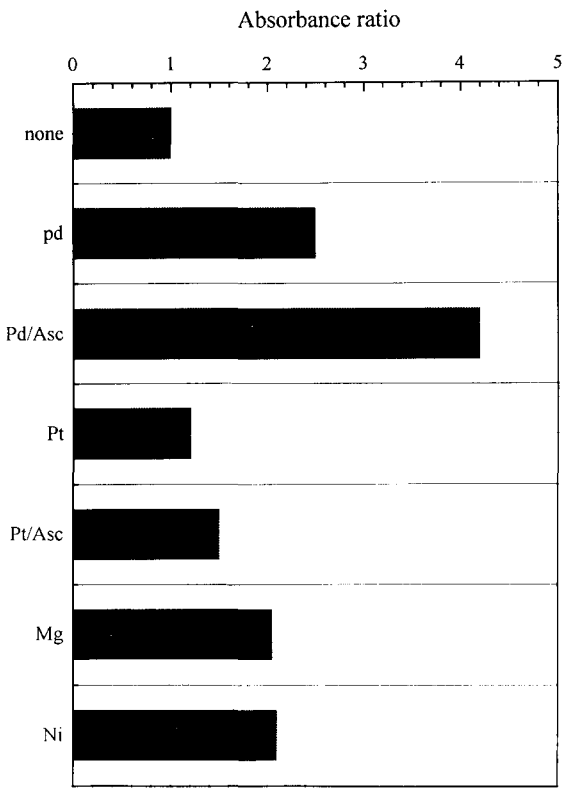

Fig. 2. The effects of matrix modifiers on the atomic absorbance of selenium: Se = 0.1 μg ml^{-1}, matrix modifiers = 100 μg ml^{-1}, atomic absorbance ratios are normalized to 1 when no iron is present.

Table 3
Recovery of selenium separated from high purity iron by coprecipitation with various carriers and reductants

Carrier	Recovery (%)			
	Reductant			
	Ascorbid acid	Hydrazine sulfate	$NaHSO_3$	$NaHSO_3$ + Hydrazine sulfate
Pd	100.4	not detected	not detected	93.4
Pt	32.4	not detected	not detected	26.8

3.2. Effects of matrix modifier on the determination of selenium by ET-AAS

The effects of matrix modifier on the determination of selenium by ET-AAS under the conditions mentioned in Table 1 were examined. Results are shown in Fig. 2. The employed method was as follows: the solutions containing 0.1 μg ml^{-1} selenium and 100 μg ml^{-1} (1000 times the concentration of selenium) of various matrix modifiers were prepared, and the atomic absorbance of selenium was measured. As matrix modifiers, palladium, platinum, magnesium and nickel were used. The increase in atomic absorbance was the highest in the presence of palladium and ascorbic acid. Therefore, for the matrix modifier studied, the combination of palladium and ascorbic acid appeared to be the most useful modifier for the ET-AAS determination in combination with the ascorbic acid solution which is injected into a graphite furnace with the sample solution. When the effects of iron and matrix modifiers on the ET-AAS determination of tellurium were examined, the same results were obtained as for selenium.

3.3. Selection of carrier and reductant for coprecipitation

In order to select a suitable carrier and reductant for the coprecipitation and separation of trace amounts of selenium and tellurium from high purity iron, the effects of carriers and reduc-

tants were examined. The results are shown in Table 3. The employed method was as follows: 1 g of high purity iron and 100 μg of selenium were dissolved in HNO_3 and HCl, then H_2SO_4 and H_3PO_4 were added, and heated to fumes. Selenium was separated and concentrated by coprecipitation with various carriers and reductants. The precipitate was dissolved and diluted to 10 ml, then selenium was determined by inductively coupled plasma atomic emission spectrometry (ICP-AES). Palladium and platinum were used as carriers, since they have lower redox potentials than selenium and tellurium, and the effects of the matrix modifier were evaluated by ET-AAS. As reductant, ascorbic acid, sodium hydrogensulfite ($NaHSO_3$), hydrazine sulfate and both $NaHSO_3$ and hydrazine sulfate were examined. When palladium was used as carrier, selenium was quantitatively recovered in combination with ascorbic acid, or both $NaHSO_3$ and hydrazine sulfate, but for platinum, the recoveries of selenium were low. When both $NaHSO_3$ and hydrazine sulfate are used, it is necessary to heat the sample solution for reductive coprecipitation. When only $NaHSO_3$ or only hydrazine sulfate was used as reductant, no precipitates were found and selenium was not recovered when palladium or platinum were used. However, when ascorbic acid is used, there is no need for heating the solution. The solution is left to stand in a stoppered flask, and the precipitate is not contaminated with other metal elements. Similarly, tellurium was quantitatively recovered by palladium and ascorbic acid. Therefore, palladium is suitable as a carrier, and ascorbic acid is suitable as a reductant for the reductive coprecipitation method for the simultaneous separation of selenium and tellurium.

3.4. Acid dissolution of sample

The effects of hydrochloric acid on the recovery of selenium were examined. The relationship between the volume of hydrochloric acid and the recovery of selenium is shown in Fig. 3. The employed method was as follows: 1 g of high purity iron and 1 μg of selenium were dissolved in 5 ml of 14 M HNO_3, in the volume range from

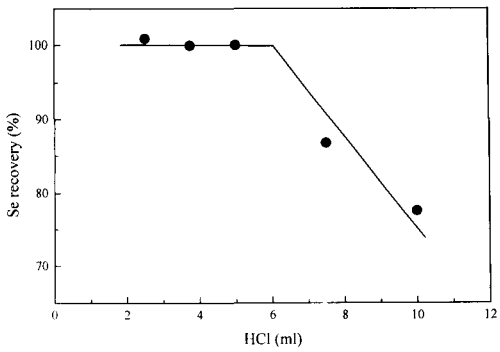

Fig. 3. The relationship between the volume of hydrochloric acid for dissolution of sample and recovery of selenium: Fe = 1 g, Se = 1 μg, HNO_3 = 5 ml.

2.5 to 10 ml of 12 M HCl and 5 ml of water. After 18 M H_2SO_4 and 15 M H_3PO_4 were added and heated to fumes, selenium was separated and concentrated by coprecipitation with palladium and ascorbic acid. The precipitate was dissolved in 1.5 ml of 14 M HNO_3 and one drop of 12 M HCl, and diluted to 10 ml with water. Then selenium was determined by ET-AAS. When more than 5 ml of HCl was used, the recovery of selenium was lower. It is assumed that selenium was vaporized as chloride during dissolution or heating to fumes, since the sublimation temperature of selenium tetrachloride ($SeCl_4$) is 196°C. When the effects on recovery of tellurium were examined, results similar to those of selenium were obtained. Therefore, the acidic mixture used for dissolution of the sample was 5 ml of 14 M HNO_3 and 5 ml of 12 M HCl.

3.5. Quantity of palladium as carrier

The effects of the quantity of palladium on the recovery of selenium were examined, and the relationship between the quantity of palladium and the atomic absorbance of selenium is shown in Fig. 4. The employed method was as follows: 1 g of high purity iron and 1 μg of selenium were dissolved and heated to fumes by the same procedure as described above, selenium was separated by coprecipitation in the range from 1 to 9 mg of palladium. The precipitate was dissolved and diluted to 10 ml by the same procedure as previous

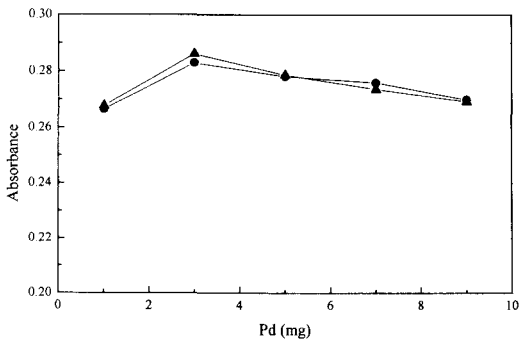

Fig. 4. The relationship between the quantity of palladium as carrier and the atomic absorbance of selenium: ●, coprecipitation; ▲, control solution.

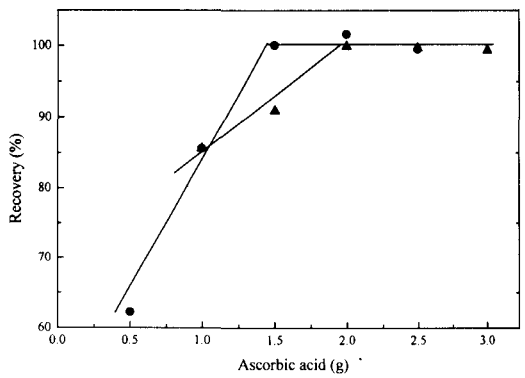

Fig. 5. The relationship between the quantity of ascorbic acid as reductor and recoveries of selenium and palladium: ●, selenium; ▲, palladium; Fe = 1 g, Se = 1 μg, Pd = 3 mg.

described, and the atomic absorbance of selenium was measured. As control solution, the solution containing 0.1 μg ml^{-1} selenium and 100–900 μg ml^{-1} palladium were prepared, respectively, and the atomic absorbance of selenium was measured. As a result, quantitative recoveries of selenium were obtained in the range from 1 to 9 mg of palladium, since the behaviour of the absorbance of employed and control solution against the quantity of palladium was the same within experimental uncertainties. Therefore, the quantity of palladium used was 3 mg, since with that amount the highest absorbance of selenium was obtained. It was also applicable for the determination of tellurium.

3.6. Quantity of ascorbic acid as reductant

The effects of quantity of ascorbic acid on the recovery of selenium were examined, and the relationship between the quantity of ascorbic acid and the recoveries of selenium and palladium is shown in Fig. 5. The employed method was as follows: 1 g of high purity iron and 1 μg of selenium were dissolved and heated to fumes by the same procedure, selenium was separated by coprecipitation using 3 mg of palladium and in the range of 0.5–3 g of ascorbic acid. The precipitate was dissolved and diluted to 10 ml by the same procedure, selenium was determined by ET-AAS, and palladium was determined by ICP-AES. As a result, when more than 1.5 g of ascorbic acid was used, selenium was quantitatively recovered, and when more than 2 g of ascorbic acid was used, palladium was quantitatively recovered within 2% error. It is assumed that when less than 2 g of ascorbic acid was used, it was consumed for the reduction of Fe(III), and it was hardly used for the reduction of Se(IV) and Pd(II). Therefore, the quantity of ascorbic acid used was more than 2 g, which was also applicable to the determination of tellurium.

3.7. Standing time for coprecipitation

The standing time for coprecipitation for the separation of selenium and tellurium was examined, and the relationship between the standing time and recovery of selenium and tellurium is shown in Fig. 6. The employed method was as follows: 1 g of high purity iron and 1 μg of

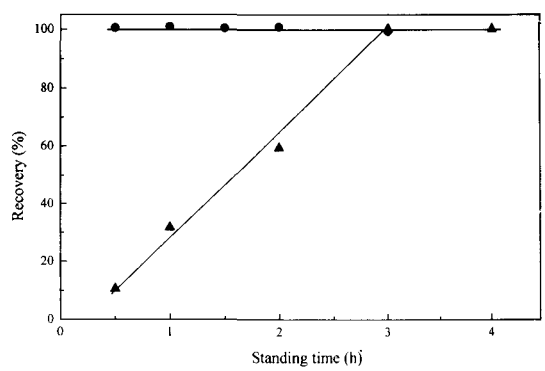

Fig. 6. The relationship between the standing time for coprecipitation and recoveries of selenium and tellurium: ○, selenium; ▲, tellurium; Fe = 1 g, Se and Te = 1 μg, Pd = 3 mg, ascorbic acid = 2 g.

selenium and/or tellurium were dissolved and heated to fumes by the same procedure. Selenium and tellurium were separated by coprecipitation using 3 mg of palladium and 2 g of ascorbic acid for 0.5–4 h. The precipitate was dissolved and diluted to 10 ml by the same procedure, then selenium and tellurium were determined by ET-AAS. As a result, when the standing time was more than 0.5 h, quantitative recovery of selenium was obtained. However, tellurium was quantitatively recovered only after more than 3 h. It is assumed that the reduction rate of Te(IV) is lower than the reduction rate of Se(IV). Both selenium and tellurium were quantitatively separated from high purity iron independent of their valence state in the solution. It was confirmed by X-ray diffraction (XRD) that selenium, tellurium and palladium in the precipitate were in their metal state. When the standing time was 3 h, selenium, tellurium and palladium in the precipitate had an amorphous structure, but in case of 15 h, they all had a crystalline structure. However, independent of structure, selenium, tellurium and palladium were quantitatively recovered.

3.8. Volume of nitric acid for the dissolution of precipitate

The volume of HNO_3 for the dissolution of precipitate was examined, and the relationship between the HNO_3 concentration and the atomic absorbance of selenium is shown in Fig. 7. The employed method was as follows: solutions containing 0.1 μg ml^{-1} selenium, 300 μg ml^{-1} palladium and in the concentration range of 0.7–3.5 M HNO_3 were prepared. The atomic absorbance of selenium was measured. As a result, in the HNO_3 concentration range from 1.4 to 2.8 M, the atomic absorbance of selenium was constant. Therefore, the HNO_3 concentration of the sample solution was selected to be 2.1 M, which means that the precipitate was dissolved in 1.5 ml of 14 M HNO_3, and the solution was diluted to 10 ml. The reason for adding one drop (about 0.05 ml) of 12 M HCl for dissolution of the precipitate is that the precipitate is hardly dissolved at room temperature in HNO_3 only. In order to dissolve the precipitate at room temperature, it is necessary that the precipitate is dissolved as soon as filtration is completed. When ascorbic acid solution was injected into a graphite furnace with sample solution, the atomic absorbance was not decreased.

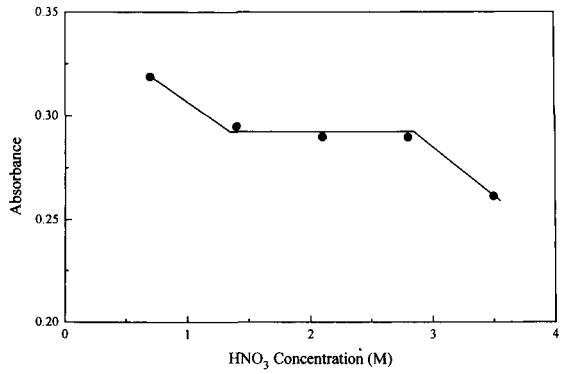

Fig. 7. The relationship between the nitric acid concentration and the atomic absorbance of selenium: Se = 0.1 μg ml^{-1}, Pd = 300 μg ml^{-1}.

3.9. Effects of foreign ions

The effects of foreign irons on the recovery of selenium and tellurium by coprecipitation were examined. The employed method was as follows: 1 g of high purity iron, 1 μg of selenium and/or tellurium and 1 mg (corresponding to 0.1% of the amounts of iron) of various metal ions were dissolved. Selenium and tellurium were separated and concentrated according to the proposed method, after which selenium and tellurium were determined by ET-AAS. The examined ions were Mn(II), Cu(II), Ni(II), V(V), Cr(III), Mo(VI), W(VI), Ti(IV), Mg(II), Ca(II), Co(II), Zn(II), Cd(II), Al(III), Pb(II) and Sn(IV). As a result, when all employed elements were contained, quantitative recovery of both selenium and tellurium was obtained within 2% error. Therefore, no effects of the foreign ions were found within this range.

3.10. Mutual effects of selenium and tellurium

The mutual influences of selenium and tellurium on the analytical results were examined.

Table 4
Analytical results of mixed solution sample

		Added (μg)	Found (μg)	Recovery (μg)	n	R.S.D. [a] (%)
Se	Fe [b], 1 g	–	$<0.01_7$	–	1	–
	Fe, 1 g + Se	1.04_0	$1.04_5 \pm 0.01_4$	100.5	5	1.18
Te	Fe, 1 g	–	$<0.01_1$	–	1	–
	Fe, 1 g + Te	1.08_6	$1.07_8 \pm 0.00_7$	99.4	5	0.71

[a] Relative standard deviation.
[b] High purity iron; Johnson Matthey, Grade 1 Powder

The employed method was as follows: the solution containing 0.1 μg ml^{-1} of either selenium or tellurium and 1–100 times higher amounts of the other elements were prepared. Selenium and tellurium were then determined. As a result, the analytical values of both selenium and tellurium were similar. Therefore, no mutual effects between selenium and tellurium on the analytical values measured by ET-AAS were found within this range.

3.11. Calibration curve

For the preparation of optimal calibration graphs an aqueous standard was used and the relationship between the atomic absorbance and the concentration of selenium and/or tellurium was examined. A straight line through the point of origin was obtained for a concentration < 0.3 μg ml^{-1} for both selenium and tellurium. The detection limit (3 times the relative standard division of the blank) of the proposed method was 0.01_7 μg g^{-1} for selenium and 0.01_1 μg g^{-1} for tellurium in 1 g of sample.

3.12. Analysis of mixed solution sample

Selenium and tellurium in a mixed solution sample, which consisted of 1 μg of both selenium and tellurium and 1 g of high purity iron, were determined according to the proposed method. The results are shown in Table 4. As a result, both elements were quantitatively determined within 2% error.

3.13. Analysis of reference sample

The proposed method was applied for the determination of selenium and tellurium in the reference sample. The results are shown in Table 5. Good agreement was found between the reference values and the values obtained via the proposed method.

4. Conclusions

Trace amounts of selenium and tellurium in high purity iron were quantitatively separated and concentrated by reductive coprecipitation using palladium and ascorbic acid. When palladium was used as matrix modifier, and ascorbic acid solution was injected into the graphite furnace together with the sample solution, the ET-AAS determination of selenium and tellurium was highly sensitive. The proposed method may be applied not only for high purity iron but also for low alloy steel.

Table 5
Analytical results of reference sample

Sample	Element	Reference [a] (μg g^{-1})	Average (μg g^{-1})	n	RSD [b] (%)
Low alloy steel [c]	Se	2.1	$2.10_8 \pm 0.03_3$	4	1.55
	Te	2	$1.98_7 \pm 0.03_8$	4	1.90

[a] Non-certified value.
[b] Relative standard deviation.
[c] NIST SRM-364.

References

[1] W. Zmijewska, H. Polkowska-Montrenko and H. Stokowska, J. Radioanal. Nucl. Chem. Art., 116 (1987) 243.
[2] N. Lavi and Z.B. Alfassi, Analyst (London), 113 (1988) 1855.
[3] G.L. Vassilaros, Talanta, 18 (1971) 1057.
[4] R. Panayappan, D.L. Venezky, J.V. Gliflish and L.S. Brirks, Anal. Chem., 50 (1978) 1125.
[5] S.G. Offley, N.J. Seare, J.F. Tyson and H.A.B. Kibble, J. Anal. Atom. Spectrom., 6 (1991) 133.
[6] J. Dedina, Spectrochim. Acta, 47B (1992) 689.
[7] J.Y. Marks, G.G. Welcher and R.J. Spellman, Appl. Spectrosc., 31 (1977) 9.
[8] K. Matsuzaki, T. Yamamoto and T. Oishi, Bunseki Kagaku, 42 (1993) 1.
[9] B.C. Severne and R.R. Brooks, Anal. Chim. Acta., 58 (1972) 216.
[10] O. Kujirai, T. Kobayashi, K. Ide and E. Sudo, Talanta, 30 (1983) 9.
[11] Z.B. Alfassi and C.M. Wai, Preconcentration Techniques for Trace Elements, CRC Press, London, 1992.
[12] Y. Terui, K. Yasuda and K. Hirokawa, Anal. Sci., 7 (1991) 397.
[13] D.L. Styris, L.J. Prell, D.A. Redfield, J.A. Holcombe, D.S. Bass and V. Malidi, Anal.Chem., 63 (1991) 508.

ELSEVIER

Analytica Chimica Acta 297 (1994) 453–464

ANALYTICA CHIMICA ACTA

Micellar effects on reaction kinetics Part II. Study of the action of dodecyltrimethylammonium bromide on the reactions between Pyrogallol Red and chromium(VI), vanadium(V) and titanium(IV)

Dolores Sicilia, Soledad Rubio, Dolores Pérez-Bendito *

Department of Analytical Chemistry, Faculty of Sciences, University of Córdoba, Córdoba, Spain

Received 10 December 1993; revised manuscript received 9 May 1994

Abstract

The complexation kinetics and equilibrium of the reactions of vanadium(V) and titanium(IV) with Pyrogallol Red (PGR), and the kinetics of oxidation of chromium(VI) by PGR were studied in micellar solutions of dodecyltrimethylammonium bromide (DTAB). The 1:1 PGR–V(V) and 2:1 PGR–Ti(IV) complexes formed in an aqueous medium associate with DTAB molecules of the micellar system to yield the new complexes 1:1:2 PGR–V(V)–DTAB and 2:1:1 PGR–Ti(IV)–DTAB. The stability constants of the ternary complexes were calculated by considering the volume fraction of micelles and were compared with those determined from the overall solution volume. The binding constants for the associates of PGR, chromium(VI), vanadium(V), titanium(IV), PGR–V(V) and PGR–Ti(IV) complexes with DTAB micelles were spectrophotometrically determined. The observed rate of formation of the PGR–Ti(IV) complex was increased by the presence of DTAB micelles, but the second-order rate constant in the micellar pseudo-phase was slightly lower than in water. Therefore, the whole rate increase observed was due to the concentration of reactants in the micellar pseudo-phase. The kinetics of formation of the PGR–V(V) complex could not be investigated by using the stopped-flow technique because the reaction was too fast in both the aqueous and the micellar medium. The second-order rate constant for the oxidation reaction between PGR and Cr(VI) was found to exceed that in aqueous solutions by a factor of ca. 55. Therefore, the increased rate observed for this reaction in the DTAB micellar medium can be ascribed to intrinsic effects of the micellar pseudo-phase on reactivity.

Keywords: Kinetic methods; Complexation; Micelles

1. Introduction

Micelles possess a high potential for multicomponent analysis as can be inferred from the results obtained in recent research on this topic [1]. Micelles can be used as special reaction media as they alter the rate, equilibrium position, products and stereochemistry of many reactions. Also, micelles change the effective microenvironment around dissolved solutes and hence their physicochemical properties such as absorptivity, equilibrium constant, spectral profile, etc. These features can help to overcome many of the analytical

* Corresponding author.

SSDI 0003-2670(94)00230-J

problems encountered in multideterminations, where, as in many other areas of analytical chemistry, micellar systems have only been applied in an empirical manner. There is, therefore, a need for additional fundamental studies of analytical micellar systems in order to clearly establish the exact origin of many of the beneficial effects micelles provide.

This paper reports on a fundamental study on the kinetics of the reactions between Pyrogallol Red (PGR) and chromium(VI), vanadium(V) and titanium(IV) in aqueous dodecyltrimethylammonium bromide (DTAB) micelles as well as on the physico-chemical features of the resulting reaction products. These reactions were previously utilized for the resolution of ternary mixtures of the three ions based on the effects of DTAB micelles on them [2]. Thus, the oxidation reaction between PGR and Cr(VI) is accelerated by the presence of the surfactant. On the other hand, the oxidation reaction between PGR and V(V) is almost completely suppressed in a DTAB micellar medium and a PGR–V(V) complex is obtained rather than the PGR oxidation product, so product distribution is altered relative to water. Likewise, DTAB micelles cause a bathochromic shift and exert a hyperchromic effect on the absorption spectrum of the PGR–Ti(IV) complex.

Kinetic studies on these reactions have so far been aimed at assessing the intrinsic reactivity of reactants in DTAB micelles. Because the rate enhancing effects of micelles can be due to medium or concentration effects [3], our aim was to determine the relative significance of both types of effects on the reactions considered. For this purpose, we estimated the binding constant for each reactant to the micelles (K_s) and the true second-order constant (k_M) in the micellar pseudo-phase. A comparison of this rate constant with that in water should reveal the significance of the medium effect of the micelle. The model used to analyse kinetic data was essentially that developed by Berezin et al. [3], implemented in the equations of Fletcher and Robinson [4] for estimation of k_M.

Our study of the physico-chemical features of the reaction products obtained in the micellar medium was focussed on the PGR–Ti(IV) and PGR–V(V) complexes, the bathochromic and/or hyperchromic effects on which arise from the presence of DTAB micelles. The nature of both complexes was comparatively investigated in the aqueous and micellar medium by determining their stability constants and stoichiometries. Metal–chelate complexes formed in micellar systems are known to be much more stable than those formed in the absence of micelles [5]. Because association of reactants and complexes to micelles involves a major concentration effect, stability constants were also determined by considering the volume fraction of micelles in order to estimate their real values using a mathematical expression derived in this work. Association of the metal–chelate complexes to surfactant molecules of the micellar system to yield a "new" complex (usually referred to as ternary complex), was also investigated since it usually equalizes bonds and results in maximal delocalization of the conjugated π-electron system, thereby altering the absorption spectrum of the complex [5].

2. Experimental

2.1. Apparatus

Absorbance measurements were made on a Hewlett Packard 8452A diode array spectrophotometer furnished with 1-cm quartz and glass cells. The spectrophotometer cell compartment was thermostated by circulating water from a Neslab RTE bath. Kinetic measurements were made on a Philips PU 8625 UV–vis spectrophotometer fitted with a stopped-flow module [6] (Quimi-Sur Instrumentation, Seville, Spain). The module, furnished with an observation cell of 0.3 cm path length, was controlled by the associated electronics via a 640 K Mitac computer for acquisition and processing of kinetic data. The solutions in the stopped-flow module and cell compartment were kept at a constant temperature by circulating water from a thermostated tank. A ordinary stalagmometer was used for surface measurements in order to determine the critical micelle concentration (c.m.c.) of the surfactant [7].

Table 1
Experimental conditions used for the determination of binding constants for various species incorporated into DTAB micelles (temperature = 25°C)

Species	[Species] (M)	DTAB concentration range (M)	Fitted wavelength (nm)
PGR	5.0×10^{-5}	1.0×10^{-3}–1.0×10^{-2}	580
Cr(VI)	1.92×10^{-4}	8.0×10^{-3}–1.8×10^{-2}	380
V(V)	3.9×10^{-4}	5.0×10^{-5}–1.0×10^{-3}	310
Ti(IV)	8.4×10^{-5}	2.0×10^{-5}–4.0×10^{-3}	310
PGR–V(V)	[PGR] = 7.0×10^{-5} [V(V)] = 1.2×10^{-5}	5.0×10^{-5}–1.5×10^{-3}	620
PGR–Ti(IV)	[PGR] = 7.0×10^{-5} [Ti(IV)] = 2.1×10^{-5}	2.0×10^{-5}–2.5×10^{-3}	640

2.2. Reagents

All chemicals used were of analytical-reagent grade and utilized as purchased, without further purification. Bidistilled water was used throughout. A stock aqueous solution of Cr(VI) (1.92×10^{-2} M) was prepared from $K_2Cr_2O_7$ (Merck). Another stock aqueous solution of V(V) (1.96×10^{-2} M) was made from NH_4VO_3 (Aldrich). A stock Ti(IV) solution (2.09×10^{-2} M) was made by dissolving 0.1 g of metal titanium (Merck) in 10 ml of HCl (1:1, v/v) with warming; after cooling,the solution was made to 100 ml with HCl (1:1, v/v). A 2.1×10^{-3} M solution of PGR (Aldrich) was prepared by dissolving 0.0840 g of the reagent in 100 ml of methanol (100%). A 0.1 M phthalate buffer of pH 3.5 was also prepared. A DTAB (Sigma) solution (9.73×10^{-2} M) was made by dissolving the required amount of surfactant in bidistilled water.

2.3. Procedure for the determination of micellar binding of the substrates or reaction products

The distribution or binding constants of PGR, Cr(VI), V(V), Ti(IV) and the PGR–V(V) and PGR–Ti(IV) complexes to DTAB micelles (K_s) were determined spectrophotometrically [8,9] from the changes (bathochromic and/or hyperchromic shifts) induced by the cationic surfactant on the absorption spectra of the species considered. A series of solutions (10 ml total volume) containing a fixed concentration of one species

Table 2
Equilibrium and kinetic parameters for the reactions of PGR with Cr(VI), V(V) and Ti(IV) in an aqueous and a DTAB micellar medium

Substrate, product or reaction	Parameter				
	K_s (M^{-1})	K_f	$K_{f_{app}}$ (M^{-3})	$k_{M,1}$ ($M^{-1}s^{-1}$)	$k_{aq,1}$ ($M^{-1}s^{-1}$)
PGR	1050 ± 5				
Cr(VI)	930 ± 60				
V(V)	6150 ± 350				
Ti(IV)	5800 ± 30				
PGR–V(V)	6300 ± 400	$(1.5 \pm 0.5) \times 10^{6}$ M^{-1}			
PGR_2–Ti(IV)	3400 ± 200	$(2.7 \pm 0.8) \times 10^{11}$ M^{-2}			
PGR–V(V)–DTA_2		$(2.4 \pm 0.2) \times 10^{2}$ M^{-3}	$(7.3 \pm 0.5) \times 10^{10}$		
PGR_2–Ti(IV)–DTA		$(2.1 \pm 0.5) \times 10^{5}$ M^{-3}	$(6.5 \pm 1.6) \times 10^{13}$		
Cr(VI) + PGR				1.1 ± 0.1	$(2.0 \pm 0.2) \times 10^{-2}$
2PGR + Ti(IV) + DTA				0.27 ± 0.02	0.44 ± 0.02

and various concentrations of DTAB at the working pH (3.5, adjusted with 0.03 M phthalate–phthalic acid buffer) was prepared. An aliquot of each solution was transferred into a 1-cm quartz cell thermostated at 25°C, and the absorbance measured at a fitted wavelength for each species. The binding constant was calculated from the expression [8,9]:

$$K_{\text{species}} = f/\{(1-f)([\text{DTAB}] - \text{c.m.c.}) - f(1-f)[\text{species}]\} \quad (1)$$

where f is the fraction of species bound to micelles at different surfactant concentrations and can be calculated from

$$f = (A - A_{\text{aq}})/(A_{\text{m}} - A_{\text{aq}}) \quad (2)$$

A, A_{aq} and A_{m} being the absorbances measured at several DTAB concentrations, in its absence and on complete incorporation of species into the micelles, respectively. The slope of the linear plot of $f/(1-f)$ against the DTAB concentration gave K_{s}. Table 1 summarizes the species concentrations and DTAB concentrations tested for the determination of the different binding constants. The fitted wavelength was that resulting in maximum absorbance in the presence of the surfactant at complete incorporation of the species into the micelles. The binding constants obtained are listed in Table 2.

2.4. Procedure for the determination of the stability constants of the ternary complexes in the micellar medium

In order to determine the stability constants of the ternary complexes formed between V(V), PGR and DTAB and between Ti(IV), PGR and DTAB a series of solutions (10 ml total volume) containing a fixed concentration of DTAB above its c.m.c. (5.84×10^{-3} M) and PGR (7.0×10^{-5} M), in addition to various concentrations of metal [Ti(IV) or V(V)], at pH 3.5 (adjusted with 0.03 M phthalate–phthalic acid buffer) was prepared. An aliquot of each solution was transferred into a 1-cm quartz cell thermostated at 25°C and the absorbance measured at a fitted wavelength for each ternary complex ($\lambda = 620$ and 640 nm for the V(V) and Ti(IV) ternary complexes, respectively).

A plot of the absorbance obtained for each solution prepared against the ratio of ligand to metal concentration gave a curve which straight-line portions were extrapolated to where they intercepted one another. The extrapolated values (A_{extp}) near the "equivalence point" on the mole-ratio plot corresponded to the overall absorbance of the complex if it was formed completely. The difference between the extrapolated value (A_{extp}) and the actual absorbance value can be used to calculate the stability constant.

We shall discuss the formation of the ternary complexes in the micellar medium on the basis of the following equation:

$$\text{M}_{\text{M}} + n\text{PGR}_{\text{M}} + m\text{DTAB}_{\text{M}} \rightleftharpoons (\text{M–PGR}_n\text{–DTAB}_m)_{\text{M}}$$

where M denotes to the metal ion and subscript M the micellar pseudophase. The complex formation constant is given by

$$K_{\text{f}} = \frac{(\text{M} - \text{PGR}_n - \text{DTAB}_m)_{\text{M}}}{(\text{M})_{\text{M}}(\text{PGR})_{\text{M}}^{n}(\text{DTAB})_{\text{M}}^{m}} \quad (3)$$

where brackets denote local concentrations in the micellar pseudo-phase.

Provided the DTAB concentration is high enough to allow complete incorporation of the metals into the micellar pseudo-phase and hence the ternary complex to be exclusively formed in the reaction medium, the overall concentrations of metal ion, PGR and DTAB can be obtained from

$$[\text{M}]_{\text{T}} = (\text{M})_{\text{M}}\phi + (\text{M} - \text{PGR}_n - \text{DTAB}_m)_{\text{M}}\phi \quad (4)$$

$$[\text{PGR}]_{\text{T}} = (\text{PGR})_{\text{M}}\phi + n(\text{M} - \text{PGR}_n - \text{DTAB}_m)_{\text{M}}\phi \quad (5)$$

$$[\text{DTAB}]_{\text{T}} = (\text{DTAB})_{\text{M}}\phi + m(\text{M} - \text{PGR}_n - \text{DTAB}_m)_{\text{M}}\phi \quad (6)$$

where ϕ is the volume fraction of the micellar pseudophase in the bulk solution, which is given by

$$\phi = ([\text{DTAB}] - \text{c.m.c.})V$$

V being the volume contributed to the micellar pseudophase per mole of micellized surfactant. The V value for DTAB is reported 0.286 mol^{-1} l [10].

The absorbance for each solution is given by

$$A = \epsilon l(\text{M} - \text{PGR}_n - \text{DTAB}_m)_{\text{M}}\phi \qquad (7)$$

where ϵ is the molar absorptivity of the ternary complex and l the cell length,

$$A = A_{\max}$$

when

$$(\text{M} - \text{PGR}_n - \text{DTAB}_m)_{\text{M}} = \frac{[\text{M}]_{\text{T}}}{\phi}$$

Therefore, the actual complex concentration is

$$(\text{M} - \text{PGR}_n - \text{DTAB}_m)_{\text{M}} = \frac{[\text{M}]_{\text{T}}}{\phi}\frac{A}{A_{\max}} \qquad (8)$$

Eqs. 3–8 allow the following expression to be derived for calculation of the stability constant of a ternary complex in the micellar medium.

$$K_{\text{f}} = \left[\phi^{n+m}\left(\frac{A}{A_{\max}}\right)\right] \times \left[\left(1 - \frac{A}{A_{\max}}\right)\left([\text{PGR}]_{\text{T}} - n[\text{M}]_{\text{T}}\frac{A}{A_{\max}}\right)^{n} \times \left([\text{DTAB}]_{\text{T}} - m[\text{M}]_{\text{T}}\frac{A}{A_{\max}}\right)^{m}\right]^{-1} \qquad (9)$$

If no volume correction is made, the apparent stability constant ($K_{\text{f}_{\text{app}}}$) for the ternary complex in the micellar medium is given by

$$K_{f_{\text{app}}} = \frac{K_{\text{f}}}{\phi^{n+m}} \qquad (10)$$

The K_{f} and $K_{\text{f}_{\text{app}}}$ values obtained for the ternary complexes formed in the micellar medium are shown in Table 2. The quoted values are the means of three values obtained from points (A, $[\text{M}]_{\text{T}}$) on the mole-ratio plots.

2.5. Kinetics

Kinetic data from both the Cr(VI)–PGR and the Ti(IV)–PGR reactions were obtained by using a stopped-flow module [6] and spectrophotometric detection. The complex-formation reaction between V(V) and PGR, which takes only a few milliseconds, could not be monitored with the stopped-flow module nor with a Sim Aminco JD-490 spectrofluorimeter. Therefore, no kinetic parameters for this reaction are reported.

In order to calculate the observed first-order rate constants, k_{obs}, for the Cr(VI)–PGR and Ti(IV)–PGR systems two solutions (A and B) were used to fill the two 10-ml reservoir syringes of the stopped-flow module. Solution A contained 6 ml of 0.1 M phthalic acid–potassium phthalate buffer (pH = 3.5), 1 ml of 2.1×10^{-3} M of PGR and various concentrations of DTAB [between 9.6×10^{-3} and 3.8×10^{-2} M for the PGR–Cr(VI) system and from 2.92×10^{-3} to 1.95×10^{-2} M for the PGR–Ti(IV) system] and bidistilled water to a final volume of 10 ml. Solution B contained 0.5 ml of 1.92×10^{-2} M Cr(VI) or 0.4 ml of 2.09×10^{-2} M Ti(IV), plus NaOH to adjust pH to 2.2 and bidistilled water to a final volume of 10 ml. After the two 2-ml drive syringes were filled with the corresponding solutions from the reservoir syringes, 0.15 ml of each was mixed in the mixing chamber in each run. The redox reaction between PGR and Cr(VI) was monitored at 380 nm (the $\lambda_{\max}$ for oxidized PGR) and the complex formation reaction between PGR and Ti(IV) at 640 nm (the $\lambda_{\max}$ for PGR–Ti(IV) complex), by recording the variation of the absorbance as a function of time at 25 ± 0.1°C. Absorbance data were collected and processed by the microcomputer using a rate-constant calculation program to obtain observed rate constants (k_{obs}). These constants were calculated from linear plots of $\ln(A_\infty - A_t)$ vs. time. The quoted k_{obs} values are the means of five measurements, so k_{obs} was estimated to better than $\pm 6\%$.

The model used to analyse kinetic data was essentially that developed by Berezin et al. [3], where the chemical reaction is assumed to take place in two pseudo-phases, one associated with the surfactant aggregates and the other with the

bulk solvent. The reaction scheme for a reversible bimolecular association reaction is

$$\begin{array}{ccc} A_m + B_m & \underset{k_{M,2}}{\overset{k_{M,1}}{\rightleftharpoons}} & C_M \\ \updownarrow K_A \quad \updownarrow K_B & & \updownarrow K_C \\ A_{aq} + B_{aq} & \underset{k_{aq,2}}{\overset{k_{aq,1}}{\rightleftharpoons}} & C_{aq} \end{array} \qquad (11)$$

where subscripts M and aq denote the micellar and aqueous pseudo-phase, respectively.

Since the investigated reactions completed within 10 s, it is reasonable to assume that partitioning of the reactants between the two pseudo-phases was quite rapid compared to the rate of chemical reaction. Hence, partitioning can be described by the equilibrium parameters K_A, K_B and K_C. The equilibrium constant K_s for species S partitioning between the two pseudo-phases is given by:

$$K_S = \frac{[S]_M}{[S]_{aq} C} \qquad (12)$$

where C is the concentration of surfactant that contributes to the micellar pseudo-phase volume, which may be taken to be ([surfactant]-c.m.c.); and $[S]_M$ and $[S]_{aq}$ are the concentrations of S in the micellar and aqueous pseudo-phase, respectively (expressed as mol l^{-1} of total solution).

From Eq. 11, the observed second-order rate constant for the formation of product C, $k_{obs,1}$, is given by

$$k_{obs,1} = \frac{k_{M,1} + k_{aq,1} K_A^{-1} K_B^{-1} C^{-1} V}{CV\left[1 + (K_A C)^{-1}\right]\left[1 + (K_B C)^{-1}\right]} \qquad (13)$$

where V is the volume contributed to the micellar pseudo-phase per mole of micellized surfactant.

When both reactants and the product partition strongly to the micellar pseudo-phase, the reaction can only occur in it; hence, under pseudo-first-order conditions (i.e. $[A]_0 \gg [B]_0$), the observed first-order rate constant is given by

$$k_{obs} = \frac{k_{M,1}[A]_0}{CV\left[1 + (K_A C)^{-1}\right]\left[1 + (K_B C)^{-1}\right]} + k_{M,2} \qquad (14)$$

For $C >$ c.m.c. and K_A and $K_B \gg C^{-1}$, Eq. 14 simplifies to

$$k_{obs} = \frac{k_{M,1}[A]_0}{CV} + k_{M,2} \qquad (15)$$

Similar equations were previously used to interpret the kinetics of reactions in micellar solutions [4]. A plot of k_{obs} vs. $[A_0]/C$ gives a straight line, the slope of which (k_s) is

$$k_s = k_{M,1}/V \qquad (16)$$

Once V is known, the "true" second-order rate constant of the reaction taking place in the micellar pseudophase ($k_{M,1}$) can readily be estimated.

The second-order rate constants for the two reactions considered in the aqueous medium ($k_{aq,1}$) were determined from the kinetic curves obtained in the absence of DTAB. The stopped-flow technique was used for this purpose. The two solutions (A and B) prepared to fill the two 10-ml reservoir syringes of the stopped-flow module contained the following:

- Solution A: 6 ml of 0.1 M phthalic acid–potassium phthalate buffer (pH = 3.5), 1 ml of 2.1×10^{-3} M PGR and bidistilled water to a final volume of 10 ml.
- Solution B: 1.1 ml of 1.92×10^{-3} M Cr(VI) or 1.0 ml of 2.09×10^{-3} M Ti(IV) and NaOH to adjust the pH to 2.2, plus bidistilled water to a final volume of 10 ml.

The $k_{M,1}$ and $k_{aq,1}$ values obtained for the two reaction considered are summarized in Table 2.

3. Results and discussion

Several experiments were carried out in order to elucidate the mechanism via which the surfactant induced the above-described changes in the features of the PGR–Cr(VI), PGR–V(V) and PGR–Ti(IV) systems. The presence of micelles in the reaction medium was essential for DTAB to exert its effect on the PGR–Cr(VI) and PGR–V(V) systems. This was concluded from the critical micelle concentration (c.m.c.) obtained under the experimental conditions used (viz. 9.2×10^{-5} M, as calculated from surface tension measurements). This concentration was substantially dif-

ferent from the c.m.c. obtained in distilled water (1.5×10^{-2} M) and lower than the analytical concentration used (5.84×10^{-4} M) [2]; this is consistent with the results, according to which the effect of DTAB on these reactions was only exerted at concentrations above 1.0×10^{-4} M. The effect of DTAB on the PGR–Ti(IV) system was observed at DTAB concentrations above 1.0×10^{-5} M, where only monomers or submicellar aggregates should be present in the reaction medium. However, the maximum hyperchromic and bathochromic shifts were only observed in the presence of micelles. The results obtained for each of the systems studied are commented on below.

3.1. Pyrogallol Red–chromium(VI) system

The only evident effect of DTAB on this redox reaction was to accelerate the formation of the oxidation product. Since micellar catalysis occurs when either all the reactants concentrate on the micellar surface (where the reaction takes place) or some of them approaches the micelles (the reaction takes place at the micelle–bulk solution interface), we investigated individual interactions of each reactant with the DTAB micelles in order to elucidate which route applied in this case. Evidence for PGR–DTAB and Cr(VI)–DTAB interaction was provided by the changes that DTAB induced in the absorption spectra of PGR (Fig. 1A) and Cr(VI) (Fig. 1B). The extent of the bathochromic shift caused by DTAB micelles on the absorption spectrum of PGR increased with increasing DTAB concentration. No bathochromic shift on the Cr(VI) spectrum was observed, but only increased absorptivity in the spectral region between 350 and 410 nm. Partition or

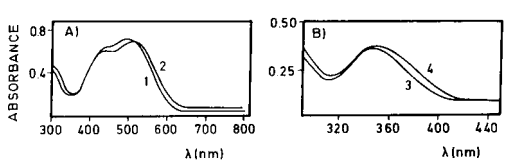

Fig. 1. Absorption spectra for (A) Pyrogallol Red and (B) chromium(VI) in the (1,3) absence and presence of (2) 7.78×10^{-3} M DTAB and (4) 1.95×10^{-2} M DTAB. [PGR] = 5.0×10^{-5} M; [Cr(VI)] = 1.92×10^{-4} M.

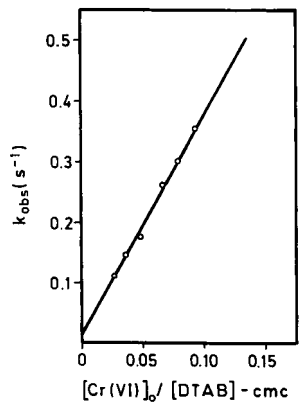

Fig. 2. Plot of k_{obs} vs. $[Cr(VI)]_0$/([DTAB]-c.m.c.) for the redox reaction between PGR and Cr(VI) at 25.0°C.

"binding" constants of these reactants to the cationic surfactant system were determined spectrophotometrically from these spectral changes by using the procedure described under Experimental. A plot of $f/(1-f)$ against the DTAB concentration for PGR was linear between 5.0×10^{-3} M and 9.0×10^{-3} M surfactant, with a slope $K_{PGR} = 1050 \pm 5$ M^{-1}. The Cr(VI) "binding" constant, $K_{Cr(VI)}$, obtained similarly, was found to be 930 ± 60 M^{-1}.

Taking into account that the DTAB concentration in the reaction medium used for the determination of the analytes (5.84×10^{-3} M) was considerably higher than those of PGR (5.0×10^{-5} M) and Cr(VI) (between 0.38×10^{-5} M and 1.54×10^{-5} M), and considering the "binding" constants of the two reactants to the micelle, the oxidation of PGR by Cr(VI) probably takes place preferentially through the reactants concentrating at the micellar surface, so the accelerating effect of the DTAB micellar medium can be ascribed to micellar catalysis, and the rate of reaction in water, $k_{aq,1}$, to be negligible. In order to confirm this hypothesis, the "true" second-order rate constant, $k_{M,1}$, for the reaction in the micellar medium was calculated by using the model of Berezin et al. [3] as described under Experimental for the quantitative treatment of the kinetic data. Since all the experimental conditions for application of Eq. 15 were fulfilled, a typical plot of the observed first-order rate constant (k_{obs})

against $[Cr(VI)]_0/C$ gave a straight line (see Fig. 2). The slope of the plot provided a value of $3.8 \pm 0.4\ s^{-1}$ for k_s (see Eq. 16). The true second-order rate constant in the micellar phase, $k_{M,1}$, was calculated by assuming the molar volume, V, of the surfactant to be $0.286\ mol^{-1}\ l$ [11]; $k_{M,1}$ was thus found to be $1.1 \pm 0.1\ M^{-1}\ s^{-1}$. Since the second-order rate constant obtained for the redox reaction between PGR and Cr(VI) in the aqueous medium was $k_{aq,1} = (2.0 \pm 0.2) \times 10^{-2}\ M^{-1}\ s^{-1}$, the "true" second-order rate constant in the DTAB micellar phase was greater by a factor of ca. 55 relative to water alone. Such a large value for a medium effect from DTAB was also confirmed by calculating the $k_{M,1}/k_{aq,1}$ ratio from the following equation

$$\left(\frac{k_{obs,1}}{k_{aq,1}}\right)_{max} = \frac{k_{M,1}}{k_{aq,1}} \frac{K_{Cr(VI)}K_{PGR}}{V\left(\sqrt{K_{Cr(VI)}} + \sqrt{K_{PGR}}\right)^2} \quad (17)$$

where $(k_{obs,1}/k_{aq,1})_{max}$ is the maximum accelerating effect on the reaction in the micellar medium, $k_{obs,1}$ being the second-order rate constant at the optimum surfactant concentration [3]. This maximum value was found to be 4.2×10^4. Also, the $k_{M,1}/k_{aq,1}$ ratio obtained from Eq. 17 was ca. 48 and thus similar, within experimental errors, to the result provided by the kinetic treatment described under Kinetics (see Experimental). This value suggests a change in the reactant reactivities on transfer from water to the micellar phase.

While uncommon, changes in the reactivity of reactants involved in bimolecular reactions induced by micelles have occasionally been reported. Some such changes have been ascribed to an altered dielectric constant for the electric double-layer around the micelles relative to that in the bulk aqueous phase in reactions sensitive to solvent polarity [10], or to a modified hydratation state of inorganic ions on incorporation into micelles [12]. While determining the real origin of the reactivity change induced by DTAB on the PGR–Cr(VI) system is beyond the scope of this work it makes quite an interesting challenge in order to find other similar systems and study their analytical potential.

3.2. Pyrogallol Red–vanadium(V) system

Vanadium(V) is known to oxidize PGR over the pH range 1–7 [13]. Complexes of vanadium ion and PGR have only been reported for V(IV) [14], which forms a 1:2 complex at pH 4.4 absorbing maximally at 540 nm.

The absorption spectra for the PGR–V(V) system in an aqueous medium recorded over the pH range 1–7 included an absorption signal above 600 nm that cannot be attributed to the oxidized form of PGR since this is involved in the disappearance of the 490 nm band for PGR and the very slow appearance of a new band at 390 nm [15]. On the other hand, the band at 600 nm was not observed for the PGR–Cr(VI) system, which gives the same oxidation product. This absorption band, which is hardly perceptible at V(V) concentrations below 1.0×10^{-5} M in an aqueous medium, was well defined at V(V) concentrations above 1.0×10^{-4} M and resulted in maximum absorption at 620 nm when dissolved PGR–V(V) was recorded against solutions of PGR alone (Fig. 3A.1). Bearing in mind that a PGR–V(V) complex might have been formed simultaneously (to a lesser extent though) with the oxidation reaction between PGR and V(V) under the working experimental conditions [2], the complex stoichiometry and stability constant were determined at 620 nm. Use of a mole-ratio method provided a well-defined intercept at a V(V) to PGR ratio of 1:1 and the working pH (3.5). Under these conditions, the stability constant for the V(V)–PGR complex was $(1.5 \pm 0.5) \times 10^6\ M^{-1}$.

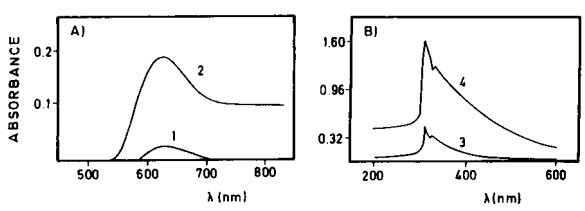

Fig. 3. Absorption spectra for (A) the Pyrogallol Red–V(V) complex, ($[V(V)] = 1.2 \times 10^{-5}$ M and $[PGR] = 7.0 \times 10^{-5}$ M) and (B) V(V) ($[V(V)] = 3.9 \times 10^{-4}$ M) in the (1, 3) absence and presence (2) of 1.5×10^{-3} M DTAB and (4) 1.0×10^{-3} M DTAB.

Addition of DTAB to the reaction medium suppressed the oxidation reaction between PGR and V(V) virtually complete above pH ≃ 3 and significantly increased the absorption at 620 nm, which is indicative of formation of the PGR–V(V) complex. Therefore, DTAB micelles essentially alter product distribution relative to an aqueous medium. Since the absorption spectrum for the PGR–V(V) complex in the DTAB micellar medium showed a maximum signal at ca. 620 nm, no bathochromic shift with respect to the aqueous medium was observed. It was unclear whether the hyperchromic effect observed in the micellar medium was due to sensitization or simply the result of the altered product distribution in the presence of DTAB. The possibility of PGR complexing V(IV) following the oxidation reaction was ruled out (at least for the micellar medium), since no decrease in the absorbance at 490 nm, which diminished for oxidized PGR, was observed. The hyperchromic effect observed in the micellar medium was used to calculate the constant of "binding" of the PGR–V(V) complex to the DTAB cationic micelles using the procedure described under Experimental and the conditions shown in Table 1. A value of 6300 ± 400 M^{-1} was obtained for $K_{PGR-V(V)}$, which suggest that the complex is retained at the micellar surface as it is formed. In order to determine whether the complex formation reaction between V(V) and PGR occurred preferentially on the micellar surface, the extent of incorporation of V(V) into the DTAB micellar pseudo-phase was determined under the experimental conditions given in Table 1. This ion is likely to be present almost entirely as $H_3V_2O_7^-$ in the reaction medium, although it may also exist in a condensed form such as $HV_6O_{17}^{3-}$ [16], so it may concentrate at the surface of cationic micelles. The extent binding of V(V) to DTAB was determined through the hyperchromic shift that DTAB causes on the absorption spectrum of the metal (Fig. 3B) and was found to be 6150 ± 350 M^{-1}. Since PGR is also strongly bound to micelles ($K_{PGR} = 1050 \pm 5$ M^{-1}), the complex-formation reaction probably takes place at the micellar surface.

Because the PGR–V(V) complex-formation reaction was quite rapid in both the aqueous and the micellar medium, no kinetic data could be obtained by using the stopped-flow technique, the only technique for this purpose available in our laboratory. Therefore, it could not be ascertained whether micellar catalysis actually occurred.

Several experiments were conducted in order to determine the nature of the PGR–V(V) complex in the micellar medium. Because micelles were indispensable for the effect of DTAB on this reaction to be observed, we investigated whether the binary complex was only adsorbed on the micelles or formed a true ternary complex with the surfactant. Only if this latter assumption was correct would a given molecular ratio of chelate to surfactant be meaningful. The composition of the ternary complex was investigated by using the mole-ratio method and an initial large excess of DTAB. A molar ratio of V(V) to PGR of 1:1 was provided by varying the concentration of metal. Similar experiments were carried out by using increasing DTAB concentrations and a constant, excess concentration of PGR to ascertain the possibility of a definite stoichiometry of PGR–V(V) to DTAB. The concentration of V(V) was above 9.2×10^{-5} M (c.m.c. of DTAB). The two straight lines intersected at a definite value of [DTAB]/[V(V)] of ca. 2. Thus, the ternary complex has a PGR–V(V)–DTAB molecular stoichiometry of 1:1:2. The stability constant for this ternary complex, at the DTAB concentration where the complex was maximally incorporated into the micelles, was determined by using Eq. 10. A value of K_f of $(2.4 \pm 0.2) \times 10^2$ M^{-3} was obtained by taking V to be 0.286 mol^{-1} l for DTAB. From Eq. 11, the apparent stability constant for the ternary complex was calculated to be $(7.3 \pm 0.5) \times 10^{10}$ M^{-3}, which reveals the significance of the concentration effect. Therefore, the surfactant appears to play a twofold role in the ion-association process: first, it secures a minimum concentration for micelles to be formed, below which little or no ion-association occurs; second, its cationic form, DTA^+, reacts with the complex to yield the ternary ion-association complex.

Previous studies [17] showed the chelating groups of some dissolved compounds to lie normal to the surface of charged micellar systems,

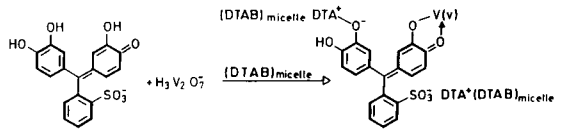

Fig. 4. Incorporation of the PGR–V(V)–DTA_2 ternary complex into DTAB micelles.

thereby facilitating coordination with the incoming metal ion. This occurs preferentially when the compound concerned possesses other ionizable groups facing the functional groups. With PGR, metal coordination probably occurs through the *ortho*-hydroxyquinone group [18], so, it is reasonable to believe that the complex associates to micelles through electrostatic interactions between the sulphonate and hydroxyl groups symmetric to the carbonyl group and the positively charged head group of the surfactant [5]. Therefore, incorporation of the PGR–V(V) complex into DTAB micelles may occur as shown in Fig. 4.

3.3. Pyrogallol Red–titanium(IV) system

PGR–Ti(IV) complexes of 1:1 and 2:1 stoichiometry have been reported to occur in aqueous media at pH 2–5 [19]. Under our experimental conditions, a substantial bathochromic shift and a hyperchromic effect on the absorption spectrum for the PGR–Ti(IV) complex was observed in the presence of DTAB relative to water (Fig. 5A). This spectral change allowed calculation of the constant of "binding" of the PGR–Ti(IV) complex to the DTAB micelles under the experimental conditions given in Table 1. A binding constant $K_{PGR-Ti(IV)}$ of $3400 \pm 200\ M^{-1}$ for the PGR–Ti(IV) complex was obtained. Accordingly, the complex binds strongly to the positively charged DTAB micellar surface and is retained by this pseudo-phase as it is formed.

Since PGR actually binds to DTAB micelles ($K_{PGR} = 1050 \pm 5\ M^{-1}$), we also studied whether Ti(IV) incorporated into the micellar surface in order to determine whether the PGR–Ti(IV) complex formation reaction takes place at the micellar pseudo-phase with both reactants in dissolved form or between dissolved (PGR) and insolubilized [Ti(IV)]. This ion is known [20] to give oxochloro complexes in aqueous hydrochloric acid the exact nature of which depends on the acid concentration. Some of the likely complexes include $TiOCl_4^{2-}$, $TiO_2Cl_4^{4-}$ and $TiOCl_5^{3-}$. Since Ti(IV) solutions were made in 1:1 HCl (see Reagents, under Experimental), this ion was likely to be present in the oxochloro complex form and, although the exact nature of the complex(es) could not be elucidated, all oxochloro complexes could be attracted by coulombic interaction to the positively charged DTAB micellar surface. Binding of titanium(IV) to DTAB was investigated spectrophotometrically (see Table 1 for the experimental conditions used) through the hyperchromic shift that this surfactant causes on the absorption spectrum of the metal (Fig. 5B). A value of $5800 \pm 30\ M^{-1}$ was found for the binding constant ($K_{Ti(IV)}$). Therefore, both reactants

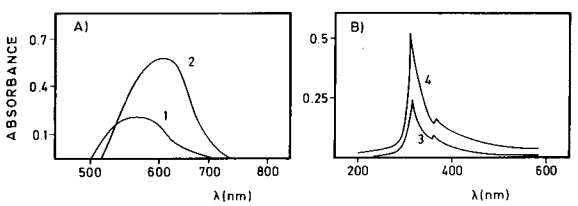

Fig. 5. Absorption spectra for (A) the Pyrogallol Red–Ti(IV) complex ($[Ti(IV)] = 2.1 \times 10^{-5}$ M and $[PGR] = 7.0 \times 10^{-5}$ M) and (B) Ti(IV) ($[Ti(IV)] = 8.4 \times 10^{-5}$ M), in the (1, 3) absence and presence (2) of 2.0×10^{-3} M DTAB and (4) 4.0×10^{-3} M DTAB.

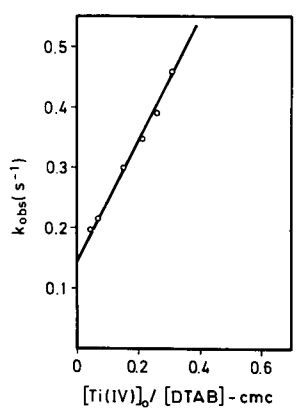

Fig. 6. Plot of k_{obs} vs. $[Ti(IV)]_0$/[DTAB]-c.m.c.) for the complex formation reaction between PGR and Ti(IV) at 25.0°C.

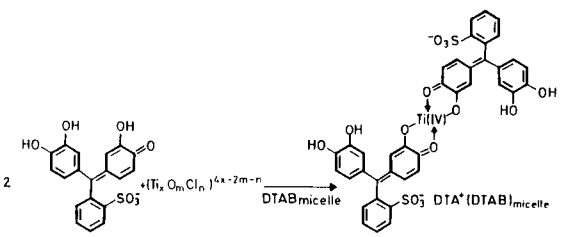

Fig. 7. Incorporation of the PGR_2–Ti(IV)–DTA ternary complex into DTAB micelles.

[Ti(IV) and PGR] and the product [PGR–Ti(IV) complex] are exclusively located in the micellar surface region, so Eq. 7 is applicable. Fig. 6 shows a plot of k_{obs} vs. $[Ti(IV)]_0/C$. The k_s, (0.95 ± 0.06) s^{-1}, allows the true second-order rate constant in the micellar pseudophase for the complex-formation reaction between PGR and Ti(IV) to be calculated [$k_{M,I} = 0.27 \pm 0.02$ s^{-1} M^{-1}]. Taking into account that the molar volume, V, of the surfactant is 0.286 mol^{-1} l [11], this rate constant is ca. 1.5 times less than that in bulk aqueous solution (0.44 ± 0.02) s^{-1} M^{-1}, so the increase in the rate of formation of the PGR–Ti(IV) complex observed in the presence of DTAB can be attributed to the increase in reactant concentrations in the micellar phase.

The nature of the complex obtained in both the aqueous and the micellar medium was investigated. The molar ratio of Ti(IV) to PGR in the binary complex and its stability constant in the aqueous medium, determined by the molar ratio method, were 1:2 and $(2.7 \pm 0.8) \times 10^{11}$ M^{-2}, respectively. The possibility of a ternary complex being formed in the presence of DTAB was investigated by using the molar ratio method and an initial large excess of surfactant. A molar ratio of Ti(IV) to PGR of 1:2 was obtained by varying the concentration of metal. Similar experiments were carried out by using increasing DTAB concentrations, and constant, excess concentration of PGR. A molar ratio of DTAB to Ti(IV) of 1:1 was obtained. Thus, the ternary complex has a PGR–Ti(IV)–DTAB molecular stoichiometry of 1:2:1. The stability constant for this ternary complex at a DTAB concentration where incorporation of the complex into the micelles was maximal, was found to be $(2.1 \pm 0.5) \times 10^5$ M^{-3}. The apparent stability constant, as calculated from Eq. 11, was $(6.5 \pm 1.6) \times 10^{13}$ M^{-3}; this value again stresses the significant of the reactant concentration on the micellar surface.

If one assumes that Ti(IV) coordination occurs through the *ortho*-hydroxyquinone group of PGR, and the sulphonate group facing the chelating site can interact favourably with a surfactant molecule, the most likely reaction sequence is that shown in Fig. 7.

Acknowledgement

The authors gratefully acknowledge financial support from the Spanish CICyT (Project no. PB91-0840).

References

[1] D. Pérez-Bendito and S. Rubio, Trends Anal. Chem., 12 (1993) 9.
[2] D. Sicilia, S. Rubio and D. Pérez-Bendito, Anal. Chim. Acta, 284 (1993) 149.
[3] I.V. Berezin, K. Martinek and A.K. Yatsimirskii, Russ. Chem. Rev., 42 (1973) 787.
[4] P.D.I. Fletcher and B.H. Robinson, J. Chem. Soc. Faraday Trans. I, 80 (1984) 2417.
[5] W.L. Hinze, in K.L. Mittal (Ed.), Solution Chemistry of Surfactants, Vol 1, Plenum Press, New York, 1979, pp. 79–127.
[6] A. Loriguillo, M. Silva and D. Pérez Bendito, Anal. Chim. Acta, 199 (1987) 29.
[7] P. Mukerjee and K.J. Hysels, Critical Micelle Concentrations of Aqueous Surfactant Systems, NSRDS-NBS 36, US Department of Commerce, Washington, DC, 1971.
[8] L. Sepúlveda, J. Colloid Interface Sci., 46 (1974) 372.
[9] C.A. Bunton, F. Ramírez and L. Sepúlveda, J. Org. Chem., 43 (1978) 1166.
[10] Y. Miyake, M. Shigeto and M. Teramoto, J. Chem. Soc. Faraday Trans. I, 82 (1986) 1515.
[11] D.E. Guveli, J.B. Kayes and S.S. Davis, J. Colloid Interface Sci., 82 (1981) 307.
[12] J.R. Cho and H. Morawetz, J. Am. Chem. Soc., 94 (1972) 375.
[13] J. Medina-Escriche, A. Sevillano-Cabeza and M. de la Guardia-Cirugeda, Analyst, 108 (1983) 1402.
[14] J. Medina-Escriche, A. Sevillano-Cabeza and M. Llobat, Quím. Anal., 5 (1986) 229.
[15] J. Medina-Escriche, A. Sevillano-Cabeza and M. de la Guardia-Cirugeda, Analyst, 110 (1985) 719.

[16] G. Charlot, Les Reactions Chimiques en Solution, Masson, Paris, 1969, pp. 334–335.
[17] H. Kohara, Bunseki Kagaku, 23 (1974) 39.
[18] N.S. Poluektov, L.A. Ovchar, S.F. Ogaichenko and R.S. Lauer, Zavod. Lab., 37 (1971) 895; Chem. Abstr., 75 (1971) 147423x.
[19] D. Abromaityte and S. Ramonaite, Liet TSR Mokyly Mokslo Darbai, Chemija ir Chem. Technol., Nauch. Tr. Vyssh. Ucheb. Zavedenii Lit SSR. Khimiya i Khim, Tekhnol., (1975) 5.
[20] F.A. Cotton and G. Wilkinson, Advanced Inorganic Chemistry, Willey, New York, 3rd ed., 1972, pp. 810–811.

ELSEVIER

Analytica Chimica Acta 297 (1994) 465–468

ANALYTICA CHIMICA ACTA

Book Reviews

Larry R. Taylor, Richard B. Papp and Bruce D. Pollard, *Instrumental Methods for Determining Elements*, VCH, New York, 1994 (ISBN 1-56081-038-6). ix + 322 pp. Price DM128.00.

For reasons that are not completely clear, analytical texts have historically fallen into two distinct types: those which describe the theory and construction of instrumentation and those which are sometimes described as recipe books. There have been few books which have largely concentrated on the advantages and disadvantages of different techniques and why a particular technique might be chosen.

This book tackles the missing area. It covers the major instrumentation: atomic absorption and emission, electrochemical techniques, chromatography, X-ray fluorescence, combustion-based procedures and others such as electrophoresis, flow injection, MS and NAA. General overviews of applications are also provided. The emphasis of the book is less on describing the theory of the techniques than on features involved in the selection of alternative configurations. In the chapter covering atomic absorption spectrometry, for example, sections are to be found covering flame, furnace, glow discharge and vapour generation methods under headings such as elemental coverage, limits of detection, dynamic range, sample type, multi-element capability, selectivity and interferences, sample throughput and preparation, precision, capital and operating costs, etc. The information contained in the chapter is valuable but the structure results in six "Flame AAS" headings just within Section 3.4. It is difficult to avoid the conclusion that some clarity has been sacrificed in the adoption of a very regimented structure.

Whilst the book is in general clearly presented and contains relatively few typographical errors, there are places where spaces between sections have been omitted. This results in Section 3.3.4, a minor subsection on Glow Discharge AA, containing the concluding remarks Section 3.3. The diagrams are generally clearly presented, if not at times rather unconventional and obviously the product of an un-tamed computer drawing package which believes that chromatography peaks are triangular.

Overall this book is well worth reading. Its emphasis is a refreshing change from the conventional instrument texts and it will provide the reader with a greater insight into the choice of suitable analytical instrumentation.

Alan G. Howard

Gabriele Wagner and George G. Guilbault (Eds.), *Food Biosensor Analysis*, Marcel Dekker, New York, 1993 (ISBN 0-8247-9150-9). 272 pp. Price US$125.00.

Medical applications were a predominant feature of early biosensor research. However, the need for simplified measurement of biochemical parameters is by no means a prerogative in medicine, and applies to a whole range of areas of applied biology. This collection of reviews has appropriately targetted an area of both growing general and legislative concern; food analysis. The biosensor systems covered (electrochemical, optical, thermometric, piezoelectric) hold no major surprises, but the particular application emphasis, coupled with several contributions by food scientists, provides for sufficient new material for even the "well-heeled" in the field. The technological slant to most of the chapters is helpful and the general reader is not overburdened with theory. The first chapter deals succinctly with basic principles, and a second chapter, by a food scientist, helps

SSDI 0003-2670(94)00410-2

define context and assay needs. Enzyme-based electrodes have been extensively reported for food analysis, and much of the growing literature is presented in chapter three with, for once, a fairly balanced representation of "real sample" problems. Fluorometric and luminometric sensors are afforded individual chapters, perhaps more in expectation than that major inroads have yet been made into food analysis; the authors do, however, give readable basic descriptions. Three chapters on piezoelectric immunosensors, whole cell biosensors and thermistors illustrate with some well chosen examples the diversity of biotransduction principles available; though experience in these lies mainly in the hands of dedicated enthusiasts, these may satisfy important niche requirements in future. A recurrent theme in these reviews is the need for sample preparation and presentation, and a chapter on biosensors combined with HPLC highlights one route to this. The final chapter, by a food scientist, presents the end-user perspective that goes some way to identify relevance. Overall, this is a readable, self-contained text, that would be a good starting point for anyone new to the field.

Pankaj Vadgama

J.W. Kiceniuk and S. Ray (Eds.), *Analysis of Contaminants in Edible Aquatic Resources: General Considerations, Metals, Organometallics, Tainting, and Organics*, VCH, New York, 1994 (ISBN 1-56081-528-0). xiii + 551 pp. Price DM260.00/£105.00.

Analysis of foodstuffs for contaminants is now an extremely important and widespread activity, The present text is divided into two "Books", the first dealing with certified reference materials, quality aspects, chemometrics, and laboratory automation and management systems, as well as cadmium and inorganic and organic forms of Pb, As, Hg, Se and Sn, sensory evaluation, and isolation of odoriferous components. Book II covers organic contaminants CPCBs, PCTs and PCNs, dioxins and furans, chlorinated pesticides, chlorinated ethers, PAHs, phenols, nitrosamines and antimicrobials), diarrhetic shellfish poisoning, detection by immunoassay and sample pretreatment (extraction, clean up, etc.) of organochlorine compounds. Each of the 24 chapters is written by well-known authors, and includes a considerable amount of detail. This is an essential text for food and environmental scientists, and will be of great interest to analytical scientists generally.

Alan Townshend

H. Jork, W. Funk, W. Fischer and H. Wimmer, *Thin-layer Chromatography: Reagents and Detection Methods*, Vol. 1b, *Physical and Chemical Detection Methods: Activation Reactions, Reagent Sequences, Reagents II*, VCH, Weinheim, 1994 (ISBN 3-527-28205-X). xvi + 496 pp. Price DM198.00/£81.00.

This is the second volume of what is stated to be a multi-part multi-volume series and appears well separated in time (4 years) from Vol. 1a. The text is divided into two main parts, the first "specific detection methods" is subdivided into activation reactions (photo-, thermo- and electrochemical), reagents for the recognition of functional groups and reagent sequences. Part 2, the major portion of the text, gives detailed reports/reviews of 70 reagents alphabetically (acridine orange through to vanillin-sulfuric acid). Each fully referenced report contains a summary of applications, details of preparation of the reagent, the reaction, discussion of method and procedures tested. The text concludes with manufacturers addresses, lists of named reactions and reagent acronyms and a collective index to Vols. 1a and 1b. This is a beautifully produced, scholarly volume and will be welcomed in view of the current interest and developments in modern high-performance thin-layer chromatography equipment and plates.

D. Thorburn Burns

J.D. Ingle Jr., and S.R. Crouch, *Spectrochemical Analysis*, Prentice Hall, New Jersey, 1988 (ISBN 0-13-826876-2). xv + 590 pp. Price £24.95.

Spectrochemical Analysis is intended as a text book for graduate and advanced undergraduate stu-

dents, but it is also an excellent reference source for analytical spectroscopists. The main strength of the book is the combination of detailed background theory and practical information on a range of atomic and molecular spectroscopy techniques, a coverage not provided by most books in this subject area.

The first two chapters provide basic definitions and give an introduction to spectrochemistry and spectrochemical measurements based on the radiation, emission, absorption and luminescence and light scattering methods. Chapters 3–5 are concerned with general instrumentation and provide a useful description of the optical and electronic components on which most spectrometric systems are based. In Chapter 3, the laws of optics are reviewed and the use of phenomena such us interference, diffraction and polarisation of radiation is described. Blackbody radiation concepts, optical sources, detectors and signal processing are described in Chapter 4. A separate chapter (No. 5) is devoted to the important topic of signal-to-noise ratio considerations, which is essential reading for all spectroscopists, especially those involved in the development of research instruments. General methodology in spectrochemical analysis is covered in Chapter 6, which provides a clear introduction to error assessment and calibration methods. *Spectrochemical Analysis* is worth buying for the first six chapters alone!

Chapters 7–11 deal with atomic spectrometry theory and techniques. Chapter 7, commendably, provides more detailed background theory on atomic states, spectral line profiles and spectral intensities than most course text books on atomic spectrometry. It is pleasing to find a book at this level that accurately describes the difference between self-absorption and self-reversal of atomic lines! Practial aspects of flame and plasma atomic emission spectrometry are described in Chapter 8 and similar information about arc and spark emission sources is provided in Chapter 9. The fundamental principles of the different emission sources are discussed, although greater emphasis could have been given to the inductively coupled plasma, particularly in relation to atom excitation and ionisation mechanisms. The lack of information on how atoms and molecules are formed/ excited/ ionised in spectrochemical sources is probably the main weakness of the book. Chapter 10 covers atomic absorption spectrometry, giving details about the main atomization systems, flame, furnace and hydride generation. As in most chapters, emphasis is placed on signal measurement topics and factors that affect the signal-to-noise ratio. Background correction procedures are described, but only a superficial coverage of atomization mechanisms and chemical interference effects is provided. Chapter 11 gives information on the different types of electronic transitions which cause atomic fluorescence. Instrumentation is discussed and the theory of fluorescence reviewed. Chapters 8 to 11 give basic information such as detection limits or different elements by the various atomic spectrometry techniques, but few details on analytical applications are provided to illustrate the usefulness of the techniques.

Chapter 12 provides a brief but thorough introduction to molecular spectroscopy techniques involving absorption or emission of radiation. Chapter 13 concerns UV–visible molecular absorption spectrometry. Conditions which cause deviation from Beer's Law are described, instrumental features are discussed and there is a good section on applications of the technique. Infrared spectrometry is covered in Chapter 14. In addition to sections on the basis of IR absorption and instrumental features, details are given on quantitative IR absorption analysis, near-IR and far-IR absorption spectrometry and IR reflectance and emission methods. Chapter 15 provides a good grounding in molecular luminescence spectrometry. Fluorescence, phosphorescence and chemiluminescence methods are described in separate sections. Lifetime and polarisation measurements are also discussed. Molecular scattering methods are covered briefly in Chapter 16. The principles of elastic and inelastic scattering of radiation are described. There are sections on resonance Raman spectroscopy, turbidimetry and nephelometry, laser scattering methods and remote sensing with lasers. The final chapter surveys developing techniques such as thermal lens spectroscopy and laser enhanced ionisation atomic spectrometry. Many readers will find the Appendices extremely useful, information is provided on statistics, the properties of optical materials, characteristics of optical filters, photomultiplier tube specifications, sample preparation, atomic and molecular transitions, and abbreviations, units and conversion factors.

Each chapter has a set of problems, useful when considering the book as a course text, although answers are not provided. Also, a list of appropriate sources of further reading is provided at the end of each chapter. Overall, this is a textbook I strongly recommend for students, teachers, researchers and practitioners of analytical spectroscopy techniques. *Spectrochemical Analysis* conveniently provides information that is normally obtained by looking at three or more separate text books. Furthermore, it is written by authors who really know their subject, is the product of a successful teaching course implemented over many years, and is good value for money.

David Littlejohn

V.R. Meyer, *Practical HPLC*, 2nd edn., Wiley, New York, 1993 (ISBN 0-471-941-328). Price £24.95.

A wide range of chromatographic techniques (from classic procedures to the most recent liquid chromatographic methods) is described in 23 chapters and 3 indexes. The explanations provide a clear guide to understanding the different kinds of chromatographic techniques, even for non-English speaking people. The instruments, packing materials, detection methods and solving separations are well written for beginners. All mathematical equations for evaluating columns and optimizing separations, are collected and explained, with examples to clarify the meaning of each equation. The details can be further studied using well-selected references. In practice, we may not use all the equations; however an understanding of these equations is very important to optimize a system. Such study methods are not given in other HPLC-related books. A few of the illustrations are less than optimal, however, this does not disqualify the value of this textbook. I recommend that beginners in the field of liquid chromatography should read this book first, then study the details of complicated phenomena taking place inside chromatographic columns.

Toshihiko Hanai

V.S. Bagotsky, *Fundamentals of Electrochemistry*, Plenum Press, New York, 1993 (ISBN 0-306-44338-4). xvii + 589 pp. Price US$115.00.

This book, from the renowned Frumkin Institute of Electrochemistry, is a translation of the 1987 Russian edition to which new chapters on photoelectrochemistry, electrokinetic processes and bioelectrochemistry have been added. The 23 chapters are grouped under the headings of Basic Concepts, Properties of Electrolytes and Interfaces, Electrochemical Kinetics and Applied Electrochemistry. Electrochemical Methods of Analysis are summarised in 11 pages in Chapter 20. The expositions, usually presented from a historical perspective, are clear, though overly concise sometimes, and translation is good. However, the diagrams of cell vessels with liquids indicated by horizontal dashes of various lengths, are off-putting and reminiscent of the papers of the pioneers of the last century! The book would be useful for undergraduate and first year postgraduate level courses were it not for the large number of good texts in electrochemistry currently available.

A.K. Covington

D. Coleman (Ed.), *Directory of Capillary Electrophoresis (TrAC Supplement No. 1)*, Elsevier, Amsterdam, 1994 (ISBN 0-444-81798-0), paperback. iii + 150 pp. Price Dfl.137.00/US$70.00.

This directory is published as part of the Library Edition of TrAC (a review of which has been published before) and is also available separately. It lists authors in the field of capillary electrophoresis, with addresses, interests, etc, a classification of authors according to techniques and country, a company index classified according to the nature of their products and services, and lists of authors grouped under techniques and areas of application.

ELSEVIER

Analytica Chimica Acta 297 (1994) 469–471

ANALYTICA CHIMICA ACTA

Author Index

ELSEVIER

Analytica Chimica Acta 297 (1994) 473

ANALYTICA CHIMICA ACTA

Corrigendum

corrected 26 Jan. 95 /AP

HOLMES: a program for target factor analysis, *Analytica Chimica Acta*, 295 (1994) 119–125, by D. González-Arjona, J. Antonio Mejías and A. Gustavo González

During the creation of the data matrix (Table 1, page 122) an error was introduced which caused a small bias in the outputs of HOLMES presented in Table 3. The modified table is shown below:

Table 3
Factor loadings for the best reproduction of data matrix using HOLMES and TARGET90

Solute	HOLMES (RMS = 0.052)		TARGET90 (RMS = 0.060)	
	π^{*} [a]	Unity	π^{*}	Unity
HNCA	−6.3(2)	10.0(2)	−6.3(1)	9.9(1)
gly1	−4.4(1)	7.5(1)	−4.38(9)	7.5(1)
gly2	−1.18(9)	10.95(9)	−1.18(9)	10.95(9)
PropK	−6.5(3)	12.3(3)	−6.4(2)	12.4(2)
Sal1	−5.8(2)	9.6(2)	−5.8(2)	9.5(2)
Sal2	−5.4(6)	19.3(6)	−5.4(4)	19.3(4)

[a] Values in parentheses are the errors associated with the last figures.

SSDI 0003-2670(94)00437-4

PUBLICATION SCHEDULE FOR 1995

	O'94	N'94	D'94	J	F	M	A	M	J	J	A	S
Anal. Chim. Acta	296/2 296/3 297/1–2	297/3 298/1 298/2	298/3 299/1 299/2	299/3 300/1–3 301/1–3	302/1 302/2–3 303/3							
Vib. Spec.		8/1		8/2		8/3		9/1		9/2		9/3

INFORMATION FOR AUTHORS

Detailed "Instructions to Authors" for *Analytica Chimica Acta* was published in Volume 289, No. 3, pp. 381–384. Free reprints of the "Instructions to Authors" of *Analytica Chimica Acta* and *Vibrational Spectroscopy* are available from the Editors or from: Elsevier Science B.V., P.O. Box 330, 1000 AH Amsterdam, The Netherlands. Telefax: (+31-20) 5862 459.

Manuscripts. The language of the journal is English. English linguistic improvement is provided as part of the normal editorial processing. Authors should submit three copies of the manuscript in clear double-spaced typing on one side of the paper only. *Vibrational Spectroscopy* also accepts papers in English only.

Rapid publication letters. *Letters* are short papers that describe innovative research. Criteria for letters are novelty, quality, significance, urgency and brevity. Submission data: max. of 2 printed pages (incl. Figs., Tables, Abstr., Refs.); short abstract (e.g., 3 lines); *no* proofs will be sent to the authors; submission on floppy disc; *no* revision will be possible.

Abstract. All papers, reviews and letters begin with an Abstract (50–250 words) which should comprise a factual account of the contents of the paper, with emphasis on new information.

Figures. Figures should be suitable for direct reproduction and as rich in contrast as possible. One original (or sharp glossy print) and two photostat (or other) copies are required. Attention should be given to line thickness, lettering (which should be kept to a minimum) and spacing on axes of graphs, to ensure suitability for reduction in size on printing. Axes of a graph should be clearly labelled, along the axes, outside the graph itself.

All figures should be numbered with Arabic numerals, and require descriptive legends which should be typed on a separate sheet of paper. Simple straight-line graphs are not acceptable, because they can readily be described in the text by means of an equation or a sentence. Claims of linearity should be supported by regression data that include slope, intercept, standard deviations of the slope and intercept, standard error and the number of data points; correlation coefficients are optional.

Photographs should be glossy prints and be as rich in contrast as possible; colour photographs cannot be accepted. Line diagrams are generally preferred to photographs of equipment. Computer outputs for reproduction as figures must be good quality on blank paper, and should preferably be submitted as glossy prints.

Nomenclature, abbreviations and symbols. In general, the recommendations of IUPAC should be followed, and attention should be given to the recommendations of the Analytical Chemistry Division in the journal *Pure and Applied Chemistry* (see also *IUPAC Compendium of Analytical Nomenclature, Definitive Rules*, 1987).

References. The references should be collected at the end of the paper, numbered in the order of their appearance in the text (*not* alphabetically) and typed on a separate sheet.

Reprints. Fifty reprints will be supplied free of charge. Additional reprints (minimum 100) can be ordered. An order form containing price quotations will be sent to the authors together with the proofs of their article.

Papers dealing with vibrational spectroscopy should be sent to: Dr J.G. Grasselli, 150 Greentree Road, Chagrin Falls, OH 44022, U.S.A. Telefax: (+1-216) 2473360 (Americas, Canada, Australia and New Zealand) or Dr J.H. van der Maas, Department of Analytical Molecular Spectrometry, Faculty of Chemistry, University of Utrecht, P.O. Box 80083, 3508 TB Utrecht, The Netherlands. Telefax: (+31-30) 518219 (all other countries).

0003-2670/94/$07.00

Find out more... *with Wiley*

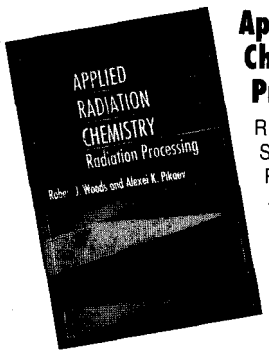

Applied Radiation Chemistry Radiation Processing

R.J. WOODS, University of Saskatchewan, Canada, and A.K. PIKAEV, Russian Academy of Sciences, Russia

Takes a long, hard look at the entire field of radiation processing: its history, the current state of technology, level of use, controversial applications, and promising developments. The only book of its kind, *Applied Radiation Chemistry* places as much emphasis on the chemical changes and principles that produce the observable results, as it places on the techniques in question. This enables the reader to understand applications in chemical terms, rather than as a series of recipes. Applications include processing of polymers and the sterilization of medical disposables.

0471544523 548pp 1993 £62.00/$86.50

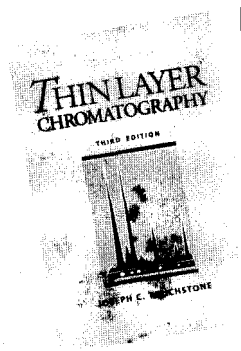

Practice of Thin Layer Chromatography

Third Edition

J.C. TOUCHSTONE, University of Pennsylvania, USA

Using a clear step-by-step approach, this valuable guide outlines the procedural basics of thin layer chromatography, detailing the specifics of each step in single chapter. An extensive glossary as well as several tables and figures which serve to illustrate key points supplement the text. Not only has the informative breadth of the present edition been expanded, each chapter has undergone updating and revision in keeping with the field's escalating technological advances.

0471612227 394pp 1992 £77.00/$109.00

Voltammetric Determination of Molecules of Biological Significance

W. FRANKLIN SMYTH, University of Ulster, Coleraine, Northern Ireland

This book presents a critical account of recent applications of voltammetry to the identification and determination of selected molecules of biological significance such as pollutants, drugs, food additives and contaminants, amino acids and neurotransmitters. Intended as a concise practical guide, the book has been divided where possible according to the nature of the eloctroactive functional groups in the overall molecular structure.

0471933457 144pp 1992 £51.00/$86.95

An Introduction to Laboratory Automation

V. CERDA, University of the Balearic Islands, Spain and G. RAMIS, University of Valencia, Spain

This definitive, hands-on and up-to-date text will allow you to smoothly automate your lab in as cost-effective and efficient a style as possible. The versatility of the tools and techniques described are suitable for professional settings as wide as the industrial lab, municipal lab, analytical services, environmental control services, and health services.

Series: Chemical Analysis Series
0471618187 336pp 1990 £92.00/$129.00

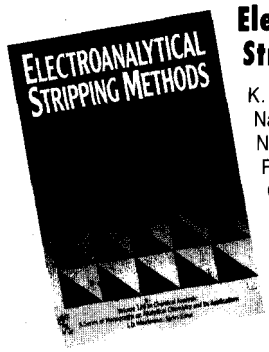

Electroanalytical Stripping Methods

K. BRAININA, Sverdlovsk Institute of National Economy, Russia and E. NYMAN, Central Special Inspection of Russian Environmental Protection Committee, Russia

Bringing together the latest theoretical and experimental Developments in the field over the past decade, this valuable guide emphasizes the theory associated with the most progressive stripping electroanalytical methods (SEAMSs) and their application to environmental monitoring and industry. Important information on the main advantages of these methods is given, including their low detection limit, the low cost of the instruments used, the possibility of speciation analysis, and their use in the investigation of solids as well as solutions.

CONTENTS: Discharge-Ionization of Metals; The Choice and Formation of Analytical Signals; Electrodes and Electrolyzers; Stripping Electroanalytical Methods in the Analysis of Solutions; Phase Analysis of Solids; Investigation of Specific Features of the Structure of a Solid; References

Chemical Analysis: A Series of Monographs on Analytical Chemistry and Its Applications
0471595063 224pp 1994 £49.50/$68.95

Remember for chemistry...read Wiley

Order from your Bookseller - or directly from Wiley. Cheques made payable to 'John Wiley & Sons Ltd', marked for the attention of Nicky Douglas. For credit card orders phone +44 (0)243 770392 or fax +44 (0)243 531712. All prices are correct at time of going to press. Please add £2.00/$5.00 to cover postage. Save money - order more than one book and postage is ***FREE!***

John Wiley & Sons Ltd
Baffins Lane Chichester
West Sussex PO19 1UD UK

WILEY